Exploring neutrophil heterogeneity in health and cancer

Frederick Mark Peakman

University College London

and

The Francis Crick Institute

PhD Supervisor: Dr Ilaria Malanchi

A thesis submitted for the degree of

Doctor of Philosophy

University College London

September 2019

Declaration

I, Frederick Mark Peakman, confirm that the work presented in this thesis is my own. Where information has been derived from other sources, I confirm that this has been indicated in the thesis.

Abstract

Interactions between cancer cells and their microenvironment are critical for tumour initiation, growth and metastasis. Consequently, a greater understanding of these interactions may offer novel opportunities for therapy. Neutrophils are innate immune cells that form a component of the tumour microenvironment. Both pro- and anti-tumour effects of neutrophils are reported in the literature, suggesting context-dependent complexity in neutrophil-tumour interactions. This complexity is further deepened by recent reports demonstrating that neutrophil populations are more heterogeneous than previously appreciated, but it is unclear what significance this may have in a cancer context. This thesis therefore aimed to investigate how tumours perturb neutrophil heterogeneity and the potential functional consequences of this perturbation for neutrophil-tumour interactions.

I first used mass cytometry to perform high-dimensional analysis of mouse neutrophil surface marker expression across tissues and control and tumour-bearing contexts, using the MMTV-PyMT mouse model of breast cancer. This revealed a number of neutrophil populations defined by their differential expression of surface markers, with shifts in the populations observed between control and tumour-bearing mice. In particular, a population of neutrophils defined by low expression of L-Selectin ($CD62L^-$) expands in the bone marrow, circulation and periphery of tumour-bearing mice. This phenotype was observed in a number of other mouse cancer models.

Analysis of nuclear morphology found that $CD62L^-$ neutrophils have a more hyper-segmented nucleus than $CD62L^+$ neutrophils, suggesting potential functional differences between these populations. However, a range of

functional assays did not identify differences between the two populations. Instead, comparison of the total neutrophil population from control mice and tumour-bearing mice discovered differences in functionality. Most significantly, when comparing neutrophils from control and tumour-bearing mice I found changes in kinase activity, reactive oxygen species and *in vitro* interactions with cancer cells, indicating broad shifts in neutrophil phenotype during the switch from a healthy state to cancer.

Impact Statement

In recent years neutrophils have been implicated in cancer pathology, with both pro- and anti-tumorigenic neutrophil effects reported. In addition, there is mounting evidence that neutrophils are a heterogeneous population with extensive phenotypic plasticity. My thesis aimed to investigate the intersection between these emerging concepts, to improve understanding of the contribution of neutrophil heterogeneity to cancer processes.

My findings in this thesis primarily impact academic science but also have implications for clinical oncology. My principal discoveries are: firstly, the expansion of a CD62L- neutrophil population across tissues in tumour-bearing mice. Secondly, the observation of extensive alterations in functional activity between neutrophils from control and tumour-bearing mice; most significantly, I find differences in kinase activity and levels of reactive oxygen species.

My work is the first, to my knowledge, to demonstrate a systemic expansion of $CD62L^-$ neutrophils in tumour-bearing mice, in a range of mouse carcinoma models. Although I am unable to identify a functional significance for the $CD62L^-$ neutrophil population, my results suggest that the presence of a tumour can manipulate neutrophil phenotypes systemically. In addition, there is evidence in the literature to suggest functional differences in neutrophil populations based on CD62L expression. Thus, my results indicate a future avenue for research in this area focused on dissecting the functional importance of variable CD62L expression by neutrophils in a tumour context.

Significantly, a number of studies have demonstrated higher levels of $CD62L^-$ neutrophils in the circulation of cancer patients compared to healthy volunteers. My findings therefore have relevance to clinical oncology, and offer the potential to link the expansion of $CD62L^-$ neutrophils I identify in mice with that observed in humans. This will require further investigation of this population in cancer patients, and diligent functional characterization of these populations in both mouse and human settings. If this can be achieved, exploration of the function of $CD62L^-$ neutrophils in mice

could be used to inform our understanding of the roles of these cells in human disease. Whilst mouse models are an imperfect facsimile of human cancer, they would offer a manipulable experimental setting, allowing testing of cytokines, inhibitors or other factors in order to probe the effects of $CD62L^-$ neutrophils on tumours, with potential implications for human disease and therapy.

My observations of shifts in kinase activity are novel findings in the neutrophil field. Whilst there has been extensive analysis of neutrophil transcription, there has been limited focus on kinase activity, which is critical in signalling pathways involved in neutrophil development and activation. In particular, I find shifts in kinase activity and levels of reactive oxygen species between neutrophils at different stages of development in the bone marrow. Although it is well established that tumours can perturb granulopoiesis, my findings offer a novel route to analyse and understand the consequences of these phenotypes, by focusing on kinases and reactive oxygen species. Further analysis of kinase activity in mouse neutrophils could be complemented by analysis of human neutrophils, which may reveal new insights into neutrophil phenotypes in human disease.

Acknowledgements

I cannot thank Ilaria enough for her excellent supervision over the last four years. Her hard work, passion and ideas have all been instrumental in this project. I am eternally grateful for the opportunity to have been a student in her lab.

I also want to thank all members of the Malanchi lab, past and present, for creating a great atmosphere. I am grateful for the technical support, the scientific discussion and the beers! I've thoroughly enjoyed working with everyone in the lab and I will miss you all.

I am indebted to the Francis Crick Institute Biological Research Facility and Flow Cytometry Science Technology Platform. Without the excellent support from these facilities it would have been impossible to perform many of the experiments in this thesis.

I would like to thank my family for a lifetime of love and support, and in particular my parents for motivating and inspiring me over the years.

Finally, I would like to thank Kate from the bottom of my heart, for all her love and support over the last four years, and for always being there for me.

Table of Contents

Table of figures

List of tables

Abbreviations

ATP	Adenosine triposphate
BSA	Bovine Serum Albumin
CD	Cluster of differentiation
CMP	Common myeloid progenitor
CXCL	Chemokine C-X-C motif ligand
CXCR	Chemokine C-X-C motif receptor
DAPI	4′,6-diamidino-2-phenylindole dihydrochloride
ddH20	Double-distilled water
DMEM	Dulbecco's Modified Eagle's Medium
EDTA	Ethylenediaminetetraacetic acid
EGF	Epidermal Growth Factor
FACS	Fluorescence-activated cell sorting
FCS	Foetal calf serum
FSC	Forward scatter
G-CSF	Granulocyte-colony stimulating factor
GFP	Green fluorescent protein
GM-CSF	Granulocyte –macrophage-colony stimulating factor
GMP	Granulocyte myeloid progenitor
HBSS	Hanks' balanced salt solution
IL	Interleukin
L	litre
LPS	Lipopolysaccharide
Ly6g	Lymphocyte antigen 6 complex , locus G
M	Molar
M-MDSC	Monocytic-myeloid-derived suppressor cell
MDSC	Myeloid-derived suppressor cell
MHC	Major histocompatibility complex
MMP9	Matrix metallopeptidase 9
MMTV	Mouse mammary tumour virus
NET	Neutrophil extracellular trap
NLR	Neutrophil : lymphocyte ratio

PBS	Phosphate-buffered saline
PD-L1/2	Programmed death-ligand 1/2
PMA	12-*O*-Tetradecanoylphorbol-13-acetate
PMN	Polymorphonuclear
PMN-MDSC	Polymorphonuclear-myeloid-derived suppressor cell
PyMT	Polyoma middle T antigen
ROS	Reactive oxygen species
RPMI-1640	Roswell Park Memorial Institute 1640
SSC	Side scatter
TAN	Tumour-associated neutrophils
TGF	Transforming growth factor
TIL	Tumour-infiltrating lymphocyte
TNF	Tumour necrosis factor
t-SNE	t-distributed stochastic neighbour embedding

Chapter 1. Introduction

1.1 Cancer: an unmet global health burden

Cancers are a heterogeneous group of diseases in which abnormal cells grow in an uncontrolled manner, with the capacity to invade local tissue and spread to other regions of the body. Cancer is today the second leading cause of death worldwide (Ferlay et al., 2015). Current trends predict an increase in cancer incidence and mortality over the coming decades, predominantly due to increasing global development and demographic trends that are producing an ageing population (Bray et al., 2012).

Decades of research have resulted in enhanced diagnostic tests and significant advances in treatment options, improving detection and lengthening survival rates (Siegel et al., 2019). Despite this progress, survival rates for a number of cancer types have remained stubbornly low. For example, in the UK, five- and ten-year survival rates for lung, pancreatic, brain and oesophageal cancer have barely increased since 1970 (Quaresma et al., 2015). In 2011, ten-year survival rates for these cancers were below 20%, and below 5% in the case of lung and pancreatic cancer. Even in cancers where survival rates have dramatically improved, such as breast cancer, there is still 20% mortality ten years following diagnosis, and for many cancers, ten year survival rates are in the region of 40-60% (Quaresma et al., 2015).

Additionally, there is controversy over the claimed improvements in survival rates, which typically measure patient survival five or ten years following diagnosis: these metrics do not quantify overall mortality, which has shown much more modest decreases over the last 40 years (Siegel et al., 2019). Furthermore, it has been argued that much of this decrease was due to changes in public health, primarily declining rates of tobacco smoking, rather than improved diagnostic techniques and therapies (Thun and Jemal, 2006).

In summary, whilst progress has been made in improved diagnosis and treatment of cancer over the last 40 years, the disease remains a stubborn global health burden

and death sentence for many patients. This fact, in tandem with the predicted increase in cancer incidence over the coming decades, underlines the urgent demand for novel and improved therapeutic options.

The precise molecular and cellular origins of cancer are the subject of intense debate and controversy (Blanpain, 2013, Visvader, 2011, Chaffer and Weinberg, 2015). It is not within the scope of this introduction to fully explore the range of ideas in this field, but I will briefly summarize general principles of cancer biology. Cancer is broadly accepted to arise from a failure of control of cellular proliferation. Aberrant, excessive activation of growth-promoting oncogenes is coupled with diminished activity of tumour suppressor proteins that control and limit growth, this results in the uncontrolled expansion of transformed cells (Hanahan and Weinberg, 2000). Tumour growth and further mutations produce malignant cells with invasive capacity, that can spread within a tissue and ultimately detach from the tumour, enter the circulation, and invade tissues around the body, a process known as metastasis that is responsible for over 90% of cancer mortality (Valastyan and Weinberg, 2011).

1.2 The tumour microenvironment

In recent years it has become increasingly clear that a tumour is not simply a collection of malignant transformed cells, but a dynamic ecosystem in which cancer cells are surrounded by untransformed “normal” host cells: immune cells, fibroblasts, parenchymal cells, endothelial cells and an extracellular matrix (Balkwill et al., 2012). The interactions between these elements and cancer cells create what is termed the tumour microenvironment. These interactions are critical for the survival and growth of cancer cells, and are also central to processes such as tumour invasion and metastasis (Quail and Joyce, 2013). For example, fibroblasts and macrophages can alter the extracellular matrix to facilitate invasion and metastasis (Kalluri, 2016, Yang et al., 2018) and tumour-associated endothelial cells can improve blood supply to a tumour (Hida et al., 2018).

The microenvironment is consequently an attractive target for novel therapeutic avenues, though it must be emphasized that interactions between cancer cells and the microenvironment are highly specific and context-dependent, therefore careful elucidation of microenvironmental interactions and their underlying mechanisms is required before novel therapies can be effectively designed and realised. Therefore, improving our understanding of the tumour microenvironment is an important step in the development of new avenues for treatment. Therapies targeting the microenvironment have been developed and met with significant success in some cases, most notably immunotherapies that target interactions between cancer cells and the T cells of the adaptive immune system (Dougan et al., 2019).

A major component of the tumour microenvironment is inflammatory cells. This was in fact first observed by Rudolf Virchow in 1863 (Virchow, 1863), and has since become an established “hallmark” of cancer (Hanahan and Weinberg, 2011, Mantovani et al., 2008). Inflammation is a significant contributor to the initiation of tumours: chronic inflammation is associated with an increased risk of certain cancers, and tumour-initiating events, such as UV radiation or viral infection, often involve inflammation (Kundu and Surh, 2008). More significantly, inflammation can enhance the growth, invasion and metastasis of established tumours. Therefore, regardless of the origins of a tumour, inflammation can have a major effect on the outcome of that tumour (for example, the response to therapy) (Grivennikov et al., 2010). A central cellular component of inflammation is the neutrophil, a bone marrow-derived myeloid cell that is a critical arm of the innate immune system. Neutrophils can comprise a significant element of the tumour microenvironment (Powell and Huttenlocher, 2016), and have been implicated in processes at all stages in the life of a tumour (Coffelt et al., 2016). Notably, they are the first circulating immune cells to respond to inflammatory signals emanating from a tissue (Kruger et al., 2015), and have extensive inflammatory capabilities (Mayadas et al., 2014). However, the effects that neutrophils exert appear contradictory, with reports showing neutrophils have the capacity to enhance or impede tumour progression depending on the context (Uribe-Querol and Rosales, 2015). Neutrophils therefore represent an attractive microenvironmental target for further research that may inform the development of new therapies.

In this introduction, I will first describe the biology of neutrophils, detailing their functions, origins and life cycle, and the emerging concept of neutrophil heterogeneity. Then, I will explore the relationship between neutrophils and cancer, covering clinical and basic science evidence implicating neutrophils in tumour processes. Next, I will explain how tumours can in turn affect neutrophils, and impinge upon neutrophil heterogeneity. Finally, I will summarize outstanding questions in the neutrophil-cancer field, and outline the aims for my experimental investigations.

1.3 Neutrophils: foot soldiers of the immune response

Neutrophils originate in the bone marrow, which they leave upon maturation. After exiting the bone marrow, neutrophils spend their mature lifespan in the circulation, where they are the predominant leukocyte population in humans, comprising 50-70% of circulating leukocytes, in mice they are less dominant, comprising 10-25% (Mestas and Hughes, 2004). The induction of inflammation within a tissue, which can be due to the detection of pathogens or sterile damage to the tissue, produces a rapid (in the order of minutes) influx of neutrophils from the circulation into the tissue, where neutrophils perform their central functions of pathogenic destruction (Mayadas et al., 2014). They are highly adapted to fulfil this role, with an armoury of anti-microbial weapons: firstly, they have extensive phagocytic capability, allowing them to engulf numerous pathogens in a phagosome. In a process termed the respiratory burst, neutrophils then use NADPH oxidase to generate reactive oxygen species (ROS) in the form of superoxide radicals, which generate hydrogen peroxide. The key enzyme myeloperoxidase then combines hydrogen peroxide and chloride to form hypochlorous acid, which effects the destruction of engulfed pathogens. Neutrophils can also release ROS into the extracellular space, where these species can contribute to microbial destruction (Kruger et al., 2015).

The cytoplasm of neutrophils is studded with granules and secretory vesicles. These contain a plethora of anti-microbial proteins and enzymes, including myeloperoxidase, elastase, lysozyme, defensins and more. Degranulation thereby

allows neutrophils to rapidly flood their surroundings with anti-microbial factors, granules can also be released into phagosomes to destroy engulfed pathogens (Kruger et al., 2015). Granules also contain matrix metalloproteases and other enzymes that modify the extracellular matrix, facilitating neutrophil migration and the entry of more neutrophils and other immune cell types into the site of inflammation (Kolaczkowska and Kubes, 2013).

In 2004, a novel aspect of neutrophil biology was identified: the neutrophil extracellular trap (NET) (Brinkmann et al., 2004). These are large structures of decondensed chromatin studded with antimicrobial proteins from granules and the cytosol. The chromatin traps pathogens, which prevents their spreading, and allows their destruction by the antimicrobial proteins and other immune cells. NETs are released in a process known as NETosis, which can be a fatal final act for the neutrophil, but can also be achieved in a more controlled manner (Papayannopoulos, 2017). Both of these mechanisms result in NETs spreading out from the cell, which can then trap and kill pathogens. NETs have additionally been implicated in processes ranging from atherosclerosis to metastasis, and have immunomodulatory effects via signalling to other immune cells, highlighting their role beyond killing pathogens (Papayannopoulos, 2017).

1.4 Neutrophil functions beyond microbial destruction

These three methods, phagocytosis, degranulation and NETosis, are the principal weapons neutrophils utilize to combat pathogens. The classical view of neutrophils has posited that these cells are vital yet one-dimensional; arriving at sites of inflammation, using the above three mechanisms to destroy pathogens, and then undergoing apoptosis (or indeed NETosis) once they have exhausted their antimicrobial arsenal, but performing little beyond this function. In recent years this view has been challenged and it is now abundantly clear that neutrophils are much more multifaceted than was previously appreciated (Mayadas et al., 2014). This allows neutrophils to influence a diverse range of processes, and it is unlikely that the full extent of their participation has been discovered. It has also transpired that

neutrophils have much greater plasticity than previously appreciated, with the capacity to respond to and coordinate a range of signals within the inflammatory environment (Giese et al., 2019, Fridlender et al., 2009).

Perhaps the most important findings are those that have demonstrated the extensive immunomodulatory capabilities of neutrophils. Neutrophils can secrete, from their granules and the cytosol, an enormous range of cytokines and chemokines that can influence other immune cell types, other neutrophils and also stromal and parenchymal cells within the tissue (Leliefeld et al., 2015). This ability allows neutrophils to aid in the marshalling of a specific immune response against different types of pathogen; they can recruit and activate a multitude of other immune cell types, including dendritic cells, macrophages and T cells, and pro-inflammatory cytokines such as Interleukin-6 can contribute to systemic inflammation (Mantovani et al., 2011). Neutrophils express numerous pattern recognition receptors that detect microbial moieties and signals of tissue damage. Engagement of these receptors induces release of immunomodulatory cytokines, with different receptors activating different pathways, thereby allowing neutrophils to fine-tune the immune response to a specific pathogenic threat. Neutrophils can also secrete anti-inflammatory, angiogenic and fibrogenic factors that contribute to the resolution of inflammation and wound healing (Mantovani et al., 2011).

Arguably one of the most important neutrophil abilities that has been recently revealed is their capacity to suppress T cells responses. This has been extensively documented in both mice and humans, and occurs in numerous contexts, notably cancer but also in other settings, including bacterial and viral infections (Leliefeld et al., 2015), where this suppressive ability may be important in the resolution of inflammation following pathogen clearance. There are a range of mechanisms by which neutrophils suppress T cells, these include neutrophil-secreted proteases that degrade activating cytokines and T cell surface molecules (Bank and Ansorge, 2001), ROS and arginase inhibiting T cell proliferation (Leliefeld et al., 2015), and direct inhibition of T cell responses by neutrophil expression of PD-L1 or release of Prostaglandin E2 (Cheng et al., 2018, Veglia et al., 2019).

In contrast to their immunosuppressive capabilities, neutrophils can also use major histocompatibility II (MHC-II) molecules to present antigens to T cells, in both mice and humans (Singhal et al., 2016, Lin and Loré, 2017). Chemokines from neutrophils can also attract T cells to sites of inflammation (Pelletier et al., 2010b). In the spleen neutrophils have been shown to aid the activation of marginal zone B cells by secreting factors such as interleukin-21 and pentraxin 3, thereby influencing humoral immunity (Chorny et al., 2016).

Neutrophils also have the ability to participate in tissue restoration and angiogenesis following inflammation and wounding. This has been demonstrated in a variety of contexts, including infected skin wounds and sterile internal injuries, in both mice and humans (Phillipson and Kubes, 2019). For example, neutrophils can release anti-inflammatory cytokines and mediators that dampen inflammation following pathogen clearance (Bui et al., 2018). Neutrophils can also directly induce angiogenesis at sites of wounding and injury (Christoffersson et al., 2012b, Christoffersson et al., 2017). Matrix metalloproteases and other enzymes released by neutrophils can degrade the extracellular matrix to enhance angiogenesis (Christoffersson et al., 2012a). Illustrating the importance of neutrophils in these processes, depletion of neutrophils during sterile liver injury significantly delayed revascularization (Wang et al., 2017), and genetic impairment of neutrophil migration slows epithelialization after wounding (Devalaraja et al., 2000).

The above examples are not an exhaustive list, but they demonstrate the extensive capabilities of neutrophils beyond microbial destruction, and the elemental plasticity of neutrophils. This has consequences for how neutrophils may influence cancer progression, demonstrating that neutrophils can interact with tumour cells and other cells in the tumour microenvironment in a range of ways.

1.5 The origins of neutrophils: granulopoiesis

It is estimated that in humans 10^{11} neutrophils are produced daily from the bone marrow, in mice the figure is 10^{7} (Borregaard, 2010).This is necessitated by the comparatively short lifespan of neutrophils, meaning continuous production is

required on a daily basis to maintain neutrophil numbers within homeostatic limits. In humans and mice with cancer or other inflammatory conditions, neutrophil production can be increased further. (this is explored in further detail in Section 1.9).

The process of neutrophil production is termed granulopoiesis, and is a subdivision of haematopoiesis; the generation of blood cells. This process begins with haematopoietic stem cells, which generate a pool of multipotent progenitors. These then produce lineage-committed granulocyte-monocyte myeloid progenitors (GMPs). These cells differentiate into mature neutrophils via the following sequence: GMPs, myeloblast, promyelocyte, myelocyte, metamyelocyte, band cell, immature neutrophil, mature neutrophil (Borregaard, 2010, Hidalgo et al., 2019) (Figure 1.1).

Unlike other immune cell types, neutrophils leave the bone marrow as terminally differentiated mature cells. Consequently, they undergo extensive changes during maturation. Production of granules begins at the promyelocyte stage, and continues throughout neutrophil development, resulting in mature neutrophils with large stores of granules in their cytoplasm (Häger et al., 2010).

Changes in expression of cell surface molecules accompany neutrophil differentiation: as they mature neutrophils increase expression of a number of cell surface proteins, including Ly6g, which is used as a biomarker to identify neutrophils and delineate them from other myeloid cell types (Daley et al., 2008, Lund-Johansen and Terstappen, 1993). Ly6g in particular is the canonical neutrophil marker in mice, though it is not expressed by human neutrophils. Neutrophils also upregulate expression of functional cell surface molecules, such as integrins, selectins and Toll-like receptors. Additionally, expression of two C-X-C chemokine receptors is critical in neutrophil development, as these markers mediate the retention and egress of neutrophils in the bone marrow. CXCR4 is highly expressed from the haematopoietic stem cell stage of development onwards. It binds to its ligand, CXCL12, which is present at high concentrations in the bone marrow microenvironment due to constant release by stromal cells. This sequesters maturing precursors and immature neutrophils within the bone marrow, ensuring they do not leave the bone marrow before they are fully developed. As cells proceed down the neutrophil maturation pathway they downregulate CXCR4 expression. In tandem, the chemokine receptor

CXCR2 is expressed at the promyelocyte stage, and is upregulated as neutrophils mature (McKinstry et al., 1997). CXCR2 binds to numerous chemokines, including CXCL1,2,3,5,6,7,8 (Veenstra and Ransohoff, 2012). CXCL1 and CXCL2 are produced by endothelial cells and megakaryocytes in the blood. In this way, mature bone marrow neutrophils, expressing high levels of CXCR2, are attracted into the circulation by CXCL1 and CXCL2, and their low expression of CXCR4 ensures they are no longer sequestered by CXCL12 in the bone marrow niche (Eash et al., 2010). This system regulates neutrophil exit from the bone marrow, ensuring that only sufficiently differentiated neutrophils, with high CXCR2 expression and low CXCR4 expression, can enter the circulation. Though it is important to note that this system can be dysregulated under inflammatory conditions and other contexts (Manz and Boettcher, 2014). Once in the circulation, neutrophils use CXCR2 to detect and respond to inflammation: CXCL-X chemokines are released from cells in tissues in response to inflammatory stimuli. Neutrophils bind these chemokines with CXCR2, promoting their chemotaxis through the tissue to the site of inflammation (Veenstra and Ransohoff, 2012).

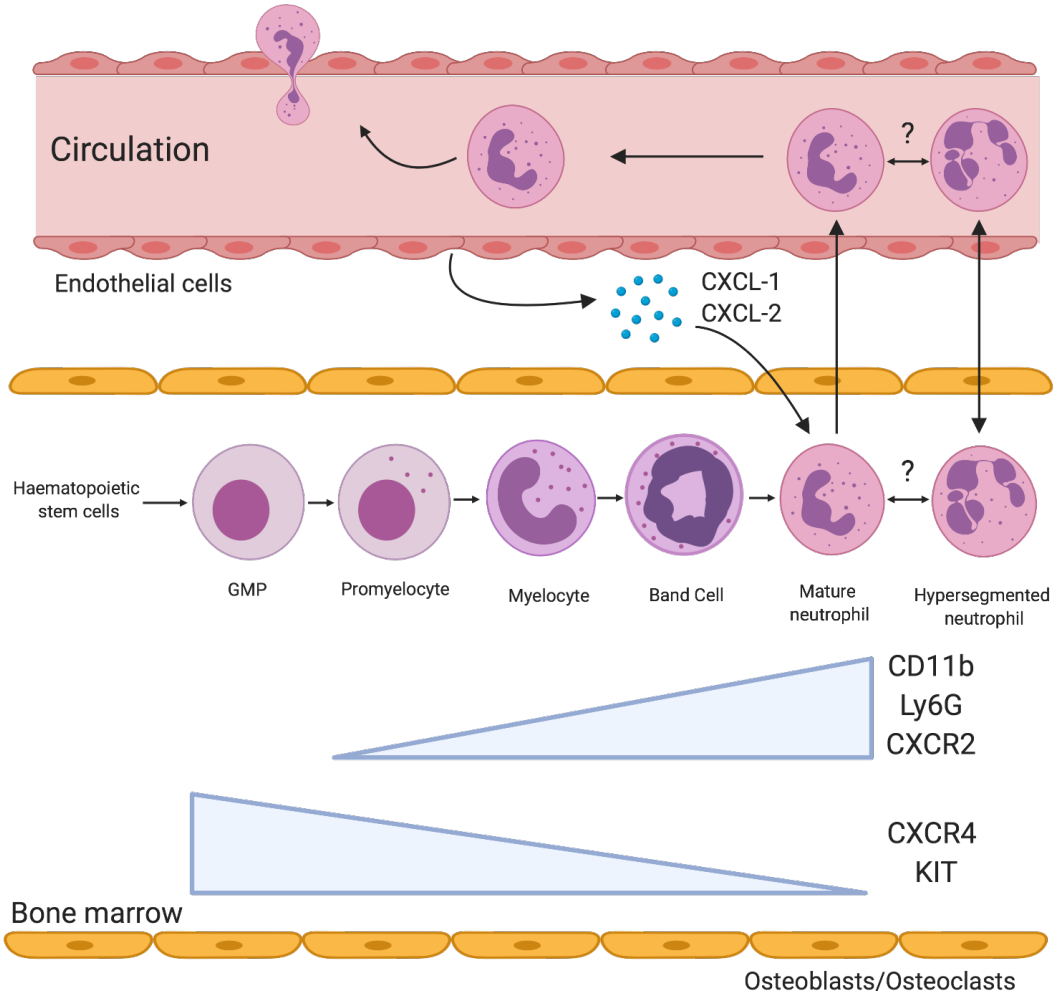

Figure 1.1 Bone marrow granulopoiesis

Diagram displaying granulopoiesis and the egress of neutrophils from the bone marrow into the circulation. Haematopoietic stem cells generate granulocyte myeloid progenitors (GMPs), which generate neutrophils, passing through promyelocyte, myelocyte, and band cell stages. Note that not all neutrophil developmental stages are shown for simplicity. As they undergo granulopoiesis, neutrophils upregulate a range of surface markers, most importantly CD11b, Ly6g and CXCR2. They also downregulate CXCR4 and KIT, among others. CXCL-1/2 can stimulate egress of mature neutrophils from the bone marrow by activating CXCR2, inducing chemotaxis. Hypersegmented neutrophils can be found in the circulation and bone marrow in mice, and have been observed in the circulation in humans. However, the relationship between these neutrophil populations is not yet fully defined, and where and how hypersegmented neutrophils are generated Is still subject to debate. Image created with Biorender.com

Another important aspect of neutrophil maturation is the changes in nuclear morphology that occur during differentiation (Figure 1.2) (Pillay et al., 2013). Haematopoietic stem cells and GMPs have quintessential round nuclei. However, when developing cells reach the myelocyte stage they begin to develop a concave nucleus. At the promyelocyte stage they develop a ring-shaped nucleus, enclosing cytosol. Bulges in the nucleus begin to appear at the band cell stage, further differentiation results in these bulges forming lobes in the nucleus. The number and size of these lobes increases as cells develop into immature neutrophils and then into mature neutrophils, by which point they will typically have between two and five lobes, linked by thin filaments of nucleoplasm, in an open horseshoe-like structure (Skinner and Johnson, 2017). Analysis of neutrophil nuclear morphology is therefore a useful tool for assessing the maturity of different neutrophil populations.

The precise significance of the lobed nuclei of neutrophils is unclear. There is some speculation that it facilities the transmigration of neutrophils across the endothelium, allowing them to squeeze between tight endothelial cell junctions (Hoffmann et al., 2007). The nuclear morphology may also aid in the formation of NETs. Similar granulocytic cells, such as eosinophils, basophils and mast cells also have lobular nuclei, these cells have quite distinct functions and capabilities from neutrophils, which implies that the abnormal nuclear morphology may not be related to specific neutrophil abilities.

Mature neutrophils can also undergo further increases in lobe number and segmentation of their nuclei to form hypersegmented neutrophils. This is generally believed to only occur outside the bone marrow in certain contexts, though it has been suggested that there may be a population of hypersegmented neutrophils residing in the bone marrow whose release is induced by LPS stimulation (Pillay et al., 2012, Tak et al., 2017). Thus, hypersegmented neutrophils do not necessarily represent a more differentiated population than segmented neutrophils.

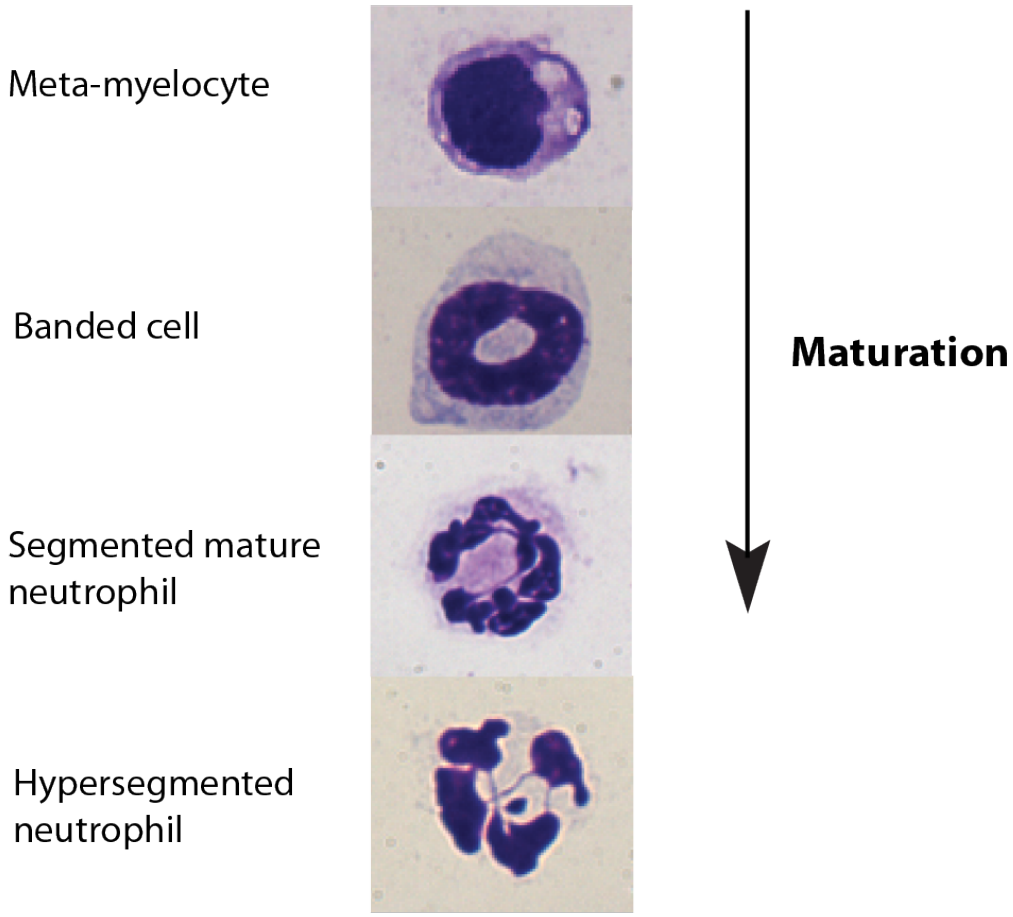

Figure 1.2 Neutrophil nuclear morphology during development and beyond

Microscope images of neutrophils stained with Wright-Giemsa stain (see Materials and Methods section 2.13 for the methods used to produce neutrophil images). Changes in nuclear morphology begin at the metamyelocye stage, when the nucleus begins to develop a concave shape. Banded cells develop lobes in the nuclei as it forms a ring shape, the size and number of these lobes increases to form segments by the mature neutrophil stage. Mature neutrophils can undergo further lobe formation and segmentation to form hypersegmented nuclei.

The master regulator of neutrophil production and differentiation is granulocyte-colony stimulating factor (G-CSF) (Bendall and Bradstock, 2014). The G-CSF receptor is expressed from the GMP stage onwards up to even mature neutrophils (McKinstry et al., 1997), and its activation by G-CSF induces proliferation and differentiation of granulocytes. Mice lacking G-CSF or its receptor display severely impaired neutrophil production, though they are still able to produce small numbers of mature neutrophils (Liu et al., 1996), suggesting redundancy in this system. Indeed, other factors, including Interleukin-6 (IL-6), KIT and granulocyte-macrophage-colony stimulating factor (GM-CSF), can all induce neutrophil production (Coffelt et al., 2016). G-CSF can be produced by a range of different cell types and tissues, including cancer cells, thereby allowing production of neutrophils to be stimulated by numerous sources and signals. G-CSF can also enhance neutrophil egress from the bone marrow, by increasing release of CXCR2 ligands, and inducing downregulation of CXCR4 expression by neutrophils (Köhler et al., 2011, Kim et al., 2006).

Under homeostatic conditions, neutrophil production is tightly regulated, principally by an IL-23/IL-17/G-CSF axis (Wirths et al., 2014), in which IL-23 from macrophages stimulates Il-17 production by various lymphocyte subsets, Il-17 in turn induces G-CSF production by stromal cells, and this stimulates granulopoiesis in the bone marrow. Apoptotic neutrophils are phagocytosed by macrophages in the liver and bone marrow, and this induces the macrophages to downregulate IL-23 expression, in turn lowering Il-17 and G-CSF production from lymphocytes and stromal cells respectively. In this way increased or decreased neutrophil levels ultimately influence the production of G-CSF, fine-tuning granulopoiesis to maintain neutrophil numbers within homeostatic limits. This system can be dysregulated during infection, inflammation and cancer, leading to increased granulopoiesis (Coffelt et al., 2015).

Under both homeostatic and inflammatory conditions, including cancer, extramedullary haematopoiesis can occur in the spleen and other tissues (in both mice and humans) (Kim, 2010). Though it is not yet established to what extent this process has functional significance for neutrophil production or tumour progression.

1.6 The neutrophil lifecycle

Once they have exited the bone marrow, neutrophils enter the circulation and travel around the body in the blood. Compared to most other immune cells, the lifespan of neutrophils is short: their half-life in the circulation is estimated to be between six and ten hours in humans and mice (Galli et al., 2011). These figures have been the subject of intense debate, with some studies positing half-lives as long as two days, and a total lifespan of up to 5.4 days (Pillay et al., 2010). Findings of differing neutrophil lifespans may reflect differing experimental techniques, and in particular the findings of longer lifespans have been challenged on experimental grounds (Tofts et al., 2011). The precise lifespan of neutrophils in the circulation remains an open topic of debate, but there is abundant evidence that neutrophils within tissues, sites of inflammation and tumours can have extended lifespans, up to several days (Hidalgo et al., 2019). This appears to be principally achieved by inhibition of apoptosis, which can be induced by an array of signals, including pro-inflammatory cytokines, tissue damage signals, pathogen-derived signals and environmental factors such as hypoxia (Geering et al., 2013, Silvestre-Roig et al., 2016). Neutrophil lifespan can also be boosted *in vitro* by a variety of cytokines and factors (Colotta et al., 1992). Importantly, an increased neutrophil lifespan implies increased capacity for neutrophils to alter their phenotype and function, and of course allows neutrophils more time to perform a particular function. For example, tissue hypoxia during bacterial-driven inflammation was found to activate pro-survival pathways in neutrophils in the inflammatory milieu and this enhanced their bacterial killing activity (Peyssonnaux et al., 2005).

Marginated pools of neutrophils have been identified in tissues including the bone marrow, spleen, lungs and liver (Hidalgo et al., 2019). The precise nature of these populations remains unclear, but there is evidence that these neutrophils are longer-lived than neutrophils in the circulating pool, and may have distinct functional phenotypes. For example, the aforementioned neutrophil population that can aid the activation of marginal zone B cells in the spleen (Chorny et al., 2016).

Evidence also has emerged that neutrophils can reverse migrate out from tissues and sites of inflammation, and re-enter the circulation (Colom et al., 2015). The precise functional consequences of this activity are not fully established, nor are the reasons why neutrophils decide to reverse migrate (Nourshargh et al., 2016). A recent study found that neutrophils migrated out from a sterile injury in the liver, and travelled to the lungs and then bone marrow, via CXCR4 upregulation, where they died by apoptosis (Wang et al., 2017). It has been speculated that this process may contribute to the resolution of inflammation, perhaps in concert with neutrophil apoptosis at the site of injury, or may allow neutrophils to relay signals to immune cells in other regions of the body (Garner and de Visser, 2017). Nevertheless, these findings further illustrate that neutrophil lifespan is more complex and potentially of greater length than previously appreciated.

Several recent reports have explored the concept of neutrophil ageing; as neutrophils persist in the circulation in the absence of inflammatory stimuli they begin to develop an “aged” phenotype (Casanova-Acebes et al., 2013). The precise timings for this are unclear, as a consequence of uncertainty around neutrophil lifespan in the circulation, but the circadian nature of neutrophil ageing suggests neutrophils age within 6-8 hours of egress from the bone marrow. Aged neutrophils upregulate CXCR4, which allows them to home back to the bone marrow for destruction. This was shown to occur in a circadian fashion, with the destruction of aged neutrophils reducing haematopoiesis at certain times of the day, regulating neutrophil production in a rhythmic circadian fashion, thereby maintaining homeostasis in haematopoiesis and neutrophil production. Additionally, aged neutrophils have a hypersegmented nuclear morphology, downregulate expression of CD62L (also known as L-Selectin), and have an enhanced capacity for inflammatory activation and NET formation compared to mature circulating neutrophils (Zhang et al., 2015).

1.7 Neutrophil heterogeneity

In the last decade, it has become apparent that, in addition to their multi-faceted nature, neutrophils may be a more heterogeneous population of cells than was previously appreciated (Silvestre-Roig et al., 2016). Evidence also suggests that neutrophils have a large degree of plasticity in their phenotypes, which can be altered by microenvironmental and systemic cues, and this plasticity in turn can contribute further to heterogeneity. These developments in the understanding of neutrophil biology were not unexpected, given the diversity and heterogeneity that exists across other immune cell populations, in particular in monocytes, macrophages and dendritic cells, which are the myeloid “cousins” of neutrophils. However, much of the precise nature and consequences of neutrophil heterogeneity remains to be established.

In the literature, different populations of neutrophils have been defined based on a number of characteristics including:

- Size
- Density
- Nuclear morphology
- Surface molecule expression

Differences in these characteristics have been linked to altered transcriptional states, protein synthesis, activation states and ultimately different functional phenotypes.

For example, a subpopulation of low density neutrophils was isolated from the circulation of patients with systemic lupus erythematous (SLE) (Denny et al., 2010, Villanueva et al., 2011). These neutrophils were found to have a more pro-inflammatory phenotype compared to higher density neutrophils, with increased production of type I interferons but decreased phagocytic activity. They were also more prone to releasing NETs, even in the absence of stimulation, which the authors suggest contributes to SLE pathology.

Another study found that a population of hypersegmented neutrophils expanded in the blood of humans following LPS stimulation (Pillay et al., 2012). This population was found to have stronger T cell suppressing ability than segmented neutrophil populations from the same blood, and also downregulated CD62L. A more recent paper from the same group demonstrated that the hypersegmented population has a significantly different proteome from the segmented population, further indicating functional differences between these populations (Tak et al., 2017).

The aged neutrophils in mice described in the previous section (section 1.6) were defined by their hypersegmented nuclear morphology and surface molecule expression ($CXCR4^+$ $CD62L^-$ compared to mature neutrophils which were $CXCR4^-$ $CD62L^+$). These differences reflected altered functionality, including increased inflammatory and NET-forming capacities (Zhang et al., 2015).

At the surface marker level, an important study used a 38-parameter antibody panel to interrogate surface marker expression in the mouse myeloid system across different tissues (Becher et al., 2014). The authors investigated all myeloid cell populations but, unexpectedly, automated clustering analysis separated the neutrophil pool into five different clusters based on differential surface marker expression. Notably, different tissues were found to contain differing relative ratios of the clusters, implying tissue-specific organisation of neutrophil heterogeneity. Importantly, this study did not further investigate the phenotypes of these populations, so it is unclear whether the differing surface marker expression between these populations reflects underlying functional phenotypic differences.

A more recent study from the same group investigated populations of developing neutrophils in the mouse bone marrow, identifying a novel population of “Pre-neutrophils,” committed, proliferative precursors that fall between the band cell and immature neutrophil stages of development (Evrard et al., 2018). These cells differentiated into immature and then mature neutrophil populations, which could be distinguished by their differential expression of several surface markers. All three populations were shown to have distinct transcriptional signatures, indicating underlying phenotypic differences between them. Significantly, an inflammatory stimulus or the induction of a tumour caused expansion of Pre-neutrophils and

induced the entry of immature neutrophils into the circulation, periphery and tumour. This study therefore demonstrated that immature neutrophils can exit the bone marrow before they are fully developed and potentially participate in inflammatory or tumour-related processes, provided that the right stimuli are present. A number of other studies have also found an expansion of immature neutrophils in the circulation under inflammatory conditions, including cancer (Wellenstein et al., 2019)

The above list of examples provides an overview of the various characteristics by which neutrophil heterogeneity can be defined, and illustrate how neutrophil heterogeneity can have functional consequences, with different populations having differing capacities for activities such as immune suppression and NET formation.

It is important to note that there is little evidence to suggest that neutrophil heterogeneity represent genuine subsets in the same manner as those found in T or B cells (Ng et al., 2019). Subsets of lymphocyte populations represent cells committed to a lineage, with extensive epigenetic and transcriptional differences that underpin this commitment. This is reflected in the highly specific functions that different lymphocyte subsets perform, for example $CD8^+$ T cells directly kill infected cells, whereas $CD4^+$ T cells aid in the activation of B cell humoral responses. These subsets have more limited plasticity, and lack the ability to perform each other's functions: a $CD4^+$ T cell lacks the granzyme and perforin proteins required for cytotoxic killing of infected cells. In contrast, neutrophil heterogeneity appears to be a system of neutrophils in different states of activation, polarization or maturation. Systemic and microenvironmental signals can perturb neutrophils during development in the bone marrow, or once they are in the circulation or in a tissue. An early landmark study in neutrophil heterogeneity offers an instructive example of these concepts in a cancer setting: in mice with subcutaneous mesotheliomas, neutrophils were found to infiltrate the tumours, where they suppressed $CD8^+$ T cells, thereby aiding tumour growth (Fridlender et al., 2009). Treatment of the mice with an inhibitor of transforming growth factor β (TGF-β) resulted in a switch in neutrophil phenotype, with neutrophils in the tumour now displaying cytotoxic activity towards tumour cells, mediated by ROS. This population also had hypersegmented nuclei and increased expression of pro-inflammatory cytokines. Depletion of neutrophils had contrasting effects depending on TGF-β blockade: depletion of neutrophils in

control mice decreased tumour growth, because neutrophils were no longer suppressing T cell activity against tumour cells. But in mice treated with TGF-β inhibitors, neutrophil depletion enhanced tumour growth, as these neutrophils were no longer present to kill cancer cells. This study therefore elegantly demonstrated how a single signal can polarize neutrophils and alter their functional phenotype. The authors of this study propose an "N1 vs N2" nomenclature for these neutrophil populations, resembling the M1/M2 nomenclature in the macrophage field, with the N1 population being the pro-inflammatory cytotoxic neutrophils, and N2 denoting the immunosuppressive neutrophils. However, these designations have been criticised on similar grounds to the M1/M2 macrophage nomenclature as being an oversimplification of neutrophil heterogeneity (Coffelt et al., 2016).

Another example involved human patients receiving G-CSF treatment. This caused an expansion of immature neutrophils in the circulation, these cells had less segmented, band cell-like nuclei than the mature neutrophils, which had fully segmented nuclei (see figure 1.2). Additionally, the study found these cells could be distinguished by their expression of CD10, with mature neutrophils positive for this marker. The mature neutrophils were found to have enhanced immunosuppressive properties compared to the immature population (Marini et al., 2017). This study illustrates that a systemic stimulus can induce immature neutrophils to depart the bone marrow before they are fully mature, and also showed phenotypic functional differences between mature and immature neutrophils in humans.

In summary, a number of characteristics have been used to define neutrophil heterogeneity, primarily surface marker expression and nuclear morphology. These characteristics broadly reflect different underlying functional phenotypes, that have consequences for how neutrophils influence a range of processes. The field is still in its infancy, and at this stage broad principles of neutrophil heterogeneity are still lacking, particularly surface marker expression patterns that could define neutrophil populations and relate to functional phenotypes. Furthermore, the precise transcriptional, epigenetic and protein-level programs underlying differences between neutrophil populations have yet to be fully elucidated, as do the complete range of signals that govern the formation of different neutrophil populations.

1.8 Neutrophils and cancer: a complex relationship

Historically, there has been limited examination of the potential roles of neutrophils in cancer, with immuno-oncology research generally focussed on T cells, macrophages and other immune cell types. But over the last two decades, mounting evidence, at both the clinical and basic science levels, has implicated neutrophils at all stages of carcinogenesis, from tumour initiation to metastasis. However, the precise roles that neutrophils play appear contradictory, with neutrophils able to bolster or hinder tumour progression, depending on the context (Fridlender et al., 2009). This further illustrates both the extensive plasticity of neutrophils and the complexity of neutrophil-tumour interactions, which still require extensive research to be fully dissected.

The short lifespan of neutrophils (see section 1.6) results in technical difficulties involved in performing experiments with these cells: it is extremely challenging to culture neutrophils *ex vivo* for longer than 3 days, additionally, they cannot be immortalised into a cell line and are extremely sensitive to activating signals *ex vivo* and *in vitro,* and even excessive mechanical manipulation can activate them. Consequently, much of the data on neutrophil involvement in cancer comes from animal models, although there have been a number of studies performed at the clinical level, predominantly using neutrophils isolated from the blood of cancer patients, though there are a number of studies using neutrophils isolated from patient tumours (Shaul and Fridlender, 2019).

Much of the data amassed at the clinical level is based on the neutrophil: lymphocyte ratio (NLR) in the blood. This is simply a measure of the neutrophil blood count relative to the lymphocyte blood count, but a higher NLR correlates strongly with poor prognosis; a recent meta-analysis of NLRs from 100 studies involving over 40,000 patients found that the NLR is a powerful indicator of negative prognostic outcomes in a range of solid tumour types (Templeton et al., 2014). These data have been interpreted as demonstrating that neutrophils support cancer progression (Coffelt et al., 2016), however it is not necessarily the case that neutrophils are the causative factor in poor prognostic outcomes arising from increased NLRs: lymphocytes can

of course have significant interactions with tumour cells and hence influence clinical outcomes: tumour-infiltrating lymphocytes (TILs) within a tumour correlate with positive prognostic outcomes in a range of solid tumours (Gooden et al., 2011). Importantly, the NLR is a ratio, and can thus be altered by changes in the levels of both neutrophils and lymphocytes. Differential NLRs could therefore reflect changes in blood lymphocyte levels which in turn could affect intratumoral lymphocyte levels, and thereby influence tumour progression. This is of course conjecture and has not yet been proven, however it illustrates that the correlation between a high NLR and negative prognosis has not yet been shown conclusively to be a causative relationship.

Focus on neutrophil counts specifically has revealed that neutrophil numbers increase in the circulation of cancer patients (Uribe-Querol and Rosales, 2015, Schmidt et al., 2005, Shaul and Fridlender, 2019), replicating findings from mouse models (Wculek and Malanchi, 2015, Coffelt et al., 2016, Coffelt et al., 2015). This is consistent with extensive evidence that tumours can boost granulopoiesis (Wu et al., 2014, Ueda et al., 2005).

Further complicating this picture is the fact that quantification of intratumoral neutrophils (also known as tumour-associated neutrophils, TANs) has much less consistent prognostic power: for example, in gastric carcinoma TANs correlate with positive outcomes (Caruso et al., 2002), but in renal carcinoma and melanoma TANs predict negative prognosis (Jensen et al., 2009, Jensen et al., 2012) and in lung cancer there is no correlation (Carus et al., 2013). However, a recent meta-analysis including almost 4000 patient samples from a range of solid cancers found a strong correlation between TANs and negative prognostic outcomes (Shen et al., 2014). Quantification of TANs relies on histological determination of nuclear morphology and the use of several different markers such as CD66b, CD15 and MPO. The complex inflammatory environment within a tumour may affect the nuclear morphology of neutrophils and their expression of these proteins, complicating quantification (Ng et al., 2019). The histological quantification can also be subject to bias and variability from experimental techniques and different experimenters, further contributing to the discrepancies in prognostic power of intratumoral neutrophils.

Several studies have investigated gene signatures within human tumours, and have found that enrichment of neutrophil-associated genes is correlated with poor prognosis (Blaisdell et al., 2015, Gentles et al., 2015). In particular, one study investigated gene signatures from over 18,000 human tumours across 39 different cancer types, and found that neutrophil gene signatures were the strongest predictors of poor prognosis out of all immune cell signatures (Gentles et al., 2015). This approach lacks the aforementioned drawbacks of histological quantification of intratumoral neutrophils, and is therefore more robust evidence that neutrophils contribute to cancer progression. These studies are perhaps the best evidence that neutrophils overall exert a negative effect on cancer prognosis in solid tumours.

Investigations at the clinical level have also used neutrophils obtained from cancer patients in *ex vivo* experiments, despite the technical difficulties involved, providing a closer look at neutrophil function within tumours in humans. In human colorectal cancer samples, IL-17 from $\gamma\delta$-T cells was found to induce migration of neutrophils into tumours. These neutrophils used ROS and arginase to inhibit proliferation of T cells, promoting tumour growth (Wu et al., 2014). Another study showed TANs using the same mechanisms to suppress T cells in ovarian cancer samples (Cui et al., 2013). In hepatocellular carcinoma, GM-CSF from tumour cells was shown to induce PD-L1 expression on TANs, which enhanced the ability of TANs to suppress activation and proliferation of $CD3^+$ T cells within the tumour (He et al., 2015). In another study of hepatocellular carcinoma, TANs released chemokines that attracted macrophages and regulatory T cells into the tumour microenvironment, where they respectively increased angiogenesis and suppressed T cell responses (Zhou et al., 2016). TANs can also enhance invasion and metastasis of hepatic cancer cells directly by secreting hepatocyte growth factor (He et al., 2016). This study replicated a previous finding that GM-CSF from tumour cells can attract neutrophils into the tumour microenvironment.

The above examples show a range of mechanisms by which TANs can promote tumour growth. However, two studies investigating TANs in early-stage lung cancer samples have found an anti-tumour effect of neutrophils in the tumour microenvironment. (Eruslanov et al., 2014, Singhal et al., 2016). These studies found that TANs from early lung tumour samples had a more pro-inflammatory phenotype

than circulating neutrophils, and were able to present antigen to T cells, initiating an anti-tumour response by the T cells. The TANs could also enhance the T cell response by cytokine release and expression of T cell-activating co-stimulatory molecules on their surface. This activity of TANs was dependent on Interferon-γ and GM-CSF within the tumour: tumour with low levels of these factors did not have TANs with antigen-presenting capabilities. A study using colorectal cancer patient samples also found TANs could enhance the activation and proliferation of $CD8^+$ T cells (Governa et al., 2017).

The above examples illustrate the range of mechanisms used by TANs to influence tumour processes in human patient samples. The majority of studies performed with TANs from patient samples have found a pro-tumour effect of these cells, consistent with correlative evidence linking high NLRs, TAN numbers and TAN gene signatures to poor prognostic outcomes (Shaul and Fridlender, 2019, Gentles et al., 2015, Templeton et al., 2014). However, several studies have found an anti-tumour effect for TANs, suggesting that the correlative findings may not apply to all tumour types and stages.

At the basic science level, a multitude of studies using mouse models of cancer to explore neutrophil behaviour have been published in the last decade. These studies provide the most detailed mechanistic evidence for neutrophil involvement in all tumour processes: neutrophils are able to interact directly with cancer cells, and can also influence other cells in the tumour microenvironment, principally immune cells, ultimately affecting tumour progression. These findings replicate and expand upon preliminary clinical studies using human samples. The majority of these reports demonstrate a pro-tumour role for neutrophils, however anti-tumour roles have also been established, mimicking the conflicting data at the clinical level (Mishalian et al., 2016).

Neutrophils have been found to promote tumorigenesis in a range of mouse model studies. Inflammation is an important factor in tumour initiation (Kundu and Surh, 2008), and given the centrality of neutrophils to inflammation is not unexpected that neutrophils may contribute to tumorigenesis in this manner. Mouse cancer models using chemical carcinogens to drive tumour initiation have shown roles for

neutrophils in the development of skin and colon cancer, with neutrophils invading inflamed regions before tumours are observed. CXCR2-deficient mice, in which neutrophils have impaired migration to sites of inflammation, have reduced tumorigenesis from chemical carcinogens (Katoh et al., 2013, Jamieson et al., 2012). A number of genetic models of lung cancer also involve neutrophil infiltration during tumorigenesis, and in these models depletion of neutrophils or inhibition of CXCR2 signalling both reduce tumour formation (Gong et al., 2013). Neutrophil elastase was found to be mechanistically involved in promoting lung tumorigenesis (Houghton et al., 2010), and other neutrophil factors such as ROS, proteases and immunosuppression are also believed to play a role (Coffelt et al., 2016).

Once tumours have formed, neutrophils can promote or hinder tumour growth and progression, depending on the context, although the majority of studies find that neutrophils boost tumour growth (Mishalian et al., 2016). Antibody-based depletion, genetic ablation of neutrophils and genetic inhibition of neutrophil migration have all been used to probe the effects of neutrophils on tumour growth. In pancreatic, ovarian, fibrosarcoma, lung and prostate cancer models, neutrophils boost cancer growth, principally through induction of angiogenesis by neutrophil-secreted matrix metalloprotease 9 (MMP9) (Charles et al., 2009, Tazzyman et al., 2011, Nozawa et al., 2006, Bekes et al., 2011). In these studies, depletion of neutrophils and inhibition of neutrophil migration led to reduced tumour growth. In another study, co-injection of neutrophils with lung carcinoma or colon carcinoma tumour cells boosted tumour growth and vascularization in an MMP9-dependent fashion (Yang et al., 2004). Neutrophils have other mechanisms by which they can boost tumour growth: in a model of prostate cancer, neutrophil release of interleukin-1 receptor agonist inhibited senescence of prostate cancer cells, enhancing proliferation and boosting tumour growth (Di Mitri et al., 2014), and neutrophil elastase can enhance lung tumour cell proliferation by degrading insulin receptor substrate 1 (Houghton et al., 2010). Finally, a well-documented method by which neutrophils can aid tumour growth is through the suppression of anti-tumour immune responses (Talmadge and Gabrilovich, 2013).

In contrast, there are studies finding that neutrophils inhibit tumour growth: in a melanoma model, neutrophils can enhance cytotoxic T cell activity against tumour

cells (Chang et al., 2016). Neutrophil secretion of hydrogen peroxide can induce cell death in breast and lung carcinoma models (Gershkovitz et al., 2019), and neutrophil secretion of inducible nitric oxide synthase, stimulated by tumour-necrosis factor alpha in the tumour microenvironment, produced nitric oxide which killed tumour cells and inhibited metastasis (Finisguerra et al., 2015).

Perhaps the most well established and important neutrophil function in tumours is the suppression of T cell activity, which can significantly enhance tumour survival and progression (Veglia et al., 2018). This has been extensively documented in both mice and humans and there is evidence this phenomenon can play a significant role in the outcome of a tumour. Significantly, immunosuppression by neutrophils may diminish the efficacy of therapies that enhance T cell-mediated destruction of tumour cells (Fleming et al., 2018).

There are a range of mechanisms that neutrophils use to suppress T cell responses in cancer (described in Section 1.4), including proteases, arginases, nitric oxide, ROS, PD-1 checkpoint blockade, secretion of prostaglandins, and recruitment of regulatory T cells (Kumar et al., 2016). The use of these different mechanisms is highly context-dependent, but their ultimate function is to inhibit the activation, proliferation, migration and cytotoxic function of T cells in the tumour microenvironment, all to the benefit of tumour cell survival.

The extensive suppressive capabilities of neutrophils have led to the designation of populations of neutrophils as myeloid-derived suppressor cells (MDSCs). This term has previously been used to encompass suppressive myeloid cells of both monocytic and granulocytic origin. To resolve this confusion a recent review proposed MDSCs of monocytic origin be designated M-MDSCs and those of granulocytic origin be designated PMN-MDSCs (polymorphonuclear-MDSCs) (Bronte et al., 2016a).

The term MDSC is controversial, and has been particularly criticized for describing a heterogeneous population of cells by a single function, thereby implying that these cells exist for this purpose alone, and cannot perform other activities (Shaul and Fridlender, 2019, Coffelt et al., 2016). This is in contrast to extensive evidence that neutrophils, and more broadly cells of granulocytic origin, are highly plastic, dynamic

cells able to perform numerous different functions in different contexts. In addition, recent findings demonstrating the heterogeneity of neutrophil populations suggest that there may be heterogeneity within PMN-MDSC populations, further diluting the utility of the term.

Finally, the differences between neutrophils and PMN-MDSCs are ill-defined; any neutrophil that has suppressive capabilities can be termed a PMN-MDSC, but it is unclear what value the MDSC designation adds beyond simply describing that cell as a “suppressive neutrophil.”

Further to this, there are currently no surface markers that differentiate neutrophils and PMN-MDSCs (Bronte et al., 2016a). It has been argued that MDSC represent a more immature population of neutrophils, and can therefore be distinguished upon this basis (Mazzoni et al., 2002). However, mature neutrophils can also have immunosuppressive abilities: in a recent study in humans mature neutrophils were shown to have greater immunosuppressive capacity than immature neutrophils from the same patient, therefore maturation state is insufficient for delineating PMN-MDSCs from neutrophils (Lang et al., 2018, Marini et al., 2017).

Neutrophils can also make significant contributions towards invasion and metastasis. MMP9 and other pro-angiogenic factors released by neutrophils can facilitate the migration of tumour cells from the tumour into the circulation (Bald et al., 2014, Coffelt et al., 2016). At sites of metastasis, neutrophils can aid cancer cells through a variety of mechanisms. In a model of breast cancer, tumour cells at sites of metastasis induced NET formation from local neutrophils (Park et al., 2016). These NETs boosted cancer cell growth, enhancing metastasis. Dnase I treatment, which destroys NETs, was found to decrease metastasis, as was genetic inhibition of neutrophil NET formation. This study also found NETs in primary tumours and lung metastatic lesions of breast cancer patients (Park et al., 2016), and another recent study found the same phenomenon in a colon cancer model (Al-Haidari et al., 2019).

Neutrophils can suppress T cell responses at sites of metastasis (Coffelt et al., 2015). This study importantly demonstrated a complex chain of signalling that resulted in neutrophil expansion and immunosuppression: tumour-associated macrophages in

mammary tumours secreted IL-1-ß, which stimulated IL-17 from gamma-delta T cells, boosting G-CSF expression (Section 1.5), resulting in increased neutrophil production from the bone marrow. This also converted neutrophils to a more immunosuppressive phenotype, allowing them to suppress $CD8^+$ T cells at sites of metastasis, allowing cancer cells to evade destruction, thereby aiding metastasis.

Previous work in the Malanchi laboratory examined the role of neutrophils in metastasis in a model of breast cancer (Wculek and Malanchi, 2015). This work used the mouse mammary tumour virus-polyoma middle T antigen (MMTV-PyMT) model of breast cancer (Guy et al., 1992). This model is a widely used and well characterized model in which mice spontaneously develop luminal mammary tumours with similar morphology and progression to that found in human breast cancers (Christenson et al., 2017, Lin et al., 2003). These tumours progressively lose oestrogen and progesterone receptor expression, and have low levels of erbB-2 (also known as HER2) expression. They also spontaneously metastasize to the lungs (Lin et al., 2003). In this model, it was found that lung neutrophils in tumour-bearing mice secrete leukotriene B4, which expanded the pool of metastasis-initiating tumour cells in the lungs, bolstering metastasis. Treatment with the drug Zileuton, which inhibits leukotriene B4 synthesis, significantly reduced metastasis, and this result was replicated with two other breast carcinoma cell lines. Genetic inhibition of neutrophil leukotriene B4 synthesis also reduced metastasis (Wculek and Malanchi, 2015). Importantly, the presence of a tumour induced extensive increases of neutrophils in the bone marrow, lungs and spleen before metastasis had begun to occur. Accumulation of neutrophils in the lungs preceded the arrival of metastasizing cancer cells, thus neutrophils aided in the generation of what is termed the pre-metastatic niche. This term describes the way in which sites of future metastasis are converted to a more favourable microenvironment for arriving metastatic cells, thereby enhancing the metastatic potential of these tumour cells (Sceneay et al., 2013). In this model, neutrophil-released leukotriene B4 was found to be critical for the generation of a favourable pre-metastatic niche.

Intriguingly, genetic and antibody-based depletion of neutrophils significantly reduced metastasis in this study, but had no effect on primary tumour growth, a finding that has been replicated in other breast tumour models (Coffelt et al., 2015,

Szczerba et al., 2019). This suggests neutrophil behaviour towards cancer cells is highly dependent on the microenvironmental context.

Neutrophils can also enhance the proliferation of circulating tumour cells, before they have begun to lodge and form a site of metastasis (Szczerba et al., 2019). This study found tumour cells bound to neutrophils in the circulation of tumour-bearing mice and breast cancer patients. The neutrophils increased cell cycle progression of the tumour cells, enhancing their metastatic potential.

As with other tumour processes, there is evidence that neutrophils can act in an anti-metastatic fashion: depletion of neutrophil results in reduced metastasis in renal carcinoma and breast cancer models (Granot et al., 2011, López-Lago et al., 2013). This was found to be mediated by hydrogen peroxide produced by neutrophils. In breast and prostate cancer models, neutrophil release of thrombospondin-1 inhibited metastasis in the lungs (Catena et al., 2013).

The above descriptions are not an exhaustive list of neutrophil-cancer interactions, but highlight a variety of neutrophil activities that can promote or hinder tumour cells, across all stages of cancer. These examples illustrate the vast range of mechanisms by which neutrophils can influence tumours, and demonstrate that neutrophils can promote or inhibit tumours depending on the context.

1.9 How tumours affect neutrophils

In the previous section I explored how neutrophils can interact with cancer cells, promoting or inhibiting tumour progression. In turn, tumours, and the immune and stromal cells within them, can manipulate neutrophils, enhancing granulopoiesis and affecting neutrophil heterogeneity, polarizing neutrophils into pro- and anti-tumour phenotypes.

It is well established that tumours can significantly perturb haematopoiesis, and more specifically granulopoiesis. In tumour-bearing mice and human cancer patients expansion of neutrophils in the circulation and peripheral tissues is observed in most types of cancer and tumour models (Coffelt et al., 2016, Shaul and Fridlender, 2019), and is a result of increased granulopoiesis and possibly also signals, such as G-CSF, that increase neutrophil lifespan (Ng et al., 2019). The increase in granulopoiesis is driven by signals, such as G-CSF and GM-CSF, that can be produced by tumour cells, immune cells and stromal cells (Coffelt et al., 2015, Morris et al., 2014). Higher levels of G-CSF and other factors such as CXCL1 and CXCL2, also affect the mechanisms that control neutrophil egress from the bone marrow. This results in the premature exit of immature neutrophils from the bone marrow, a process known as emergency granulopoiesis (Manz and Boettcher, 2014). In mouse models and cancer patients, immature neutrophils, defined principally by their less segmented nuclear morphology, have been found in the circulation (Sagiv et al., 2015, Ueda et al., 2005, Wu et al., 2014). For example, in mice the presence of a pancreatic carcinoma led to increased numbers of immature neutrophils in the circulation, these neutrophils had distinct gene expression signatures from mature neutrophils, suggesting they may have different interactions with tumour cells (Evrard et al., 2018). A study in humans found that G-CSF treatment resulted in the appearance of immature neutrophils in the circulation. This population had decreased immunosuppressive capacity compared to mature neutrophils (Marini et al., 2017). Thus, the presence of a tumour can increase neutrophil production from the bone marrow and also potentially alter the phenotypes of the neutrophils exiting the bone marrow (Mackey et al., 2019).

Tumours can also alter the phenotypes of neutrophils in the circulation, periphery and tumour microenvironment. In a mouse model of lung cancer, tumours perturbed the bone marrow niche, inducing the generation of a population of neutrophils expressing high levels of Siglec-F (typically used as a biomarker of eosinophils), which travelled to the lungs to promote tumour growth. This population was not present in control mice, and had extensive tumour-promoting abilities compared to Siglec-F^- neutrophils. Significantly, inhibiting the production of this population reduced lung tumour outgrowth (Engblom et al., 2017). This study demonstrated both the ability of tumours to affect neutrophils by modifying the bone marrow, and the ability of tumours to alter neutrophil heterogeneity. Another study found that IFN-γ and GM-CSF in the tumour microenvironment of human lung samples could polarize neutrophils into an anti-tumour phenotype, inducing them to present antigens to T cells and activate T cells against tumour cells (Singhal et al., 2016). In a study in mice TGF-β was shown to induce a switch in neutrophil phenotype, from pro-tumour to anti-tumour (Fridlender et al., 2009). Another mouse study found that G-CSF drove the production of immunosuppressive neutrophils in mice with breast tumours. These immunosuppressive neutrophils boosted lung metastasis by suppressing $CD8^+$ T cell activity against tumour cells (Coffelt et al., 2015).

As described in section 1.7, evidence from the literature suggests neutrophil heterogeneity is not a system of discrete subsets, but instead a system of polarization and activation of neutrophils, with neutrophils in different maturation states responding differently to polarization signals, further increasing heterogeneity. The above examples show that tumours can alter neutrophil heterogeneity, polarizing neutrophils into a particular phenotype, or inducing the production of different neutrophil populations, that can then participate in different interactions with tumour cells or other immune cells (Shaul and Fridlender, 2019, Ng et al., 2019).

1.10 Project aims

The study of neutrophil heterogeneity and cancer is still in its infancy, and much remains unclear. Many studies, at the clinical and basic level, have found differing roles for neutrophils, with both pro- and anti-tumour phenotypes observed. These results are likely a consequence of differing tumour types and stages that have been investigated but it is not yet established precisely how these differing contexts affect neutrophil heterogeneity and manipulate neutrophils into a particular pro- or anti-tumour phenotype.

Additionally, surface markers distinguishing neutrophil populations are poorly defined, in both health and cancer (Ng et al., 2019). Although one study in mice identified five neutrophil populations across several tissues, these populations were not further characterized, so it is unclear how different they may be as a result of their differential surface marker expression (Becher et al., 2014). We also do not know how these putative populations may be affected by the presence of a tumour.

A number of signals that induce switches in neutrophil phenotype have been discovered, for example TGF-β (Fridlender et al., 2009), but it is unlikely they are all accounted for. Investigations typically focus on either the bone marrow neutrophil pool or TANS in the tumour microenvironment, neglecting changes in circulating neutrophils, and the pools of neutrophils within tissues. The latter populations may be particularly important in metastasis, with several studies finding a role for lung neutrophils in this process (Wculek and Malanchi, 2015, Coffelt et al., 2015). Circulating neutrophils may also be consequential, as they will supply neutrophils to the tumour and to tissues where metastasis may be occurring. Investigating systemic changes in neutrophils during cancer may therefore offer new insights into how neutrophil heterogeneity and cancer interact with each other.

Previous work in the Malanchi laboratory has demonstrated that in the MMTV-PyMT mouse model of breast cancer neutrophils aid the metastasis of breast cancer cells to the lungs (described in section 1.8) (Wculek and Malanchi, 2015). In this work, the authors also characterized lung neutrophil dynamics and phenotype during cancer

progression in this model: neutrophil numbers in the lungs increase consistently with time following tumour induction (Figure 1.3a,b). Cancer cells enter the lungs approximately four weeks after tumour induction, and increase in number until the beginning of metastatic outgrowth, approximately six weeks following tumour induction (Figure 1.3b). Characterization of lung neutrophils in the pre-metastatic lung revealed minor changes in the lung neutrophil compartment compared to control lungs (Figure 1.3c). Although only a limited number of markers were used in this analysis, and the changes it found were small, it did suggest that the presence of a tumour can alter the lung neutrophil compartment.

In summary, preliminary results from previous work in the Malanchi laboratory suggest that lung neutrophil phenotype may be affected by cancer cells. More broadly, there is evidence that tumours can alter neutrophil heterogeneity but the precise nature of these alterations remains unclear, as do the mechanisms underlying tumour-induced changes in neutrophil heterogeneity. Finally, how different neutrophil populations might affect tumour processes is an open area of investigation.

Based on findings from the Malanchi laboratory, and the wider literature, I hypothesize that there may be different populations of neutrophils, across and within tissues, that differ in their functional phenotypes and their interactions with tumour cells. I hypothesize further that the presence of a tumour can perturb these populations, altering their relative proportions and functional phenotypes, with potential consequences for neutrophil-tumour interactions.

I therefore wanted to characterize systemic changes in the heterogeneity of neutrophil populations induced by tumours, investigating not just the lungs but other tissues, in order to generate a broader picture of how a tumour can perturb neutrophil phenotypes. I then wanted to understand the functional consequences these alterations might have for neutrophil-tumour interactions.

Therefore, the aims for my experimental investigations in this thesis were:

- **To investigate neutrophil heterogeneity across tissues**
- **To determine how the presence of a tumour perturbs this heterogeneity**
- **To investigate the functional consequences of neutrophil heterogeneity for tumour cells**

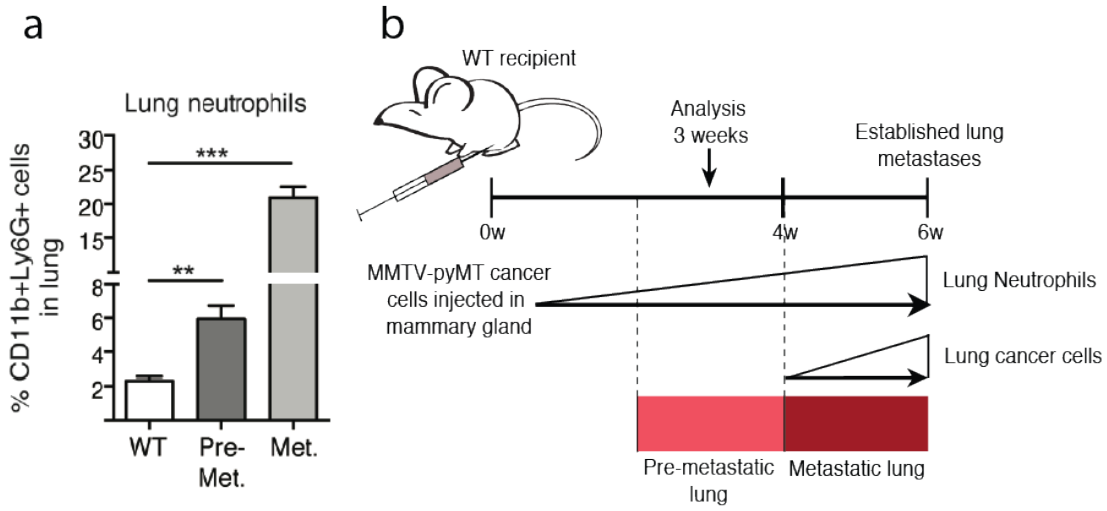

c Characterization of neutrophils accumulating in the pre-metastatic lung

Analysis of neutrophils in the lung				
	Wildtype	Pre-metastatic		
Cytometric analysis:	Mean intensity of CD11b+ Ly6G+		Significance	
Cell size (FSC)	84295 ± 199.0	87223 ± 628.1	N=4, P=0.0044	**
Cell granularity (SSC)	54932 ± 1467	62774 ± 2020	N=4, P=0.0200	*
Surface expression:	Percent positive of CD11b+ Ly6G+			
CXCR2+	97.90 ± 0.524	98.45 ± 0.150	N=4, P=0.3522	
CD31+	31.58 ± 3.728	49.45 ± 1.900	N=4, P=0.0053	**
MHC-I+	30.60 ± 1.696	28.77 ± 2.381	N=4, P=0.5533	
MHC-II+	28.18 ± 0.820	22.82 ± 1.415	N=4, P=0.0170	*
ICAM1+	23.90 ± 2.515	24.20 ± 1.119	N≥3, P=0.9008	
Fas+	99.35 ± 0.050	99.50 ± 0.058	N≥2, P=0.1697	
mRNA expression:	Change relative to wildtype		Neutrophil purity ≥ 90%	
TNFα	1	0.9585 ± 0.1735	P=0.8334	
Arginase 1	1	0.7667 ± 0.1924	P=0.3492	
VEGF-A	1	0.6814 ± 0.1494	P=0.1666	
CCL2	1	0.4157 ± 0.0932	P=0.0245	*
CCL3	1	0.7391 ± 0.1584	P=0.2414	
iNOS	1	1.0360 ± 0.4653	P=0.9506	
CCL5	1	0.0517 ± 0.0042	P<0.0001	***

Figure 1.3 Characterization of lung neutrophil dynamics and phenotype in the MMTV-PyMT mouse model of breast cancer

(**a**) Flow cytometric quantification of lung neutrophils from wild-type (WT) or MMTV-PyMT tumour-bearing mice, at either pre-metastatic (Pre-Met.) or metastatic (Met.) stages. n = 5 (WT), n = 4 (Pre-Met., Met.). Data are shown as mean ± standard error of the mean (s.e.m.). (**b**) Representation of timing and dynamics of neutrophil and cancer cell infiltration into the lung of mice grafted with two mammary tumours by orthotopic injection of 10^6 MMTV-PyMT tumour cells. (**c**) Flow cytometric analysis for cell size (forward scatter (FSC)), granularity (side scatter (SSC)) and expression of surface markers CXCR2, CD31, MHC-I, MHC-II, ICAM1 and Fas (*n* is indicated) as well as mRNA expression analysis of *Tnfa*, arginase1,*Vegfa*, *Ccl2*, *Ccl3*, *iNOS* (also known as*Nos2*) and *Ccl5* by quantitative polymerase chain reaction (PCR) of $CD11b^+Ly6g^+$wild-type (WT) or pre-metastatic (Pre-met.) lung neutrophils 3 weeks after primary tumour graft ($n = 3$ (pre-metastatic compared with one normal lung reference)). Statistical analysis by two-sided *t*-test (flow cytometry) and one-sample *t*-test (mRNA). Data are represented as mean ± s.e.m. $^*P < 0.05$, $^{**}P < 0.01$, $^{***}P < 0.001$.

Chapter 2. Materials & Methods

2.1 Media components for *in vitro* experiments

- Dulbecco's Modified Eagle Medium/Nutrient Mixture F-12 (DMEM-F-12) (Thermo Fisher Scientific, 11330-032)
- Dulbecco's Modified Eagle Medium (DMEM), high glucose (Thermo Fisher Scientific, 41965-039)
- Roswell Park Memorial Institute (RPMI) 1640 (Thermo Fisher Scientific, 21875-034)
- Foetal Calf Serum (FCS) (Labtech, FB-1001-/500)
- Bovine Serum Albumin (BSA) (Sigma Aldrich, A7906)
- Penicillin/Streptomycin (P/S) (Thermo Fisher Scientific 15140-122)
- HEPES (Thermo Fisher Scientific, 15630-080)
- Insulin solution human (Sigma Aldrich, 19278)
- Epidermal Growth Factor (EGF) Recombinant Human Protein (Thermo Fisher Scientific PHG0311)
- Glutamax (Thermo Fisher Scientific, 35050-038)
- PureCol® Bovine Type 1 Atelo-Collagen Solution (Advanced BioMatrix, #5005-100ml)
- 2-mercaptoethanol (Thermo Fisher Scientific, 21985-023)
- 0.25% Trypsin (Thermo Fisher Scientific 25050-014)
- Hank's Balanced Salt Solution (HBSS), no calcium, no magnesium, no phenol red (Thermo Fisher Scientific, 14175-053)

2.2 Complete media for *in vitro* culture

- MMTV-PyMT and MMTV-PyMT GFP$^+$ primary cells
  - DMEM/F12, 2% FCS, 100U/ml P/S, 20ng/ml EGF, 10µg/ml insulin solution
  - These cells were cultured on plates coated with collagen. Collagen coating solution (HBSS, 100µg/ml BSA, 20mM HEPES, 30µg/ml PureCol®) was pipetted on to plates, immediately aspirated, and then plates incubated for at least 15 minutes at 37^{o}C before cells were plated.
- 4T1, RENCA and B16 cells
  - DMEM high glucose, 10% FCS, 100U/ml P/S
- E0771 cells
  - DMEM high glucose, 10% FCS, 100U/ml P/S, 20mM HEPES
- Conventional T cells (freshly isolated from mouse spleen)
  - RPMI 1640, 10% FCS, 50µM 2-mercaptoethanol, 5mM HEPES

All cells were cultured in incubators maintained at 37^{o}C and 5% CO2.

2.3 Primary cells and cell lines

MMTV-PyMT and MMTV-PyMT GFP$^+$ tumour primary cells were obtained from tumours from transgenic mice. Tumours were dissected, minced manually and digested for 60 minutes at 37^{o}C in a shaker in HBSS with Liberase Tm, Liberase Th (Roche, 5401127001 and 5401151001 respectively) and DNaseI (Sigma-Aldrich (D4527) and then mashed through a 100µm cell strainer. Cells were washed once with DMEM-F12 10% FCS, then twice with HBSS before being plated and cultured overnight in complete media on collagen-coated plates. Cells were detached using treatment with 1mM EDTA in PBS for eight minutes, followed by treatment with 0.25% trypsin for five minutes, which was quenched with 10% FCS in DMEM-F12. Cells were washed once with complete media then frozen at -160^{o}C until thawing before use *in vitro* and *in vivo*.

4T1, RENCA, E0771 and B16 cell lines were obtained from the Cell Services platform at the Francis Crick Institute. Cells were grown in culture for up to seven days before detachment as described above and transplantation into mice.

The 4T1 cell line is a breast cancer cell line isolated from the mammary tumour of a BALB/CJ mouse (Pulaski and Ostrand-Rosenberg, 2000). The RENCA cell line is a renal cancer cell line isolated from a renal adenocarcinoma in a BALB/CJ mouse (Murphy and Hrushesky, 1973). The E0771 cell line is a breast cancer cell line isolated from the mammary tumour of a C57BL/6 mouse (Casey et al., 1951). The B16 cell line is a melanoma cancer cell line isolated from melanoma on a C57BL/6 mouse (Overwijk and Restifo, 2001).

2.4 Mouse strains and breeding

Wildtype mice of pure FvB/NJ, C57BL/6 and BALB/Cj background (more than 10 generations) were used for all experiments except those using transgenic mice. MMTV-PyMT, MMTV-PyMT Actin-GFP and Rag1 KO transgenic mice were all used on a pure FvB/NJ background (more than 10 generations). MMTV-PyMT mice were also used on a pure C57BL/6 background. LSL-Kras$^{G12D/+}$;LSL-Trp53$^{R172H/+}$;Pdx-1-Cre transgenic mice were used on a C57/BL6 background (Lee et al., 2016). B1-8$^{flox/flox}$ Igκ-$^{Ctm1Cgn/tm1Cgn}$ BCR-restricted transgenic mice were used on a pure C57/BL/6 background (Nowosad et al., 2016, Zou et al., 1993, Sonoda et al., 1997).

All mouse lines (wildtype and transgenic) were bred and maintained under specific-pathogen-free conditions by The Francis Crick Institute Biological Research Facility. Mice were used between 6 and 12 weeks of age. Breeding and all animal procedures were performed at the Francis Crick Institute in accordance with UK Home Office regulations under project license P83B37B3C.

2.5 Mouse experiments

For tumour cell transplantations, mice were anaesthetised with IsoFlo® (Isoflurane, Abbott Laboratories 0044-5260-05).

Female FvB/NJ, C57BL/6 and Rag1 KO mice were used for MMTV-PyMT tumour cell transplantations. Thawed MMTV-PyMT cells were cultured overnight in complete media on collagen coated plates (section 2.2). Cells were detached as described previously (section 2.3), washed once with PBS, counted, and $5x10^5$ primary MMTV-PyMT cells were resuspended in 50µl of growth factor-reduced Matrigel (Costar, 356231) and transplanted by injection into the fourth mammary fat pad on one flank (or both flanks where indicated in the Results section).

Female BALB/CJ mice were used for 4T1 and RENCA tumour cell transplantations. $2x10^5$ 4T1 cells were resuspended in 50µl of PBS and transplanted by injection into the fourth mammary fat pad on one flank. $5x10^5$ RENCA cells were resuspended in 50µl of growth factor-reduced Matrigel and injected subcutaneously into the right flank.

Female C57/BL6 mice were used for E0771 and B16 tumour cell transplantations. $5x10^5$ E0771 cells were resuspended in 50µl of growth factor-reduced Matrigel and transplanted by injection into the fourth mammary fat pad on one flank. $2x10^5$ B16 cells were resuspended in 50µl of growth factor-reduced Matrigel and injected subcutaneously into the right flank.

2.6 Tissue digestion for cell isolation and analysis

Lungs were dissected, minced manually, and digested for 30 minutes at 37^{o}C in a shaker with Liberase Tm and Liberase Th (Roche, 5401127001 and 5401151001 respectively) and DNaseI (Sigma-Aldrich, D4527) in HBSS and then mashed through a 100µm cell strainer. Alternatively, where specified, lungs were dissected, minced manually and then digested using the Lung Dissociation Kit, mouse (Miltenyi 130-095-927) and gentleMACS Octo Dissociator (Miltenyi 130-096-427). Spleen and liver were dissected, minced manually and mashed through a 100µm and 70μm cell strainer successively. Bone marrow cells were isolated by crushing the femur and tibia in HBSS and passed through a 100µm cell strainer. Blood was obtained by cardiac puncture and washed once with HBSS.

Cell isolates from all tissues were next passed through a 20μm strainer to generate a single-cell suspension, and then subjected to hypotonic lysis (Red Blood Cell Lysis Solution, Miltenyi 130-094-183) for 10 minutes to remove erythrocytes, then washed with 1×PBS/2mM EDTA/0.5% BSA (MACS buffer).

2.7 Flow cytometry analysis and cell sorting

For extracellular staining, prepared single cell suspensions were resuspended at a concentration of 2 x 10^7 cells/ml in MACS buffer, and then incubated on ice for 10 minutes with 5% mouse FcR Blocking Reagent (Miltenyi). Cells were then incubated on ice for 20 minutes with specific pre-labelled antibodies (see Table 1 for antibody list and concentrations).

For intracellular staining, cells were first stained with LIVE/DEAD™ Fixable Blue Dead Cell Stain Kit (Thermo Fisher Scientific L34961) for 30 minutes on ice. Cells were then washed and fixed and permeabilized using eBioscience™ Foxp3/Transcription Factor Staining Buffer set (Thermo Fisher Scientific, 00-5523-00). Cells were washed and then stained with antibodies for 30 minutes at room temperature, washed and then acquired on a flow cytometer.

For extracellular staining, dead cells were stained with 4′,6-diamidino-2-phenylindole (DAPI, Sigma-Aldrich D9542). The LSR Fortessa cell analyser running FACSDiva software (BD Biosciences) was used to analyse cells and FlowJo software used for data analysis Gating strategy to identify live, single cells is displayed in Figure 2.1. For imaging flow cytometry, cells were analysed with the Imagestream®X Mark II (Luminex Corporation). Fluorescence activated cell sorting (FACS) was run on the Influx and Aria cell sorters running FACS Sortware sorter software and FACSDiva software respectively (BD Biosciences). To ensure accurate discrimination between positive and negative populations Fluorescence-Minus-One controls for all fluorophores were used in all flow cytometry analysis and sorting experiments.

When sorting neutrophil populations for NET-formation, Immunosuppression and 3D co-culture assays depletion of T and B cell populations was performed prior to sorting to enrich neutrophils and increase the yield from sorting. T and B cells were stained, as described above, with CD3, CD19 and B220 antibodies, all conjugated to the fluorophore APC. EasySep^{TM} Mouse APC Positive Selection Kit (Stem Cell Technologies 18452) was used to deplete APC^{+} cells per the manufacturer's instructions. Briefly, cells were incubated with EasySep^{TM} APC Selection cocktail at room temperature for 15 minutes, then magnetic beads were added and cells incubated for a further 10 minutes. Cells were then incubated in magnets for 5 minutes and the supernatant containing APC^{-} cells was then taken for sorting.

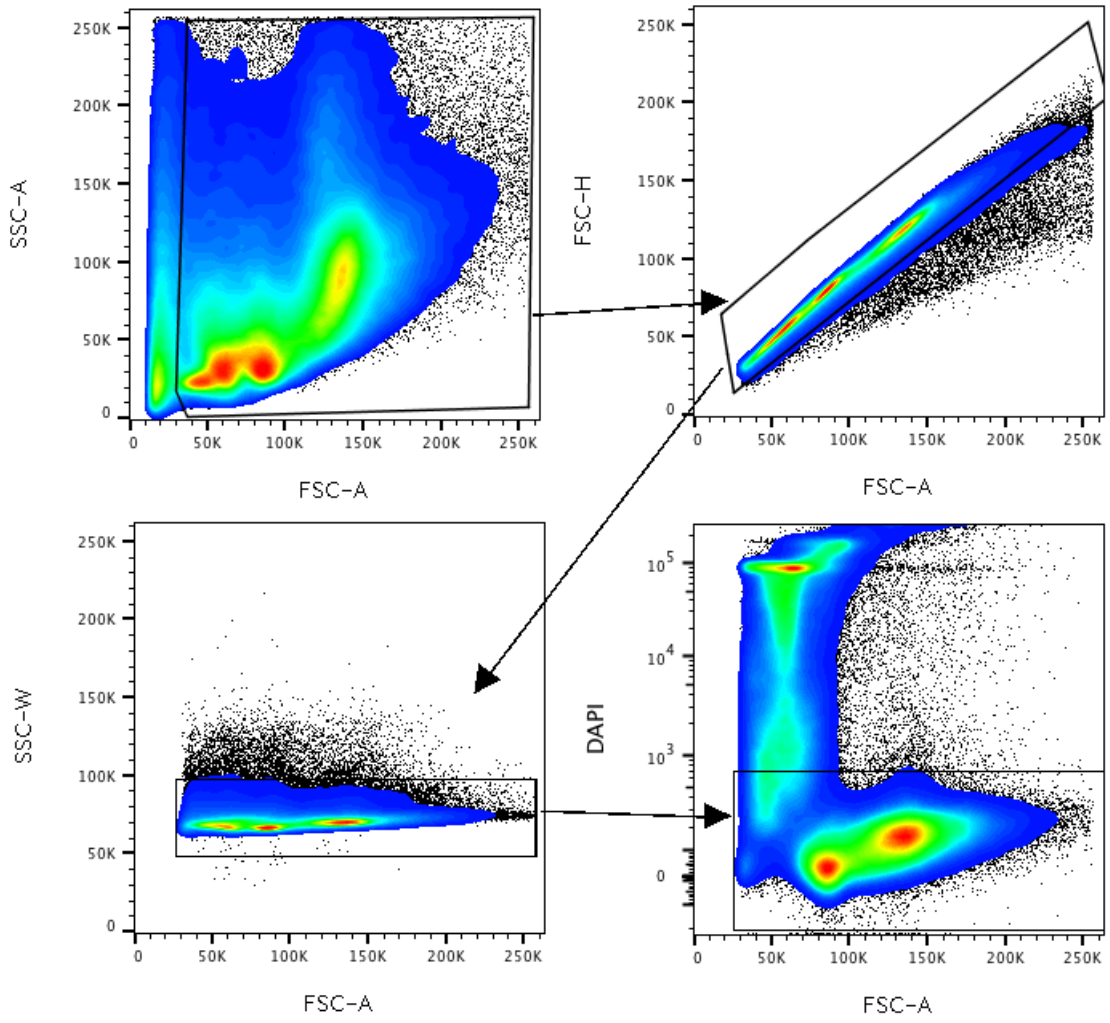

Figure 2.1 Gating strategy for flow cytometry

Flow cytometry plots displaying the gating strategy used to select live singlet cells in all flow cytometry experiments. Debris was excluded by Forward scatter (FSC)- and Side scatter (SSC) -area. Doublets are next excluded by FSC-height and FSC-Area, and remaining doublets removed by SSC-width and FSC-area. Finally, $DAPI^-$ alive cells are selected. Sample used is bone marrow cells from a control FvB/NJ mouse.

Antibody	Clone	Manufacturer	Concentration/ $2x10^6$ cells	Fluorophores
Ly6G	1A8	Biolegend/eBioscience	100ng	BV421, BV510, BV605, FITC, APC, PE, PE-Cy7, APC-Cy7
CD11b	M1/70	BioLegend	100ng	APC, BV421, FITC, APC-Cy7
CXCR2 (CD182)	SA04G44	BioLegend	100ng	FITC, PE
CXCR4 (CD184)	2B11	BD Biosciences	200ng	BV421
CD62L	MEL-14	BioLegend	100ng	BV421, APC, PE-Cy7
MHC-II	M5/114.15.2	BioLegend	50ng	FITC, APC-Cy7
F4/80	BM8	BioLegend	200ng	BV421, APC, PE
Siglec-F	E50-2440	BD Biosciences	200ng	PE
CD115	AFS98	BioLegend	200ng	PE
C-Kit	2B8	BioLegend	100ng	PE-Cy7
CD34	RAM34	eBioscience	200ng	FITC
Lineage	17A2/RB6-8C5/RA3-6B2/Ter-119/M1/70	BioLegend	50ng	BV421
Sca-1	D7	BioLegend	100ng	APC
CD16/32	2.4G2	BD Biosciences	100ng	APC-Cy7
Ki67	B56	BD Biosciences	200ng	PE
CD3	17A2	BioLegend	100ng	FITC, APC, PE
CD19	eBio1D3	eBioscience	100ng	FITC, APC, PE
B220	RA3-6B2	eBioscience	100ng	BV510, FITC, APC
IgM	11/41	Invitrogen	100ng	APC
IgD	11-26c.2a	BioLegend	100ng	PerCP-Cy5.5
CD4	GK1.5	BioLegend	100ng	FITC
CD25	PC61	Biolegend	100ng	APC
CD21	7E9	BioLegend	100ng	BV421
CD23	B3B4	BioLegend	100ng	PE

Table 1 Flow Cytometry Antibodies

Table displays antibodies used in flow cytometry experiments in this thesis, including clones, manufacturers, the concentration of antibody used in staining per $2x10^6$ cells and the fluorophores conjugated to these antibodies.

2.8 Mass cytometry analysis

Single cell suspensions of mouse tissues were generated as described in section 2.6. For live/dead discrimination cells were stained with cisplatin (25μM in PBS) for 1 minute, before quenching with 10% FCS. Next, cells were stained, as described in section 2.7, with mouse FcR Blocking Reagent (Miltenyi) followed by metal-conjugated antibodies (obtained from either Fluidigm or labelled by the Flow Cytometry Facility at Guy's Hospital, London, see Table 2 for further details). Cells were then fixed in 2% paraformaldehyde for 12 hours, washed once with 1×PBS/2mM EDTA/0.5% BSA, stained with an Iridium DNA stain (Flow Cytometry Platform at Guy's and St Thomas' Biomedical Research Centre, London) for 30 minutes and then washed twice with ddH20. Cells were resuspended in ddH20 with equilibration beads spiked into each sample for signal normalization. Samples were run on a Helios mass cytometer (Fluidigm) and data analysed by FlowJo software. The gating strategy used to identify live singlet cells is shown in Figure 2.2. Live singlet cells were selected and exported into Cytobank and Phenograph software for bioinformatics analysis. For analysis, $Ly6g^+$ cell events were evenly sampled from the tissue live cell events from 8-10 mice per condition. For the spleen, 15,000 $Ly6g^+$ cell events were sampled, for the lungs 30,000, and for the bone marrow 67,000.

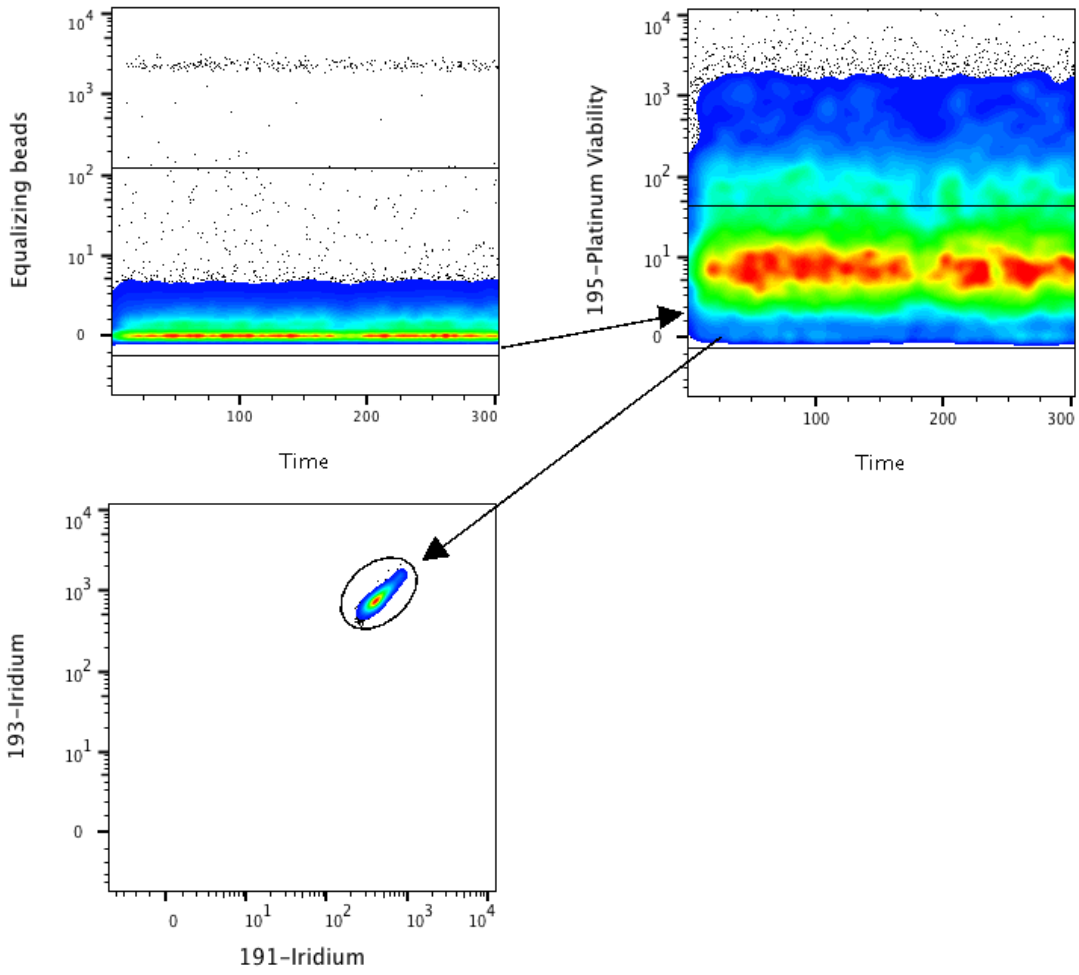

Figure 2.2 Gating strategy for mass cytometry

Cytometry plots displaying the gating strategy used to select live singlet cells in all mass cytometry experiments Non-bead cell events are first selected. Live, cisplatin$^-$ cells are then gated. Finally, Iridium$^+$ cell events are selected. Sample used is lung cells from a control FvB/NJ mice.

Antibody	Clone	Manufacturer	Concentration/ 2x106 cells	Conjugate
CD45	30-F11	Fluidigm	50ng	89 Y
Ly6G	1A8	Fluidigm	100ng	141 Pr
CD11c	N418	Fluidigm	100ng	142 Nd
CD115	AFS98	Fluidigm	200ng	144 Nd
CD16/32	93	Fluidigm	100ng	153 Eu
F4/80	BM8	Fluidigm	200ng	146 Nd
CD24	M1/69	BioLegend	100ng	160 Gd
Ly6C	HK1.4	Fluidigm	100ng	162 Dy
CD25	3C7	Fluidigm	100ng	150 Nd
CD64	X54-5/7.1	Fluidigm	100ng	151 Eu
CD48	HM48-1	Fluidigm	100ng	154 Sm
CD54	YN1/1.7.4	Fluidigm	100ng	163 Dy
CD38	90	Fluidigm	100ng	171 Yb
CD11b	M1/70	Fluidigm	100ng	148 Nd
CD86	GL1	Fluidigm	100ng	172 Yb
MHCII	M5/114.15.2	Fluidigm	50ng	174 Yb
FcEr1	MAR-1	Fluidigm	100ng	176 Yb
CD31	390	Fluidigm	100ng	165 Ho
CD62L	MEL-14	Fluidigm	100ng	164 Dy
PDL2 (CD273)	TY25	BioLegend	100ng	169 Tb
PDL1 (CD274)	10F.9G2	BioLegend	100ng	159 Tb
CCR5 (CD195)	HM-CCR5	Novus Biologicals	200ng	166 Er
CXCR4 (CD184)	2B11	eBioscience	200ng	168 Er
CXCR2 (CD182)	SA044G4	BioLegend	100ng	156 Gd
CD3	145-2C11	Fluidigm	100ng	152 Sm

Table 2 Mass cytometry antibodies

Table displays antibodies used in mass cytometry experiments in this thesis, including clones, manufacturers, the concentration of antibody used in staining per $2x10^6$ cells and the fluorophores conjugated to these antibodies. Antibodies acquired from Fluidigm were obtained already conjugated by the manufacturer, all other antibodies were conjugated by the Flow Cytometry Platform at Guy's and St Thomas' Biomedical Research Centre, London, after purchase from the listed manufacturer. Y, Yttrium, Pr, Praseodymium, Nd, Neodymium, Eu, Europium, Gd, Gadolinium, Dy, Dysprosium, Sm, Samarium, Yb, Ytterbium, Ho. Holmium, Tb, Terbium, Er, Erbium.

2.9 *In vitro* 3D scaffold co-culture

Thawed primary MMTV-PyMT GFP$^+$ cells were cultured overnight on collagen-coated dishes in complete media, detached and washed once with complete media (as described in section 2.5).

Alvetex scaffold 96-well plates (Reprocell, AVP009-2) were activated, per the manufacturer's instruction, with 200µl 70% ethanol, followed by three washes with 200µl PBS. Collagen coating solution (35µl, section 2.2) was then added directly onto the scaffold and the plate incubated for 1 hour at room temperature. Following aspiration of the collagen solution 5x10^3 GFP$^+$ PyMT cells were added onto the scaffold in a volume of 50µl. Plates were then incubated at 37^{o}C and 5% CO2 for 24 hours. Neutrophils populations were purified by FACS (section 2.7). FACS-purified neutrophils were washed once with media and then 1x10^5 neutrophils were added to the scaffold, to a final volume of 100µl. Images of wells were acquired with a Stereo Lumar.V12 stereomicroscope (Zeiss) 1 day and 6 days after neutrophils were added. GFP integrated density was quantified using ImageJ software.

2.10 *In vitro* immunosuppression assay

Conventional T cells (T_{conv}), regulatory T cells and neutrophil populations were purified from spleens of control and tumour-bearing mice using FACS (section 2.7). T_{conv} were washed once with media, then resuspended at a concentration of 1x10^6 cells per millilitre in PBS with 5µM Cell Trace Violet (Thermo Fisher Scientific, C34571), and incubated for 20 minutes at 37^{o}C. T_{conv} were washed twice with media and plated into U-bottom 96 well plates, then stimulated with anti-CD3/CD28 beads (Thermo Fisher Scientific, 11452D), per the manufacturer's instructions at a bead: cell ratio of 1:1. Neutrophils or T_{regs} were next added to the T_{conv} wells at T_{conv}: neutrophil/T_{reg} ratios of 1:1, 1:2 and 1:4, to a final volume of 100µl. Cells were then incubated for 72 hours and T_{conv} proliferation determined by flow cytometry.

2.11 Analysis of reactive oxygen species levels

Single-cell suspensions of cells were generated from blood, spleen and bone marrow, and, after FcR blocking, stained with antibodies (section 2.6, 2.7). Cells were then washed once and then incubated in MACS buffer with 5μM CellROX® Deep Red reagent (Thermo Fisher Scientific C10422) for 30 minutes at 37^{o}C. Cells were next washed twice with 1×PBS/2mM EDTA/0.5% BSA before analysis by flow cytometry.

2.12 Neutrophil extracellular trap formation

FACS-purified neutrophils were washed once with MACS buffer and then resuspended in HBSS with either 2.5% FCS or 2.5% mouse serum. Neutrophils were plated onto lysine-coated 24-well plates and allowed to settle for 30 minutes at 37^{o}C. Next, neutrophils were stimulated with 100nM phorbol 12-myristate 13-acetate (PMA, Sigma Aldrich, P1585) for 16 hours and then fixed with 2% paraformaldehyde. Sytox® Green (1μM, Invitrogen S7020) and Hoechst 3342 (1μgml, Invitrogen H3570) were added to visualize DNA, images acquired with a Leica DM IRB (Leica Camera AG) and analysed with ImageJ software.

2.13 Nuclear morphology analysis

Cells were purified using FACS (section 2.7). Purified cells were washed once with MACS buffer, then resuspended in PBS. 5x10^{4} cells in 50μl PBS were centrifuged (7 minutes at 800rpm) on to poly-lysine-coated slides (Thermo Fisher Scientific, P4981) using a Cytospin 3 (Thermo Shandon). Cells were fixed in 100% methanol at -20 ^{o}C for 5 minutes, washed once with PBS, then stained with Wright-Giemsa stain (VWR Chemicals, 352603R) for 30 minutes. Slides were then washed 3 times with ddH20 before mounting. Images were acquired on an Observer Z.1 (Zeiss) and analysed using ImageJ software. A minimum of 120 cells from images from each slide were classified as banded, segmented or hypersegmented. Then the number of cells in

each classification was converted to a percentage of the total counted cells from that slide.

2.14 Kinase activity assay

Neutrophils were purified by FACS (section 2.7) and washed with 1xPBS. Cells were resuspended in M-PER™ Mammalian Protein Extraction Reagent (Thermo Fisher Scientific, 78501) with Halt™ Protease and Phosphatase inhibitors (Thermo Fisher Scientific, 1861278 and 78428 respectively). Cells were lysed on ice for 30 minutes with mixing every five minutes, then centrifuged for 10 minutes at 15,000 rpm to pellet debris. Supernatant was snap frozen and stored at -80^{o}C until use. Protein concentration was determined using a BCA assay (Thermo Fisher Scientific, 23225). For each sample, 5µg of protein lysate was loaded onto a phosphotyrosine kinase PamChip® (Pamgene 86402) and the chip run on a Pamstation®12 (Pamgene). A table of all kinase target peptide sequences used in the phosphotyrosine kinase chip assay can be found in the Appendix. Kinase activity data was analysed using ClustVis (Metsalu and Vilo, 2015)

Chapter 3. High-dimensional analysis reveals neutrophil heterogeneity in control and tumour-bearing mice

3.1 Chapter Aims

- **Use mass cytometry to investigate mouse neutrophil heterogeneity across different tissues**
- **To determine how the presence of a mammary tumour impacts upon this heterogeneity**

3.2 PyMT breast tumours induce expansion of neutrophils in the bone marrow, circulation and periphery.

Before investigating neutrophil heterogeneity, it was necessary to confirm previous results from the Malanchi laboratory, which found increases in neutrophils in the lungs and other tissues in mice with MMTV-PyMT breast tumours (section 1.8, 1.10) (Wculek and Malanchi, 2015). This expansion of neutrophils has also been observed in other mouse tumour models in the literature (Section 1.9) (Coffelt et al., 2015, Coffelt et al., 2016) . I find that neutrophil numbers increase in the bone marrow, blood, lungs, liver and spleen of MMTV-PyMT tumour-bearing mice (Figure 3.1). Consistent with previous results, I also find that the size and stage of a tumour affects the increase in neutrophils with larger, later stage, metastatic tumours showing a greater expansion of neutrophils (see Section 4.6 and Figure 4.8). Unless otherwise stated, this is the case for all experimental results involving MMTV-PyMT tumour-bearing mice, including mass cytometry experiments.

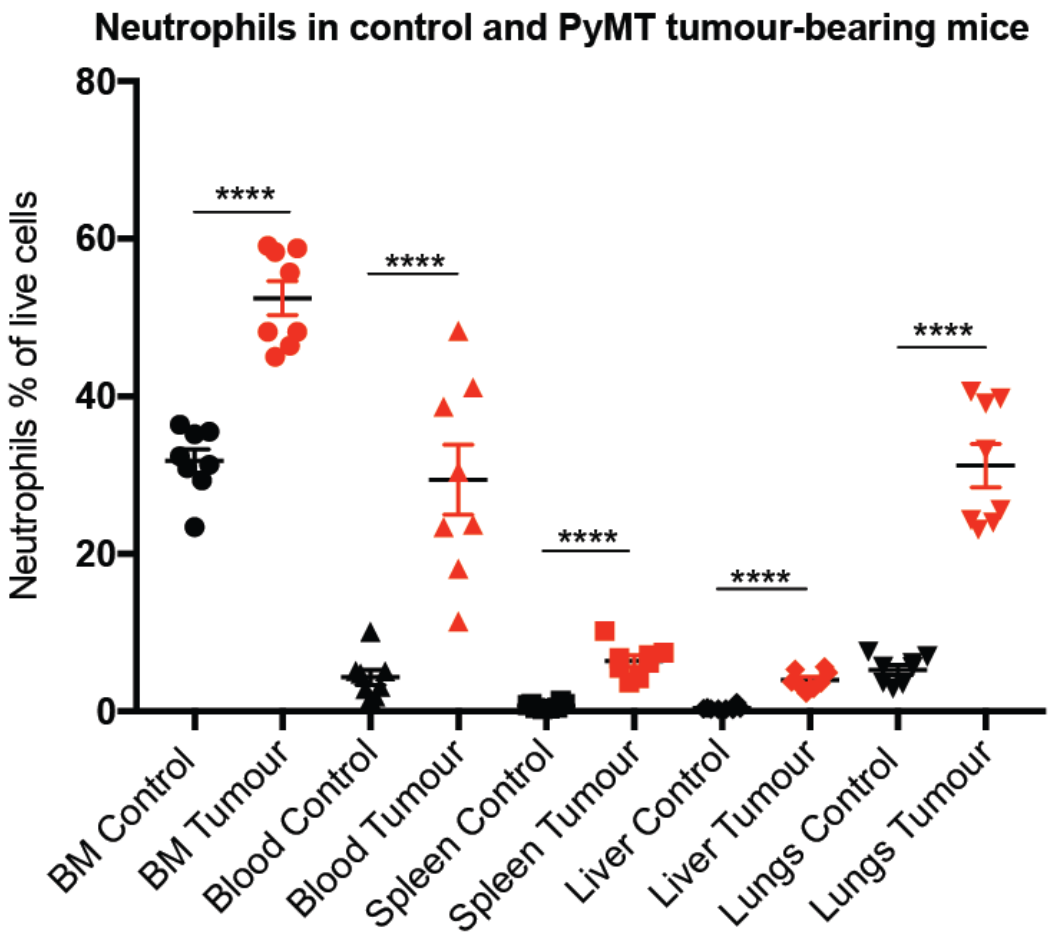

Figure 3.1 Neutrophils increase across tissues in tumour-bearing mice

Flow cytometric analysis of $Ly6g^{+}$ $CD11b^{+}$ neutrophils in bone marrow (BM), blood, spleen, liver and lungs of control and tumour-bearing (Tumour) mice. Female FvB/NJ mice were orthotopically injected with PyMT cells into the mammary fat pad and tumours grown for 3.5 weeks before analysis by flow cytometry, with age-matched naïve female FvB/NJ mice used as controls. Neutrophils were analysed as a percentage of live single cells in the tissue. n=8 mice per group. Data are displayed as mean ± standard deviation (SD). Statistical analysis by two-sided t-test. **** $P < 0.0001$.

3.3 High-dimensional analysis reveals neutrophil heterogeneity in surface marker expression

Analysis of cell surface marker expression is used extensively in immunology, and other fields, to define and characterize heterogeneous populations of cells. It therefore represents an attractive experimental method for investigating neutrophil heterogeneity. A recent novel technique for investigating surface marker expression at a high dimensional level is mass cytometry (Spitzer and Nolan, 2016). This technique is based on traditional fluorescence-based flow cytometry, but uses antibodies conjugated to heavy metal ions, which are then detected with a mass spectrometer. There is minimal spectral overlap between heavy metal ions when analysed by this method, allowing up to 40 different parameters to be used simultaneously. Mass cytometry thus allows high-dimensional, single cell analysis of surface marker expression, making it ideally suited for interrogating neutrophil heterogeneity.

In order to determine what effects a tumour might have on neutrophil heterogeneity I used the MMTV-PyMT mouse model of breast cancer (Guy et al., 1992): breast tumours can be induced by the injection of primary MMTV-PyMT cells in to the mammary fat pad of FvB/NJ mice (section 2.5). As described in section 1.8 and 1.10, previous work in the Malanchi laboratory suggested that in this model the presence of a breast tumour may locally affect lung neutrophil phenotypes. I wanted to extend this work, investigating how a tumour may perturb neutrophil heterogeneity more systemically.

If neutrophil heterogeneity is altered by the presence of a tumour, the stage of the tumour (and metastatic disease) may also impact the overall effect on heterogeneity. The MMTV-PyMT model offered two different time points for investigating how a tumour, and the stage of a tumour, might affect neutrophil heterogeneity:

1. The pre-metastatic stage, three weeks after tumour induction. At this stage neutrophil numbers have increased significantly in the lungs (Figure 3.2a, Figure 1.3), and neutrophils are contributing to the pre-metastatic niche, but cancer cells have not yet metastasised to the lungs.
2. The metastatic stage, six weeks after tumour induction. At this point neutrophil numbers have further increased to the extent that they represent almost 25% of cells in the lungs (Figure 3.2a, Figure 1.3) Cancer cells are present in the lungs, and metastatic outgrowth can be detected. The overall tumour burden is high at this time point.

Therefore, I designed a mass cytometry analysis to investigate neutrophil heterogeneity in three different conditions:

1. Control: naïve, unchallenged mice
2. Pre-metastatic: mice with one MMTV-PyMT breast tumour, 3-4 weeks post-injection
3. Metastatic: mice with two MMTV-PyMT breast tumours, 6 weeks post-injection (I used two tumours to enhance tumour burden and metastasis, with the intention of accentuating differences between metastatic and pre-metastatic conditions, to ensure that potential changes in neutrophil heterogeneity were more readily detectable)

(Figure 3.2a shows the time points for each condition)

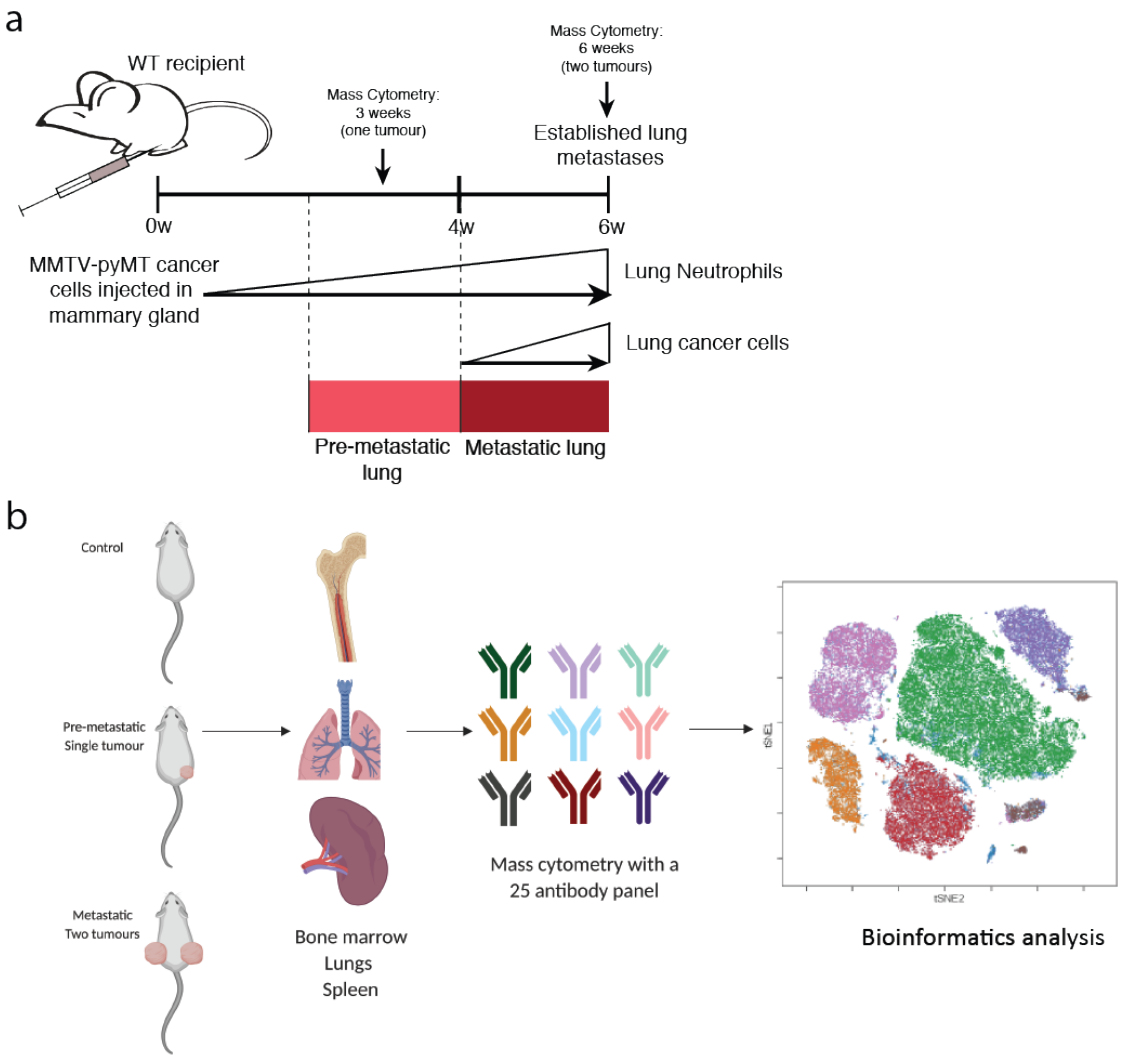

Figure 3.2 Experimental design for mass cytometry investigations

(**a**) Representation of timing and dynamics of neutrophil and cancer cell infiltration into the lungs of mice grafted with mammary tumours by orthotopic injection of MMTV-PyMT tumour cells. Time points of analysis for mass cytometry experiments are shown (top arrows). **Reprinted by permission from Springer Nature Customer Service Centre GmbH: Springer Nature, Nature, *Neutrophils support lung colonization of metastasis-initiating breast cancer cells*, Wculek SK, Malanch I, 2015.** (**b**) Experimental workflow for mass cytometry experiments. Mice in three different conditions were sacrificed and bone marrow, lungs and spleen dissected, dissociated and cells stained with metal-conjugated antibodies followed by mass cytometry analysis. Bioinformatics analysis was then performed on mass cytometry data.

Previous work in the Malanchi laboratory discussed thus far focused principally on neutrophils in the lungs. However, there is evidence for neutrophil heterogeneity within and between tissues in the whole body, and evidence that tumours can affect this (section 1.7, 1.9). I therefore performed mass cytometry analysis on the lungs, spleen and bone marrow, in order to obtain a more comprehensive picture of neutrophil heterogeneity. I did not investigate neutrophils in the tumour itself because in the PyMT model, genetic and antibody-based depletion of neutrophils decreases metastasis of cancer cells but has no effect on primary tumour growth. Moreover, there is limited infiltration of neutrophils in to tumours in this model (Wculek and Malanchi, 2015). I therefore wanted to focus on neutrophils in the periphery to investigate the systemic effects a tumour might exert on neutrophil phenotypes. I also wanted to investigate the bone marrow because this organ is the origin of neutrophils, and there is evidence that tumours can extensively perturb haematopoiesis and thereby affect neutrophil production and development (Wilcox, 2010).

I designed a 25-antibody panel for the mass cytometry analysis. Panel design was based on markers that neutrophils have been reported in the literature to express, and additionally those that have not yet been reported on neutrophils but are functional markers that immune cells and other cell types express under certain conditions that may be relevant to neutrophil function in cancer; for example, PD-L1, which is involved in T cell suppression, and is the target of a number of novel therapies. Table 3 shows the panel and provides a description of the known function and significance of each marker, including whether expression of the marker has previously been documented on neutrophils. Further information on the panel and mass cytometry analysis, including antibody clones, heavy-metal conjugates and experimental workflow, can be found in Materials and Methods section 2.8.

Marker	Function/Significance	Reported on neutrophils in literature?
CD45	Haematopoietic immune cell marker	Yes - Haematopoietic immune marker
Ly6g	Mouse neutrophil biomarker. There is some evidence that Ly6g is involved in neutrophil migration	Yes (Daley et al., 2008)
CD11c	CD11c plays roles in adhesion and cellular activation. Upregulated on neutrophils during sepsis and systemic inflammation	Yes (Lewis et al., 2015)
CD115	Receptor for macrophage-colony stimulating factor. Controls production, differentiation and function of macrophages	Yes (Becher et al., 2014)
CD16/32	Low affinity Fc receptor (antibody-binding receptor, allows neutrophils to bind and phagocytose opsonized pathogens.	Yes (Pillay et al., 2012)
F4/80	Mouse macrophage marker, possible role in immune tolerance, but function not established	Yes (Becher et al., 2014)
CD24	Function unclear. CD24 has been shown to play a role in neutrophil apoptosis.	Yes (Parlato et al., 2012)
Ly6C	Myeloid cell biomarker. Involved in cell adhesion and activation	Yes (Becher et al., 2014)
CD25	Interleukin-2 receptor alpha subunit. Function on neutrophils unclear.	Yes (Becher et al., 2014)
CD64	Fc-gamma Receptor 1 (antibody-binding receptor). Upregulated on neutrophils under inflammatory conditions and in sepsis	Yes (Sack, 2017)
CD48	Roles in adhesion and costimulation on immune cells. Upregulated in neutrophils under inflammatory conditions	Yes (McArdel et al., 2016)
CD54	Also known as ICAM-1. Involved in cell adhesion and migration, upregulated in activated neutrophils	Yes (Yao et al., 2015)
CD38	Cyclic ADP ribose hydrolase. Involved in activation and cell adhesion	No
CD11b	Myeloid cell biomarker, subunit of Complement receptor 3. Involved in activation and adhesion	Yes (Fagerholm et al., 2019)
CD86	Costimulatory molecule expressed by antigen presenting cells	No
MHCII	Antigen presenting molecule, it can be expressed on neutrophils under certain conditions	Yes (Lin and Loré, 2017)
FcEr1	Fc-Epsilon receptor 1 (antibody-binding receptor). Involved in immune activation pathways	Yes (Becher et al., 2014)
CD31	Involved in adhesion and transmigration across endothelium	Yes (Wculek and Malanchi, 2015)
CD62L	L-selectin, cell adhesion molecule, involved in adhesion and transmigration across endothelium. Also plays a role in intracellular signalling	Yes (Ivetic et al., 2019)
PDL2	T-cell inhibitory molecule, suppresses T cell responses.	Yes (Becher et al., 2014)
PDL1	T-cell inhibitory molecule, suppresses T cell responses.	Yes (Cheng et al., 2018)
CCR5	Chemokine receptor, involved in adhesion and endothelial migration	Yes (Reichel et al., 2006)
CXCR4	Sequesters immature neutrophils in the bone marrow. Upregulated on "aged" neutrophils in the periphery to induce their homing back to the bone marrow for destruction	Yes (Casanova-Acebes et al., 2013)
CXCR2	Chemokine receptor for a number of different chemokines. Role in neutrophil egress from bone marrow and chemotaxis to sites of inflammation	Yes (Becher et al., 2014)
CD3	T cell receptor. Used as internal control	No

Table 3 Antibody panel for mass cytometry experiments

I performed mass cytometry experiments as detailed in the Materials and Methods section 2.8, using the antibody panel in Table 3. Figure 3.2b shows the experimental workflow for the mass cytometry experiments. Briefly, I obtained single-cell suspensions of bone marrow, lungs and spleen from mice in all three conditions. The cells were stained with Cisplatin as a viability dye, and then stained with a cocktail of the 25 panel antibodies. Following overnight fixation, the cells were then labelled with an Iridium DNA stain and cell events acquired on a Fluidigm Helios mass cytometer. Doublets, dead cells and non-cell events were excluded before analysis. Samples from between eight and ten female FvB mice were used for each condition.

When analysing mass cytometry data, neutrophils were defined by positive expression of Ly6g, a GPI-anchor protein, which, in the literature, is specific for mouse neutrophils (Daley et al., 2008, Lee et al., 2013). The function of Ly6g is not yet established: however a recent report suggested it may be involved in neutrophil migration to sites of inflammation (Wang et al., 2012a). Regardless of the function of Ly6g, it is reportedly only expressed on mouse neutrophils (there is no known human homologue) and not on other myeloid or lymphoid cell types; I therefore used this marker to define neutrophils in analysis of mass cytometry data.

$Ly6g^+$ cells were selected from the total live cell population and analysed. For each tissue and condition, at least 15,000 $Ly6g^+$ cells evenly sampled from all 8-10 mouse samples were analysed (precise numbers of $Ly6g^+$ cells analysed for each tissue and condition are listed in Materials and Methods section 2.8).

The first stage in analysing high dimensional data is termed nonlinear dimensionality reduction, for which I used t-Distributed Stochastic Neighbour Embedding (t-SNE), from CytoBank (Kotecha et al., 2010, Maaten and Hinton, 2008). This process reduces the dimensionality of the data whilst preserving the overall data structure, allowing all 25 parameters to be incorporated on a two-dimensional map. Each cell is plotted on the map based on that cell's expression of all 25 parameters. Cells with more similar properties (i.e. more similar expression of surface markers) are plotted closer together, thereby revealing relationships between cells and allowing the visualisation of heterogeneity of surface marker expression of $Ly6g^+$ cells.

I first performed t-SNE analysis on each tissue separately, comparing between control and tumour-bearing samples, in order to provide information on the intra-tissue heterogeneity of neutrophils (Figure 3.3a-c). Results from all three tissues reveal heterogeneity in the neutrophil population in control mice, with a different pattern of heterogeneity in each tissue. Furthermore, there are shifts in the population distribution on the plot between control, pre-metastatic and metastatic samples in all three tissues, showing that the presence and stage of a tumour can impact neutrophil heterogeneity.

In the bone marrow, there are clear shifts between control and tumour-bearing samples in a number of regions of the t-SNE plot (Figure 3.3a). For example, in the pre-metastatic and metastatic samples there is an expansion of cells in the regions of the plot denoted by the red arrows, with greater expansion in the metastatic sample. Conversely, the blue arrows denote regions of the plot where cells are enriched in the control sample, but the population is diminished in the tumour-bearing samples, again more strongly in the metastatic sample.

The splenic samples produce a similar picture (Figure 3.3b), the red arrows again denote a region which is enriched in tumour-bearing samples. Additionally, there are populations which decrease in the tumour-bearing mice (Figure 3.3b, blue arrows). Both of these shifts are affected by tumour stage, as in the bone marrow.

The lungs samples display less dramatic shifts than the bone marrow and spleen samples (Figure 3.3c), however there still changes in cell populations, denoted by red arrows (increase in tumour-bearing) and blue arrows (decrease in tumour-bearing), which are also dependent on tumour stage.

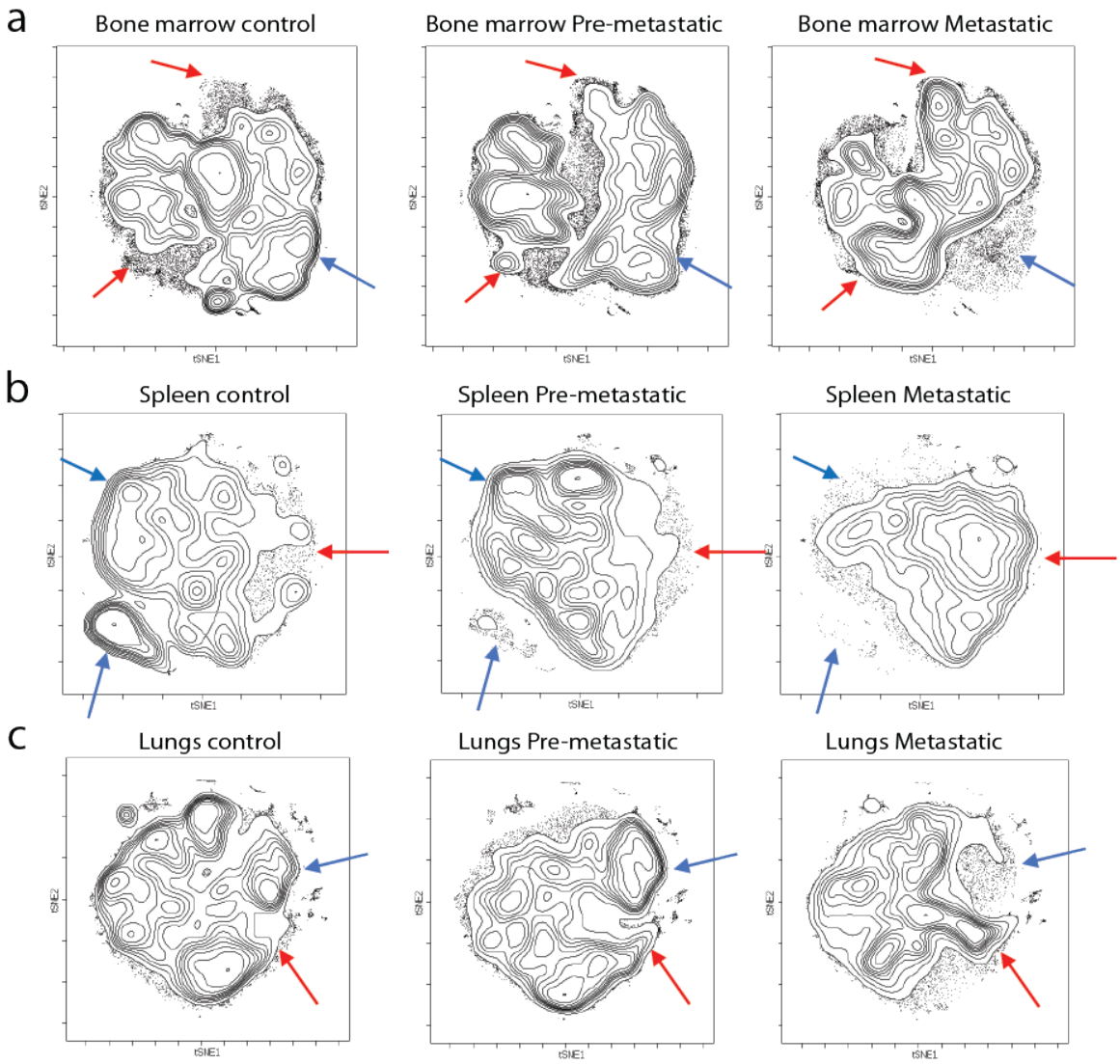

Figure 3.3 t-SNE analysis reveals neutrophil heterogeneity within tissues.

(**a-c**) t-SNE composite dimensions 1 and 2 for Ly6g$^+$ cells from bone marrow (**a**), spleen (**b**), and lungs (**c**). Left to right shows t-SNE plots for Ly6g$^+$ cells from each tissue from control, pre-metastatic tumour-bearing and metastatic tumour-bearing mice respectively. Red arrows denote cell populations that are higher in tumour-bearing mice. Blue arrows denote cell populations that are lower in tumour-bearing mice. t-SNE plots were generated by viSNE analysis on Cytobank. Live, singlet Ly6g$^+$ cell events were evenly sampled from mass cytometry results from 8-10 mice per tissue per condition, then exported into Cytobank and subject to t-SNE analysis.

The t-SNE analysis therefore provides evidence of heterogeneity in neutrophil populations within all three tissues, and demonstrates that the presence and stage of a breast tumour can perturb this heterogeneity. However, the t-SNE analysis only provides a relatively coarse picture of heterogeneity; for validation and further experiments, it is necessary to ascertain the specific markers that define the observed heterogeneity. This required an algorithm called Phenograph (Levine et al.), which runs t-SNE analysis, but also performs unsupervised clustering of cells based on their marker expression. It is therefore an unbiased method of defining cell populations. Cells can then be mapped on a t-SNE plot, and coloured according to which cluster they belong. Phenograph provides the marker expression that it uses to determine clusters and therefore allowed the identification of the markers defining the neutrophil heterogeneity observed in the initial t-SNE analysis.

In the same manner as for t-SNE analysis, $Ly6g^+$ cells were selected from total live single cells from the generated mass cytometry data and run on Phenograph. I ran the Phenograph algorithm on all three tissues together, in order to reveal clusters across all three tissues and therefore provide information on the inter-tissue heterogeneity of neutrophils. Phenograph identified 12 clusters of neutrophils across all three tissues (Figure 3.4, see Appendix 1 for a full list of population clusters defined by Phenograph). The distribution of clusters differs significantly between the tissues; the dominant clusters identified in the lungs (Figure 3.4, clusters 1 and 2) are present at much lower levels in the bone marrow and spleen. Moreover, these clusters occupy different regions of the t-SNE plot in the lungs, compared to the bone marrow and spleen, indicating that despite their overall shared expression of markers, these cells have some differences in marker expression between in the lungs compared to the other tissues

A number of clusters were identified in both the bone marrow and spleen (Figure 3.4, clusters 4, 5 and 6), suggesting that these tissues have shared neutrophil populations. These clusters could not be found in the lungs. There are also two clusters present in the spleen that could not be detected in the bone marrow or lungs (Figure 3.4, clusters 7 and 11), and two clusters found in the bone marrow, that were not present in either lungs or spleen (Figure 3.4, clusters 8 and 9).

Differences can be observed between the control and tumour-bearing samples, in a similar manner to the t-SNE results, with the metastatic samples showing larger shifts than the pre-metastatic samples. Phenograph did not identify a cell cluster unique to tumour-bearing samples in any tissue; instead in the tumour-bearing samples the relative proportions of clusters shift compared to the control samples. For example, clusters 1 and 2 increase in pre-metastatic and metastatic samples in the bone marrow and spleen, but not in the lungs. Clusters 7 and 11, found in the spleen only, decrease in tumour-bearing samples, more strongly in the metastatic sample. Clusters 8 and 9, present only in the bone marrow decrease in tumour-bearing samples, once again more strongly in the metastatic sample. Finally, clusters 4, 5 and 6, in the bone marrow and spleen, increase in tumour-bearing samples.

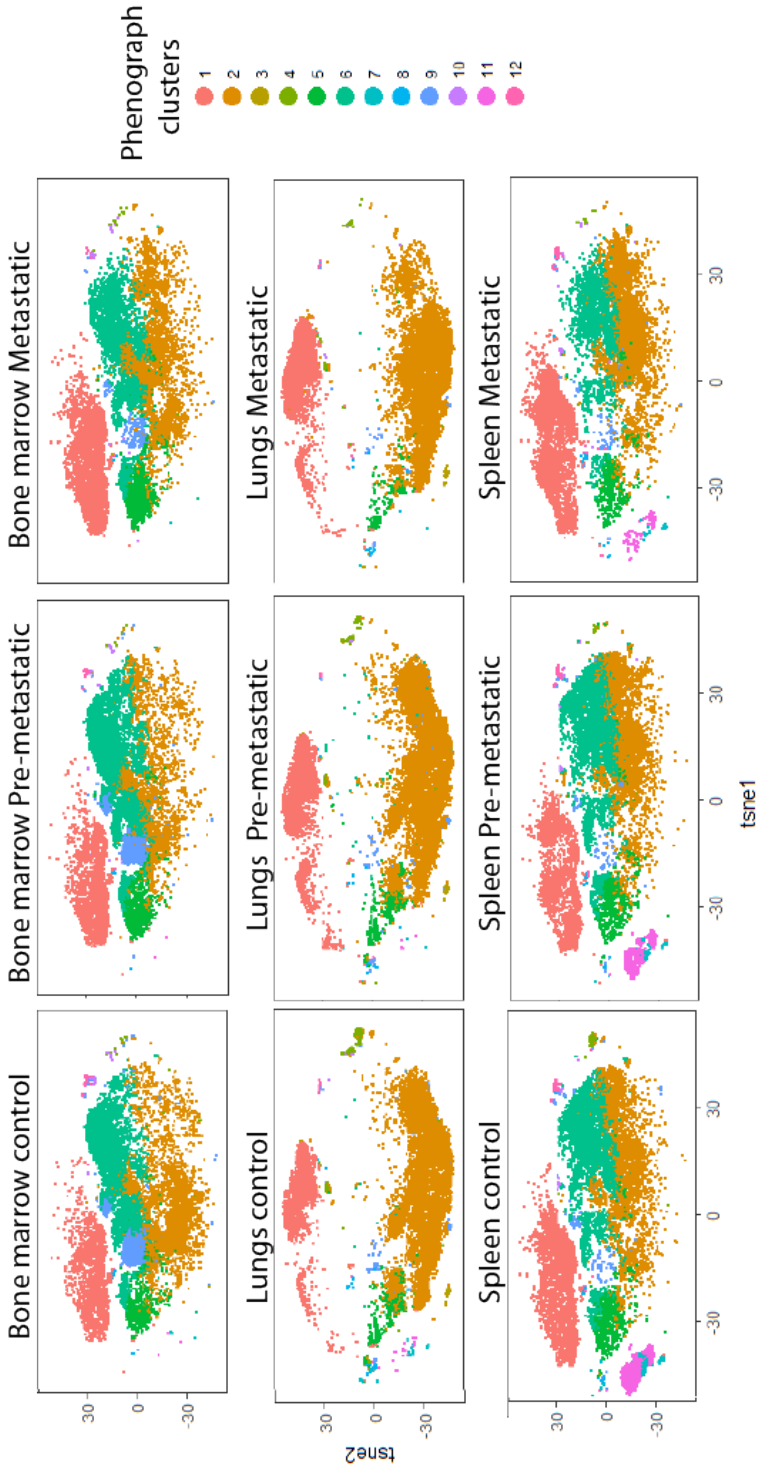

Figure 3.4 Phenograph analysis identifies 12 neutrophil clusters across bone marrow, spleen and lungs

Ly6g^{+} cells from bone marrow, spleen and lungs are plotted on t-SNE composite dimensions 1 and 2 for all samples and colour coded by Phenograph cluster. Live, singlet Ly6g^{+} cell events were evenly sampled from mass cytometry results from 8-10 mice per tissue per condition, then subject to Phenograph analysis. See Appendix 1 for a full list of population clusters defined by Phenograph analysis

Conclusions

- **I confirm previous findings demonstrating an expansion of neutrophils in the bone marrow, circulation and periphery of tumour-bearing mice**
- **Mass cytometry reveals mouse neutrophil heterogeneity at the surface marker level across bone marrow, spleen and lungs**
- **In the presence of a tumour, as neutrophils expand systemically, I observe alterations in neutrophil heterogeneity that appear dependent on tumour stage**
- **Phenograph analysis identifies neutrophil populations with differential marker expression, and finds tissue-specific populations**
- **The presence and stage of a breast tumour alters the relative proportions of neutrophil populations identified by Phenograph analysis**

3.4 Validation of mass cytometry reveals Ly6g$^+$ F4/80$^+$ and Ly6g+ MHC-II$^+$ populations in the bone marrow

Mass cytometry experiments followed by t-SNE and Phenograph analysis revealed neutrophil populations and the markers defining them. It was next necessary to validate these findings using fluorescence-based flow cytometry, to confirm the findings of the mass cytometry experiments and analysis, and to allow further investigation into identified populations. I first wanted to determine, as a proof of concept, if it was possible to observe the populations identified by mass cytometry using conventional flow cytometric methods.

To provide examples for validation, I focused on two clusters identified by Phenograph that were located principally in the bone marrow (Figure 3.5a, clusters 8 and 9). These two clusters were defined by their positive expression of F4/80 and MHC-II respectively. Both clusters were reduced in pre-metastatic and metastatic tumour-bearing samples (Figure 3.5b).

F4/80 (also known as EMR1) is a G-protein coupled receptor that has classically been used as a mouse macrophage marker; it is expressed at differing levels on different macrophage populations across the body. However, more recently its expression has been detected on microglia and certain dendritic cell subtypes (dos Anjos Cassado, 2017). It is still somewhat surprising to observe expression of F4/80 on Ly6g+ cells, particularly given that the expression is restricted to the bone marrow, suggesting that this population is not fully mature, but also suggesting that this population may downregulate expression of F4/80 later in development or upon egress from the bone marrow.

The function of F4/80 remains undetermined, but there are reports that it is involved in the formation of regulatory T cells (Lin et al., 2010). The fact that F4/80 is a G-protein coupled receptor suggests it can play a role in cell signalling pathways but these have not yet been elucidated. Therefore, the significance of F4/80 expression on neutrophils in the bone marrow is not immediately clear.

MHC-II is used to present captured antigen to T cells in order to activate the T cells against the antigen, beginning an adaptive immune response. MHC-II expression has been reported on neutrophils in specific contexts, and it has been shown in humans that neutrophils can use MHC-II to cross-present antigens to T cells (Singhal et al., 2016), and in mice a number of studies have demonstrated that neutrophils can present antigen to T cells using MHC-II (Lin and Loré, 2017). However, this expression has not previously been found in the bone marrow. Additionally, the MHC-II^{+} population could not be observed in the lungs or spleen, suggesting that this population may be a more immature population confined to the bone marrow, and may downregulate MHC-II expression during maturation before exiting the bone marrow. The functional significance of the MHC-II expression is unclear; mature T cells are not present in the bone marrow, so neutrophils would be unable to present antigen to them.

The unexpected finding of expression of these two markers on Ly6g+ cells warranted validation. I performed flow cytometry with fluorophore-conjugated antibodies for F4/80 and MHC-II, using the same antibody clones as used in the mass cytometry experiments, the tumour burden in this experiment being pre-metastatic. Flow

cytometry experiments were performed as detailed in Materials and Methods section 2.7. These experiments confirmed the expression of these markers on Ly6g+ cells in the bone marrow (Figure 3.6a). Flow cytometry also shows these populations decrease significantly in tumour-bearing mice, both as a proportion of Ly6g+ cells and as a proportion of total alive cells in the tissue (Figure 3.6b). These results demonstrate that it is indeed possible to use conventional flow cytometry to detect and interrogate populations identified by mass cytometry.

Conclusions

- **Flow cytometry can be used to identify populations defined by mass cytometry**
- **In the bone marrow, mass cytometry identifies populations of Ly6g+ cells defined by their expression of F4/80 and MHC-II**
- **Flow cytometry can also be used to detect these populations**
- **Using both mass cytometry and flow cytometry, I observe decreases in $Ly6g^+$ $F4/80^+$ and $Ly6g^+$ $MHC\text{-}II^+$ populations in mice with breast tumours**

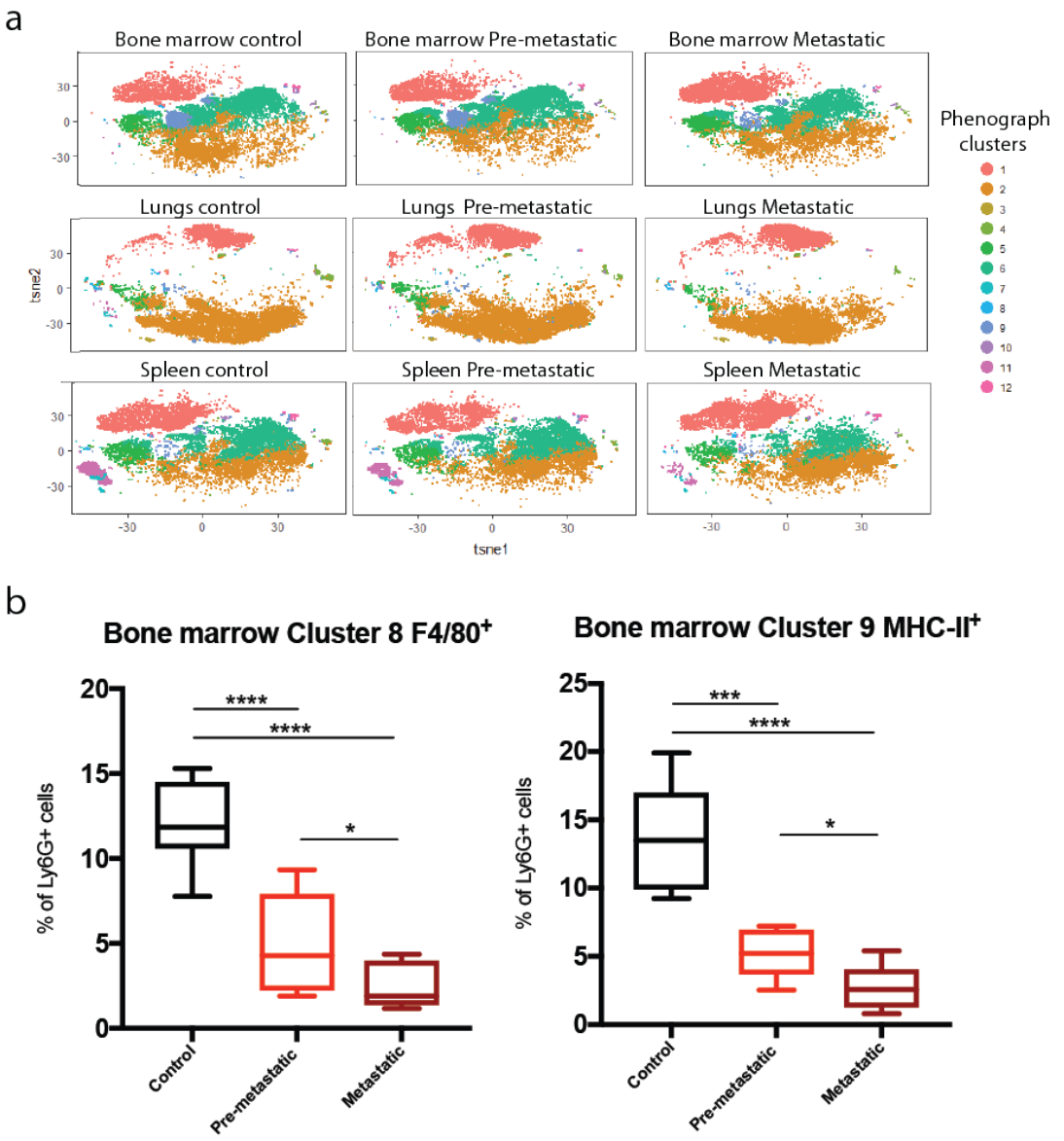

Figure 3.5 Mass cytometry identifies MHC-II$^+$ and F4/80$^+$ populations that are reduced in the bone marrow of tumour-bearing mice

(**a**)Phenograph analysis of Ly6g$^+$ cells from bone marrow, spleen and lungs of control and tumour-bearing mice. (**b**) Quantification of mass cytometry analysis of Cluster 8 Ly6g$^+$ F4/80$^+$ and Cluster 9 Ly6g$^+$ MHC-II$^+$ cells in the bone marrow. Data are displayed as Tukey box and whiskers plot, n=9 mice. Statistical analysis by two-sided t-test. * P < 0.05, ** P < 0.01, *** P < 0.001, **** P < 0.0001.

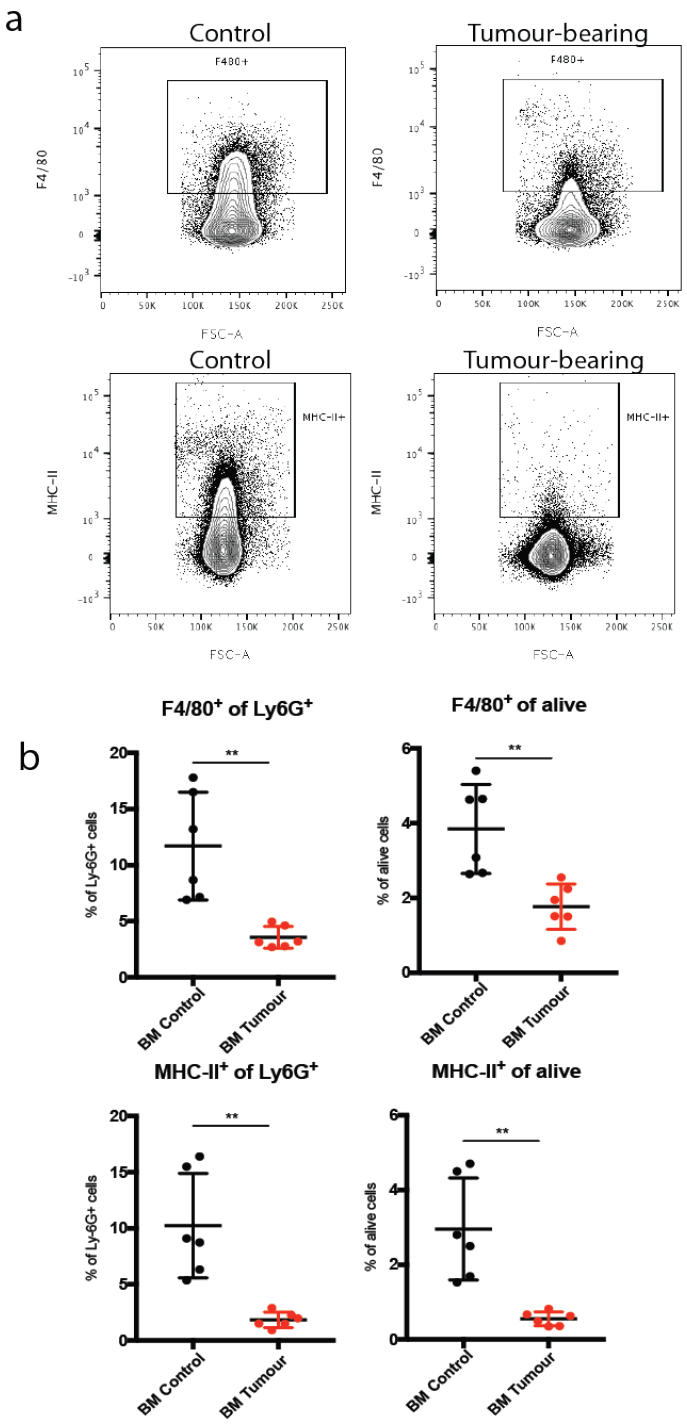

Figure 3.6 Flow cytometry detects F4/80$^+$ and MHC-II$^+$ Ly6g$^+$ populations identified by mass cytometry

(**a**) Representative flow cytometry plots, pre-gated on Ly6g$^+$ cells, showing top, the F4/80$^+$ population, and bottom, the MHC-II$^+$ population, from control and tumour-bearing mice. Flow cytometric quantification of bone marrow Ly6g$^+$ F4/80$^+$ or MHC-II$^+$ cells in control and tumour-bearing mice, analyzed as a percentage of total Ly6g$^+$ cells and a percentage of total alive cells in the tissue. Data are displayed as mean ± (SD). Statistical analysis by two-sided t-test * P < 0.05, ** P < 0.01, **** P < 0.0001.

3.5 Identification of a population of Ly6g^{+} CD11b^{-} cells in the spleen.

In the spleen, mass cytometry identified a neutrophil population that was decreased in pre-metastatic and metastatic samples (Figure 3.7a,b, cluster 11). Phenograph identified this population as defined primarily by lack of expression of CD11b; this population also expressed MHC-II, CD48 and CD86. All the other populations identified by Phenograph were Ly6g^{+} CD11b^{+}. I wanted to investigate this population using flow cytometry, as a further proof of concept that flow cytometry could be used to detect populations initially defined by mass cytometry.

CD11b is a subunit of the alpha-M beta-2 integrin (also known as Mac-1 or Complement receptor 3), which is comprised of CD11b and CD18. CD11b is expressed on neutrophils, monocytes, macrophages and natural killer cells (Jawhara et al., 2016) and is used extensively as a myeloid marker in mouse and human studies. CD11b function as part of an integrin heterodimer and on neutrophils is involved in numerous functions including extravasation from the circulation, phagocytosis, degranulation and antibody-dependent cellular cytoxicity (Fagerholm et al., 2019).

During haematopoiesis CD11b expression can first be detected at the myelocyte/pro-monocyte stage (for neutrophils and monocytes respectively), expression increases during maturation, with highest expression observed on mature myeloid cells in the circulation and periphery (van Lochem et al., 2004). Ly6g expression follows the same pattern as CD11b expression (although Ly6g is canonically only expressed on neutrophils) (Lee et al., 2013). It is therefore surprising to observe a population of cells expressing Ly6g but not CD11b, given that neutrophils will typically begin expression of both of these proteins at approximately the same point in development, and upregulate expression as they mature and leave the bone marrow.

Consequently, I performed flow cytometry experiments using the same CD11b antibody clone as used in the mass cytometry experiments, the results confirmed the presence of the Ly6g^{+} CD11b^{-} population in the spleen, and also confirmed its

absence in the bone marrow, lungs, and additionally the blood (Figure 3.8). Flow cytometry also confirmed a significant decrease in this population in tumour-bearing spleen compared to control spleen, the tumour burden in this experiment being pre-metastatic (Figure 3.9). Furthermore, the flow cytometry experiments found that Ly6g expression is lower on the $CD11b^-$ population compared to the $CD11b^+$ population, in both control and tumour-bearing mice (Figure 3.10a,b). The lower expression of Ly6g, in tandem with lack of CD11b expression, suggests this population may be more immature than the $Ly6g^+$ $CD11b^+$ population. However, as mentioned above, Ly6g and CD11b have the same pattern of expression during neutrophil development(Coffelt et al., 2016), thus, canonically, even if this population were more immature (suggested by its lower Ly6g expression) it would still be expected to display CD11b expression.

The fact that these cells could only be observed in the spleen and not any other tissues I investigated is also of interest; haematopoiesis can occur in the spleen (Kim, 2010), and it is therefore possible that the $Ly6g^+$ $CD11b^-$ population is an immature myeloid population involved in splenic haematopoiesis. It is also well established that tumours can cause significant changes in haematopoiesis, and particularly myelopoiesis, potentially explaining why this population decreases in tumour-bearing mice (Wilcox, 2010). However, these interpretations still do not explain why this population expresses Ly6g but not CD11b. This puzzling, non-canonical combination of marker expression therefore warranted further investigation.

Conclusions

- **Mass cytometry reveals a population of $Ly6g^+$ $CD11b^-$ cells in the spleen**
- **Flow cytometry confirms the identification of this population**
- **$Ly6g^+$ $CD11b^-$ cells are reduced in the spleens of tumour-bearing mice and have lower expression of Ly6g than $Ly6g^+$ $CD11b^+$ cells**

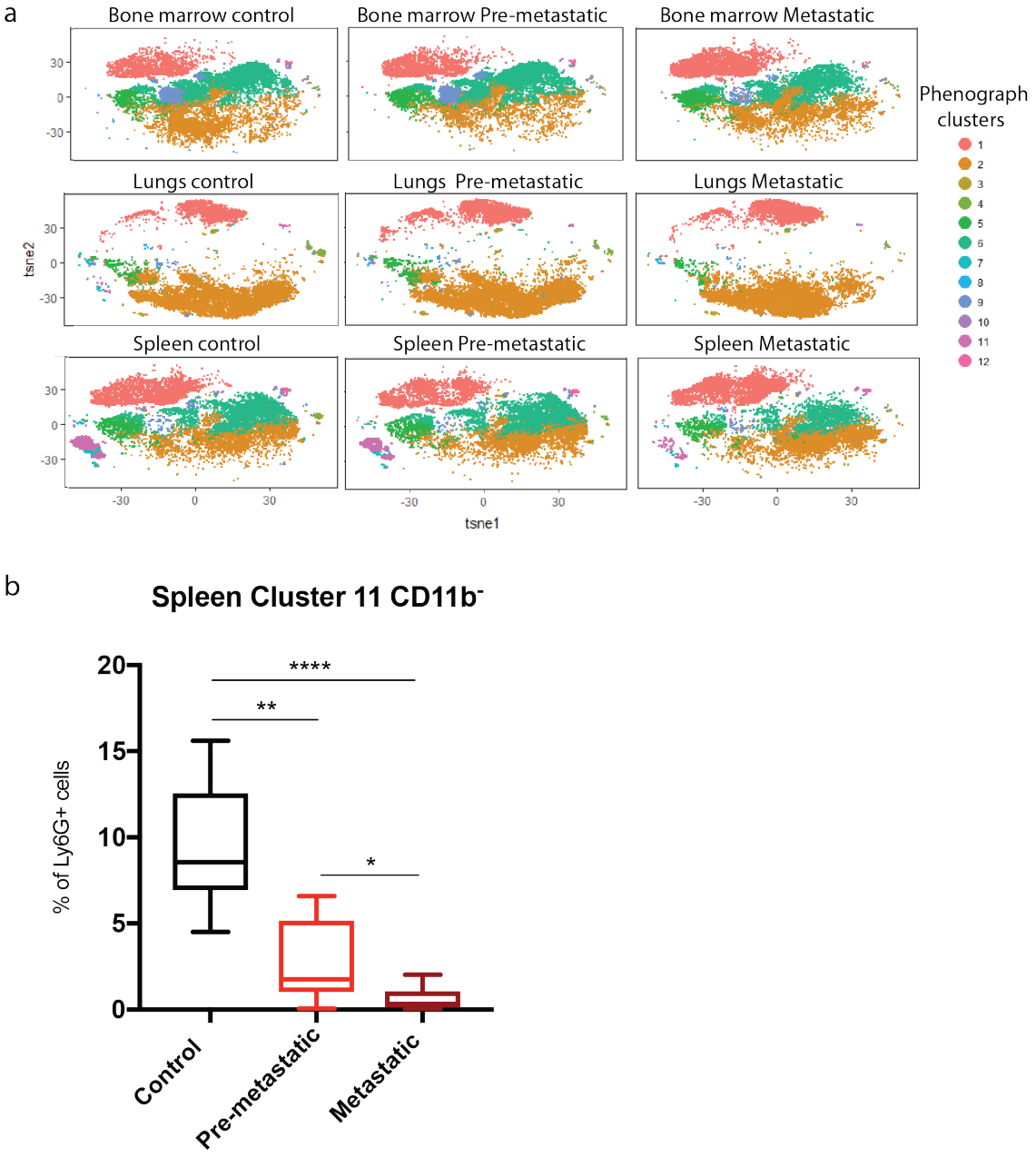

Figure 3.7 Mass cytometry identifies a population of splenic Ly6g^{+} CD11b^{-} cells that decrease in tumour-bearing mice

(**a**) Phenograph analysis of Ly6g^{+} cells from bone marrow, spleen and lungs of control and tumour-bearing mice. (**b**) Quantification of mass cytometry analysis of Cluster 11 Ly6g^{+} CD11b- cells in the spleen. Data are displayed as Tukey box and whiskers plot, n=9 mice. Statistical analysis by two-sided t test. * P < 0.05, ** P < 0.01, , **** P < 0.0001.

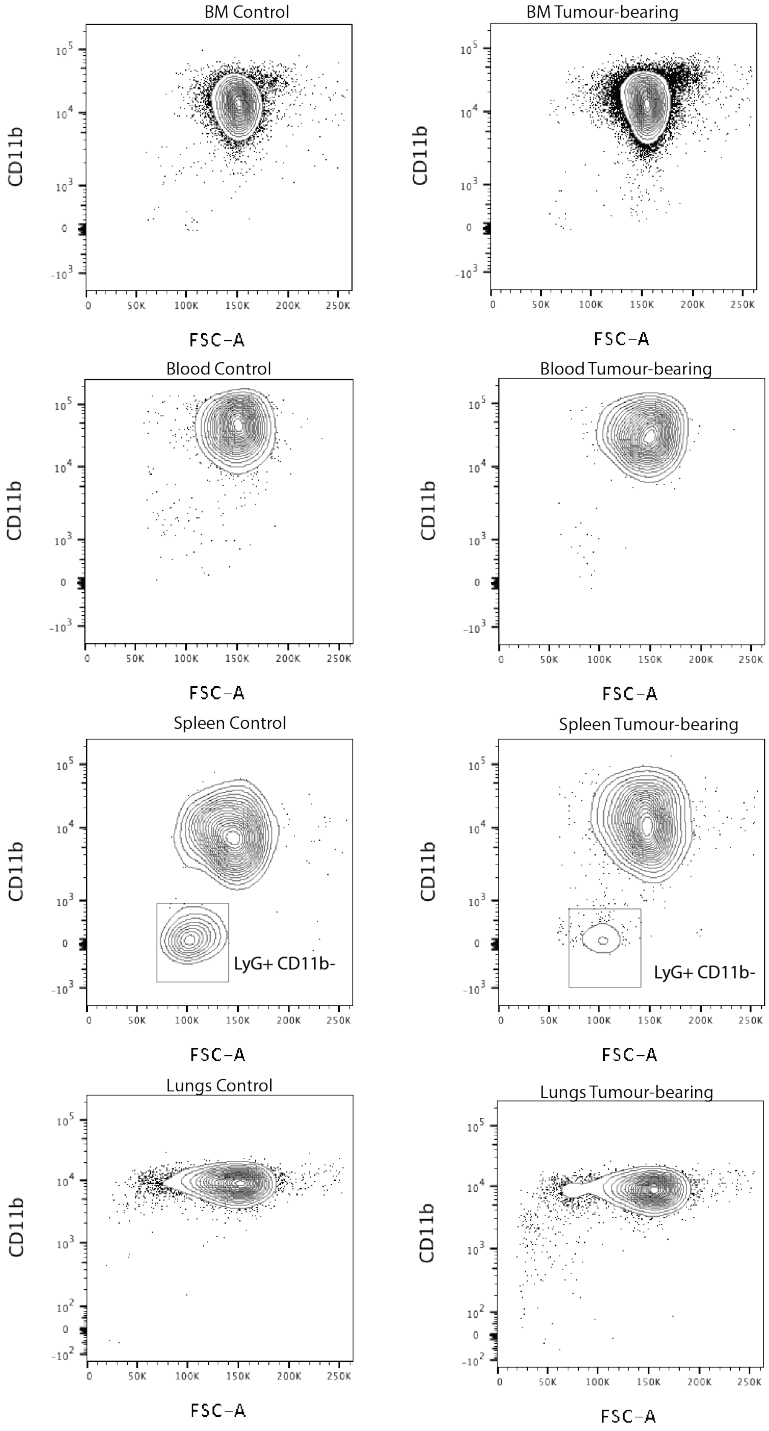

Figure 3.8 Flow cytometry identifies a population of splenic Ly6g^{+} CD11b^{-} cells

Flow cytometry plots, pre-gated on Ly6g^{+} cells, showing CD11b expression on Ly6g^{+} cells in the bone marrow, blood, liver, spleen and lungs of control and tumour-bearing mice. The Ly6g^{+} CD11b- population in the spleen is highlighted.

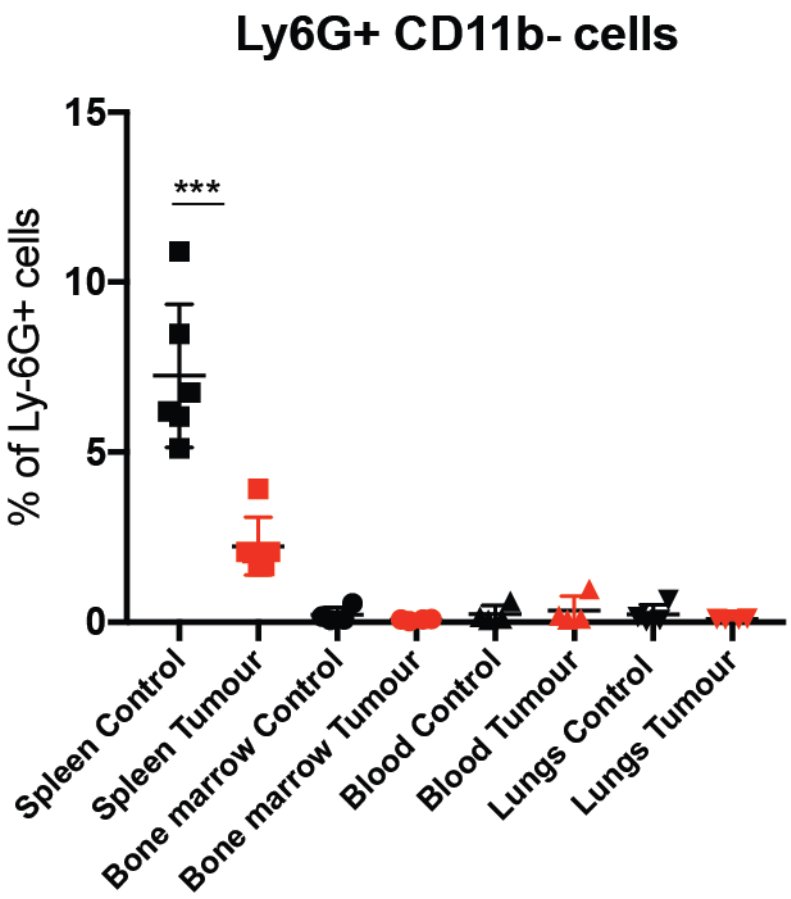

Figure 3.9 Flow cytometry confirms a decrease in splenic Ly6g^{+} CD11b^{-} cells in tumour-bearing mice

Flow cytometric quantification of the frequency of the Ly6g^{+} CD11b^{-} population across tissues in control and tumour-bearing mice. n = 6 mice per condition, data are displayed as mean ± SD. Statistical analysis by two-sided t-test. *** P < 0.001.

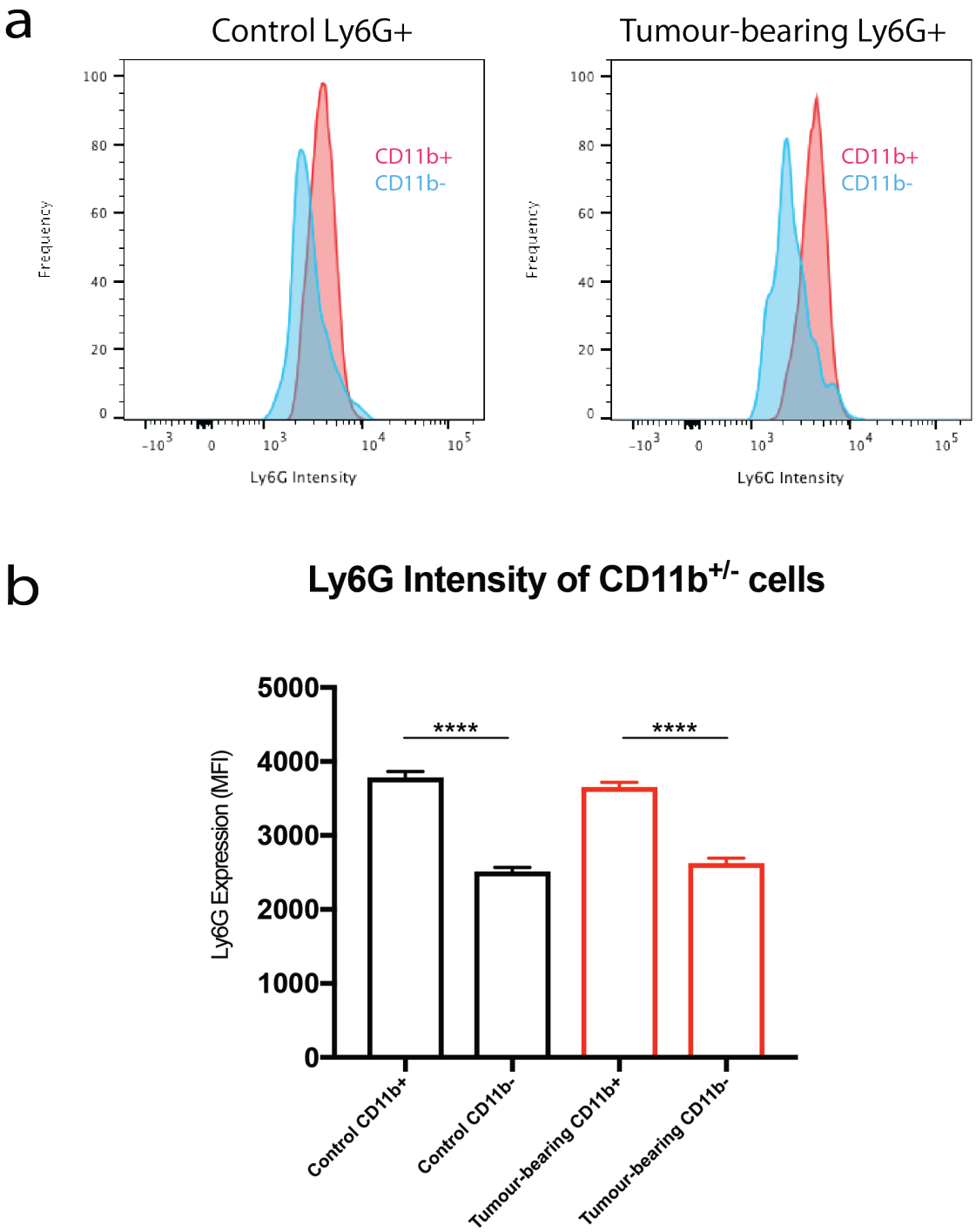

Figure 3.10 Lower Ly6g expression on Ly6g^{+} CD11b^{-} cells, regardless of tumour presence

(**a**) Ly6g intensity was determined by flow cytometry. Representative histograms showing Ly6g intensity of CD11b^{+}/- cells from control and tumour-bearing mice. (**b**) Flow cytometric quantification of intensity of Ly6g expression (mean fluorescence intensity, MFI) on Ly6g^{+} CD11b^{+} and Ly6g^{+} CD11b- cells from the spleen of control and tumour-bearing mice, n=4 mice, data are displayed as mean ± SD. Statistical analysis by two-sided t-test. **** $P < 0.0001$.

3.6 Characterization of the splenic Ly6g$^+$ CD11b$^-$ population finds that they do not have conventional neutrophil characteristics

I decided to focus further investigations on the splenic Ly6g$^+$ CD11b$^-$ population due to its non-conventional expression of myeloid markers, its restriction to the spleen, and the reduction in this population observed in tumour-bearing mice.

First, I used flow cytometry to measure the abundance of this population as a proportion of total live cells in the spleen, and used this value to calculate the total number of these cells in the spleen, in this experiment the tumour burden being metastatic. This revealed that the population does not actually differ in total number between control and tumour-bearing mice (Figure 3.11a). This is explained by the fact that the Ly6g$^+$ CD11b$^+$ population increases in the spleen in tumour-bearing mice (Figure 3.1), consequently, the Ly6g$^+$ CD11b$^-$ population decreases as a proportion of total Ly6g$^+$ cells, whilst its numbers remain unchanged. This shows that the population does not in fact decrease in response to the presence of a tumour. I also found that the population can be detected in the spleens of control BALB/CJ and C57BL/6 mice, showing it is not restricted to the FvB mouse strain (Figure 3.11b)

I then used flow cytometry to investigate the size and granularity of this population; cells scatter the laser light source as they pass through a flow cytometer, the forward and side scatter can both be detected, with forward scatter being proportional to cell size, and side scatter being proportional to cell granularity. I therefore determined the forward and side scatter of Ly6g$^+$ CD11b$^+$ and Ly6g$^+$ CD11b$^-$ cells from control and tumour-bearing mice. Surprisingly, the Ly6g$^+$ CD11b$^-$ population has significantly reduced forward and side scatter compared to the Ly6g$^+$ CD11b$^+$ population, in both control and tumour-bearing spleens, indicating that the CD11b$^-$ population is smaller and less granular (Figure 3.11c, d).

The nuclear morphology of neutrophils alters as they undergo maturation in the bone marrow (see Introduction section 1.5), and can also change in the periphery as

neutrophils age, or if they are activated by a stimulus. Nuclear morphology is therefore a useful method for categorizing neutrophils at different stages of maturation (Figure 3.12a). Given the smaller size and lower granularity of the Ly6g$^+$ CD11b$^-$ population it is possible that they have may have an altered nuclear morphology compared to Ly6g$^+$ CD11b$^+$ cells, and this may reflect a different maturation state or activation state. It is also conceivable that they are not neutrophils, in which case they may have a more typical round nucleus. Therefore, I next wanted to investigate the nuclear morphology of this population.

Using FACS, I purified Ly6g$^+$ CD11b$^-$ and Ly6g$^+$ CD11b$^+$ cells from the spleens of control and pre-metastatic tumour-bearing mice. Sorted neutrophils were affixed to slides by Cytospin centrifugation, fixed with methanol and stained with Giemsa stain to visualise neutrophil nuclei. The Ly6g$^+$ CD11b$^+$ cells had the classical segmented nuclei of mature neutrophils, as would be expected from Ly6g$^+$ CD11b$^+$ cells in the spleen (Figure 3.12b, c). Remarkably, the Ly6g$^+$ CD11b$^-$ had almost uniformly round nuclei, indicating that they are not mature neutrophils and indeed not even immature neutrophils or myelocytes, which would be expected to have a banded or doughnut-shaped nucleus. Instead these cells have the typical round nuclei typical of monocytes, lymphocytes, epithelial and stromal cells. The small size and granularity of these cells, in tandem with their round nuclei suggests that they are not neutrophils, but may be a highly immature myeloid progenitor population, or indeed, may not be myeloid cells at all.

Conclusions

- **The splenic Ly6g$^+$ CD11b$^-$ population does not change in total abundance in response to a tumour.**
- **This population can be observed in other mouse strains**
- **The Ly6g$^+$ CD11b$^-$ population is smaller and less granular than Ly6g$^+$ CD11b$^+$ cells, and has round nuclei, these traits are highly uncharacteristic of neutrophils**
- **These results suggest that these cells are myeloid progenitors at an early stage of myelopoiesis, or not of myeloid origin at all**

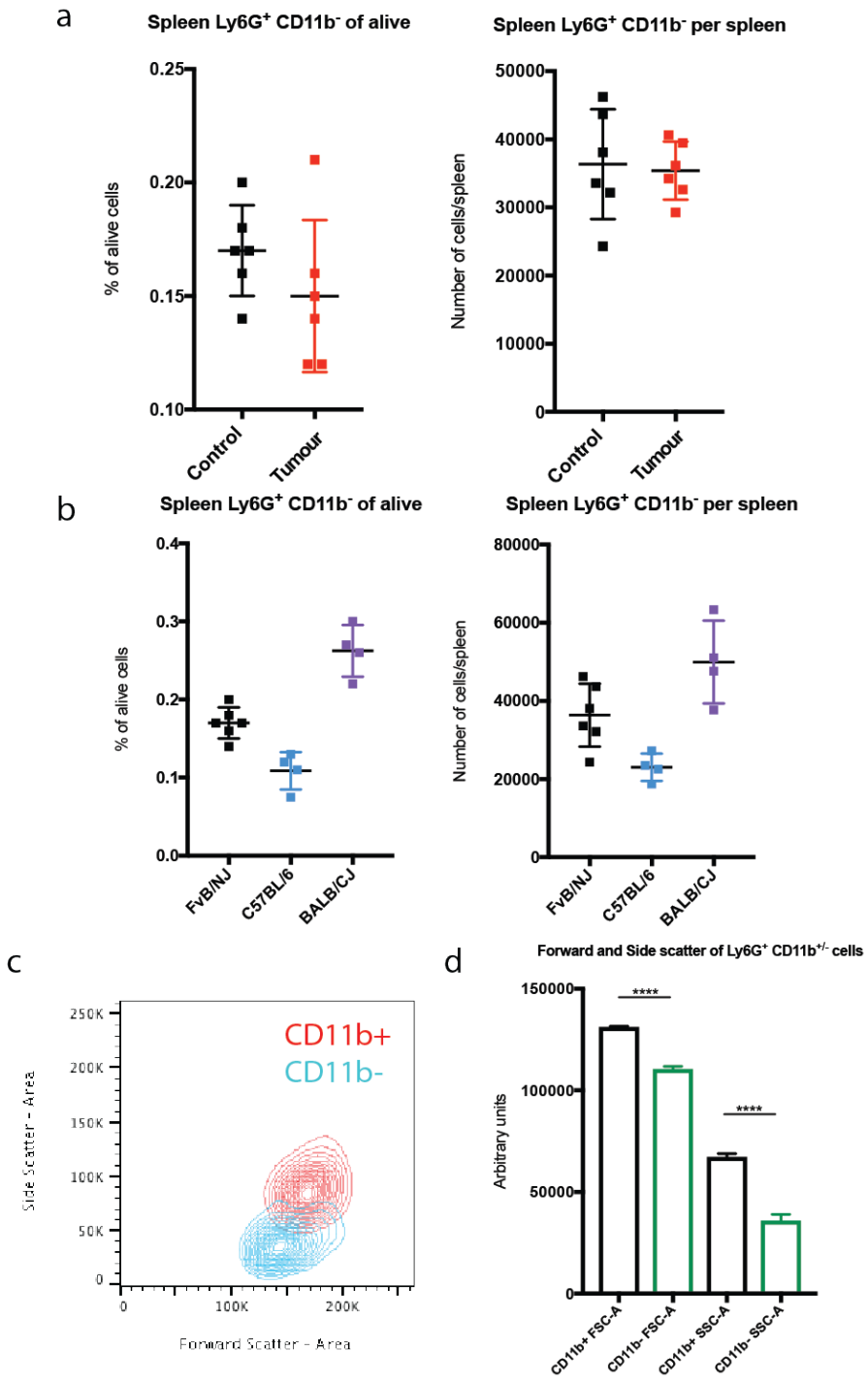

Figure 3.11 Ly6g^{+} CD11b^{-} cells do not change in total tumour in tumour-bearing mice, and are smaller and less granular than Ly6g^{+} CD11b^{+} cells

(**a**) Flow cytometric quantification of Ly6g^{+} CD11b- cells as a proportion of total alive cells in the tissue and total numbers of these cells in the spleen, n=6 mice per condition. (**b**) Flow cytometric quantification of Ly6g^{+} CD11b- cells as a proportion of total alive cells in control female FvB, BALB/CJ and C57/BL6 mice. n=6 for FvB mice n=4 for BALB/CJ and C57/BL6. (**c**) Representative flow cytometry plot showing forward and side scatter of Ly6g^{+} CD11b^{+} (red) and Ly6g^{+} CD11b- (blue) cells. (**d**) Quantification of forward and side scatter of Ly6g^{+} CD11b$^{+/-}$ cells, n=5 mice per condition. Data are displayed as mean ± SD. **** P < 0.0001.

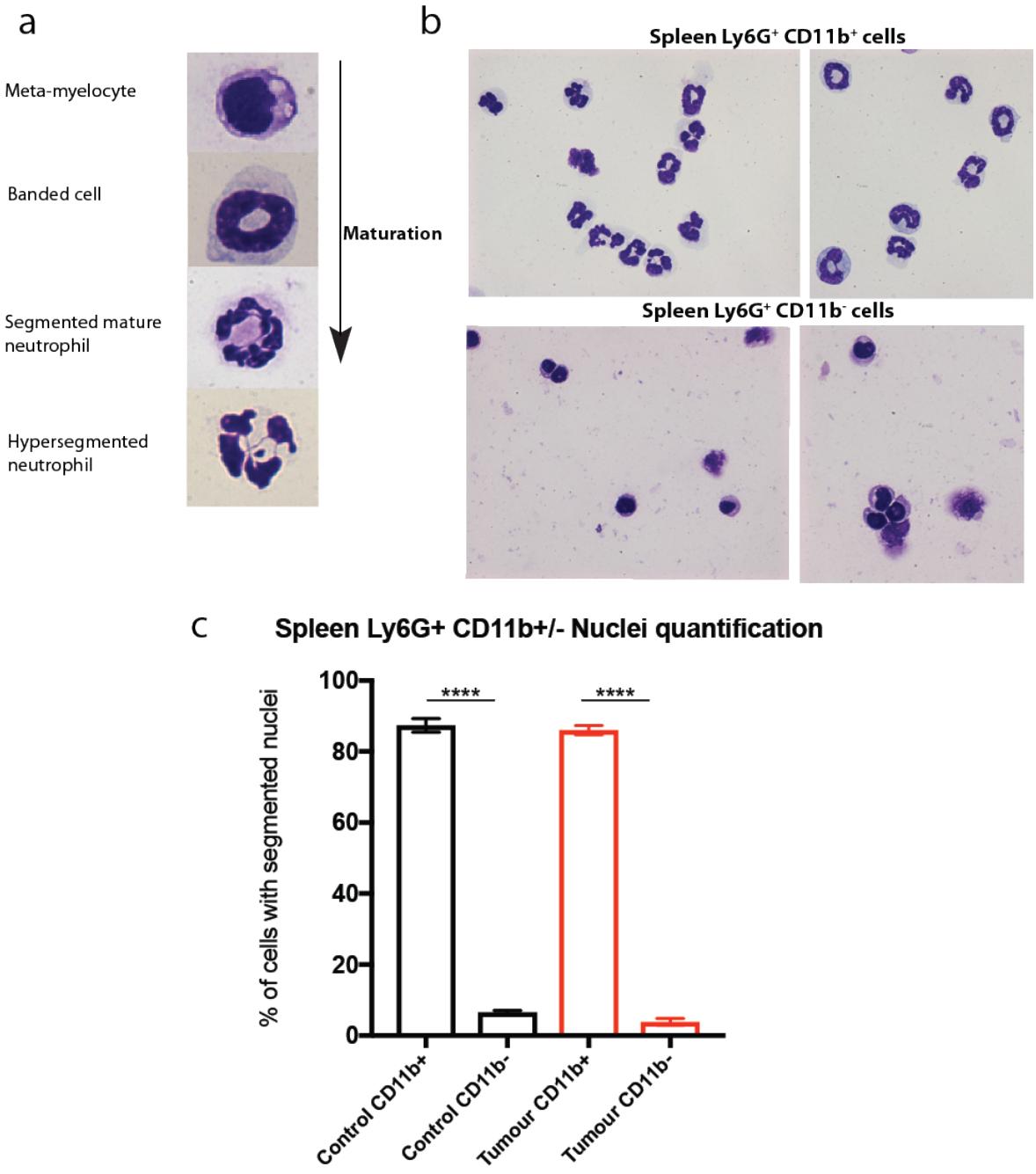

Figure 3.12 Ly6g^{+} CD11b^{-} cells do not have conventional neutrophil nuclear morphology

(**a**) Images of neutrophils at different stages of maturation stained with Wright-Giemsa stain. (**b**) Images of (top) Ly6g^{+} CD11b^{+} cells and (bottom) Ly6g^{+} CD11b- cells stained with Wright-Giemsa stain. (**c**) Quantification of cells with segmented nuclear morphology for Ly6g^{+} CD11b$^{+/-}$ cells, data are shown as mean ± SD. Statistical analysis by two-sided t-test. **** P < 0.0001.

3.7 The Ly6g$^+$ CD11b$^-$ population are B cells

To better understand the precise nature of the Ly6g$^+$ CD11b$^-$ population I decided to determine their ontogeny, taking advantage of two types of knockout mice; GCSF$^{-/-}$ and Rag$^{-/-}$. GCSF$^{-/-}$ mice lack G-CSF), which is a critical factor stimulating neutrophil production in the bone marrow (section 1.5). These mice therefore have severely impaired neutrophil numbers (Liu et al., 1996). Rag$^{-/-}$ mice lack a functional Recombination-activating gene 1 (Rag-1), which T and B cells use for VDJ DNA recombination during maturation. Loss of Rag prevents T and B cells from producing functional T cell and B cell receptors, preventing their maturation; thus Rag mice lack mature T and B cells (Mombaerts et al., 1992).

I used flow cytometry to look for the Ly6g$^+$ CD11b$^-$ population in the spleens of FvB GCSF$^{-/-}$ and FvB Rag$^{-/-}$ mice. Surprisingly, the population is present in similar numbers to wildtype FvB in the spleens of FvB GCSF$^{-/-}$ and GCSF$^{+/-}$ mice, but totally absent in the spleens of Rag$^{-/-}$ mice (Figure 3.13a). This evidence suggests that this population may not be of myeloid origin, but could be of lymphoid origin, either B or T cells. I also observed that, when measured as a proportion of total Ly6g$^+$ cells, the Ly6g$^+$ CD11b$^-$ population is significantly higher in GCSF$^{-/-}$ mice compared to wildtype FvB and GCSF$^{+/-}$ mice (Figure 3.13a, left). However, when measured as proportion of total live cells, this difference is absent (Figure 3.13a, right). This is likely due to the fact that GCSF$^{-/-}$ mice have greatly reduced numbers of Ly6g$^+$ CD11b$^+$ cells, therefore the Ly6g$^+$ CD11b$^-$ population forms a greater proportion of the total Ly6g$^+$ compartment, despite the fact that the total numbers of Ly6g$^+$ CD11b$^-$ cells are unchanged.

To confirm my observation that the Ly6g$^+$ CD11b$^-$ population is of lymphoid origin, and to determine whether the Ly6g$^+$ CD11b$^-$ cells are indeed T or B cells I used flow cytometry to look for expression of CD3 and CD19 on these cells. CD3 is the T cell receptor, expressed by mature T cells. CD19 is a B cell transmembrane protein involved in B cell receptor signalling. CD19 is expressed by all B cells from an early stage of development and is consequently a commonly used B cell biomarker (Wang et al., 2012b).

As expected, Ly6g$^+$ CD11b$^+$ cells did not express CD3 or CD19, however the Ly6g$^+$ CD11b$^-$ population showed clear expression of CD19, and no CD3 expression (Figure 3.13b), showing that this population is in fact a B cell population.

To confirm this finding, and to visualise the cell surface expression of the markers defining this population, I used the Imagestream imaging flow cytometer to generate pictures of the marker expression on the cell population. Ly6g$^+$ CD11b$^+$ cells (Figure 3.14a, top panel) display clear expression of CD11b and Ly6g on their cell membranes, and no expression of CD19, as would be expected for neutrophils. Ly6g$^+$ CD11b$^-$ cells (Figure 3.14a, bottom panel) displayed strong expression of CD19 around their whole cell membrane, and additionally Ly6g expression could be observed on these cells, though it is visibly weaker expression than that observed on Ly6g$^+$ CD11b$^+$ cells. This is consistent with previous data (Figure 3.10) showing that the CD11b$^-$ population has lower expression of Ly6g than the CD11b$^+$ population.

I next wanted to further investigate the B cell characteristics of the Ly6g$^+$ CD11b$^-$ B cell population; there a number of different B cell subpopulations, and B cells can also be found in a range of maturation and activation states. Further information on what type of B cells the Ly6g$^+$ CD11b$^-$ population are may illuminate the reason for their expression of Ly6g, or indeed the function of Ly6g (which, as previously mentioned, is currently unclear). I therefore used flow cytometry to interrogate the splenic B cell population, comparing the Ly6g$^+$ and Ly6g$^-$ B cells. The Ly6g$^+$ cells were all negative for the marker AA4.1 and positive for CD19 and B220, meaning that they are mature B cells (Allman and Pillai, 2008). The expression of CD21 and CD23 on mature B cells denotes these cells as either Follicular B cells (CD23$^+$ CD21$^-$) or Marginal Zone B cells (CD23$^-$ CD21$^+$) (Allman and Pillai, 2008). Follicular B cells principally participate in T cell-dependent antibody responses, with the capacity to become long-lived plasma cells and memory cells. Marginal zone B cells primarily function in T cell-independent responses, with consequently lower antibody specificity.

The Ly6g$^+$ population is predominantly Follicular or in the Marginal zone (Figure 3.14b, c). Compared to the Ly6g$^-$ population, the Ly6g$^+$ population is distributed

slightly more in the Marginal zone than in the Follicles, though the differences between the populations are minor. However, this result does demonstrate that the $Ly6g^+$ B cells are not restricted to a specific B cell subtype.

Conclusions

- **The $Ly6g^+$ $CD11b^-$ population disappears in $Rag^{-/-}$ mice, and expresses CD19 and a number of other B cell markers**
- **Splenic $Ly6g^+$ $CD11b^-$ cells are a population of B cells, broadly distributed in the spleen follicles and marginal zone**

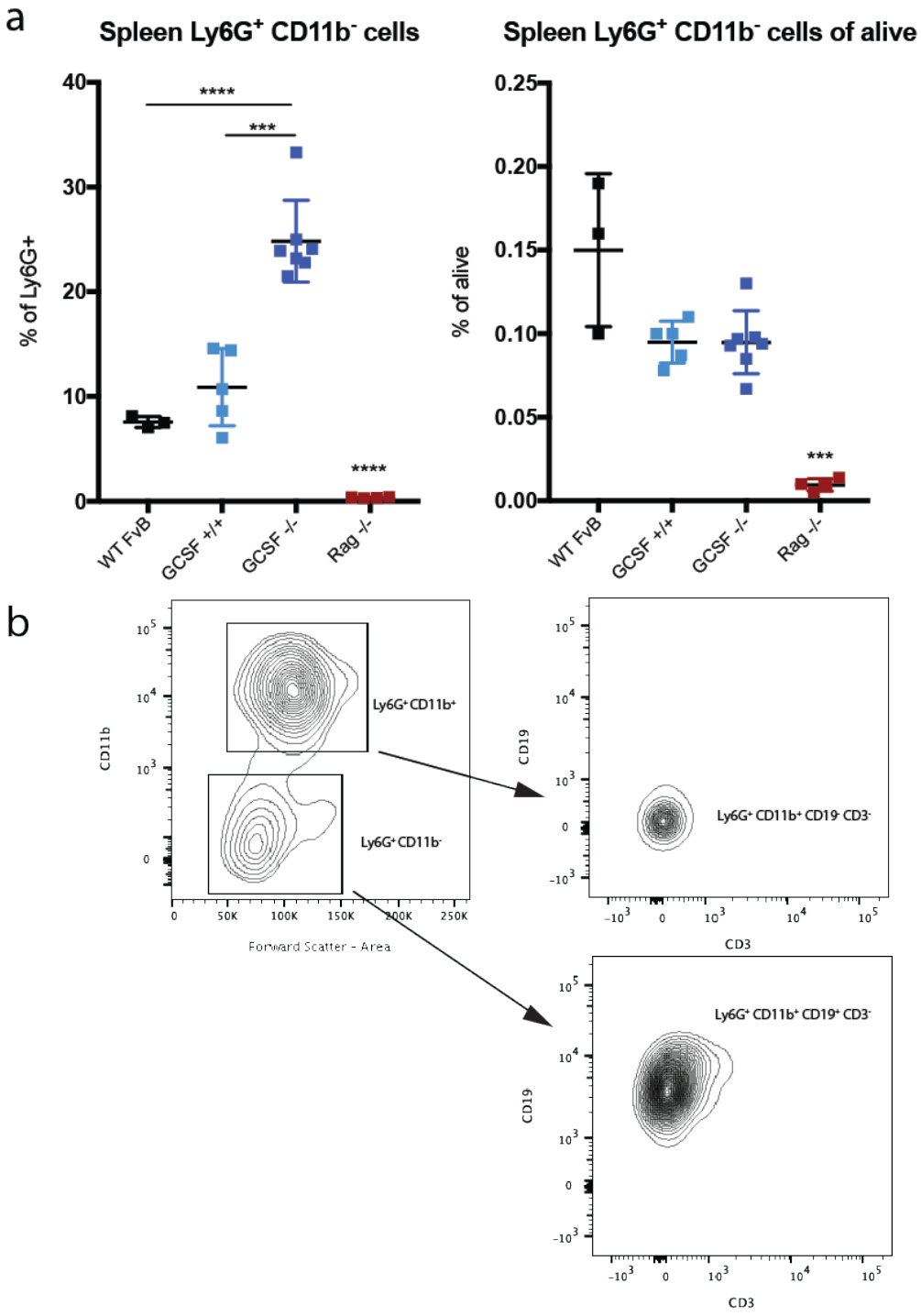

Figure 3.13 Ly6g^{+} CD11b^{-} cells are B cells

(**a**) Flow cytometric quantification of splenic Ly6g^{+} CD11b- cells in FvB, GCSF$^{+/-}$, GCSF$^{+/+}$ and Rag$^{-/-}$ mice. Analysed first as a proportion of total Ly6g^{+} cells and then as a proportion of total alive cells in the tissue. n=3 for FvB, n=5 for GCSF$^{+/-}$, n=7 for GCSF$^{+/+}$, n=4 for Rag$^{-/-}$. (**b**) Flow cytometry plots showing the expression of CD19 and CD3 on splenic Ly6g+ CD11b+ cells (top right) and splenic Ly6g^{+} CD11b- cells (bottom right). Data are displayed as mean ± SD. Statistical analysis by two-sided t-test. *** $P < 0.001$, **** $P < 0.0001$. **** on Rag$^{-/-}$ samples indicate Rag$^{-/-}$ samples are $P < 0.0001$ significantly different from all three other samples in the experiment (determined by two-sided t test).

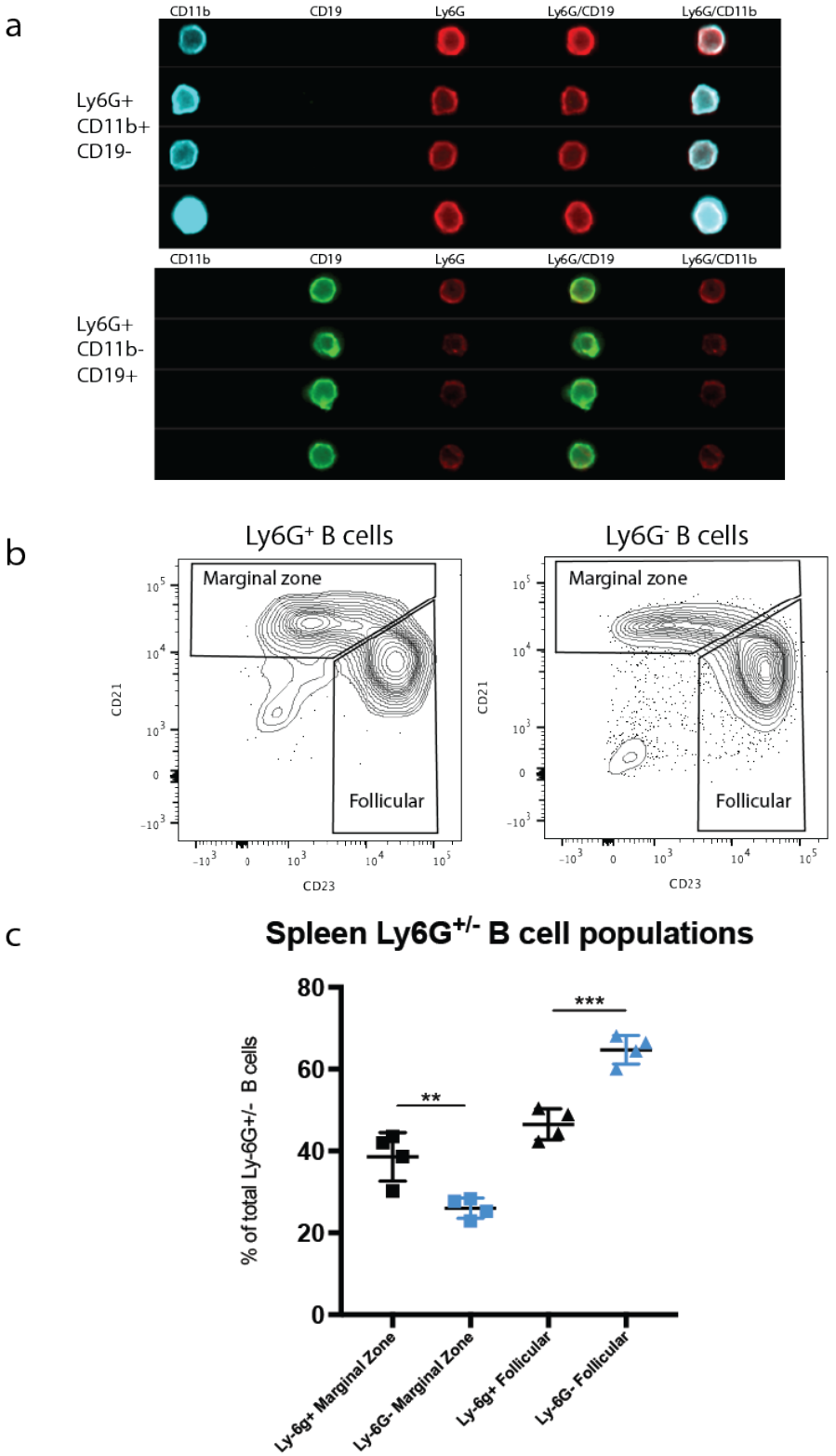

Figure 3.14 Characterization of Ly6g^{+} B cells

(**a**) Images from Imagestream imaging flow cytometer of Ly6g^{+} CD11b^{+} CD19- cells (top panel) and Ly6g^{+} CD11b- CD19^{+} cells (bottom panel). (**b**) Representative flow cytometry plots and quantification of Ly6g$^{+/-}$ follicular and marginal zone B cell populations in the spleen. n=4 mice, data are shown as mean ± SD. Data analysed by two-sided t test. ** P < 0.01, *** P < 0.001.

3.8 Ly6g expression on B cells appears to arise from B cell receptor binding to the Ly6g antibody

One possible reason for the observed expression of Ly6g on B cells is the binding of the B cell receptor (BCR) to an epitope it recognises on the Ly6g antibody. During development, antigen receptor genes in B cells undergo DNA recombination to generate diversity in the BCR repertoire. It is estimated that up to 10^{13} distinct BCRs could be generated through these mechanisms (Calis and Rosenberg, 2014), and it is therefore theoretically conceivable that a BCR antigen binding region could bind an epitope on the Ly6g antibody. This would result in erroneous positive staining and detection of expression of Ly6g during flow cytometry analysis.

This phenomenon has been previously documented in mice; a population of "Natural Killer B cells," cells with apparent characteristics of both Natural Killer cells and B cells was identified in a recent report (Wang et al., 2016). However, this population was subsequently shown to have been erroneously characterized this way due to binding of the BCR on these cells to an epitope on the Natural Killer marker antibody. This was demonstrated using MD4 genetically modified mice (Goodnow et al., 1988), which have a highly restricted BCR repertoire; in these mice the population of "Natural Killer B cells" disappeared, demonstrating that the detection of Natural killer cell markers on the B cells was due to BCR binding to epitopes on the detection antibodies (Kerdiles et al., 2017).

To test if this possibility were occurring with the $Ly6g^+$ B cell population I identified, I used transgenic mice that have a restricted BCR repertoire, such that almost all B cells in these mice express the same BCR, which recognises a given specific epitope ((Nowosad et al., 2016), eliminating the potential for a BCR to recognise and bind an epitope on the Ly6g antibody. Therefore, I performed a flow cytometry experiment using these BCR-restricted mice, comparing them to control mice. The $Ly6g^+$ B cell population completely disappears in the BCR mice (Figure 3.15), demonstrating that the observed Ly6g expression on B cells is likely due to BCR recognition and binding to an epitope on the Ly6g antibody, and unlikely to be due to actual expression of Ly6g by these cells.

Conclusions

- **Ly6g expression on these cells is due to binding of their B cell receptor to the Ly6g antibody, therefore they likely do not actually express Ly6g**

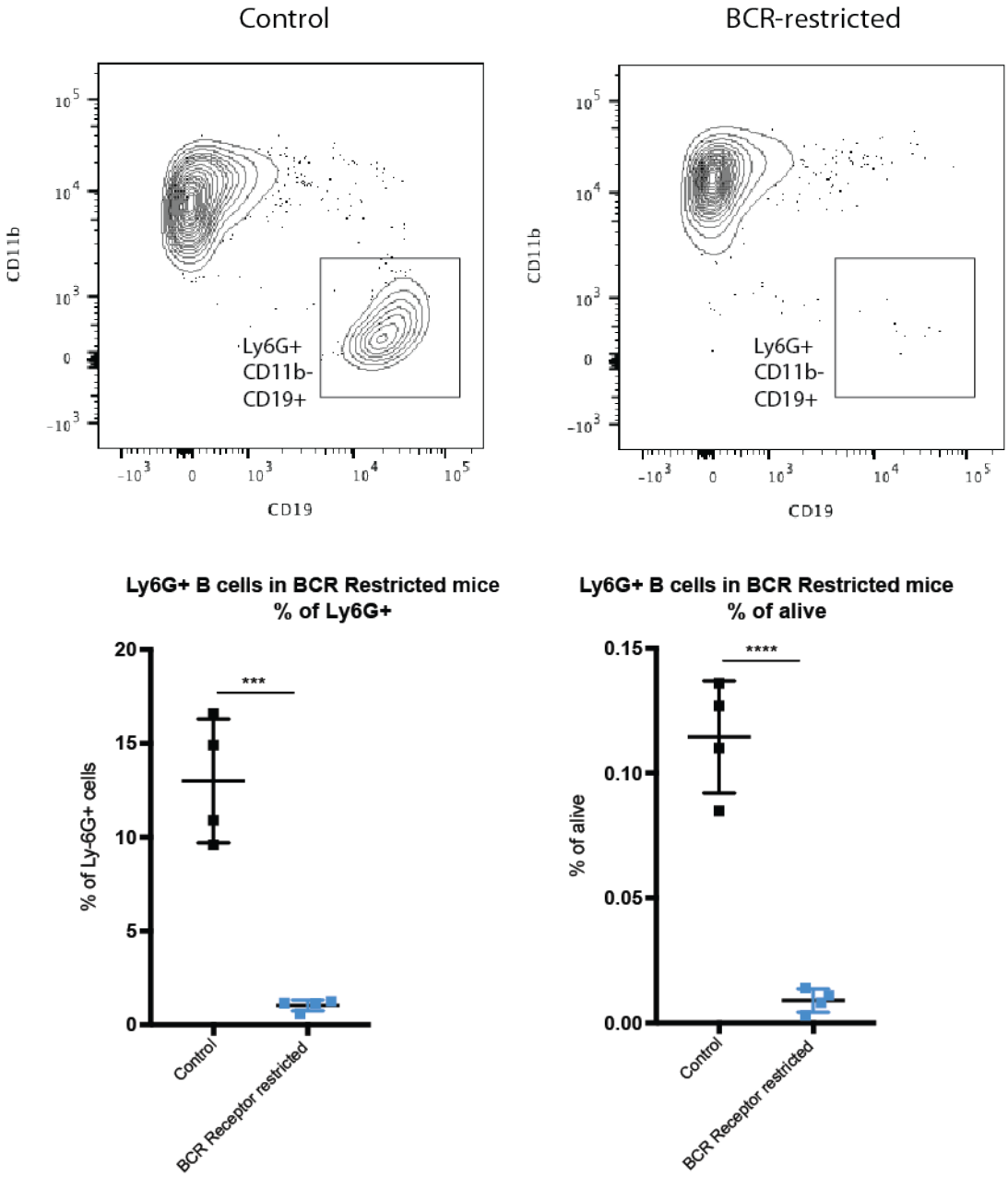

Figure 3.15 Ly6g^{+} B cell expression arises from binding of the BCR to the Ly6g antibody

Representative flow cytometry plots pre-gated on Ly6g quantification of Ly6g^{+} B cells in the spleen of control and BCR-restricted mice, n = 4 mice. Data are displayed as mean ± SD. Statistical analysis by two-sided t-test. *** P < 0.001, **** P < 0.0001.

3.9 Chapter Conclusions

- **Mass cytometry discovers mouse neutrophil heterogeneity at the surface marker level**
- **The presence and stage of a breast tumour alters this heterogeneity**
- **Populations identified by mass cytometry can also be detected using conventional flow cytometry**
- **MHC-II^{+} and F4/80^{+} populations of neutrophils decrease in the bone marrow of tumour-bearing mice**
- **A Ly6g^{+} CD11b^{-} population decreases in the spleens of tumour-bearing mice**
- **This population is in fact a mature B cell population**
- **Ly6g expression on this population is due to B cell receptor binding to the Ly6g antibody**

Chapter 4. Expansion of a CXCR2^{+} CD62L^{-} neutrophil population in the bone marrow and periphery of tumour-bearing mice

4.1 Chapter aims

In the previous chapter I described how mass cytometry analysis of control and tumour-bearing mice revealed a number of neutrophil populations that shift in response to the presence of a tumour. Bioinformatics analysis allowed the determination of markers defining these populations, this discovered a population of Ly6g^{+} CD11b^{-} cells that were ultimately revealed to be B cells. I next wanted to further investigate the heterogeneity identified by mass cytometry, in order to explore further populations and determine if the changes induced by a tumour are potentially meaningful.

Therefore, my aims in this chapter were:

- **Further exploration of neutrophil populations identified by mass cytometry**
- **To determine if the alterations in neutrophil heterogeneity observed in the MMTV-PYMT model can be observed in other mouse models of cancer**
- **Investigate how tumours perturb granulopoiesis in the bone marrow**

4.2 CXCR2$^+$ neutrophils are increased in the bone marrow and peripheral tissues in tumour-bearing mice

Mass cytometry identified almost all neutrophil populations in the lungs and spleen as CXCR2$^+$, except for the Ly6g$^+$ CD11b$^-$ population discussed in Chapter 3 Section 3.6. The Ly6g$^+$ CD11b$^-$ population were found to be B cells, which do not express CXCR2, hence why this population was not identified as CXCR2$^+$ by mass cytometry. In the bone marrow mass cytometry identified differential expression of CXCR2 on neutrophils, consistent with the literature. In particular, Phenograph analysis identified a population of CXCR2$^+$ neutrophils (Figure 4.1a b, bone marrow cluster 5), that was expanded in tumour-bearing mice, more strongly in metastatic samples.

CXCR2 (also known as CD182 or IL-8 receptor, beta) is a chemokine receptor expressed by neutrophils and a number of other cell types (but not B cells, hence why CXCR2 expression was not detected on the Ly6g$^+$ CD11b- population). CXCR2 binds to a number of ligands, principally the chemokines CXCL1,2,3,5,6,7 and 8 (Veenstra and Ransohoff, 2012). Neutrophils first express CXCR2 at the promyelocyte stage of development (McKinstry et al., 1997). As neutrophils mature, they upregulate CXCR2 expression, which allows eventual egress of mature bone marrow neutrophils, which are attracted into the circulation by the release of CXCL1 and CXCL2 from endothelial cells and megakaryocytes in the blood (Köhler et al., 2011, Eash et al., 2010). Once in the circulation, neutrophils use CXCR2 to detect and respond to inflammation: CXCL-X chemokines are released from cells in tissues in response to inflammatory stimuli. Neutrophils bind these chemokines with CXCR2, promoting their extravasation from the circulation and chemotaxis through the tissue to the site of inflammation.

Flow cytometry analysis confirmed the CXCR2 results from the mass cytometry analysis (Figure 4.1c, d), namely an expansion of the CXCR2$^+$ population in the bone marrow of tumour-bearing mice, the tumour burden in this experiment being pre-metastatic. This was only observed when the population was analysed as a proportion of Ly6g$^+$ CD11b$^+$ cells. When the CXCR2$^+$ population is calculated as a proportion of total live cells in the tissue it expands across bone marrow, and also

the lungs and spleen. I also extended my analysis into the blood and liver, to provide a broader picture of changes in neutrophil heterogeneity. I also found an increase of $CXCR2^+$ cells in the blood and liver of tumour-bearing mice (Figure 4.1d).

Therefore, I find an expansion of $CXCR2^+$ $Ly6g^+$ $CD11b^+$ cells as a proportion of total cells in the bone marrow, lungs, spleen, liver and blood of tumour-bearing mice. However, this is a consequence of the expansion of total $Ly6g^+$ cells in the tissue, because almost all $Ly6g^+$ cells outside the bone marrow are also $CXCR2^+$. Thus, the key shift in CXCR2 expression within neutrophil populations is in the bone marrow, where the increase in $CXCR2^+$ cells also occurs as a proportion of $Ly6g^+$ $CD11b^+$ cells, meaning that the bone marrow will contain more neutrophils with the capacity to leave the bone marrow and enter the circulation of tumour-bearing mice.

Conclusions

- **Mass cytometry reveals an expansion of $CXCR2^+$ neutrophils in the bone marrow of tumour-bearing mice**
- **Flow cytometry confirms this finding**

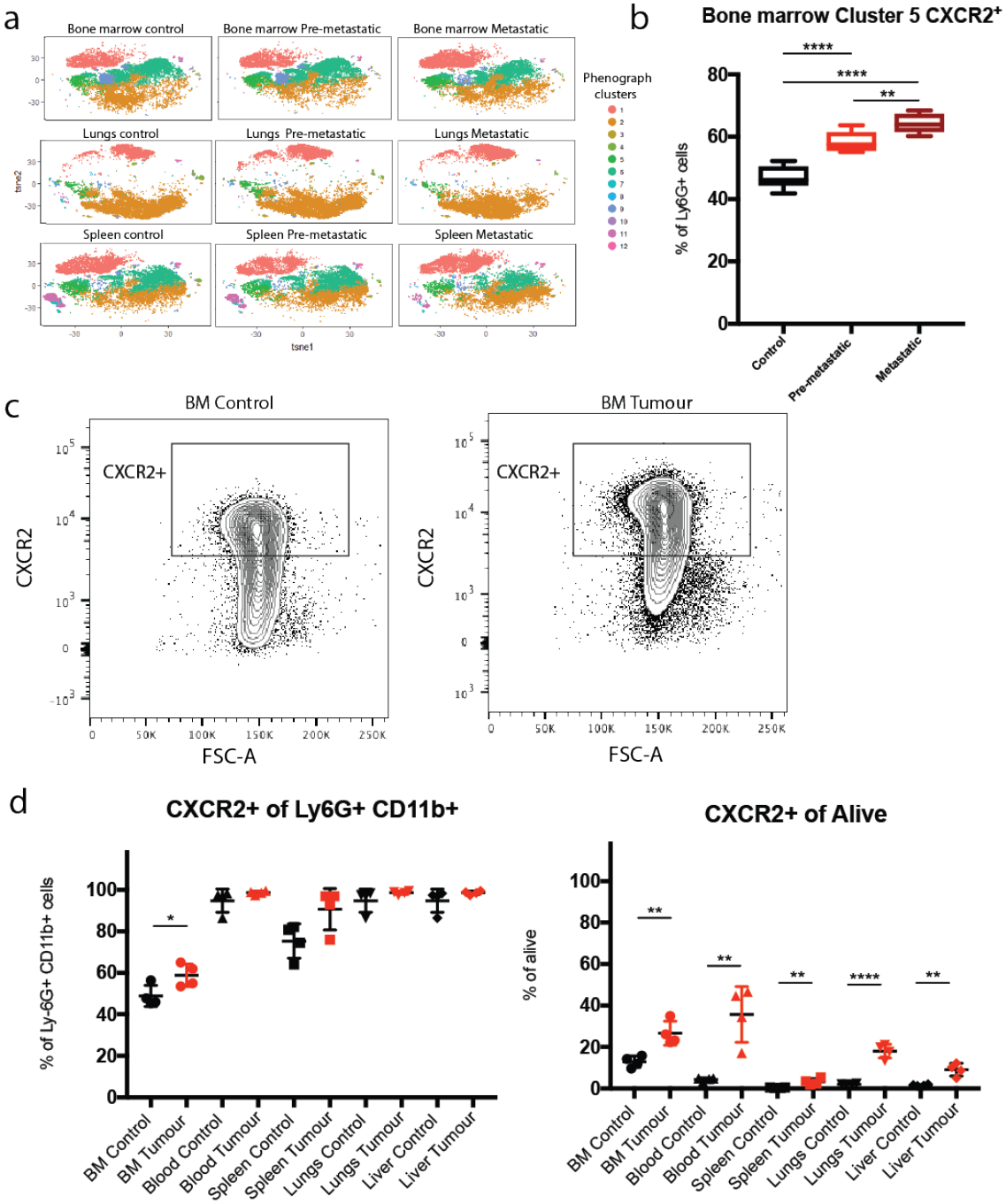

Figure 4.1 CXCR2$^+$ neutrophils are increased in the bone marrow and periphery in tumour-bearing mice

(**a**) Phenograph analysis of Ly6g$^+$ cells. (**b**) Quantification of mass cytometry analysis of Cluster 5 Ly6g$^+$ CXCR2$^+$ cells in the bone marrow. Data are displayed as Tukey box and whiskers plot, n=9 mice (**c**) Representative flow cytometry plots, pre-gated on Ly6g$^+$ CD11b$^+$ cells, showing CXCR2 expression on bone marrow neutrophils (**d**) Flow cytometric quantification of Ly6g$^+$ CD11b$^+$ CXCR2$^+$ cells in control and tumour-bearing mice, analysed as a percentage of total Ly6g$^+$ CD11b$^+$ cells and as a percentage of total alive cells in the tissue. n = 4 mice, data are displayed as mean ± SD. Statistical analysis by two-sided t-test. * P < 0.05, ** P < 0.01, *** P < 0.001, **** P < 0.0001.

4.3 CD62L$^-$ neutrophils increase in the bone marrow and peripheral tissues in tumour-bearing mice

Phenograph identified CD62L as a marker defining populations of neutrophils. In particular, CD62L$^-$ neutrophils expanded in the bone marrow and spleen in tumour-bearing mice in the mass cytometry results, with this effect dependent on tumour stage (Figure 4.2a, b, cluster 2). However, whilst this population could be detected in the lungs, there was no difference in this population between control and tumour-bearing mice. In fact, all lung neutrophils were CD62L$^-$ in the mass cytometry results.

Flow cytometry analysis validated these findings in the bone marrow, spleen, blood and liver (Figure 4.3a, b), the tumour burden in this experiment being pre-metastatic. The CD62L$^-$ population of neutrophils expands significantly in all of these tissues in tumour-bearing mice. In the blood, spleen and liver the CD62L$^-$ fraction comes to dominate the total neutrophil compartment; in the control mice CD62L$^-$ neutrophils are approximately 10%, 20% and 15% of blood, spleen and liver neutrophils respectively, but in tumour-bearing mice these neutrophils increase to become 57%, 45% and 70% of the corresponding tissue neutrophil compartment. This effect is further heightened when looking at the CD62L$^-$ neutrophils as a proportion of total alive cells in the tissue; they are almost non-existent in the blood, spleen and liver, comprising less than 0.3% of total alive cells in these tissues in control mice. But in tumour-bearing mice they rise to 13%, 3.5% and 2.5% of blood, spleen and liver cells respectively, approximately a 100-fold increase in the blood, and a 10-fold increase in the spleen and liver. This is due to a combination of the expansion of the total Ly6g$^+$ population, and the expansion of the CD62L$^-$ population within the Ly6g$^+$ compartment. The overall effect is that the CD62L$^-$ population changes from being barely present in the tissue in a control setting, to becoming at least approximately 2% of live cells in a tumour-bearing context.

Flow cytometry also validated the finding from mass cytometry that all lung neutrophils are CD62L$^-$ (Figure 4.3a, b), with no difference between control and tumour-bearing samples when this population is calculated as a percentage of total Ly6g$^+$ cells. However, the lung CD62L$^-$ neutrophil population increases significantly

in tumour-bearing mice when measured as a percentage of total alive cells in the tissue. This is again due to the expansion of total $Ly6g^+$ cells in tumour-bearing mice, and is particularly accentuated in the lungs because all the neutrophils in the lungs are $CD62L^-$. The lack of CD62L expression on lung neutrophils will be explored in further detail in section 4.4.

CD62L is a cell adhesion molecule expressed by leukocytes, including T cells, monocytes, eosinophils and neutrophils (Ivetic, 2018). In neutrophils, the established principal function of CD62L is in the tethering and rolling of neutrophils along the endothelial wall. CD62L binds to target sugar moieties on endothelial cells allowing neutrophils to arrest in the circulation and subsequently extravasate into a tissue in order to respond to an inflammatory stimulus.

CD62L is expressed by early myeloid progenitors and mature neutrophils in the bone marrow, but is downregulated at the intermediate stages of neutrophil development (Lund-Johansen and Terstappen, 1993). Another important aspect of CD62L biology is CD62L "shedding:" the extracellular domain of CD62L contains a cleavage site nine amino acids up from the cell membrane. Cleavage at this site results in "shedding" of CD62L from the cell membrane. This can be triggered by numerous cues, including during rolling and tethering to the endothelium, pro-inflammatory stimuli and neutrophil activation (Ivetic, 2018). The cytosolic tail of L-selectin can also interact with numerous cytosolic proteins, transmit signals and affect CD62L shedding (Ivetic et al., 2019).

Conclusions

- **Flow cytometry confirms a significant expansion of $CD62L^-$ neutrophils in the bone marrow and spleen of tumour-bearing mice, and additionally shows this population expands in the blood**
- **CD62L expression cannot be detected on lung neutrophils, in both control and tumour-bearing mice**

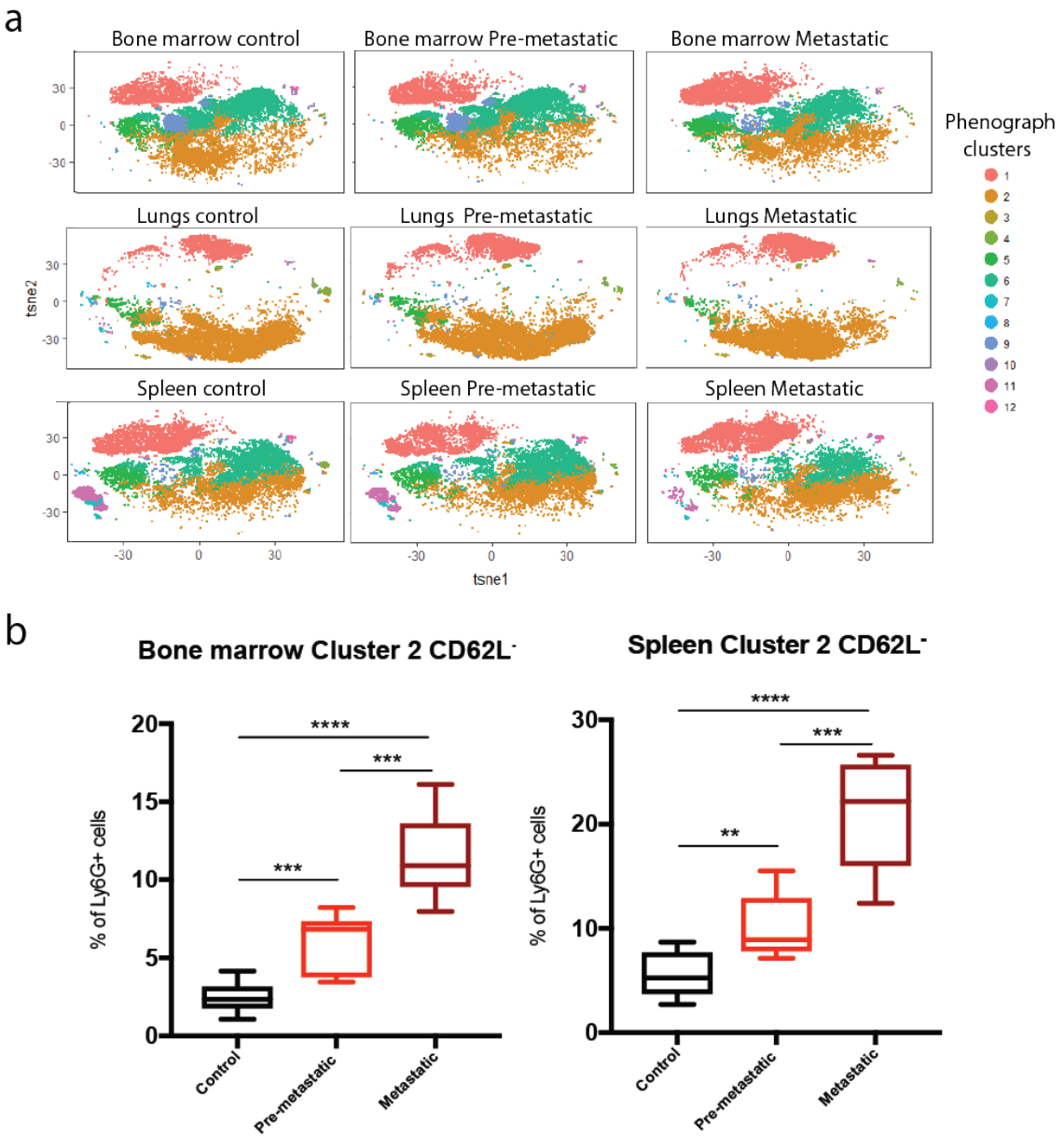

Figure 4.2 Mass cytometry identifies a CD62L- neutrophil population that is increased in tumour-bearing mice

(**a**) Phenograph analysis of Ly6g+ cells. (**b**) Quantification of mass cytometry analysis of Cluster 2 Ly6g+ CD62L- cells in the bone marrow. Data are displayed as Tukey box and whiskers plot, n=9 mice. ** P < 0.01, *** P < 0.001, **** P < 0.0001.

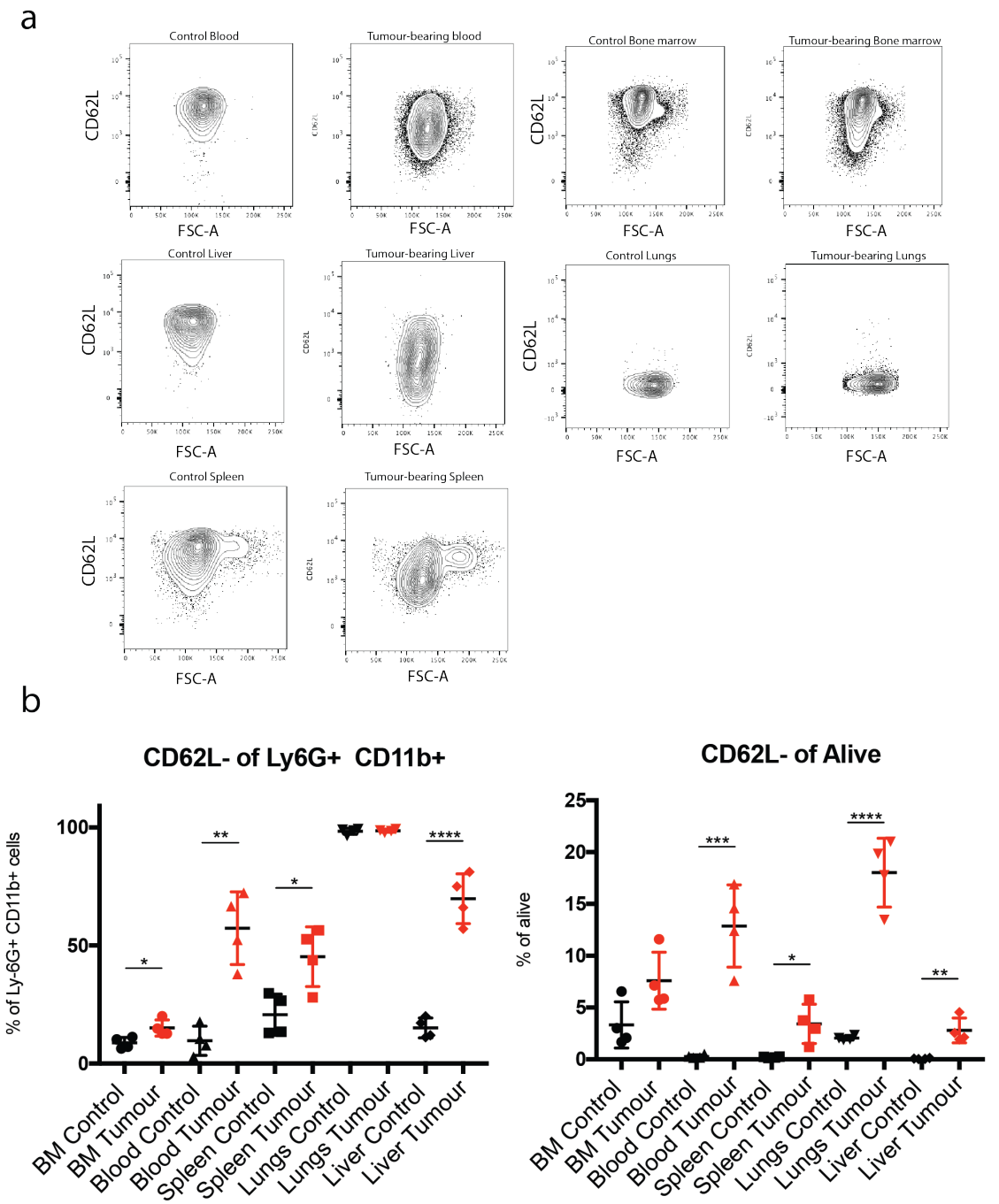

Figure 4.3 Flow cytometry reveals an expansion of CD62L$^-$ neutrophils in the bone marrow, circulation and periphery of tumour-bearing mice

(**a**) Representative flow cytometry plots, pre-gated on Ly6g+ CD11b+ cells, showing CD62L expression on neutrophils. (**b**) Flow cytometric quantification of Ly6g+ CD11b+ CD62L- cells in control and tumour-bearing mice, analysed as a percentage of total Ly6g+ CD11b+ cells and as a percentage of total alive cells in the tissue. n = 4 mice, data are displayed as mean ± SD. Statistical analysis by two-sided t-test. * P < 0.05, ** P < 0.01, *** P < 0.001, **** P < 0.0001.

4.4 Lung Neutrophils express low levels of CD62L

In the lungs, neutrophil expression of CD62L could not be detected by flow cytometry, in both control and pre-metastatic tumour-bearing mice, mimicking the mass cytometry results (Figure 4.2, Figure 4.3). One possible explanation for this is that the lungs were enzymatically digested during the generation of single cell suspensions from tissue: it has been shown that, during tissue digestion, enzymes can cleave surface markers from the cell membrane, or cleave the surface marker in such a way as to obscure the epitope recognised by the detecting antibody, resulting in a false negative lack of detection of expression by flow cytometry (Autengruber et al., 2012). This has been observed for CD62L and a number of other surface markers. For flow and mass cytometry I generated single cell suspensions of bone marrow, spleen and liver by cutting and mashing tissue, and CD62L expression was readily detectable in all these tissues. The lungs were the only tissue I subjected to enzymatic digestion, as they require this due to their more complex extracellular matrix, and they were the only tissue in which CD62L expression could not be detected. Therefore, it is possible that the lack of CD62L expression observed on lung neutrophils is due to enzymatic digestion of CD62L during sample preparation.

To test this hypothesis, I used an alternative method of lung digestion, the OctoMACS gentle dissociation kit from Miltenyi (see section 2.6) The manufacturers claim that this kit breaks down the tissues structure effectively, allowing generation of a single cell suspension, but preserves cell surface markers that are commonly cleaved by enzymatic digestion, including CD62L. I therefore took lungs from control and tumour-bearing mice, split them, and digested half by enzymatic digestion and the other half using the OctoMACS gentle dissociation kit. I then generated single cell suspensions from the digested tissue and performed flow cytometry analysis of CD62L expression. The use of the gentle dissociation kit revealed CD62L expression on approximately 20-30% of lung neutrophils, with the remaining 70-80% negative for CD62L (Figure 4.4a), with enzymatic digestion still resulting in no positive expression of CD62L. Importantly, there is no difference between control and tumour-bearing samples (Figure 4.4b), the tumour burden in this experiment being pre-metastatic. Enzymatic digestion thus appears to be responsible for a portion of

the lack of CD62L expression in enzymatically digested lungs, but does not account for at least 70% of negative CD62L expression.

Flow cytometry plots from spleens dissected from the same mice are shown for reference; these spleens were processed for flow cytometry by the standard methods described previously (Section 2.6), and the neutrophils display a pattern of CD62L expression similar to that found in previous flow cytometry and mass cytometry results, with the majority of neutrophils being $CD62L^+$ in control mice and a shift towards $CD62L^-$ neutrophils in tumour-bearing mice (Figure 4.4c).

It is possible that despite the manufacturer's claims, there is still some cleavage of CD62L by the gentle dissociation method. To explore this possibility, I also investigated CD62L expression on $CD3^+$ T cells in the lungs. In enzymatically digested lungs, I could detect almost no expression of CD62L on T cells (Figure 4.5a, left), mimicking CD62L expression on neutrophils from enzymatically digested lungs (Figure 4.4a). However, when lungs were dissociated via the gentle method I could observe a major shift in CD62L expression, with almost all T cells now expressing CD62L (Figure 4.5a, right). Comparison of CD62L expression between gentle and enzymatic dissociation shows that gentle dissociation results in a large shift in almost all T cells towards high CD62L expression, but only a minor shift for a proportion of neutrophils towards more moderate CD62L expression (Figure 4.5b).

These results indicate that the gentle dissociation kit is highly effective at preserving CD62L expression on T cell. Thus, the gentle dissociation kit appears to function effectively on cells other than neutrophils, suggesting that it is not solely enzymatic cleavage that explains my observation of low CD62L expression on neutrophils in the lungs.

There is some evidence in the literature that the tight lung vasculature can induce downregulation of CD62L expression by lung neutrophils (Kolaczkowska and Kubes, 2013, Kreisel et al., 2010) and this may explain why even gentle dissociation does not restore lung neutrophil CD62L expression to that of neutrophils in other tissues (see Discussion Section 6.2.4). Regardless of the ultimate explanation, CD62L expression was not readily detectable on lung neutrophils in a manner similar to

neutrophils in the other tissues investigated. This precluded detection, in the lungs, of the shift in CD62L expression on neutrophils observed in bone marrow, blood, spleen and liver of tumour-bearing mice.

Conclusions

- **Lung neutrophils have low or negative expression of CD62L, regardless of mouse tumour presence or stage**
- **This phenotype is not principally due to tissue dissociation methods**
- **This prevents detection of a shift in CD62L expression in the lungs of tumour-bearing mice**

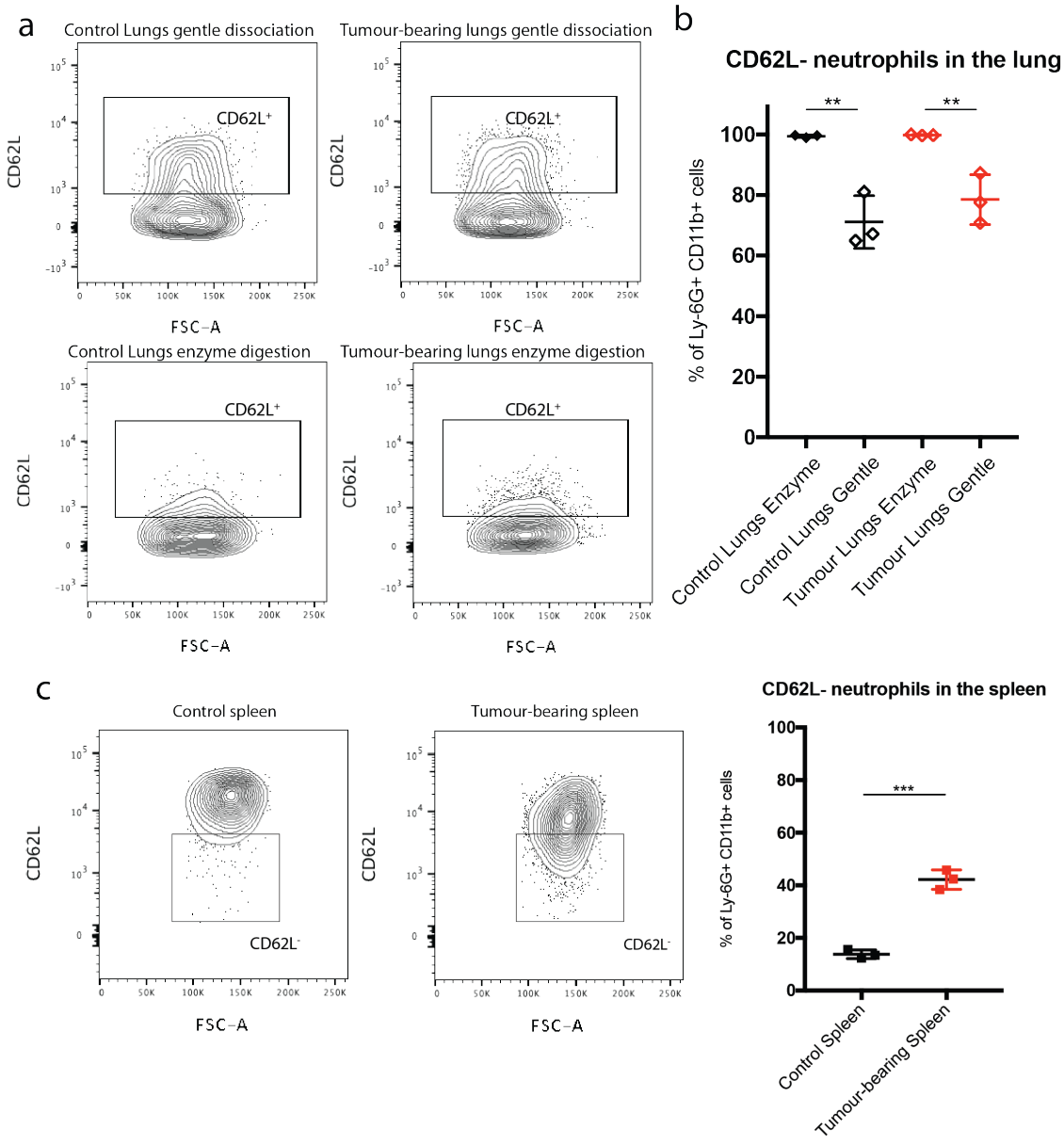

Figure 4.4 Lung neutrophils express low levels of CD62L

(**a**) Flow cytometry plots displaying CD62L expression on lung Ly6g^{+} CD11b^{+} cells from control and tumour-bearing mice. Top plots display CD62L expression in lungs digested by gentle digestion, bottom plots lungs digested by enzymatic digestion. CD62L+ cells are gated (**b**) Flow cytometric quantification of CD62L- neutrophils in lungs from control and tumour-bearing mice. Lungs were dissociated by gentle digestion or enzymatic digestion. n = 3 mice. (**c**) Flow cytometry plot and quantification of CD62L- neutrophils in the spleen of control and tumour-bearing mice (spleens were dissected from the same mice used in (**a, b**)). n = 3 mice. Data are displayed as mean ± SD. Statistical analysis by two-sided t-test. *P < 0.05, ** P < 0.01, *** P < 0.001, **** P < 0.0001.

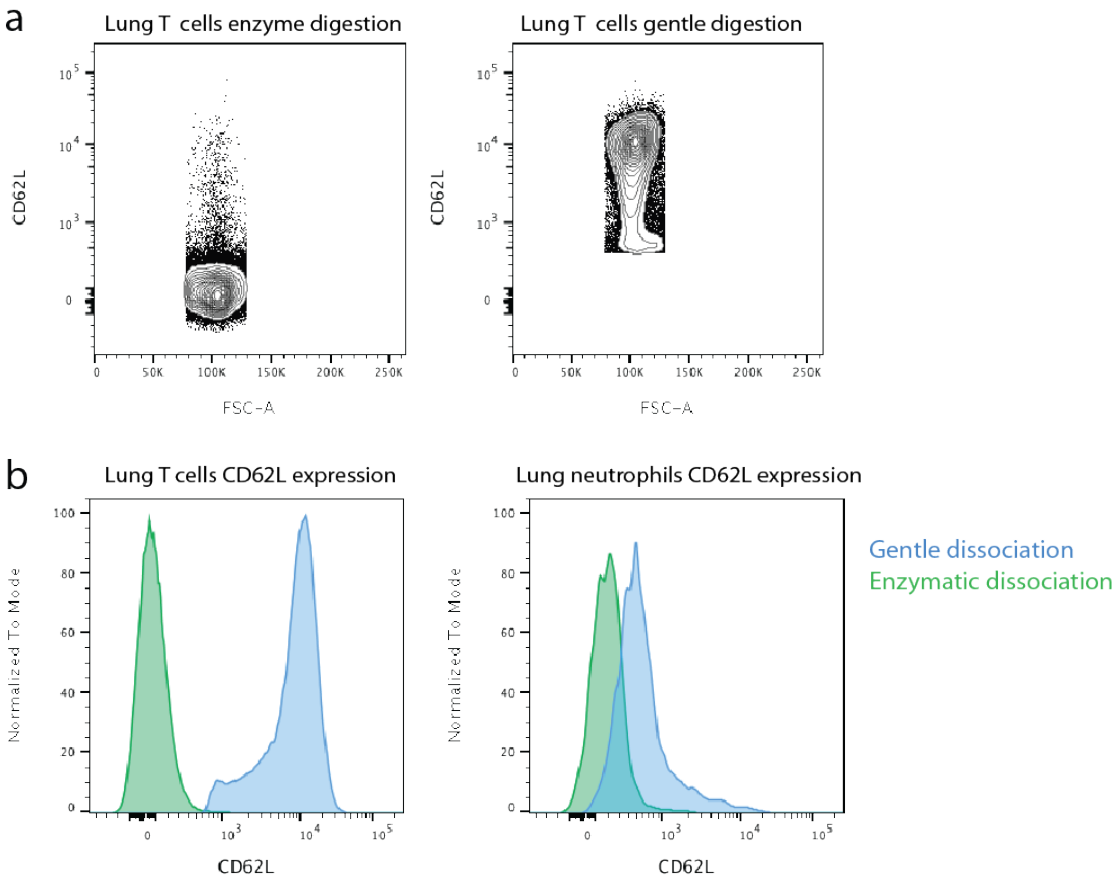

Figure 4.5 CD62L expression on lung T cells

(**a**) Flow cytometry plot displaying CD62L expression on CD3+ T cells in lungs dissociated by gentle dissociation or enzymatic digestion. (**b**) Representative histograms of CD62L expression, determined by flow cytometry, on lung T cells and lung neutrophils, from lungs either gently dissociated (blue) or enzymatically digested (green).

4.5 Intracellular staining of CD62L$^-$ neutrophils shows that they express negative internal levels of CD62L

As mentioned in section 4.3 neutrophils can shed CD62L from their cell membrane. This typically occurs during neutrophil activation and response to inflammatory stimuli and also during tethering and rolling along the endothelium (Ivetic, 2018). The flow or mass cytometry experiments I have performed only used cell surface staining for CD62L.Therefore, when flow or mass cytometry detect a neutrophil as CD62L$^-$ it is possible that this neutrophil has only transiently lost expression of CD62L from the surface due to shedding, and will soon re-express CD62L, as there is typically cytoplasmic CD62L that can be shuttled to the membrane (Ivetic et al., 2019). This is of potential significance because it might have consequences for functional phenotypic differences between CD62L$^+$ and CD62L$^-$ cells, because CD62L$^-$ cells might have the potential to re-express CD62L on their surface and therefore effects mediated by this molecule (e.g. cell migration and adhesion, intracellular signalling) could potentially occur relatively quickly in a cell initially defined as CD62L$^-$. Alternatively, CD62L$^-$ cells may have downregulated expression internally as well as losing expression on their surface, suggesting that they do not have cytoplasmic CD62L that can allow rapid re-expression of CD62L lost from the surface, meaning that effects mediated by CD62L may not be able to readily occur in these cells.

To investigate these possibilities, I took bone marrow and spleen from control and pre-metastatic tumour-bearing mice. After generating single-cell suspensions I split the samples. I performed extracellular staining for CD62L on one half, and on the other I performed intracellular staining for CD62L (for both stainings I used extracellular staining of Ly6g and CD11b to identify neutrophil populations). I found that the extracellular and intracellular stainings are very similar in both tissues from control and tumour-bearing mice (Figure 4.6a-d). There is a clear increase in CD62L$^-$ neutrophils in the bone marrow and spleen of tumour-bearing mice, regardless of intracellular or extracellular staining.

This result shows that the CD62L$^-$ neutrophils lack not just CD62L expression on their surface but also express low levels of CD62L in their cytosol. This suggests a

genuine difference in expression of CD62L between cells that are detected as $CD62L^+$ or $CD62L^-$.

Conclusions

- **$CD62L^-$ neutrophils in the bone marrow and spleen have low surface expression and low internal expression of CD62L**

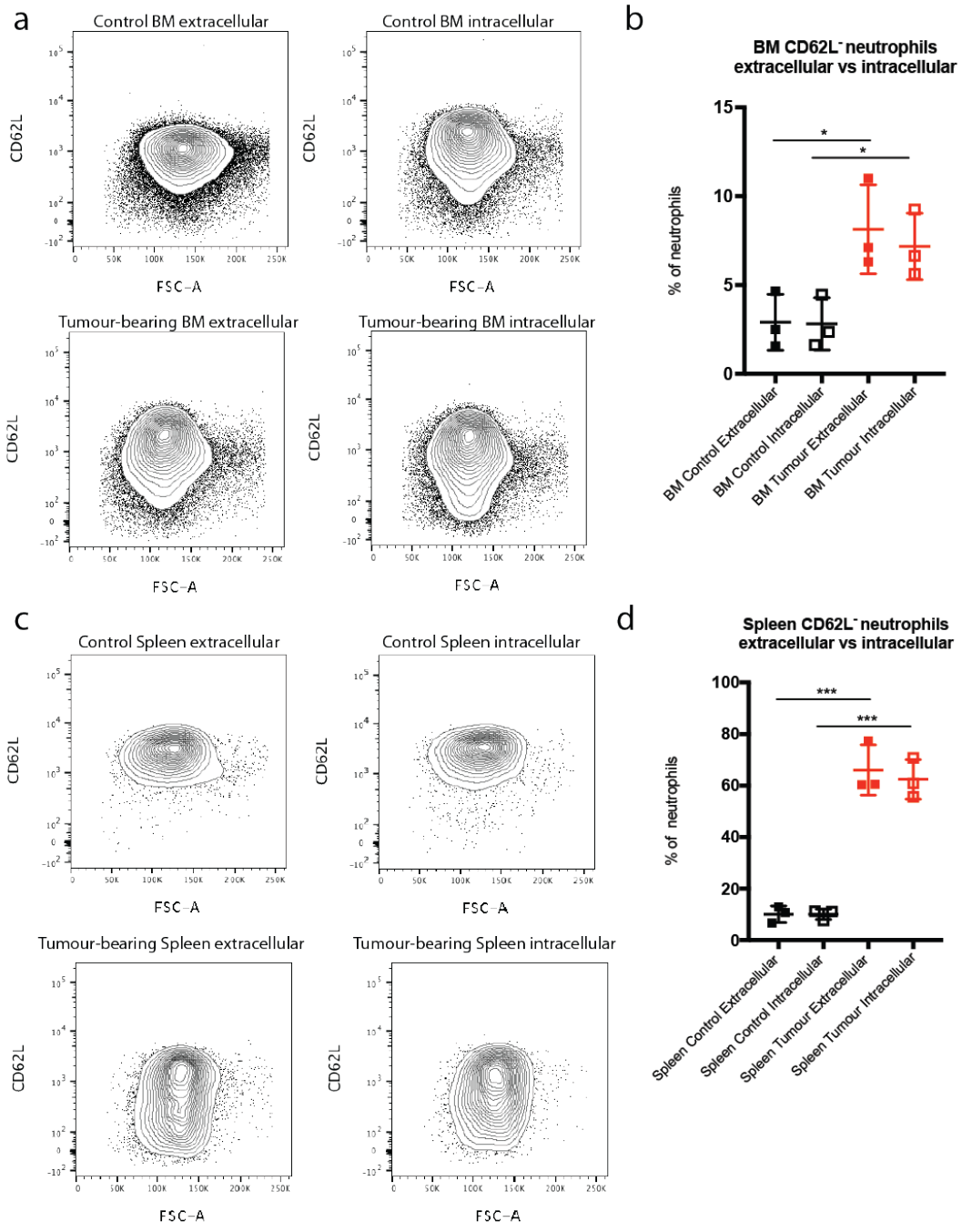

Figure 4.6 Extracellular and intracellular expression of CD62L in bone marrow and spleen neutrophils

(**a**) Flow cytometry plots displaying extracellular and intracellular CD62L expression in bone marrow neutrophils from control and tumour-bearing mice**.** (**b**) Quantification of flow cytometry analysis of CD62L- bone marrow neutrophils from control and tumour-bearing mice. n=3 mice (**c**) Flow cytometry plots displaying extracellular and intracellular CD62L expression in spleen neutrophils from control and tumour-bearing mice**.** (**d**) Quantification of flow cytometry analysis of CD62L- spleen neutrophils from control and tumour-bearing mice. n = 3 mice. Data are displayed as mean ± SD. Statistical analysis by two-sided t-test. * $P < 0.05$, ** $P < 0.01$, *** $P < 0.001$, **** $P < 0.0001$.

4.6 $CXCR2^+$ $CD62L^-$ neutrophils expand in the bone marrow, blood, spleen and liver of tumour-bearing mice. This expansion is dependent on tumour size and stage.

In sections 4.2 and 4.3 I showed that $CXCR2^+$ and $CD62L^-$ neutrophils expand in tumour-bearing mice. I next wanted to investigate co-expression of these markers on neutrophils, in order to see if this might provide further insight into how neutrophils change in response to a tumour. I therefore used flow cytometry to look at expression of both of these markers on neutrophils. I found that a population of $CXCR2^+$ $CD62L^-$ neutrophils can be detected in the bone marrow, blood, spleen and liver in control mice (Figure 4.7a), this population expands in all these tissues in pre-metastatic tumour-bearing mice, both as a proportion of $Ly6g^+$ cells, but also as a proportion of total live cells in the tissue (Figure 4.7b). In control blood, spleen and liver the mean of the $CXCR2^+$ $CD62L^-$ population is less than 0.2% of live cells, but in tumour-bearing mice, the mean of this population increases to 13% of blood cells, and slightly above 2.5% of spleen and liver cells, representing greater than a 10-fold increase in all three tissues. In the bone marrow, the change is less pronounced because the population is present in higher numbers in control mice, but there is still an increase greater than 3-fold; from a mean of 1.7% in control mice to 6.6% in tumour-bearing mice.

Over 95% of $Ly6g^+$ $CD11b^+$ neutrophils in the blood, spleen and liver are $CXCR2^+$, thus the increases in the $CXCR2^+$ $CD62L^-$ population in these tissues in tumour-bearing mice are very similar in number and proportion to the increases in CD62L-neutrophils (Figure 4.3). Therefore, the key marker defining the shift is CD62L. However, in the bone marrow, there is much greater variation in neutrophil CXCR2 expression (Figure 4.1b), with negative and positive populations; however, an increase in the $CXCR2^+$ $CD62L^-$ population can still be observed. Based on its CXCR2 expression, this population in the bone marrow is likely to be mature.

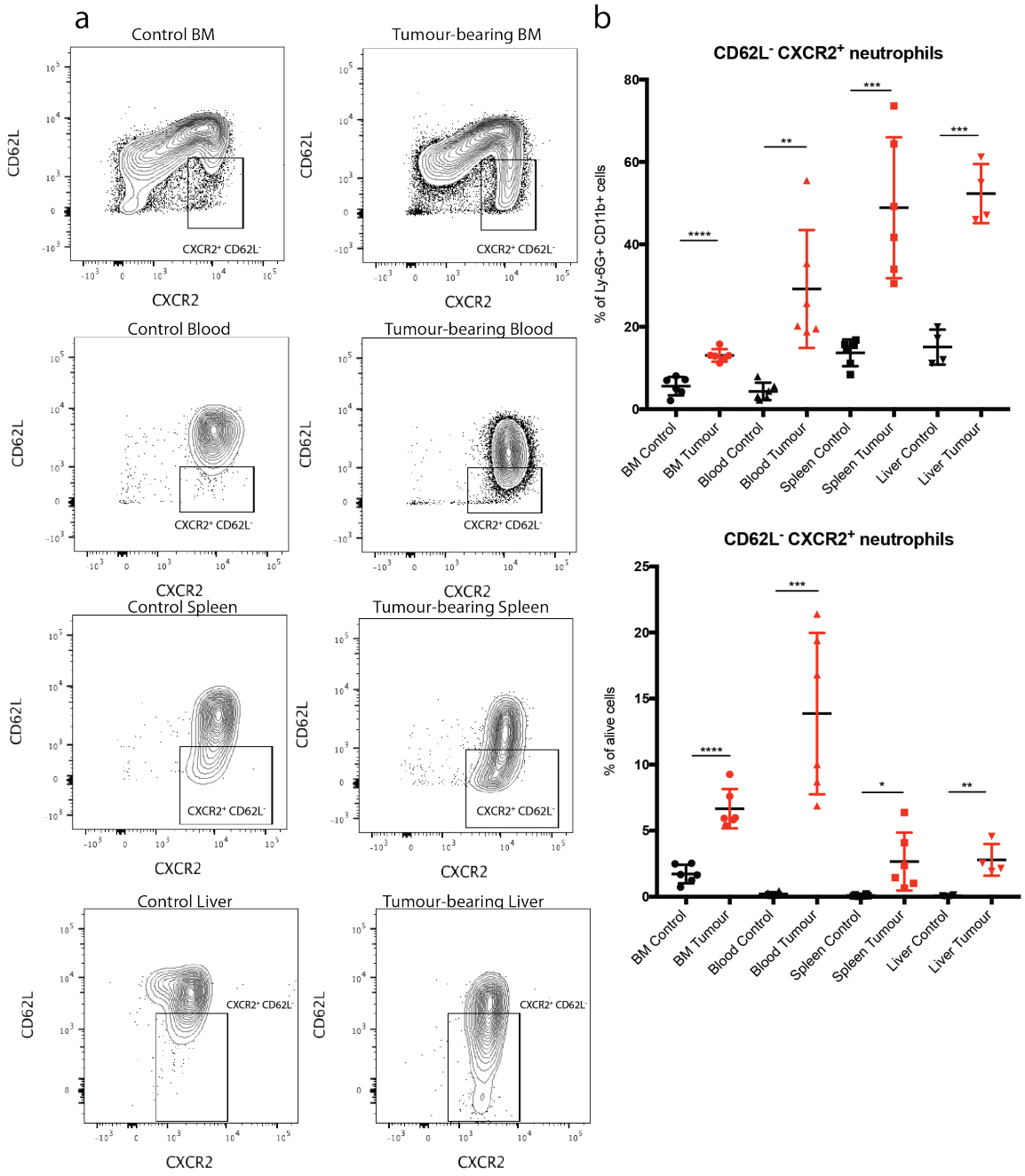

Figure 4.7 CXCR2$^+$ CD62L$^-$ neutrophils increase in the bone marrow and periphery of tumour-bearing mice

(**a**) Representative flow cytometry plots displaying expression of CXCR2 and CD62L on Ly6g$^+$ CD11b$^+$ neutrophils from control and tumour-bearing mice. Gates show the CXCR2$^+$ CD62L- population. (**b**) Flow cytometric quantification of CXCR2$^+$ CD62L- neutrophils from control and tumour-bearing mice as a proportion of Ly6g$^+$ CD11b$^+$ cells (top) or total live cells (bottom). n=6 mice for all conditions except Liver Control and Liver Tumour for which n=4 mice. Data are shown as mean ± SD. Data are displayed as mean ± SD. * P < 0.05, ** P < 0.01, *** P < 0.001, **** P < 0.0001.

I next wanted to determine how the size and stage of a tumour affects the $CXCR2^+$ $CD62L^-$ population across different tissues. I therefore used mice with induced PyMT tumours at three different stages:

- Small tumours (<0.5g), 2.5 weeks post-injection
- Medium tumours (0.5g-1.0g), 3.5 weeks post-injection
- Large tumours (1.3g-2.0g), 5 weeks post-injection

I also used MMTV-PyMT transgenic mice, which spontaneously develop tumours at 6-7 weeks of age. Instead of a single tumour from an injection, these mice will develop tumours at mammary glands all over the mouse, leading to a greater tumour burden and more metastasis. I used spontaneous PyMT mice at two stages:

- Small tumours (total tumour weight 1.0-2.0g)
- Large tumours (total tumour weight 2.5g-4.5g)

Tumour weights for all mice used are shown in Figure 4.8a.

I investigated neutrophil numbers and the $CXCR2^+$ $CD62L^-$ population in the bone marrow, spleen and blood of control mice and tumour-bearing mice at all five stages. As demonstrated previously (Figure 3.1), neutrophil numbers increase in tumour-bearing mice in the bone marrow, blood and spleen (Figure 4.8b-d). This increase is affected by tumour stage, with the large implanted tumours and large spontaneous tumours showing the greatest expansion of neutrophils, and the small implanted tumour mice displaying only a limited expansion of neutrophils compared to control mice. There is an approximate dose-response effect: as tumour size and stage increase, neutrophil numbers increase in tandem. However, this effect is not exact and varies by tissue.

The $CXCR2^+$ $CD62L^-$ population also expands in all three tissues, both as a proportion of $Ly6g^+$ cells and as a proportion of live cells in the tissue (Figure 4.9, 4.10). As with the neutrophil expansion there is an approximate dose-response effect for the $CXCR2^+$ $CD62L^-$ population and tumour size stage, but again this effect is not always exact and varies between tissues.

It is important to note that the relative contributions of tumour size versus tumour stage cannot be determined from these results.

Conclusions

- **A $CXCR2^+$ $CD62L^-$ population of neutrophils expands in the bone marrow, blood, spleen and liver of tumour-bearing mice**
- **The extent of this expansion is dependent on the size and stage of tumour, with the $CXCR2^+$ $CD62L^-$ population coming to dominate the total neutrophil population in mice with large, late-stage, metastatic tumours**

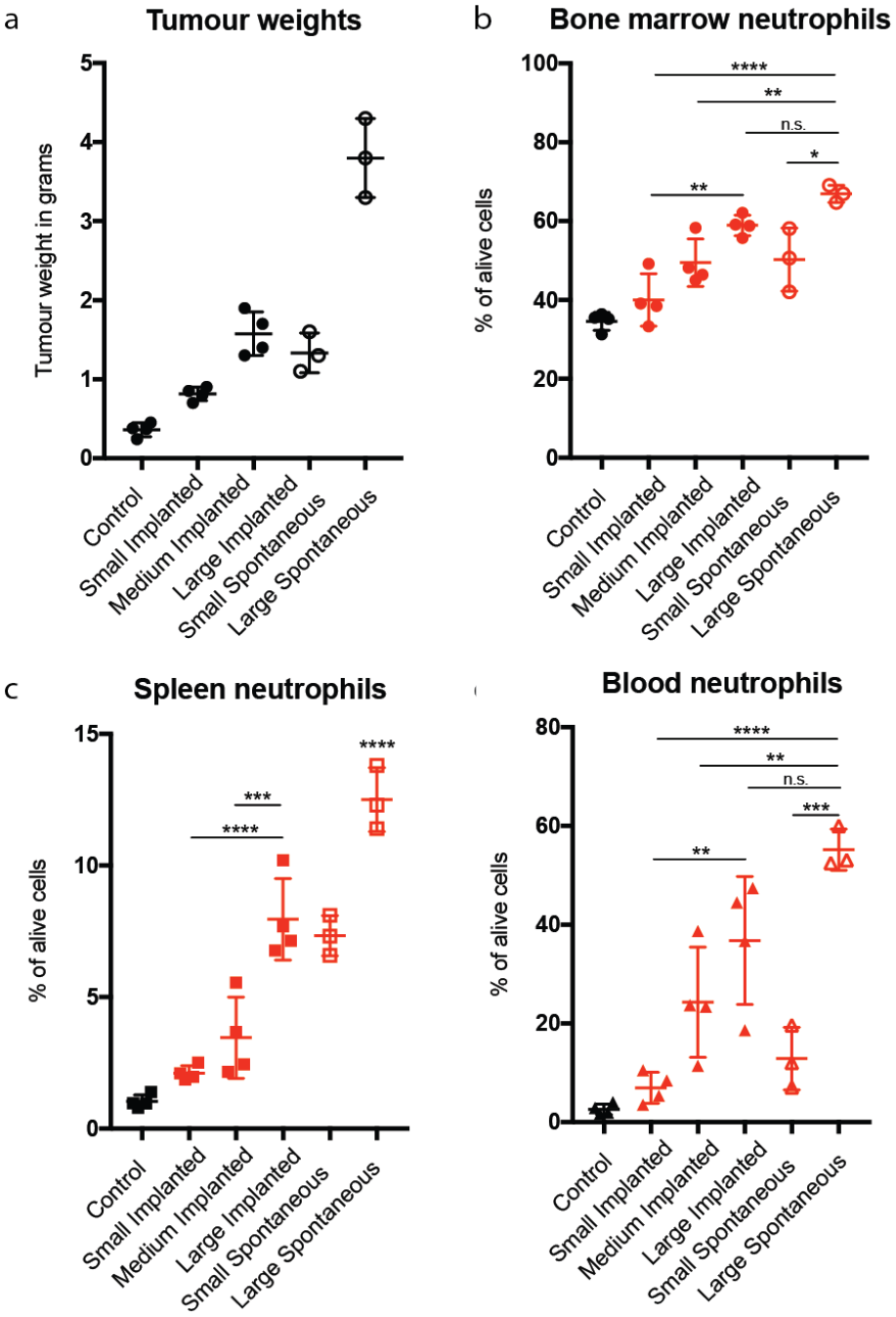

Figure 4.8 Tumour size and stage affects neutrophil numbers in the bone marrow, spleen and blood

a) Tumour weights from tumour-bearing mice at different tumour sizes and stages. (**b-d**) Flow cytometric quantification of $Ly6g^+$ $CD11b^+$ neutrophils as a proportion of total live cells in the (**b**) bone marrow, (**c**) spleen and (**d**) blood from control and tumour-bearing mice. n=4 mice for Small Induced, Medium Induced and Large Induced, n=3 for Small Spontaneous and Large Spontaneous. Data are displayed as mean ± SD. Statistical analysis by one-way ANOVA with Bonferroni's correction for multiple comparisons. Not all statistical comparisons are displayed for clarity. Tables for all statistics calculated in this experiment are in appendix section 7.2. * $P < 0.05$, ** $P < 0.01$, *** $P < 0.001$, **** $P < 0.0001$. n.s., not significant. **** on Large Spontaneous in spleen neutrophils indicates that the mean of this sample was significantly greater than all other samples at $P < 0.0001$.

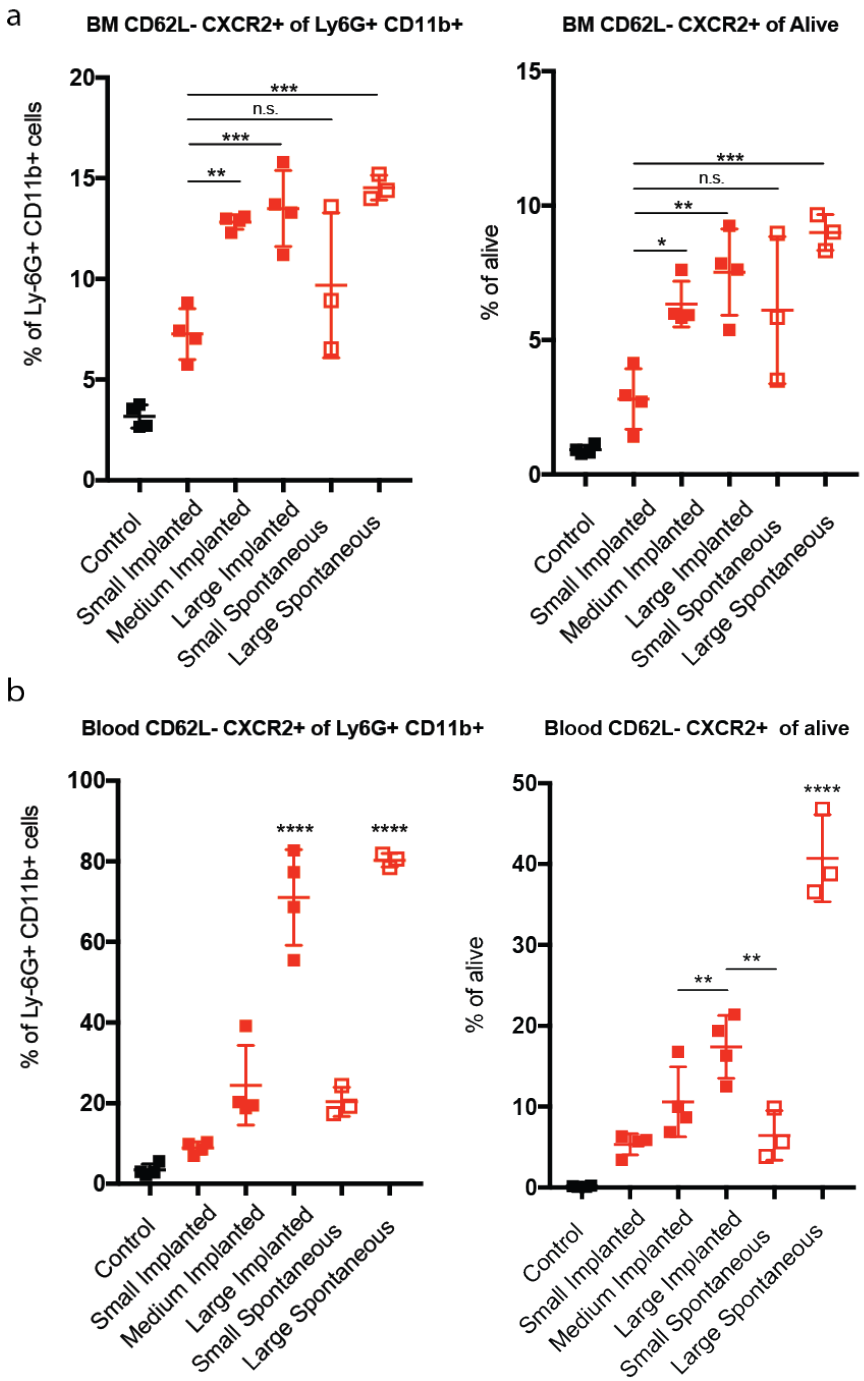

Figure 4.9 Increase of CXCR2$^+$ CD62L$^-$ neutrophils in bone marrow and blood of tumour-bearing mice is affected by tumour size and stage

(**a**,**b**) Flow cytometric quantification of CXCR2$^+$ CD62L- neutrophils from the bone marrow (**a**) and blood (**b**) of control and tumour-bearing mice, analysed as a proportion of total Ly6g$^+$ CD11b$^+$ cells and total alive cells in the tissue. n=4 mice for Small Induced, Medium Induced and Large Induced, n=3 for Small Spontaneous and Large Spontaneous. Data are displayed as mean ± SD. Statistical analysis by one-way ANOVA with Bonferroni's correction for multiple comparisons. Not all statistical comparisons are displayed for clarity. Tables for all statistics calculated in this experiment are in appendix section 7.2. * P < 0.05, ** P < 0.01, *** P < 0.001, **** P < 0.0001. n.s., not significant.

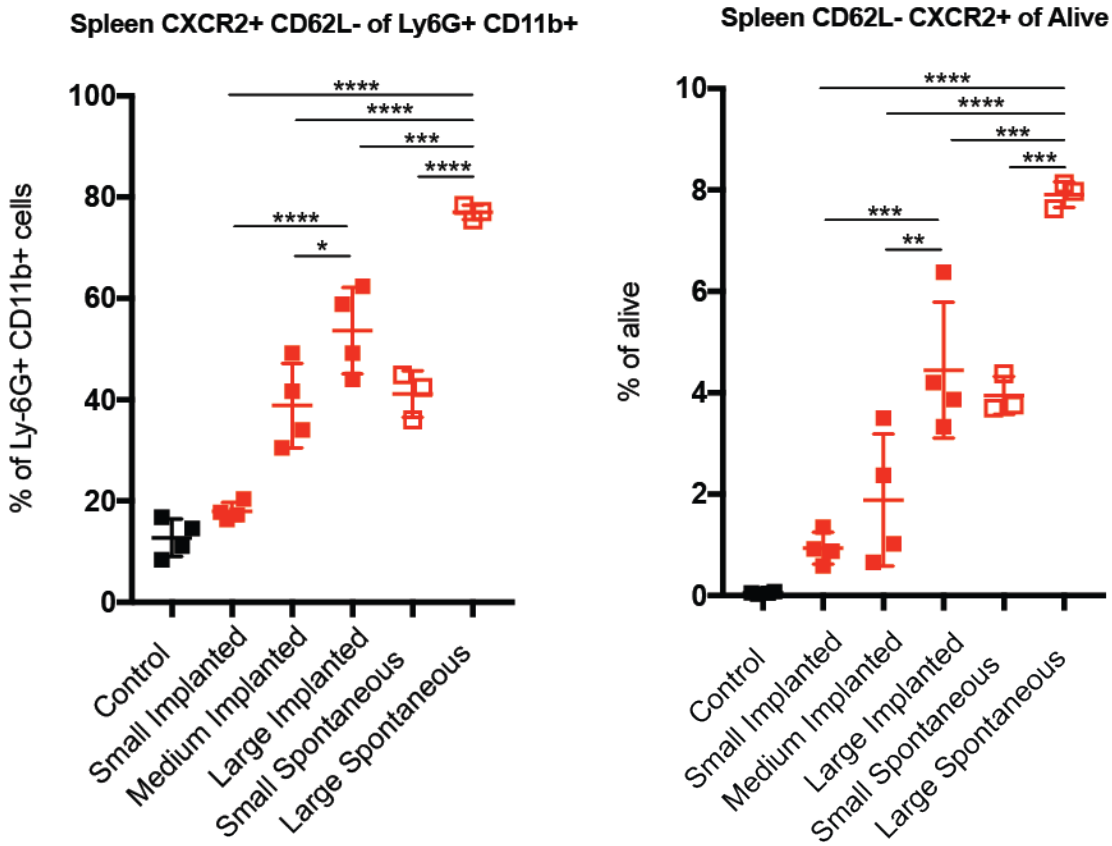

Figure 4.10 Increase of CXCR2^{+} CD62L^{-} neutrophils in spleen of tumour-bearing mice is affected by tumour size and stage

Flow cytometric quantification of CXCR2^{+} CD62L- neutrophils from the spleen of control and tumour-bearing mice, analysed as a proportion of total Ly6g^{+} CD11b^{+} cells and total alive cells in the tissue. n=4 mice for Small Induced, Medium Induced and Large Induced, n=3 for Small Spontaneous and Large Spontaneous. Data are displayed as mean ± SD. Statistical analysis by one-way ANOVA with Bonferroni's correction for multiple comparisons. Not all statistical comparisons are displayed for clarity. Tables for all statistics calculated in this experiment are in appendix section 7.2. * P < 0.05, ** P < 0.01, *** P < 0.001, **** P < 0.0001. n.s., not significant.

4.7 The CXCR2$^+$ CD62L$^-$ neutrophil population can be found in other mouse strains and increases in a range of other tumour models

In the previous sections of this chapter and chapter 3 I have established a number of aspects of neutrophil heterogeneity in the PyMT breast tumour model in FvB mice. The two principal effects of a tumour are an expansion of neutrophils across tissues and an expansion, within the neutrophil population, of CXCR2$^+$ CD62L$^-$ neutrophils. Additionally, the stage of the tumour affects these shifts, with larger, later stage tumours showing greater increases for both effects, with CXCR2$^+$ CD62L$^-$ coming to dominate the neutrophil population in mice with a large tumour burden. I next wanted to examine other mouse strains and mouse tumour models to see if I could observe similar changes in neutrophils in these settings.

I first investigated C57BL/6 mice with PyMT tumours. Tumour cells were obtained from MMTV-PyMT transgenic mice on a C57/BL6 background (see section 2.3) and stored at -160^{o}C before thawing and injection into the mammary fat pad of female C57/BL6 mice. Tumours grew for three weeks and I then performed flow cytometric analysis of neutrophil populations. I found the Ly6g$^+$ population increases in the spleen of tumour-bearing mice, but not to a statistically significant extent in the bone marrow (Figure 4.11a). However, the CXCR2$^+$ CD62L$^-$ population increases in both the bone marrow and spleen of tumour-bearing mice in this model. Therefore, the CXCR2$^+$ CD62L- population is not restricted to FvB mice, and can also expand in C57BL/6 mice with a PyMT tumour.

I then examined neutrophils in Rag$^{-/-}$ mice, which lack mature functional B and T cells (Section 3.7) (Mombaerts et al., 1992). I used an FvB Rag$^{-/-}$ strain, allowing me to use FvB PyMT tumour cells in these mice. In these mice, the Ly6g$^+$ population increases in pre-metastatic tumour-bearing mice, in the spleen and bone marrow (Figure 4.11b), and the CXCR2$^+$ CD62L$^-$ population also increases. This shows that in the FvB PyMT model, the expansion of neutrophils, and of CXCR2$^+$ CD62L$^-$

neutrophils, is not dependent on T cells (or B cells), though this has been shown in other models in the literature (Coffelt et al., 2015).

I next wanted to explore different breast tumour models, as these may have the most direct similarities with the PyMT model. In BALB/CJ mice, the 4T1 breast cancer line is used extensively in breast tumour studies (Pulaski and Ostrand-Rosenberg, 2000). The 4T1 line is triple negative, highly invasive and aggressive. Similar to the PyMT model, 4T1 breast tumours spontaneously metastasize to the lungs, lymph nodes, bone and other organs. In this model, I find a strong expansion of neutrophils in the bone marrow and spleen of 4T1 tumour-bearing mice (tumours were grown for two weeks in this experiment). In the bone marrow, there is a slight increase in $CXCR2^{+}$ $CD62L^{-}$ neutrophils, but in the spleen, there is a large increase in this population (Figure 4.11c). These results show that the $CXCR2^{+}$ $CD62L^{-}$ population can be found in BALB/CJ mice, and that 4T1 tumours can expand this population.

The E0771 model is a triple-negative breast adenocarcinoma line from C57BL/6 mice (Casey et al., 1951), that is weakly metastatic compared to the PyMT and 4T1 tumour models (Johnstone et al., 2015), and therefore offered an interesting comparator. In E0771 pre-metastatic tumour-bearing mice (tumours grown for four weeks), neutrophils expand, and the $CXCR2^{+}$ $CD62L^{-}$ population expands within neutrophils (Figure 4.12a).

Having established that two other breast tumour models have similar effects on neutrophils I then turned to models of carcinomas in other tissues. The RENCA cell line is a model of renal carcinoma in BALB/CJ mice (Murphy and Hrushesky, 1973), and is an aggressive tumour model that also spontaneously metastasizes to the lungs, lymph nodes and liver. It must be noted that I injected RENCA cells subcutaneously into the flanks of BALB/CJ mice, so in this experiment the RENCA cells were not orthotopically transplanted into the kidney. I observed an increase in both neutrophils and $CXCR2^{+}$ $CD62L^{-}$ neutrophils in RENCA tumour-bearing mice (Figure 4.12b), demonstrating that it is not only breast tumours that can affect neutrophils in this way (RENCA tumours were grown for three weeks).

To investigate neutrophils in pancreatic cancer, I used a transgenic mouse model, known as the KPC model, of this disease in which a Cre recombinase system drives expression of mutant oncogenic Kras and p53 in the pancreas (LSL-Kras$^{G12D/+}$;LSL-Trp53$^{R172H/+}$;Pdx-1-Cre) (Lee et al., 2016). These mice develop pancreatic tumours as they age, this model is therefore a spontaneous transgenic mouse model of cancer, and contrasts with the models investigated previously in this section, all of which involve tumour induction via transplantation of a tumour by direct injection of tumour cells into the mouse (although in section 4.6 I did investigate neutrophil phenotypes in mice with spontaneous MMTV-PyMT breast tumours). In the pancreatic model, pancreatic neoplasias are detectable by 10 weeks of age, and mice develop pancreatic ductal adenocarcinomas by 16 weeks of age, with extensive metastasis to the lungs, liver and other organs. I investigated neutrophils in mice with pancreatic tumours at 16 weeks of age, finding an expansion of neutrophils in the bone marrow and spleen, and an increase in CXCR2^{+} CD62L^{-} neutrophils in both of these tissues (Figure 4.13a).

Finally, I examined how a melanoma tumour might affect neutrophils, using the B16 melanoma cell line, which metastasizes to the lung, liver, spleen and other tissues (Overwijk and Restifo, 2001). I injected mice with B16 cells subcutaneously in to C57BL/6 mice and grew them for two weeks before analysis. I found that a B16 tumour has no effect on neutrophil numbers or on the CXCR2^{+} CD62L^{-} population (Figure 4.13b). This shows not every type of tumour affects neutrophils in the same fashion.

Conclusions

- **The CXCR2^{+} CD62L^{-} population is not restricted to FvB mice, but can be found in mice of BALB/CJ and C57/BL6 background**
- **The expansion of neutrophils and CXCR2^{+} CD62L^{-} neutrophils is not dependent on T cells in the PyMT model in FvB background**
- **In a range of different mouse tumour models, including two breast cancer models, I observe expansion of neutrophil numbers in the spleen and bone marrow. The only exception is a melanoma model, in which no expansion occurs**

- **In these tumour models, excepting melanoma, I also find an increase of CXCR2^{+} CD62L^{-} neutrophils in the bone marrow and spleen of tumour-bearing mice**

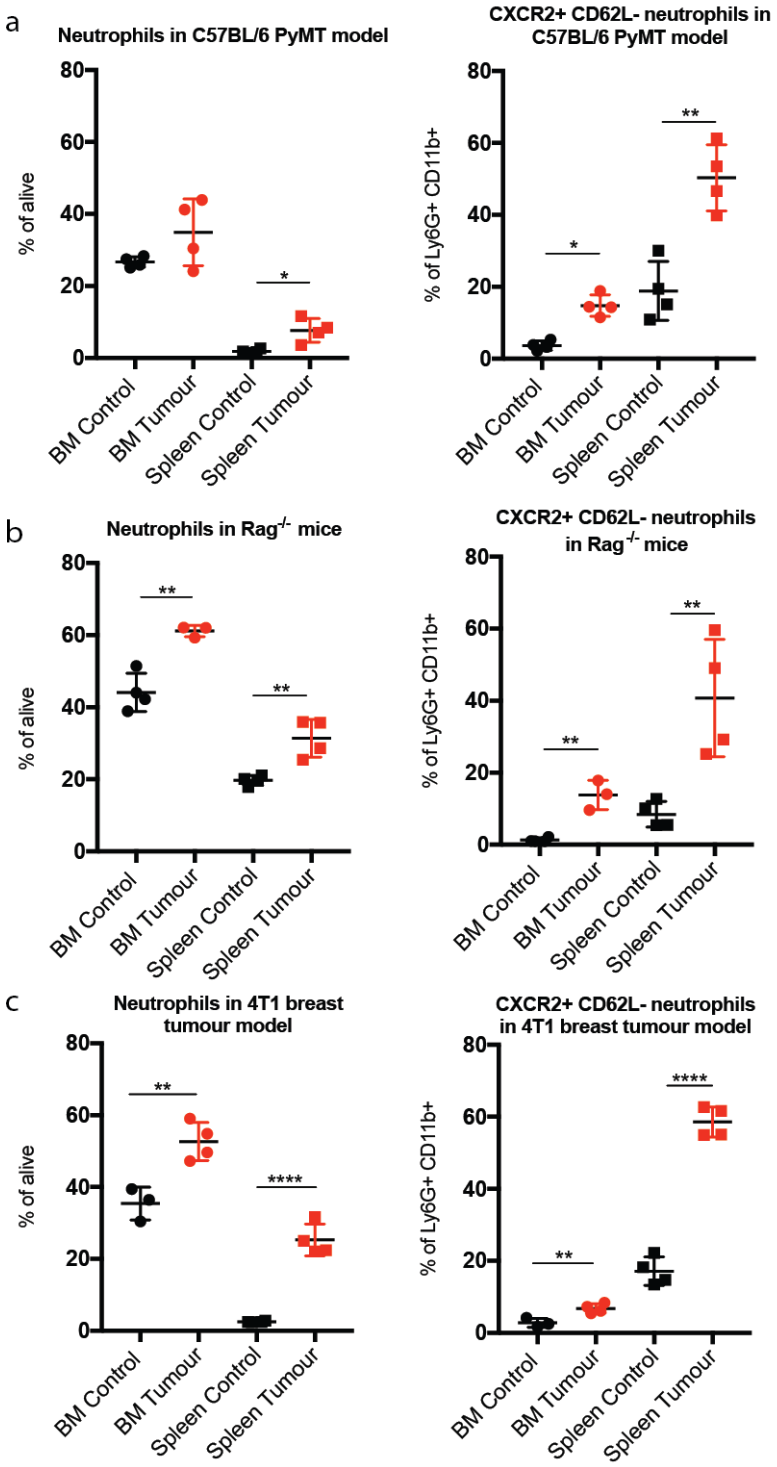

Figure 4.11 Increase of neutrophils and CXCR2^{+} CD62L^{-} neutrophils in C57/BL6 PyMT Rag$^{-/-}$ PyMT mice and 4T1 tumour-bearing mice

Flow cytometric quantification of neutrophils and CXCR2+ CD62L- neutrophils from bone marrow and spleen of control and tumour bearing mice. (**a**) MMTV-PyMT breast tumours in C57/BL6 mice. (**b**) MMTV-PyMT breast tumours in FvB Rag$^{-/-}$ mice. (**c**) 4T1 breast tumours in BALB/CJ mice. n=4 mice for all conditions, except BM tumour in Rag$^{-/-}$ mice, for which n=3. Data are displayed as mean ± SD. Statistical analysis by two-sided t test. *P < 0.05, ** P < 0.01, *** P < 0.001, **** P < 0.0001.

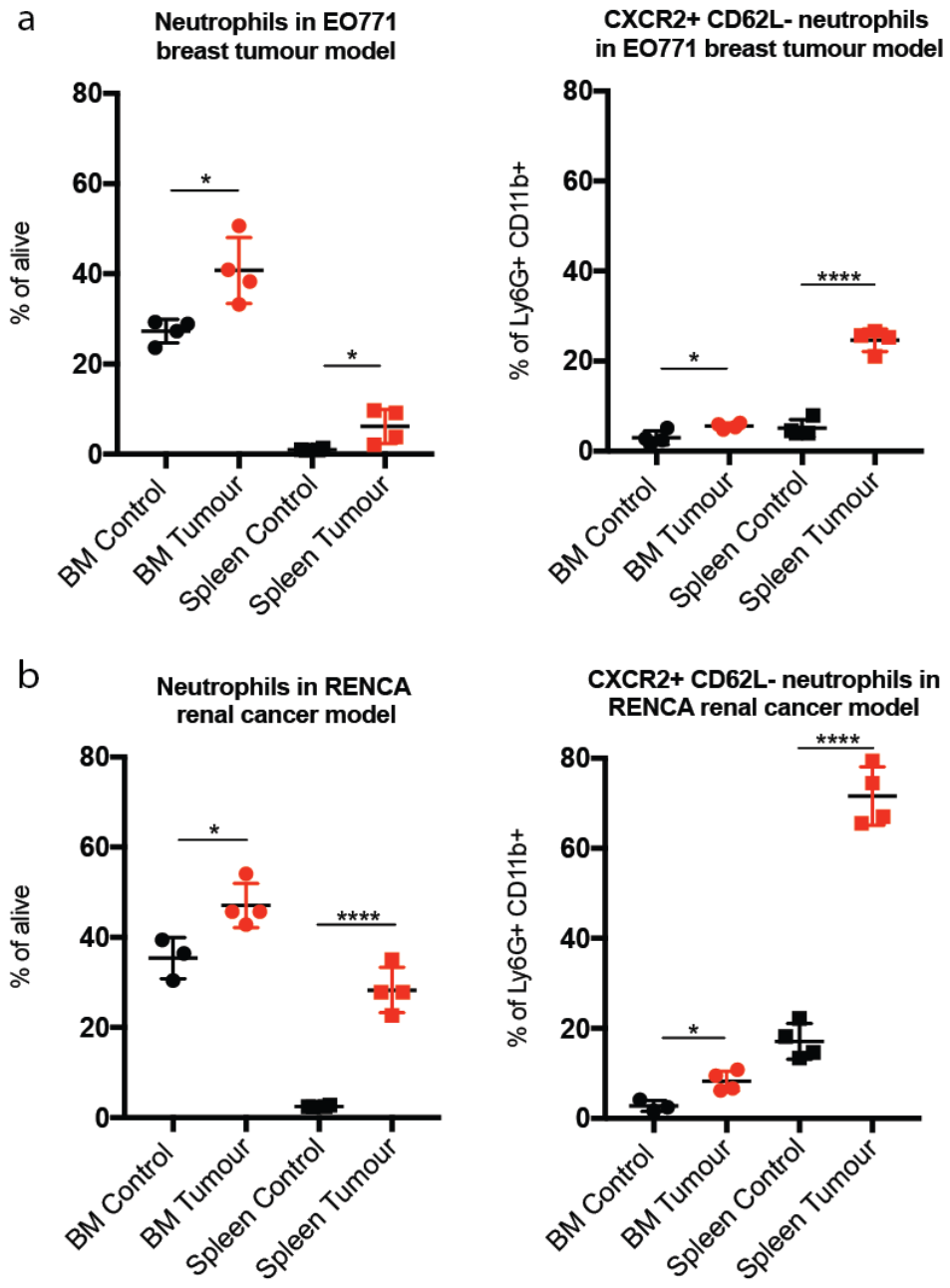

Figure 4.12 Increase of neutrophils and CXCR2^{+} CD62L^{-} neutrophils in E0771 and RENCA tumour-bearing mice

Flow cytometric quantification of neutrophils and CXCR2+ CD62L- neutrophils from bone marrow and spleen of control and tumour bearing mice. (**a**) E0771 breast tumours in C57/BL6 mice. (**b**) RENCA renal carcinoma tumours in BALB/CJ mice. n=4 mice for all conditions. Data are displayed as mean ± SD. Statistical analysis by two-sided t test. *P < 0.05, ** P < 0.01, *** P < 0.001, **** P < 0.0001.

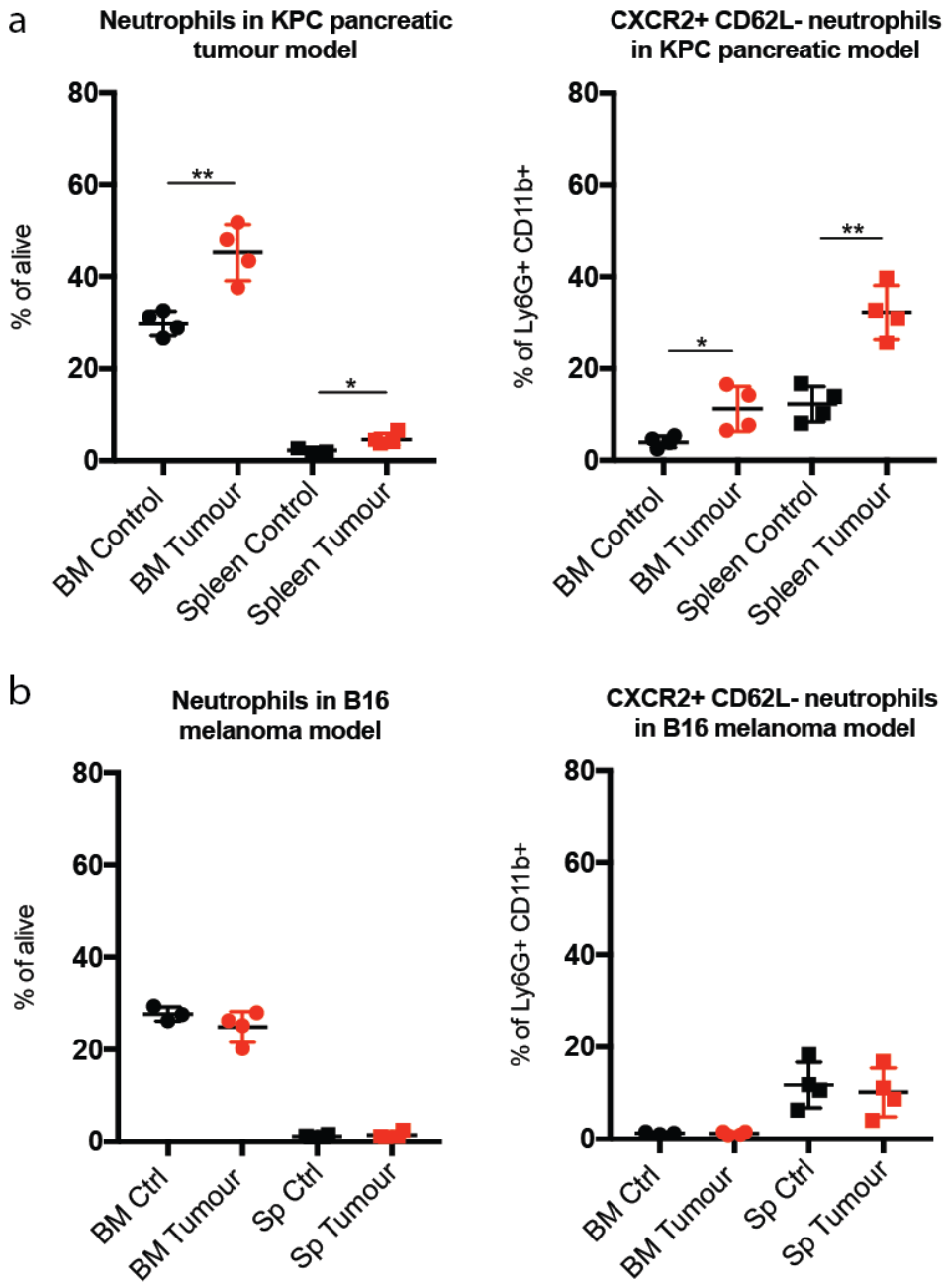

Figure 4.13 Increase of neutrophils and CXCR2^{+} CD62L^{-} neutrophils in pancreatic tumour-bearing mice, but not melanoma-bearing mice

Flow cytometric quantification of neutrophils and CXCR2+ CD62L- neutrophils from bone marrow and spleen of control and tumour bearing mice. (**a**) KPC pancreatic tumours in C57/BL6 mice. (**b**) B16 melanoma tumours in C57/BL6 mice. n=4 mice for all conditions. Data are displayed as mean ± SD. Statistical analysis by two-sided t test. *P < 0.05, ** P < 0.01, *** P < 0.001, **** P < 0.0001.

4.8 Mature bone marrow neutrophils expand in the bone marrow of tumour-bearing mice

In section 4.2 I showed that $CXCR2^+$ neutrophils increase in the bone marrow of tumour-bearing mice. Additionally, I previously found that bone marrow populations of $MHC\text{-}II^+$ and $F4/80^+$ neutrophils decrease in response to a tumour (Section 3.4, Figures 3.5, 3.6). These observations, in tandem with evidence in the literature showing that tumours can have extensive effects on bone marrow granulopoiesis (Wilcox, 2010), suggested that PyMT tumours perturb the bone marrow environment, altering granulopoiesis, with possible consequences for neutrophils. I wanted to more precisely understand how a PyMT tumour might affect these processes.

A recent study identified three neutrophil populations in the bone marrow (Evrard et al., 2018) :

- PreNeu – lineage-committed proliferative neutrophil precursors, defined by CXCR4 and C-Kit expression
- ImmNeu – non-proliferating immature neutrophils, defined by low expression of Ly6g and CXCR2
- MatNeu – non-proliferating mature neutrophils, defined by high expression of Ly6g and CXCR2

The authors show that the presence of a pancreatic tumour increases the numbers of preNeu in the bone marrow. I therefore wanted to investigate these populations in the PyMT model, using the flow cytometry gating strategy displayed in (Figure 4.14a), which was adapted from the strategy used in the study. I first examined PyMT pre-metastatic tumour-bearing mice. Compared with control mice, I found no change in PreNeu or ImmNeu populations as a proportion of total live cells in the tissue, but the MatNeu population increased significantly, from approximately 10% of alive cells to approximately 30% (Figure 4.14b). This is consistent with my previous results showing an increase in CXCR2+ neutrophils in the bone marrow of tumour-bearing mice. Next, I investigated the same populations in the bone marrow of BALB/CJ mice

with 4T1 or RENCA tumours. Given that both of these tumour models have a similar effect on neutrophils as the PyMT model (Section 4.7, Figure 4.11c, Figure 4.12b), I expected to find these tumours would have a similar effect on the bone marrow neutrophil populations and indeed in both 4T1 and RENCA tumour-bearing mice the MatNeu population expands significantly (Figure 4.15). The ImmNeu population did not change, as predicted, but surprisingly the PreNeu population decreased in the tumour-bearing mice in both 4T1 and RENCA models.

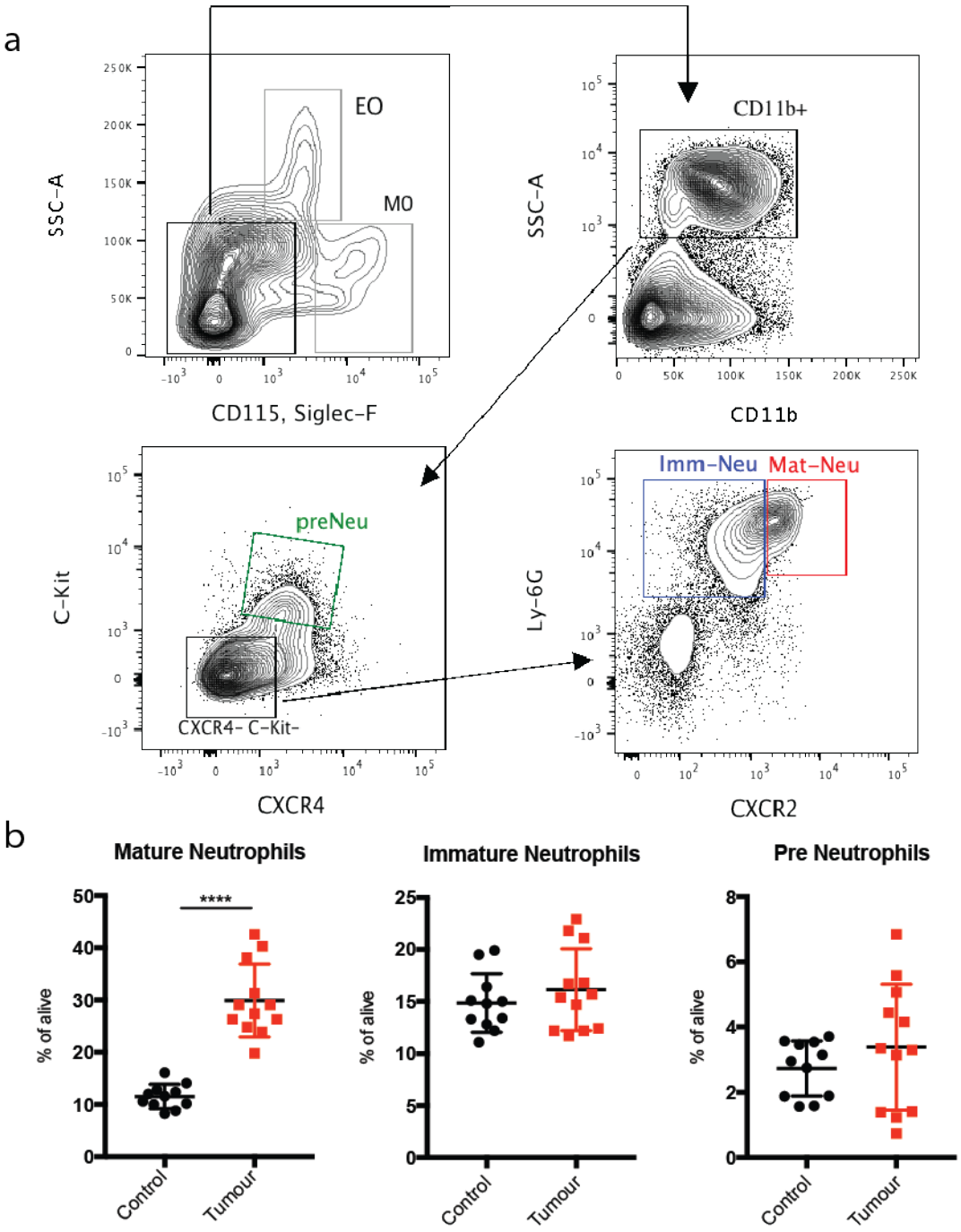

Figure 4.14 Mature neutrophils expand in the bone marrow of PyMT tumour-bearing mice

(**a**) Flow cytometry plots displaying the gating strategy used to define Pre-Neutrophils (preNeu), Immature Neutrophils (Imm-Neu) and Mature Neutrophils (Mat-Neu) in the bone marrow.The first plot is pre-gated on alive singlet bone marrow cells. Strategy adapted from (Becher et al., 2014). EO – eosinophils, M0 – macrophages. (**b**) Flow cytometry quantification of Mat-Neu, Imm-Neu and Pre-Neu neutrophil populations in the bone marrow of FvB control and FvB mice bearing PyMT tumours. n=12 mice per condition. Data are shown as mean ± SD. **** P < 0.0001

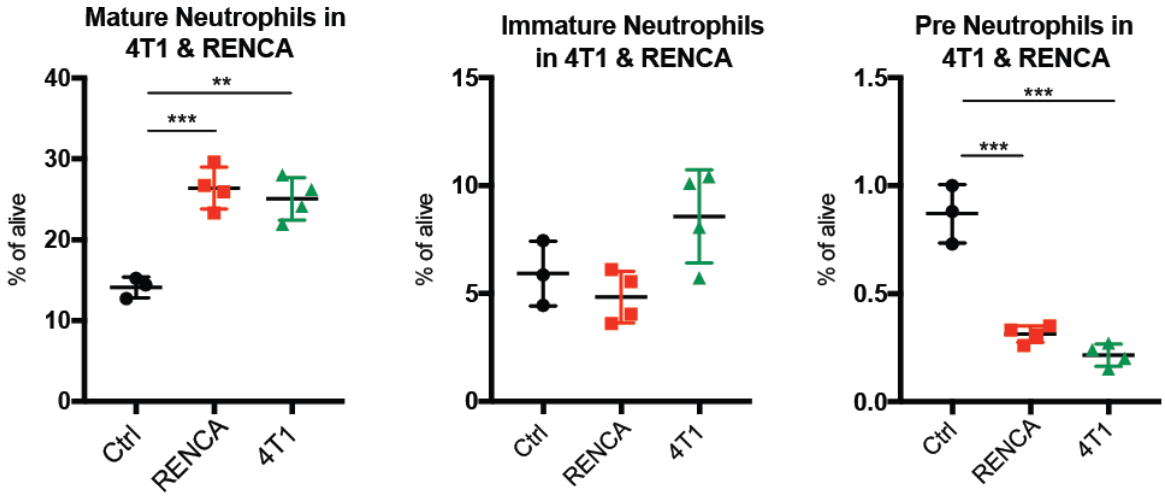

Figure 4.15 Mature neutrophils expand, and Pre-neutrophils decrease, in the bone marrow of mice with 4T1 and RENCA tumours

Flow cytometry quantification of Mat-Neu, Imm-Neu and Pre-Neu neutrophil populations in the bone marrow of BALB/CJ control mice and BALB/CJ mice bearing 4T1 or RENCA tumours. n=3 mice for control, n=4 mice for 4T1 and RENCA. Data are shown as mean ± SD. ** $P < 0.01$, *** $P < 0.001$.

In both models, the PreNeu population did not increase in tumour-bearing mice, the principal expansion being in mature neutrophils. This is surprising given the findings in the study that identified this population, which found that the PreNeu population expands in a model of pancreatic cancer. Furthermore, the mature neutrophils arise from PreNeu and other precursors, thus an expansion of mature neutrophils implies an expansion of cells at earlier stages in granulopoiesis. I therefore decided to look at changes in common myeloid progenitors (CMPs) and granulocyte-macrophage progenitors (GMPs) These two cell populations are multipotent progenitors with proliferative capacity (Section 1.5). GMPs can differentiate into granulocytes, monocytes and macrophages, CMPs can differentiate into GMPs, dendritic cells and also erythrocytes and megakaryocytes. Therefore these two populations may be affected by the presence of a tumour and may contribute to the increase in neutrophils observed in the bone marrow of tumour-bearing mice (Seita and Weissman, 2010).

I used flow cytometry to investigate GMPs and CMPs in PyMT pre-metastatic tumour-bearing mice, first selecting cells negative for lineage markers (CD3, Ly6g, Ly6C, CD11b, Ter-119 and B220, which are all expressed by mature lymphoid and myeloid cells) then selecting CMPs and GMPs. I first found a small increase in CMPs in tumour-bearing mice, with no change in GMPs (Figure 4.16a), with both populations measured as a proportion of total live cells in the bone marrow. A repeat experiment found a stronger increase in CMPs in tumour-bearing mice, whilst GMPs decreased slightly in tumour-bearing bone marrow (Figure 4.16b). In this second experiment, I also analysed expression of Ki67, a cellular biomarker of proliferation, on GMPs and CMPS, but could find no difference in Ki67 expression between the populations (Figure 4.16c). Determining the GMP and CMP populations as proportions of Lineage$^-$ cells finds an increase in both of these populations increase in tumour-bearing mice in both experiments (Figure 4.17a, b), however, the total Lineage- population decreases significantly in tumour-bearing mice (Figure 4.17c ,d), hence why the shift in GMPs and CMPs is more muted when they are measured as a proportion of total live cells. Thus overall, I can only consistently detect a small increase in CMPs in the bone marrow of PyMT tumour-bearing mice.

In summary, I observe a significant, consistent expansion of mature neutrophils in the bone marrow of tumour-bearing mice. However, I am only able to detect minor changes in neutrophil progenitor populations in tumour-bearing mice. Based on my findings, it is therefore difficult to describe a model for how the expansion of mature neutrophils is generated.

Conclusions

- **Mature neutrophils consistently expand in the bone marrow of tumour-bearing mice in the PyMT, 4T1 and RENCA models**
- **I observe no expansion of Immature and Pre-neutrophil populations in the bone marrow of PyMT-tumour bearing mice. But I do observe decreases in the Pre-neutrophil population in mice with 4T1 and RENCA tumours**
- **I can detect small changes in bone marrow granulopoietic progenitor populations in tumour-bearing mice, but these changes do not appear sufficient to explain the expansion of mature neutrophils in this context**

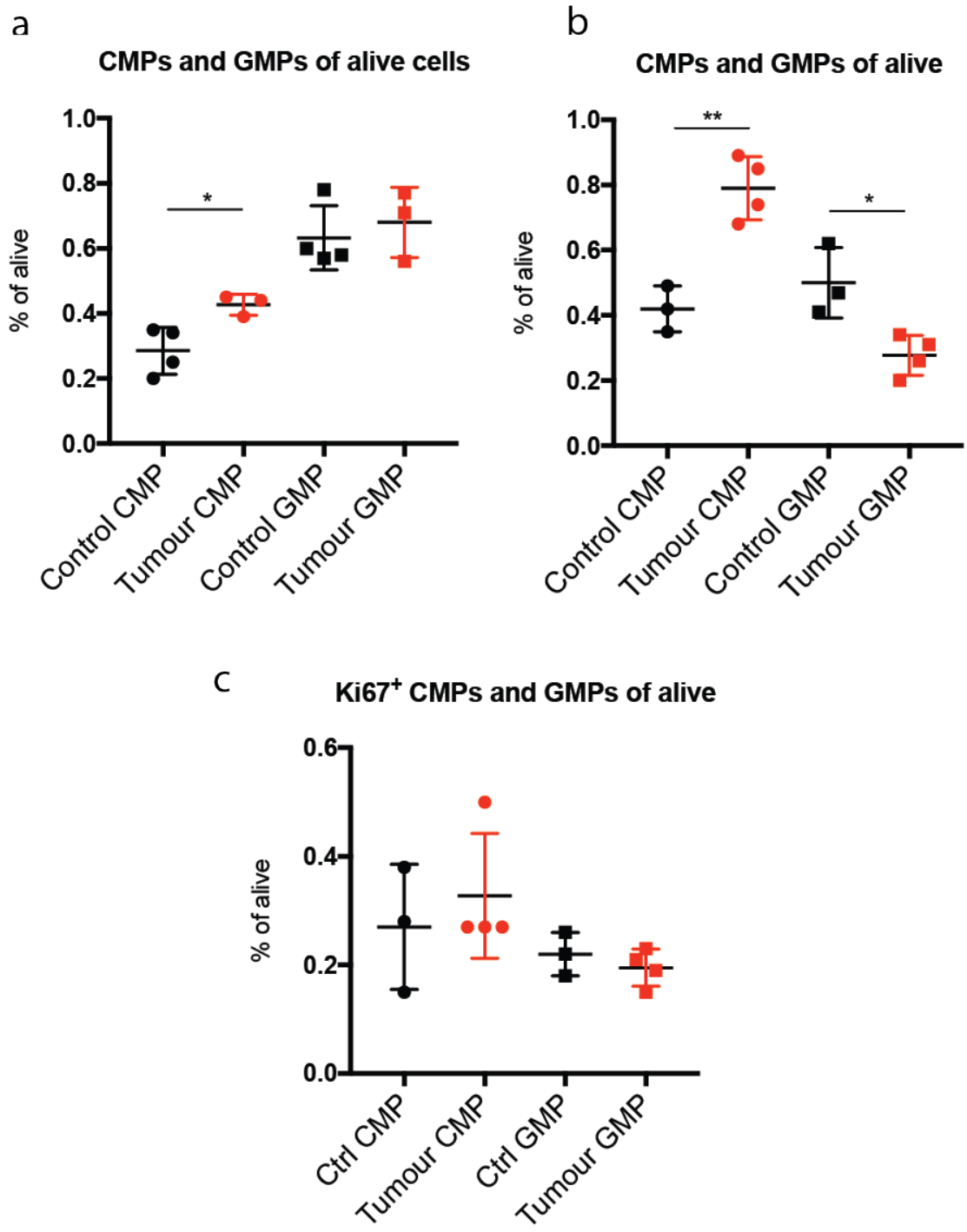

Figure 4.16 Minor changes in neutrophil progenitor populations in the bone marrow of PyMT tumour-bearing mice

(**a**) Flow cytometric quantification of GMP and CMP progenitor populations as a proportion of total alive cells in the bone marrow of control and tumour-bearing mice. n=4 (Control GMP, Control CMP), n=3 (Tumour GMP, Tumour CMP). (**b**) Repeat experiment of (**a**), with n=3 (Control GMP, Control CMP), n=4 (Tumour GMP, Tumour CMP). (**c**) Flow cytometric quantification of Ki67+ GMPs and CMPs as a proportion of total alive cells in the tissue. n=3 (Control GMP, Control CMP), n=4 (Tumour GMP, Tumour CMP). Data are shown as mean ± SD. Statistical analysis by two-sided t test. *P < 0.05, ** P < 0.01.

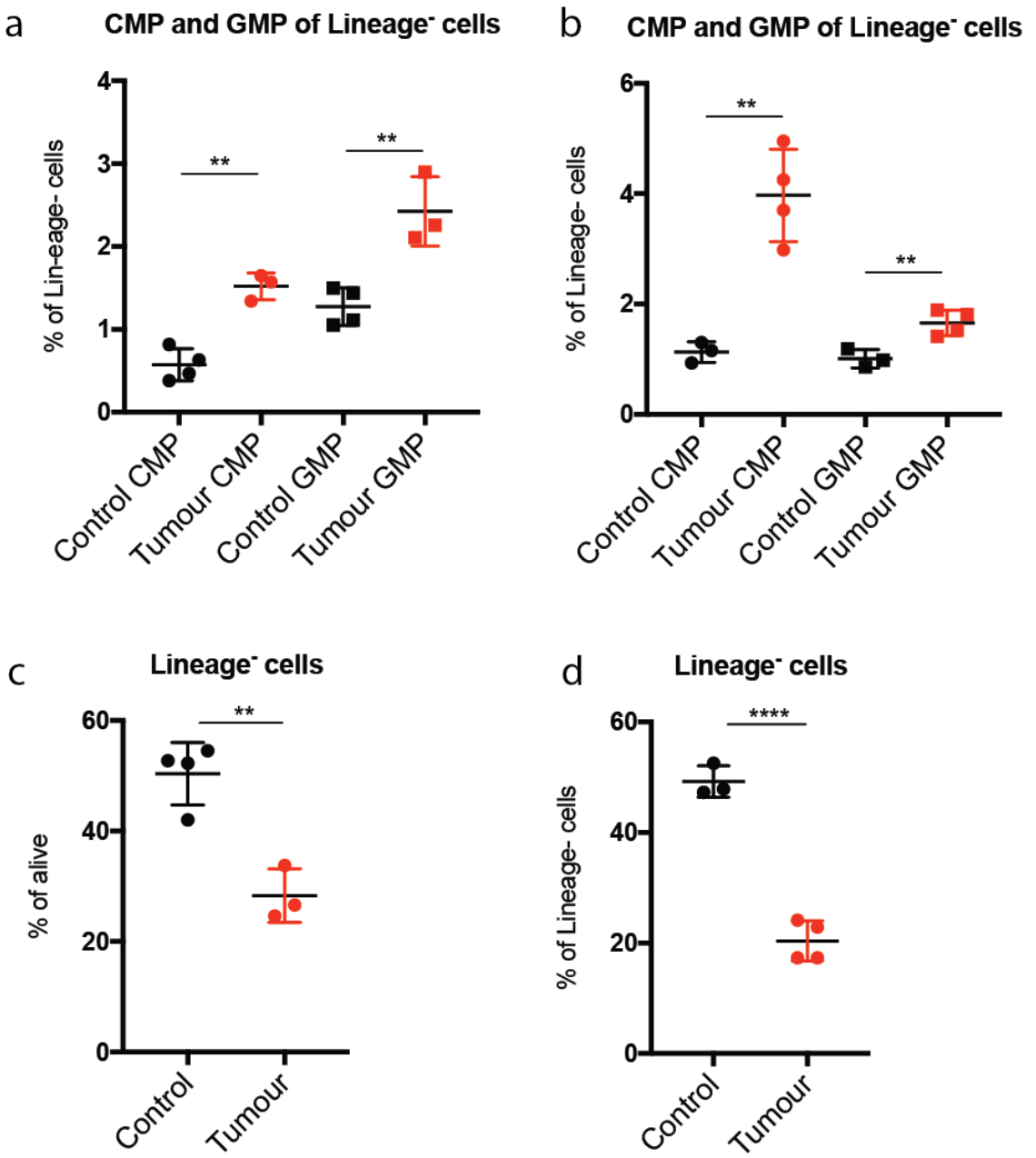

Figure 4.17 Decreases in Lineage- cells in bone marrow of PyMT tumour-bearing mice

(**a**) Flow cytometric quantification of GMPs and CMPs as a proportion of Lineage$^-$ cells in the bone marrow of control and PyMT tumour-bearing mice. n=4 (Control GMP, Control CMP), n=3 (Tumour GMP, Tumour CMP). (**b**) Repeat experiment of (**a**), with n=3 (Control GMP, Control CMP), n=4 (Tumour GMP, Tumour CMP). (**c**) Flow cytometric quantification of Lineage$^-$ cells as a proportion of alive cells. n=4 (control), n=3 (tumour). (**d**) Repeat experiment of (**c**). n=4 (tumour), n=3 (control). Data are shown as mean ± SD. ** $P < 0.01$, **** $P < 0.0001$.

4.9 Chapter Conclusions

- **$CXCR2^+$ neutrophils expand in the bone marrow of tumour-bearing mice**
- **$CD62L^-$ neutrophils expand in the bone marrow, blood, liver and spleen of tumour-bearing mice**
- **Lung neutrophils express uniformly low levels of CD62L, regardless of the presence of a tumour**
- **The $CD62L^-$ population in bone marrow and spleen has low expression of CD62L both internally and on the cell surface**
- **$CXCR2^+$ $CD62L^-$ neutrophils expand in the bone marrow, blood, liver and spleen of PyMT-tumour-bearing mice. This expansion is affected by tumour stage**
- **The $CXCR2^+$ $CD62L^-$ neutrophil population can be detected in mice of different backgrounds, and expands in a range of mouse tumour models**
- **Mature neutrophils expand in the bone marrow of PyMT- 4T1- and RENCA-tumour-bearing mice**
- **Despite observing a consistent expansion of mature neutrophils in mice with PyMT, 4T1 and RENCA tumours, I can only observe a small expansion of common myeloid progenitors in the bone marrow of PyMT-tumour-bearing mice. The mechanisms by which neutrophils expand in the bone marrow of tumour-bearing mice remain unclear**

Chapter 5. Functional characterization of neutrophil populations reveals differences between neutrophils from control and tumour-bearing mice

5.1 Chapter Aims

In the previous chapter I found that a population of $CXCR2^+$ $CD62L^-$ neutrophils is increased in the bone marrow, spleen, blood and liver of tumour-bearing mice, in a number of mouse tumour models. This population expands to comprise up to several percent of the total live cells within a tissue in tumour-bearing mice. In this chapter, in accordance with the final aim of my thesis (Section 1.10), I aimed to explore the functional consequences of neutrophil heterogeneity for cancer cells. I therefore wanted to investigate the functional characteristics of the $CXCR2^+$ $CD62L^-$ population, because this population showed a consistent expansion in a range of mouse tumour models. In addition, I wanted to compare potential functional characteristics between the $CXCR2^+$ $CD62L^+$ and $CXCR2^+$ $CD62L^-$, to determine the significance of the differential CD62L expression between these populations, particularly with respect to how these populations might interact with cancer cells.

Therefore, my aim in this chapter was:

- **Characterization of $CXCR2^+$ $CD62L^-$ neutrophils and $CXCR2^+$ $CD62L^+$ neutrophils in tumour-bearing mice, in order to explore potential functional differences between these populations that may have consequences for their interactions with tumour cells**

5.2 Analysis of neutrophil nuclear morphology reveals CXCR2$^+$ CD62L$^-$ neutrophils have more hyper-segmented nuclei than CXCR2$^+$ CD62L$^+$ neutrophils

The nuclear morphology of neutrophils is an important indicator of maturity and activation (Section 1.5) (Skinner and Johnson, 2017). In mice, at the myelocyte stage of development, cells have a classical round, spherical nucleus. At the next stage, the meta-myelocyte, the nucleus begins to become more concave. As the immature neutrophils progress to the banded cell stage the nucleus begins to form into lobes, though these do not separate, thus the overall shape is of an imperfect ring with bulges, enclosing a region of cytosol (Figure 5.1a). Progression from banded to mature neutrophils is accompanied by an increase in the number and size of lobes, with the nucleus of a mature neutrophil typically having between two and five lobes and not in a fully closed structure. Further increases in lobe number and segmentation can occur, resulting in a hypersegmented nucleus (Figure 5.1a), with numerous lobes linked by thin filaments of nucleoplasm. It is important to stress that hypersegmentation does not necessarily mean an increase in maturity. In the literature, a population of neutrophils that have “aged” in the circulation was found to have a hypersegmented nuclear morphology (Casanova-Acebes et al., 2013). In contrast, another study found a hypersegmented neutrophil population in human blood that did not differ in age (i.e. time in the circulation) from segmented mature blood neutrophils (Tak et al., 2017).

In addition, there is evidence to suggest that there are functional differences between banded, segmented and hypersegmented neutrophils (Pillay et al., 2012, Pillay et al., 2013). Therefore, determining the nuclear morphology of neutrophil populations can provide information on their maturation stage, and potentially information on their functionality and “aged” state. I wanted to investigate the nuclear morphology of neutrophil populations identified in the previous chapter, principally the CXCR2$^+$ CD62L$^-$ population, as this population expands significantly in tumour-bearing mice. I wanted to compare this population with the CXCR2$^+$ CD62L$^+$ population, which decreases in tumour-bearing mice.

I used FACS to purify neutrophil populations from blood and spleen, as I wanted to focus on changes in neutrophils in the circulation and periphery. Sorted neutrophils were affixed to slides by Cytospin centrifugation, fixed with methanol and stained with Giemsa stain to visualise neutrophil nuclei. As these neutrophils are from the periphery I expected most of these neutrophils to have segmented nuclei, and this was indeed confirmed I could also identify smaller numbers of banded and hypersegmented neutrophils (Figure 5.1b, c, display representative images showing examples of neutrophil nuclear morphologies from blood of PyMT tumour-bearing mice).

I first purified neutrophils from PyMT pre-metastatic tumour-bearing FvB mice (Figure 5.1d): in both the blood and spleen of these mice more of the $CXCR2^+$ CD62L- neutrophils are hypersegmented (mean 47% and 45% of blood and spleen $CXCR2^+$ CD62L- populations respectively) than the $CXCR2^+$ $CD62L^+$ neutrophils (mean 20% and 25% of blood and spleen $CXCR2^+$ $CD62L^+$ populations respectively). Consequently, there are fewer segmented $CXCR2^+$ $CD62L^-$ cells than in the $CXCR2^+$ $CD62L^+$ population. There are very few banded cells in either population.

In BALB/CJ mice with 4T1 tumours I was able to find a similar result in blood and spleen neutrophils (Figure 5.2a): the $CXCR2^+$ $CD62L^-$ population is more hypersegmented and less segmented than the $CXCR2^+$ $CD62L^+$ population, with a very small percentage of either population being banded cells.

In C57/BL6 mice with E0771 tumours I found that the $CXCR2^+$ $CD62L^-$ population is slightly more hypersegmented in the blood than the $CXCR2^+$ $CD62L^+$ population (mean 49% compared to 39%), but in the spleen, there is no difference in segmentation between $CD62L^-$ and $CD62L^+$ neutrophils (Figure 5.2b).

I also purified $CXCR2^+$ neutrophils from the blood of control and PyMT pre-metastatic tumour-bearing FvB mice, to compare the segmentation in the circulating mature neutrophil. Approximately 20% of blood $CXCR2^+$ neutrophils are hypersegmented, with approximately 75% segmented (Figure 5.2c). This is similar to the $CXCR2^+$ $CD62L^+$ fraction in the blood of tumour-bearing mice, and this result is consistent

with the fact that the $CXCR2^+$ population in the blood of control mice is also predominantly $CD62L^+$ (Section 4.3). There is a slight increase in hyper-segmentation in blood $CXCR2^+$ neutrophils from tumour-bearing mice compared to the control setting. This is to be expected because the $CXCR2^+$ population in tumour-bearing mice will contain more $CD62L^-$ neutrophils than the $CXCR2^+$ population in control mice, and a greater fraction of the $CD62L^-$ population is hypersegmented compared to the $CD62L^+$ population.

Conclusions

- **In three different mouse strains, with three different tumour types, the $CXCR2^+$ $CD62L^-$ population of neutrophils has more hypersegmented nuclei than the $CXCR2^+$ $CD62L^+$ population**
- **In PyMT and 4T1 tumour-bearing mice this occurs in both blood and spleen neutrophils. In E0771 tumour-bearing mice it is only observed in blood neutrophils**
- **The total $CXCR2^+$ population in the blood of control mice has a similar pattern of segmentation to the $CXCR2^+$ $CD62L^+$ population in the blood of tumour-bearing mice**

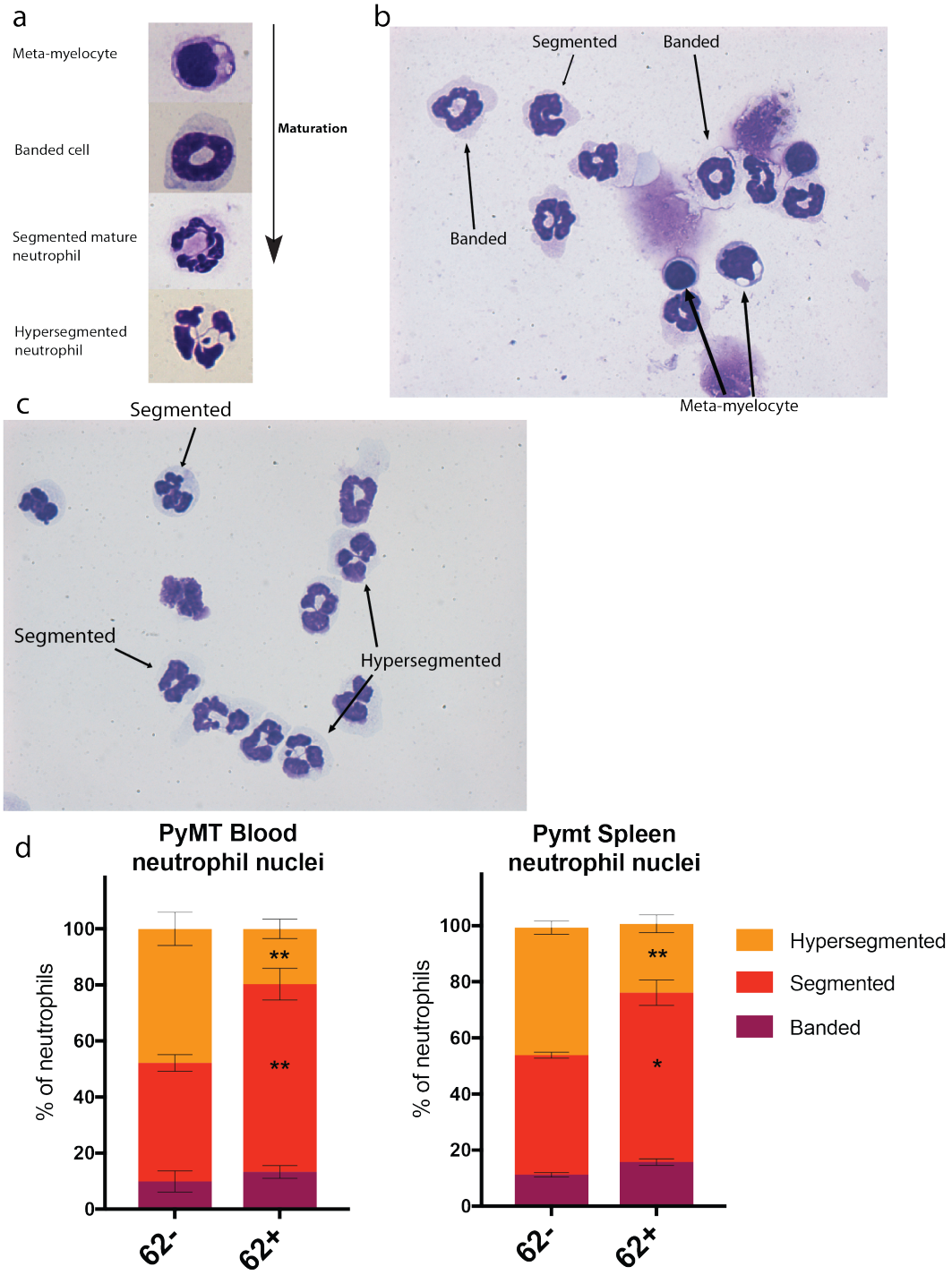

Figure 5.1 CXCR2^{+} CD62L^{-} neutrophils from blood and spleen of tumour-bearing mice have a more hypersegmented nuclear morphology

(**a**) Images of neutrophils at different stages of maturation stained with Wright-Giemsa stain. (**b,c**) Images of Wright-Giemsa-stained neutrophils, with arrows indicating meta-myelocytes, banded cells, segmented and hypersegmented neutrophils. (**d**) Quantification of nuclear morphology of CXCR2+ CD62L+/- neutrophil populations from blood and spleen of PyMT tumour-bearing mice. n=4 mice. Data are displayed as mean ± SD. Statistical analysis by two-sided t test. *P < 0.05, ** P < 0.01.

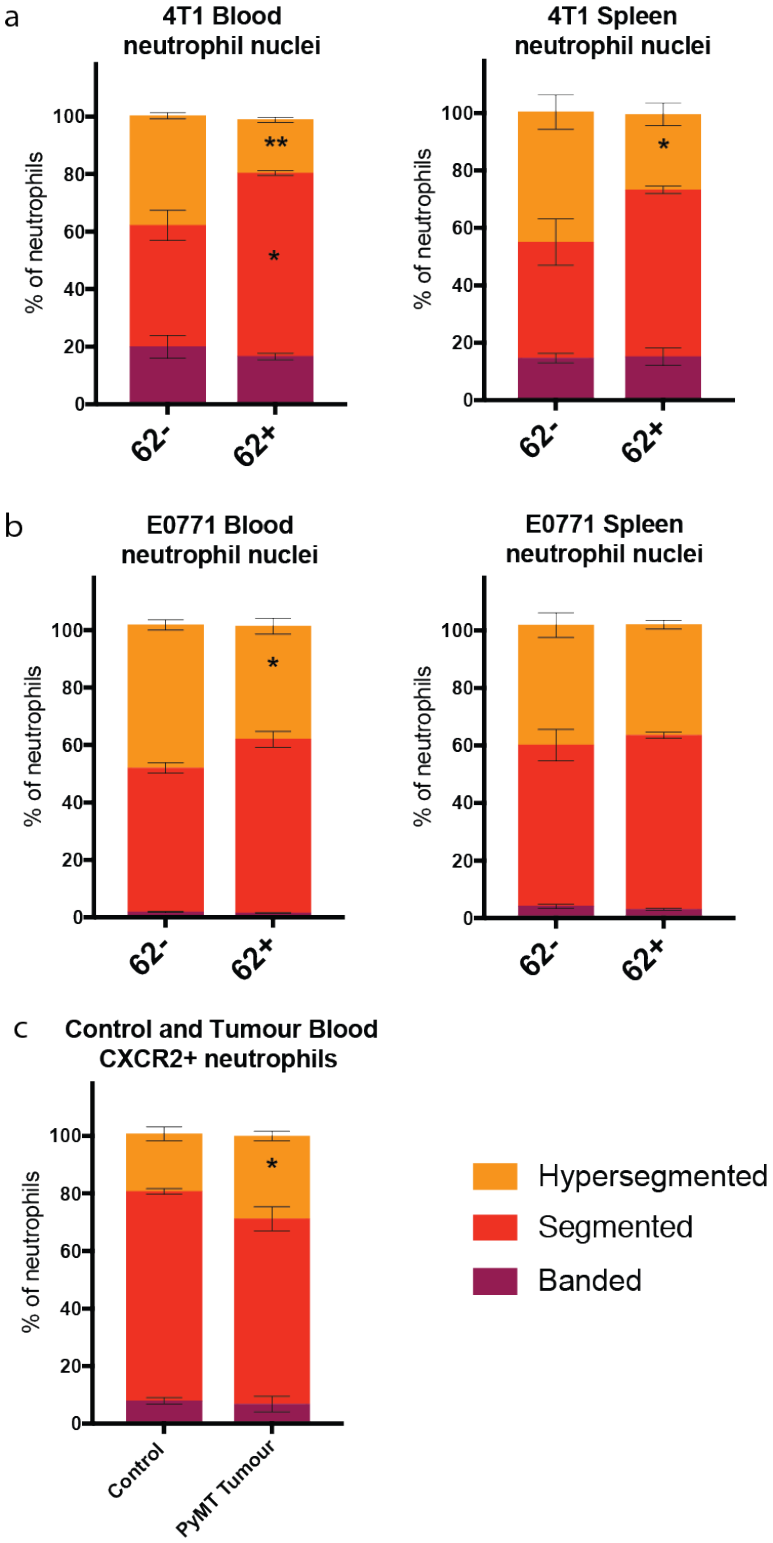

Figure 5.2 CXCR2^{+} CD62L^{-} neutrophils from 4T1 and E0771 tumour-bearing mice have a more hypersegmented nuclear morphology

Quantification of nuclear morphology of neutrophil populations from blood and spleen of 4T1 tumour-bearing mice (**a**) and E0771 tumour-bearing mice (**b**). n = 2 mice (**c**) Quantification of nuclear morphology of neutrophil populations from blood of control FvB mice. n = 3 mice. Data are displayed as mean ± SD. *P < 0.05, ** P < 0.01.

5.3 The majority of CXCR2$^+$ CD62L$^-$ neutrophils are not CXCR4$^+$ "aged" neutrophils

The finding that the CXCR2$^+$ CD62L$^-$ population is more hypersegmented is significant for a number of reasons. Firstly, there are a number of studies that have found different functional characteristics for hypersegmented neutrophils. One study revealed that a population of hypersegmented neutrophils expands in human blood in response to LPS stimulation. This population has enhanced capacity to supress T cells compared with the segmented neutrophils (Pillay et al., 2012). The same investigators later demonstrated that LPS-induced hypersegmented neutrophils in human blood have a different proteome profile compared to segmented and banded neutrophils (Tak et al., 2017). Other studies have found that hypersegmented neutrophils have reduced migration speed, increased proinflammatory cytokine secretion and enhanced cytoxicity (van Grinsven et al., 2018, Whitmore et al., 2017).

The finding that CXCR2$^+$ CD62L$^-$ neutrophils are more hypersegmented is also significant because it was found previously that there is a population of hypersegmented, CD62L$^-$ neutrophils that have "aged" in the circulation of mice (Casanova-Acebes et al., 2013). These "aged" neutrophils also express CXCR4, which binds CXCL12 in the bone marrow, allowing these "aged" neutrophils to home back to the bone marrow, where they are destroyed. The same group subsequently demonstrated that "aged" neutrophils were more primed for activation and had upregulated inflammatory activation pathways compared to typical mature neutrophils (Zhang et al., 2015). Given that the CXCR2$^+$ CD62L$^-$ neutrophils I observe in tumour-bearing mice have hypersegmented nuclei and have low CD62L expression, they may have an "aged" phenotype. This would mean that they could have the capacity home back to the bone marrow and be destroyed there. In theory, this could limit their ability to persist in the circulation and periphery and interact with tumour cells and affect tumour progression and metastasis. Therefore, I decided to examine CXCR4 expression on the CXCR2$^+$ CD62L$^-$ population, to see if this population does indeed have an "aged" phenotype. The mass cytometry experiments I performed to identify this population initially did include a CXCR4 antibody (Table

3). However, only very low levels of CXCR4 expression were detected in these experiments, with no clear expression on $CXCR2^+$ $CD62L^-$ neutrophils.

I used flow cytometry to assess CXCR4 expression on $CXCR2^+$ $CD62L^{+/-}$ neutrophils from blood and spleen of control and PyMT pre-metastatic tumour-bearing FvB mice, using the same CXCR4 antibody clone as used in my mass cytometry experiments and the aforementioned studies. In the blood, I could only detect very low levels of CXCR4 expression on neutrophils, regardless of CD62L expression, and with no difference between control and tumour-bearing mice (Figure 5.3a, b). In the spleen, I was able to detect CXCR4 expression on the $CXCR2^+$ $CD62L^-$ population, in both control and tumour-bearing mice (Figure 5.4a, b). In control mice, this population is approximately 30% of the $CXCR2^+$ $CD62L^-$ population, but decreases to approximately 3% of this population in tumour-bearing mice. Almost no CXCR4 expression could be detected on the $CXCR2^+$ $CD62L^+$ population.

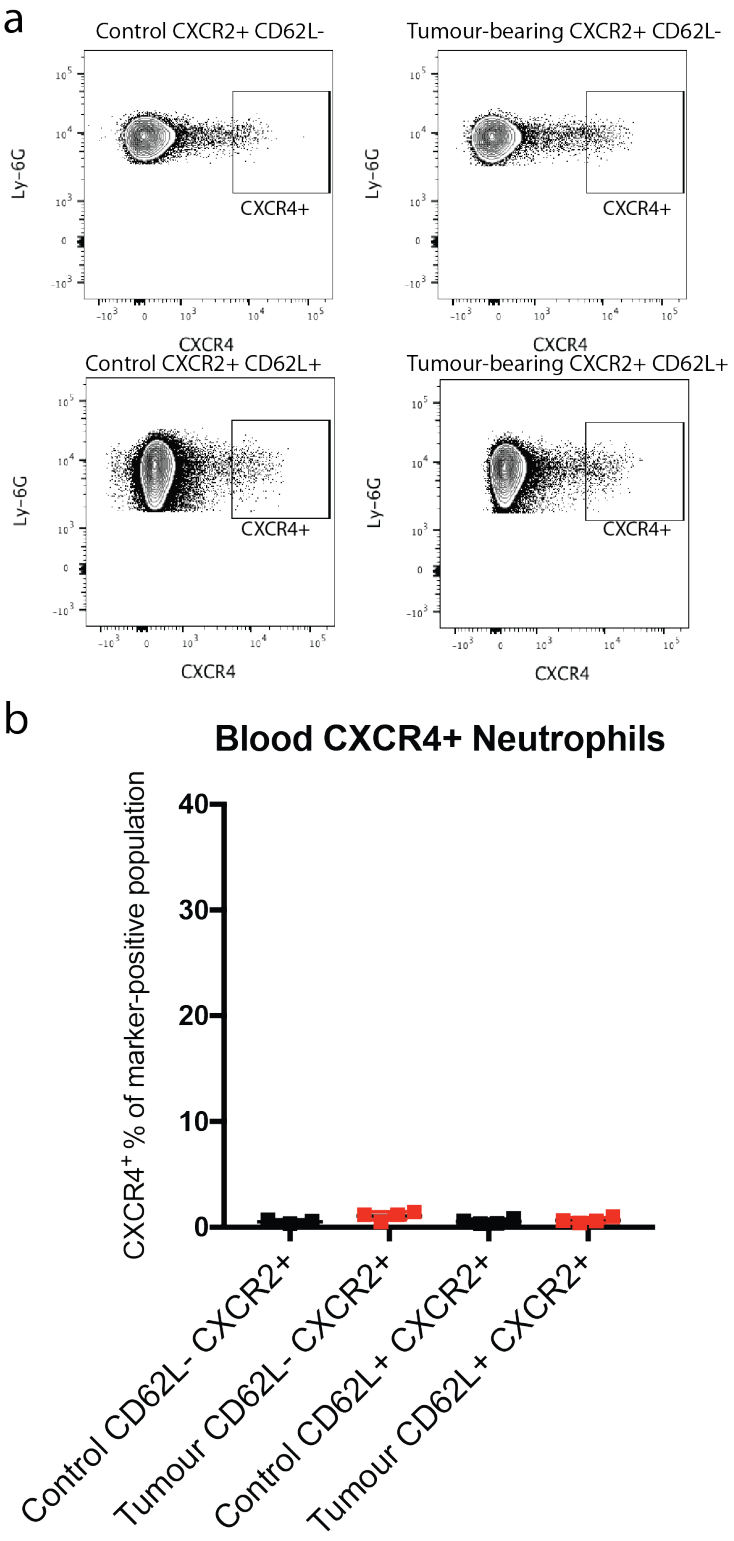

Figure 5.3 Minimal expression of CXCR4 on FvB blood neutrophil populations

(**a**) Flow cytometry plots of CXCR4 expression on $CXCR2^+$ CD62L+/- blood neutrophil populations from control and tumour-bearing mice (top CD62L-, bottom CD62L+). Gates show CXCR4+ cells. (**b**) Quantification of CXCR4+ neutrophils as a proportion of blood CXCR2+ CD62L+/- neutrophil populations from control and tumour-bearing mice. n = 4 mice per condition. Data are displayed as mean ± SD.

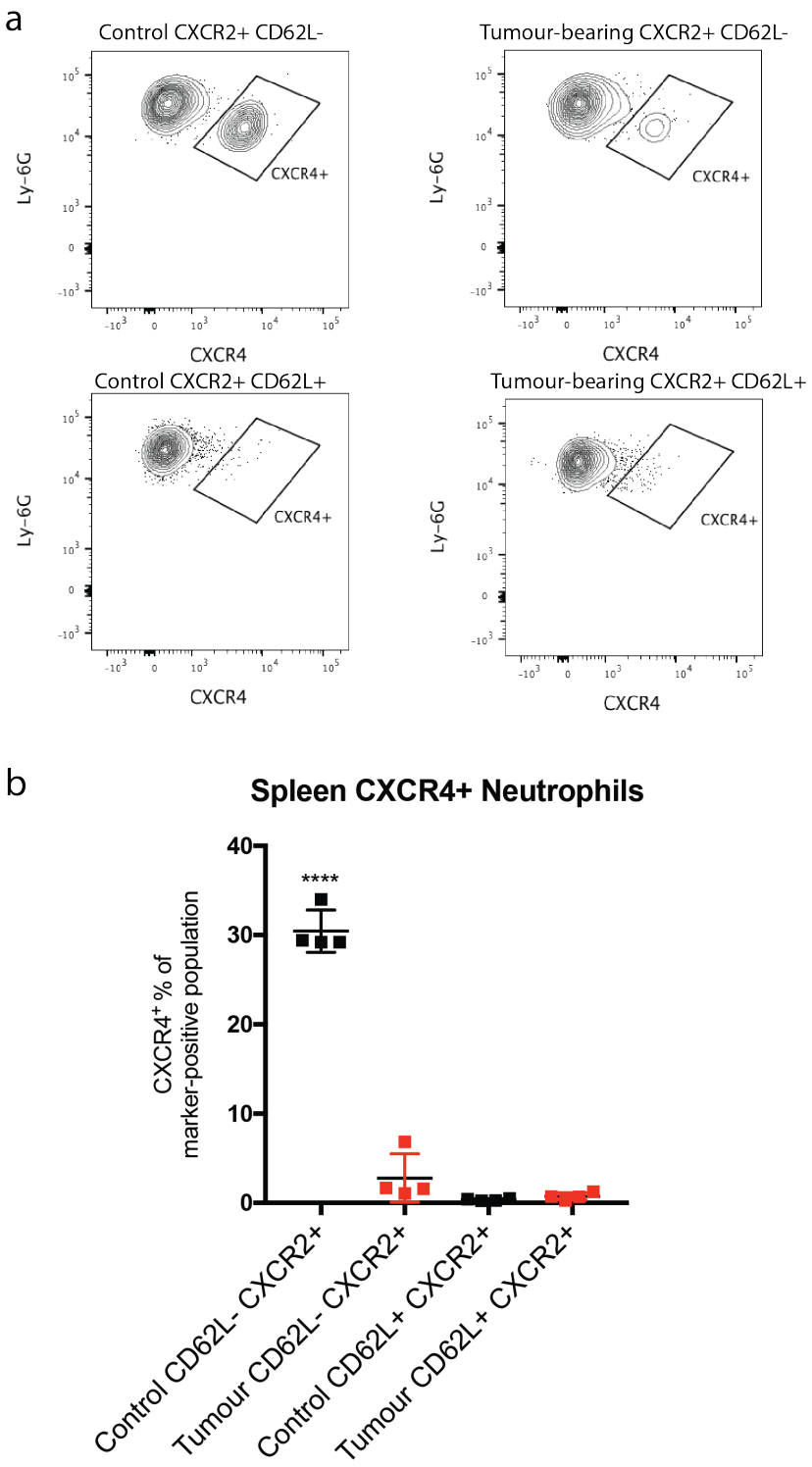

Figure 5.4 Minimal expression of CXCR4 on FvB spleen neutrophil populations

(**a**) Flow cytometry plots of CXCR4 expression on CXCR2+ CD62L+/- spleen neutrophil populations from control and tumour-bearing mice (top CD62L-, bottom CD62L+). Gates show CXCR4+ cells. (**b**) Quantification of CXCR4+ neutrophils as a proportion of spleen CXCR2+ CD62L+/- neutrophil populations from control and tumour-bearing mice. n = 4 mice per condition. Data are displayed as mean ± SD. Statistical analysis by two-sided t test **** $P < 0.0001$. Asterisks indicate that sample Control CD62L- CXCR2+ is significantly greater than all three other samples.

The lack of CXCR4 expression in the blood is surprising, given the previous studies mentioned. One explanation is the timing of the analysis: for these experiments I culled mice and harvested tissue at approximately zeitgeber time 2 (i.e. two hours after initiation of light in a 12 hours light: 12 hours dark regime). The original paper identifying this population showed the population increased as zeitgeber time progressed, peaking at zeitgeber time 9 (i.e. 10 hours after initiation of light) (Casanova-Acebes et al., 2013). I therefore repeated the experiment but this time culled the mice and harvested tissue at zeitgeber time 9. However, I was still unable to detect the population in the blood, despite confirming the previous result in the spleen (Figure 5.5a).

A further explanation for these results is that they are due to differences in mouse background: I performed these experiments in FvB mice, but C57BL/6 mice were used in the studies that identified and characterized the "aged" neutrophil population. It is possible this difference in mouse background is responsible for the difficulty identifying "aged" neutrophils in the blood. I therefore took tissue from control C57BL/6 mice at zeitgeber times 2 and 9, to see if I could detect CXCR4 expression and therefore identify "aged" neutrophils in mice of the same background as used in the original studies. I was again unable to detect CXCR4 expression on blood neutrophils, but could observe it on spleen $CXCR2^+$ $CD62L^-$ neutrophils (Figure 5.5b), additionally observing an increase in $CXCR2^+$ $CD62L^-$ $CXCR4^+$ "aged" neutrophils at zeitgeber time 9.

In summary, I am unable to reproduce the expression patterns of CXCR4 on neutrophils in the blood found in previous studies, despite controlling for differences in experimental timing and mouse background. The possibility that the $CXCR2^+$ $CD62L^-$ population I have identified are "aged" neutrophils cannot be ruled out, but I am unable to find CXCR4 expression on these cells, which suggests that they do not have the capacity to home back to the bone marrow and be destroyed. This implies that they will not be being cleared from the circulation at an accelerated rate compared to $CXCR2^+$ $CD62L^+$ neutrophils or other mature, segmented neutrophils. Furthermore, whilst I found this population has more hypersegmented cells than the $CXCR2^+$ $CD62L^+$ population, approximately 50% of $CXCR2^+$ $CD62L^-$ cells are not

hypersegmented (Figure 5.1d), which further suggests that the population as a whole does not have an “aged” phenotype

In the spleen, where I am able to find “aged” neutrophils that are $CD62L^-$ $CXCR4^+$, the “aged” neutrophils decrease significantly in tumour-bearing mice (as a proportion of the $CXCR2^+$ $CD62L^-$ population). This shows that the vast majority of $CXCR2^+$ $CD62L^-$ neutrophils in the spleen of tumour-bearing mice do not have an “aged” phenotype, and thus lack the capacity to home back to the bone marrow for destruction.

Conclusions

- **$CXCR2^+$ $CD62L^-$ neutrophils in the blood of control and tumour-bearing mice have very low expression of CXCR4 and thus do not appear to have this marker to determine an ‘‘aged’’ phenotype**
- **A small proportion of $CXCR2^+$ $CD62L^-$ neutrophils in the spleen have an ‘‘aged’’, $CXCR4^+$ phenotype. This population increases at later zeitgeber times, but decreases in the spleens of tumour-bearing mice, regardless of zeitgeber time**

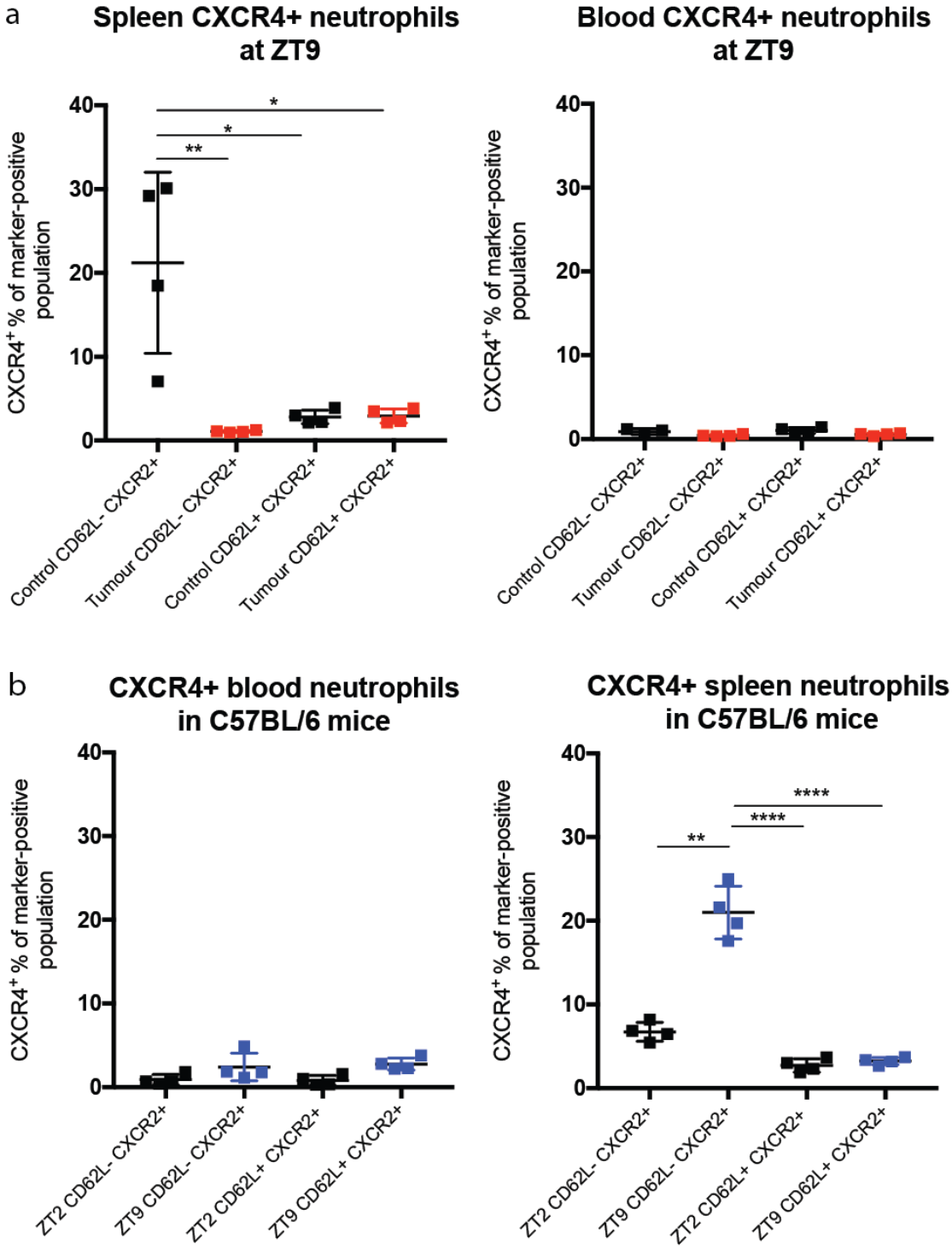

Figure 5.5 Lack of CXCR4 expression precludes identification of "aged" neutrophils in the blood of FvB and C57BL/6 mice, regardless of zeitgeber time

(**a**)Flow cytometric quantification of CXCR4+ neutrophils as a proportion of CXCR2+ CD62L+/- neutrophils in the blood and spleen at zeitgeber time 9 in control mice. n = 4 mice per condition. (**b**) Flow cytometric quantification of CXCR4+ neutrophils as a proportion of CXCR2+ CD62L+/- neutrophils in the blood and spleen at zeitgeber times 2 and 9 in control C57BL/6 mice. n = 4 mice per condition. Data are shown as mean ± SD. Statistical analysis by two-sided t test. *P < 0.05, ** P < 0.01, *** P < 0.001, **** P < 0.0001.

5.4 No differences between neutrophil populations in the formation of Neutrophil Extracellular Traps

I have shown that the CXCR2+ CD62L$^-$ and CXCR2+ CD62L+ neutrophil populations differ in their nuclear morphology. This observation, in tandem with their differential expression of CD62L, suggests that there are potential differences between these populations, which may have consequences for their interactions with tumour cells. I therefore next wanted to perform functional assays with these populations. I first investigated the *in vitro* formation of neutrophil extracellular traps (NETs) by different neutrophil populations.

NETs are structures of condensed chromatin, studded with cytosolic and granule proteins, released by neutrophils under inflammatory conditions. The condensed chromatin can bind to pathogens, trapping them, and the proteins on the chromatin, such as neutrophil elastase, have antimicrobial function (Papayannopoulos, 2017). Recently, NETs have been found to play a role in cancer in a range of different processes, including tumour progression, tumour inflammation, angiogenesis and metastasis (Erpenbeck and Schön, 2016). In addition, “aged” neutrophils have been shown previously to have enhanced NET formation (Zhang et al., 2015), so it is possible that different neutrophil populations may have differing NET-forming capacity, and their NETs may have important effects on cancer cells.

I used FACS to purify neutrophil populations from bone marrow, blood and spleen. From pre-metastatic tumour-bearing mice I compared the CXCR2+ CD62L$^{+/-}$ populations, and I also compared the CXCR2$^+$ populations (i.e. all mature neutrophils) from control and pre-metastatic tumour-bearing mice, in order to observe if there were any differences between mature neutrophils in a control and tumour setting. Neutrophils were left to attach to poly-lysine coated plates and then stimulated with phorbol 12-myristate 13-acetate (PMA), a potent inducer of NETs. After fixation cells were stained with Hoechst 33342 and Sytox Green and NET formation quantified by microscopy (Figure 5.6a, Hoechst can cross cell membranes and stain DNA in both live and dead cells, Sytox Green cannot cross cell membrane, and so stains dead cells and also the extracellular DNA in NETs).

I found very low rates of NET formation with bone marrow neutrophils, below 0.3% for all samples (Figure 5.6b), with no differences between any of the samples. Neutrophils from the blood and spleen had higher rates of NET formation than the bone marrow, on average between 1% and 2% of neutrophils forming NETs. I was unable to observe any differences between groups in these tissues (Figure 5.6c, d).

The rates of NET formation by bone marrow neutrophils are low, but not unexpectedly so, as these neutrophils are not fully mature and may lack NET-forming capacity. The low NET formation observed in blood and spleen neutrophils is somewhat surprising, as these cells are mature neutrophils. One explanation is the use of FCS as a media supplement; this has been shown to impair NET formation in some contexts and it has been suggested that mouse serum may be more effective for NET formation (Neubert et al., 2019). I therefore repeated the NET formation assay using mouse serum in place of FCS: I found the same result with bone marrow neutrophils (Figure 5.7a). Blood and spleen neutrophils had slightly increased rates of NET formation, though still low, and again with no differences between any populations (Figure 5.7b, c).

Conclusions

- **No differences in NET formation between $CXCR2^+$ $CD62L^+$ and $CXCR2^+$ $CD62L^-$ neutrophils from tumour-bearing mice**
- **Low rates of NET formation observed in all neutrophil populations from the blood and spleen of control and tumour-bearing mice**
- **Almost absent NET formation from bone marrow neutrophils**

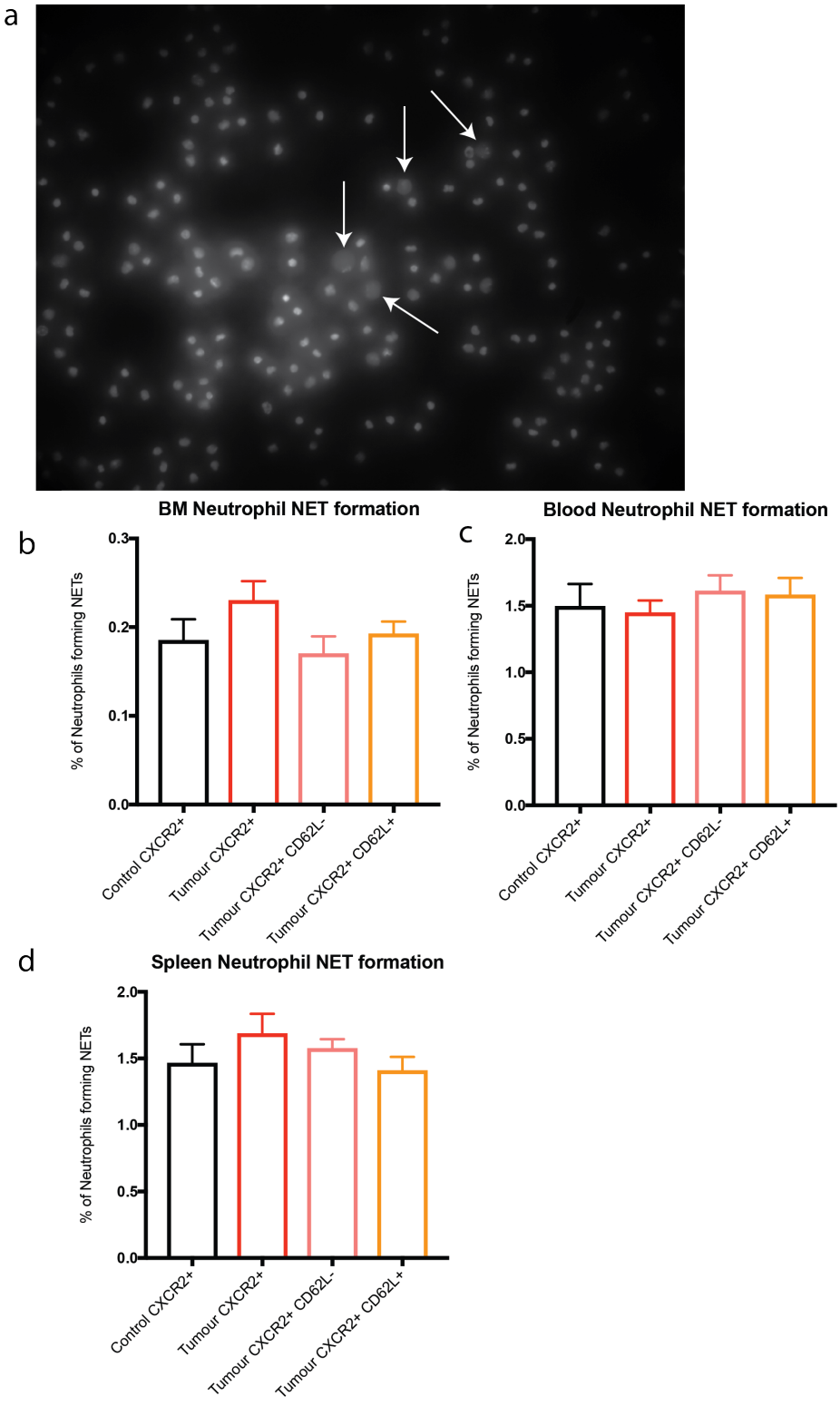

Figure 5.6 No differences in NET formation between neutrophil populations

(**a**) Image displaying neutrophils after 16 hours of PMA stimulation. DNA stained with SyTOX green. White arrows indicate NETs from neutrophils. (**b-d**) Quantification of NET formation by neutrophil populations from bone marrow (**b**) and blood (**c**) and spleen (**d**) of control and tumour-bearing mice. n=6 (3 technical replicates each from 2 mice per condition). Data are displayed as mean ± SD.

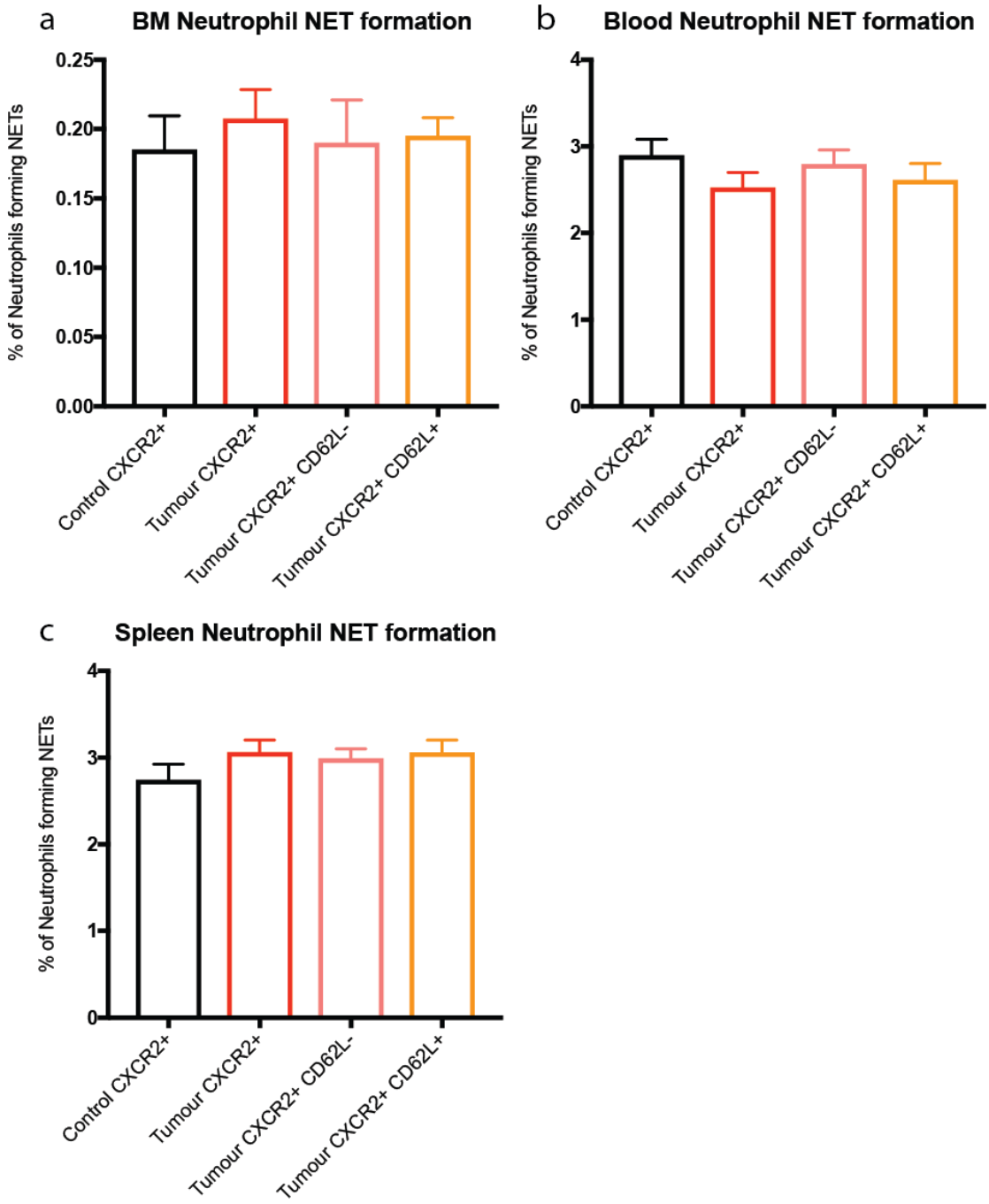

Figure 5.7 No differences in NET formation between neutrophil populations, repeat experiment using mouse serum in place of foetal calf serum

(**a-c**) Quantification of NET formation by neutrophil populations from bone marrow (**a**) and blood (**b**) and spleen (**c**) of control and tumour-bearing mice. n=6 (3 technical replicates each from 2 mice per condition). Data are displayed as mean ± SD.

5.5 Neutrophils from tumour-bearing mice have enhanced *in vitro* immunosuppressive capacity

Neutrophil suppression of immune responses has been extensively documented and observed in a number of different contexts, including cancer, chronic inflammation, infection, and autoimmunity (Pillay et al., 2013, Bronte et al., 2016b). There are a limited number of reports that show neutrophils can inhibit B cells and Natural Killer cells, but neutrophils principally suppress T cells (Bronte et al., 2016b). In cancer, neutrophil suppression of T cells has been found to occur through a variety of mechanisms, including the release of reactive oxygen species, release of immunomodulatory cytokines and through expression of PD-L1. Immune suppression by neutrophils can lead to enhanced tumour growth and metastasis, illustrated by the fact that both ablation of neutrophils and pharmacological inhibition of their suppressive mechanisms can impair tumour growth and metastasis (Coffelt et al., 2015, Veglia et al., 2019). Additionally, there is evidence that in humans a population of immunosuppressive CD62L-DIM, hypersegmented neutrophils expands in the blood following LPS stimulation (Pillay et al., 2012), and a similar population was identified in a small sample of cancer patients (Hao et al., 2013). Given the evidence for the importance of neutrophil suppression in cancer, and the possible role of $CD62L^{-}$ immunosuppressive neutrophils in humans, I wanted to investigate the suppressive capabilities of different populations of neutrophils.

I therefore performed *in vitro* T cell suppression assays, comparing $CXCR2^{+}$ $CD62L^{+/-}$ neutrophils from pre-metastatic tumour-bearing mice, and comparing $CXCR2^{+}$ neutrophils from control and pre-metastatic tumour-bearing mice. I used FACS to purify neutrophil populations from the spleens of control and tumour-bearing mice. I also purified Tconv cells (also known conventional T cells, T_{conv}) from the spleens of the same mice. For these assays neutrophils were co-cultured with T_{conv} cells from the same mice; i.e. neutrophils from control mice were co-cultured with T_{conv} cells from the same control mice, and neutrophils from tumour-bearing mice were co-cultured with T_{conv} cells from the same tumour-bearing mice.

T_{conv} cells were first incubated with Cell Trace Violet. This dye diffuses into cells and stably binds amines. The dye can be used to determine cell proliferation, because it progressively loses intensity with each cell division. Labelled Tconv cells were then stimulated with anti-CD3/CD28 beads, which activates and induces them to begin proliferating. After 72 hours, Cell Trace Violet expression can be analysed by flow cytometry (Figure 5.8a).

In addition to purifying neutrophils, I also purified $CD4^+$ $CD25^+$ regulatory T cells (also known as Tregs). Tregs cells suppress T_{conv} cells and were therefore used as a positive control in the suppression assay. Labelled, bead-activated T_{conv} cells were co-cultured with Tregs or FACS-purified neutrophil populations for 72 hours and then Cell Trace Violet expression analysed. I performed the assay with three ratios of suppressive cells: T_{conv} cells (1:1, 1:2, 1:4). For a negative control of immune suppression, labelled, bead-activated T_{conv} cells were cultured alone.

I first found that Tregs do indeed suppress T_{conv} cells, with similar levels of suppression between control and tumour-bearing samples (Figure 5.8b). Increasing the ratio of Tregs to T_{conv} cells decreases the suppression, with a 1:4 ratio abrogating suppression by Tregs.

I next compared the total $CXCR2^+$ neutrophil population (i.e. mature neutrophils) from control and tumour-bearing mice. Both populations were able to suppress T cell proliferation, but the tumour-bearing population suppressed the T cells more strongly at all ratios (Figure 5.9a, b). Indeed, at a 1:4 neutrophil : T cell ratio, there is no longer suppression by $CXCR2^+$ neutrophils from control mice, but still significant suppression by $CXCR2^+$ neutrophils from tumour-bearing mice.

Both the $CXCR2^+$ $CD62L^-$ and $CXCR2^+$ $CD62L^+$ neutrophil populations could strongly suppress T cell proliferation (Figure 5.10a, b), much more so than the Tregs, and in a ratio-dependent manner, although even a neutrophil: T cell ratio of 1:4 did not completely abrogate neutrophil suppression. However, there was no difference in suppression between the two populations.

Conclusions

- **Mature splenic neutrophils from control mice can suppress T cell proliferation *in vitro***
- **Mature splenic neutrophils from tumour-bearing mice have enhanced suppression of T cell proliferation**
- **There is no difference in suppressive capacity between splenic $CXCR2^+$ $CD62L^-$ and $CXCR2^+$ $CD62L^+$ neutrophils from tumour-bearing mice**

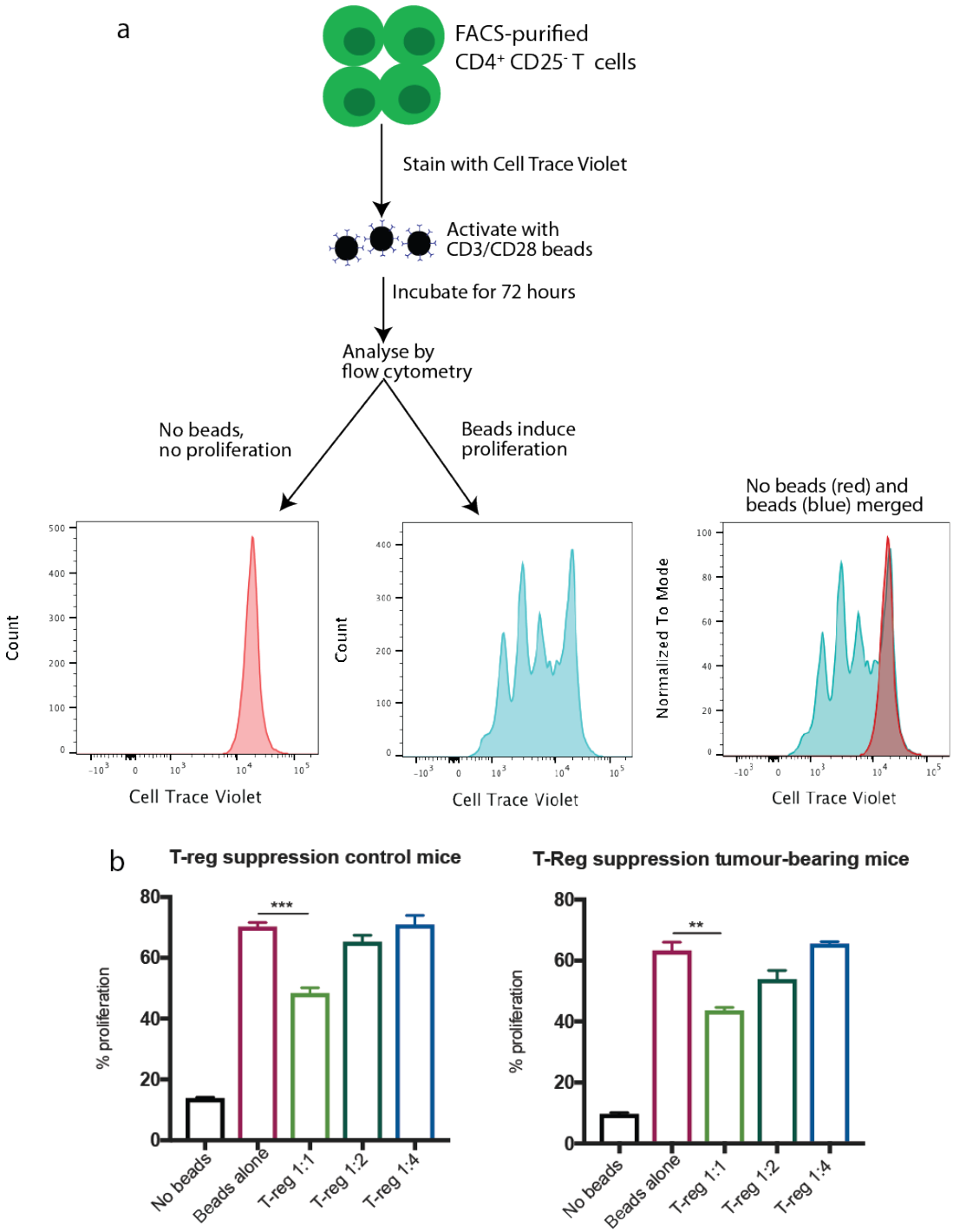

Figure 5.8 Tregs suppress T cell proliferation *in vitro*

(**a**) Schematic of T cell stimulation assay. Histograms show intensity of Cell Trace Violet on T_{conv} cells determined by flow cytometry. (**b**) Quantification of suppression of proliferation of T_{conv} cells by T-regs from control and tumour-bearing mice. n=4 (2 technical replicates each from two mice). Data are displayed as mean ± SD. Statistical analysis by two-sided t test. ** P < 0.01. *** P < 0.001.

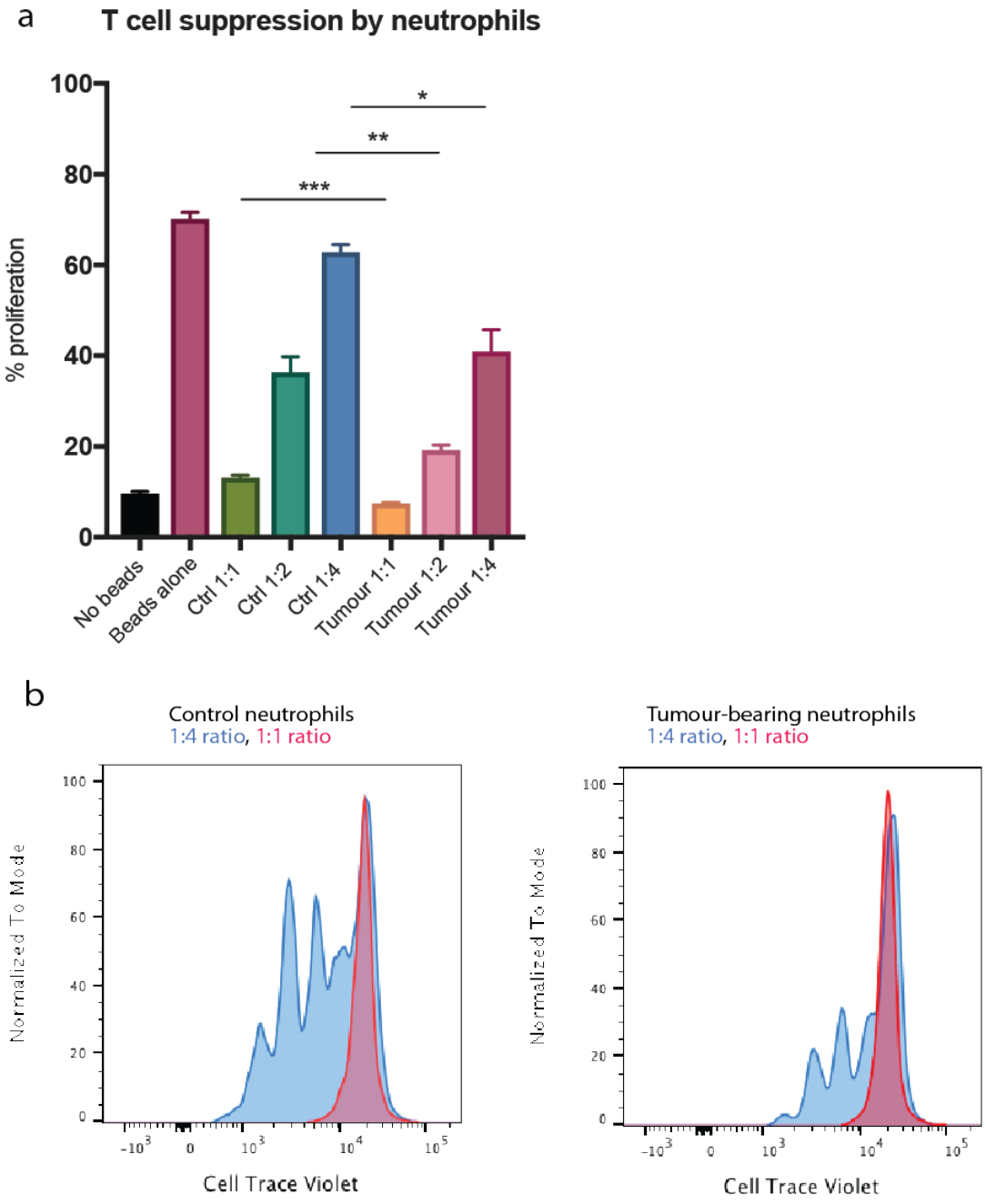

Figure 5.9 Neutrophils from PyMT tumour-bearing mice display enhanced suppression of T cells *in vitro*

(a)Flow cytometric quantification of suppression of proliferation of T_{conv} cells by CXCR2+ neutrophils from the spleen of control and tumour-bearing mice. n=8(2 technical replicates each from 4 mice). Data are displayed as mean ± SD. Statistical analysis by two-sided t test. *P < 0.05, ** P < 0.01, *** P < 0.001. (**b**) Representative histograms of Cell Trace Violet expression on T cells co-cultured with neutrophils from control or tumour-bearing mice, at either 1:1 or 1:4 ratios. Cell Trace Violet intensity is displayed as Normalized to Mode. This normalization corrects for differences in cell numbers between samples.

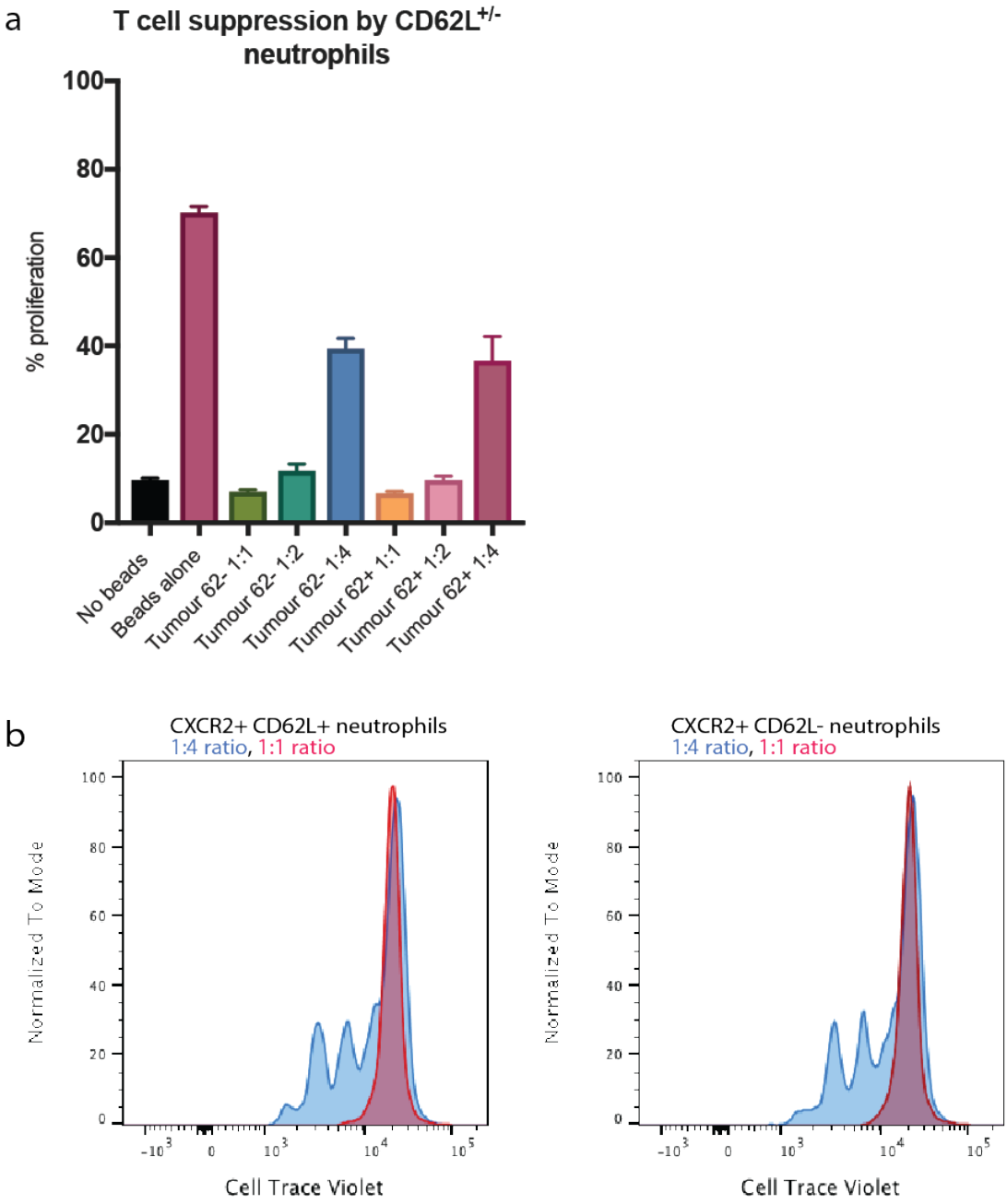

Figure 5.10 No difference in immunosuppression between CXCR2$^+$ CD62L$^-$ and CXCR2$^+$ CD62L$^+$ neutrophils from the spleen of tumour-bearing mice

(**a**)Flow cytometric quantification of suppression of proliferation of T_{conv} cells by CXCR2+ CD62L+/- neutrophils from the spleens of control and tumour-bearing mice. n=8 (2 technical replicates each from 4 mice). Data are displayed as mean ± SD. Statistical analysis by two-sided t test. *P < 0.05, ** P < 0.01, *** P < 0.001. (**b**) Representative histograms of Cell Trace Violet expression on T cells co-cultured with neutrophil populations from r tumour-bearing mice, at either 1:1 or 1:4 ratios.

5.6 Neutrophils from tumour-bearing mice boost cancer cell growth in an *in vitro* 3D co-culture system

I next wanted to investigate direct interactions between neutrophils and cancer cells. These have been observed in the literature in primary tumours and at sites of metastasis, neutrophils have primarily pro-tumour functions in these interactions (Coffelt et al., 2016). For example, neutrophil elastase has been shown to enhance tumour cell growth in lung and prostate cancer (Houghton et al., 2010, Lerman et al., 2017), and in the PyMT model neutrophils aid lung metastasis by secreting leukotrienes that boost cancer cell growth (Wculek and Malanchi, 2015).

I therefore wanted to test whether the different neutrophil populations I identified might have direct effects on cancer cells. To do this, I took advantage of a novel 3D cell culture system, Alvetex, which is a highly porous 3D polystyrene scaffold (Smith et al., 2017). Traditional 2D culture of cancer cells (and indeed other cell types) on plastic plates is used extensively but is highly non-physiological and can alter cell behaviour significantly. Indeed, switching cells from 2D to 3D culture systems induces changes in morphology, growth and drug sensitivity, among other factors (Belgodere et al., 2018). 3D culture systems offer a more tissue-like microenvironment, which may better recapitulate the interactions between cancer cells and neutrophils that occur in a tissue.

I used PyMT cells expressing GFP to allow me to track their growth by microscopy. I first seeded these cells alone on the 3D scaffold, to establish how these cells grow in this environment. I found that PyMT cells grow consistently with time, with integrated density of GFP expression approximately doubling six days after seeding (Figure 5.11a,b). I next seeded GFP^+ PyMT cells on the scaffold and allowed them to settle for 24 hours. I then used FACS to purify neutrophil populations from bone marrow, blood and spleen of control and pre-metastatic tumour-bearing mice. Neutrophils were then added to the scaffold and PyMT growth measured after six days (Figure 5.11c).

I first found that bone marrow neutrophils have no effect of PyMT growth in the 3D assay (Figure 5.12a), regardless of their CD62L expression, or origin from control or tumour-bearing mice.

Blood $CXCR2^+$ neutrophils from control mice had no effect on PyMT growth (Figure 5.12b). The same population from tumour-bearing mice boosted PyMT growth by approximately 50% compared to PyMT cells grown alone or with blood $CXCR2^+$ neutrophils from control mice. There was no difference in growth between cancer cells cultured with $CXCR2^+$ $CD62L^-$ or $CXCR2^+$ $CD62L^+$ neutrophils from the blood of tumour-bearing mice, these populations had the same effect as the total $CXCR2^+$ population.

Splenic $CXCR2^+$ neutrophils from control mice had a slight boosting effect on cancer growth, but splenic $CXCR2^+$ neutrophils from tumour-bearing mice had superior growth-boosting capacity, almost doubling growth compared to cancer cells alone, and significantly greater than $CXCR2^+$ neutrophils from control mice (Figure 5.12c, d). There was no difference in growth between PyMT cells cultured with $CXCR2^+$ $CD62L^-$ and $CXCR2^+$ $CD62L^+$ neutrophils from the spleen of tumour-bearing mice; these populations had the same effect as the total $CXCR2^+$ pool from tumour-bearing mice.

Conclusions

- **Spleen neutrophils can boost cancer cell growth in a 3D co-culture scaffold assay**
- **Spleen and blood neutrophils from tumour-bearing mice have significantly greater enhancement of cancer cell growth than neutrophils from control mice**
- **There is no difference in growth-boosting ability between $CXCR2^+$ CD62L- and $CXCR2^+$ $CD62L^+$ neutrophils from tumour-bearing mice.**

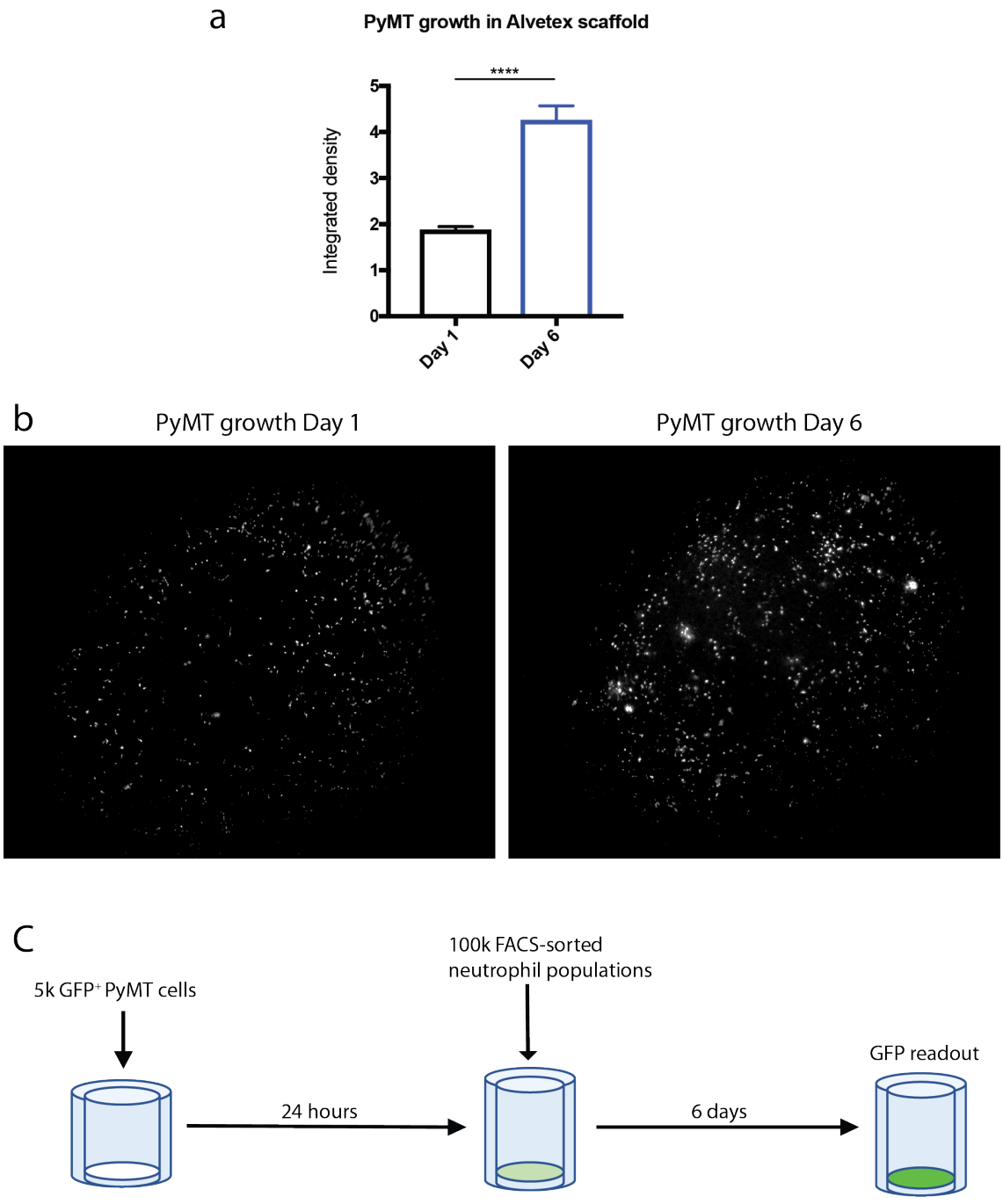

Figure 5.11 Alvetex scaffold 3D co-culture system

(**a**) MMTV-PyMT GFP+ cell growth in Alvetex scaffolds, quantified by microscope analysis of GFP+ expression on scaffold. Data are displayed as mean ± SD. **** P < 0.0001. n=12 wells combined from 2 independent experiments of 6 wells each. Each experiment used a different preparation of MMTV-PyMT GFP+ cells. (**b**) Images displaying representative GFP intensity of scaffolds 1 day and 6 days after seeding of MMTV-PyMT GFP+ cells. (**c**) Schematic of 3D scaffold co-culture experiments

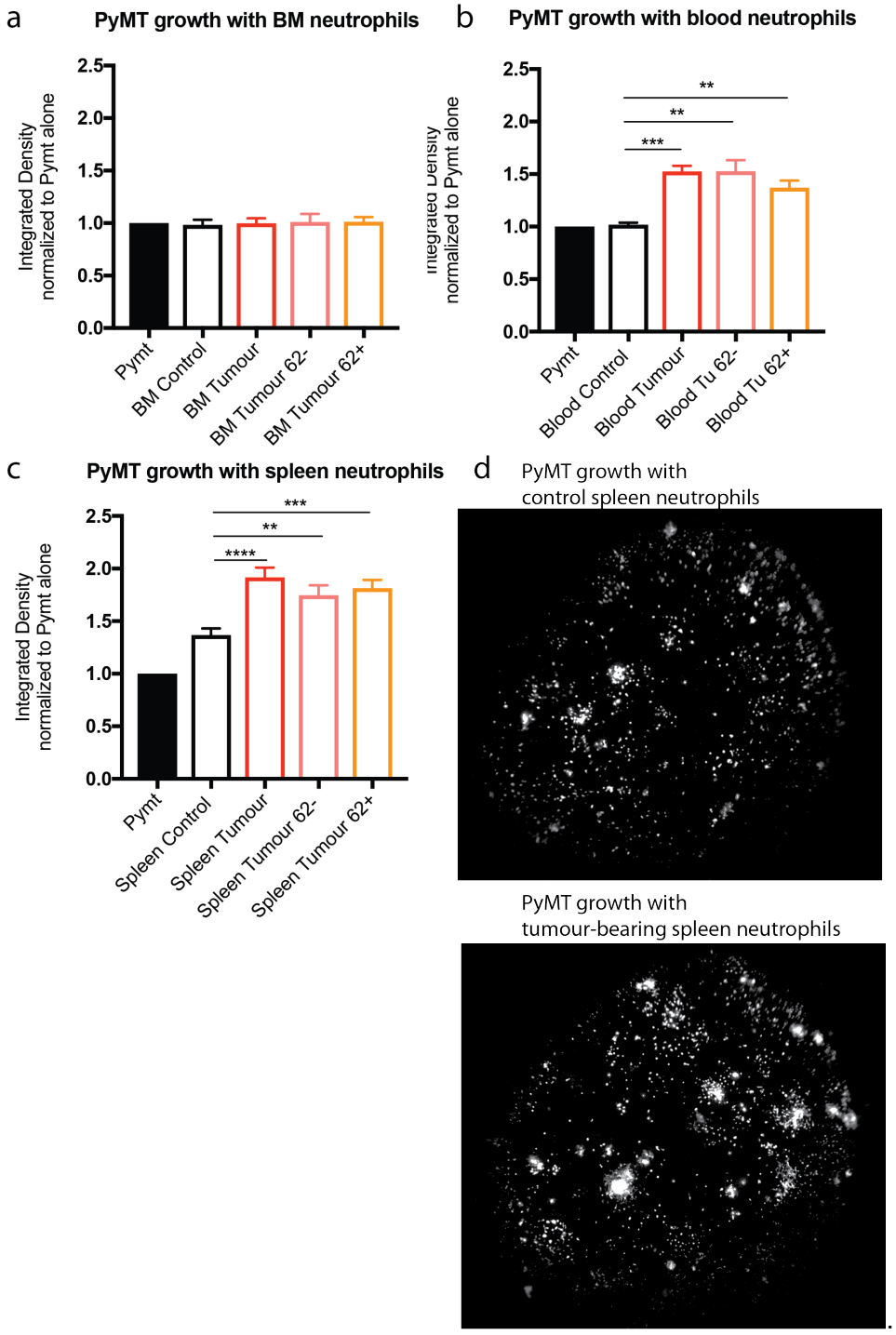

Figure 5.12 Enhanced boosting of cancer cell growth *in vitro* by blood and spleen neutrophils from tumour-bearing mice

(**a-c**) Quantification of growth of MMTV-PyMT GFP+ cells 6 days of after co-culture with bone marrow (**a**), blood (**b**) and spleen (**c**) neutrophil populations, normalized to PyMT growth alone. n = 2 independent experiments of 4 wells for each condition for bone marrow and blood, n = 3 independent experiments of 4 wells for each condition for spleen. Each independent experiment used a different preparation of MMTV-PyMT GFP+ cells. (**d**) Images displaying representative GFP intensity of scaffolds after 6 days of co-culture with spleen neutrophils. Data are shown as mean ± SD. *P < 0.05, ** P < 0.01, *** P < 0.001, **** P < 0.0001.

5.7 Bone marrow neutrophils from tumour-bearing mice have reduced reactive oxygen species levels

Results from the immune suppression assays and co-culture of neutrophil populations with cancer cells had revealed functional differences between neutrophils from control and tumour-bearing mice, whilst not finding any differences between the $CXCR2^+$ $CD62L^-$ and $CXCR2^+$ $CD62L^+$ populations in tumour-bearing mice. I wanted to explore what might be underlying the differences in functionality between control and tumour-bearing neutrophils, and also further investigate possible differences between the $CD62L^{+/-}$ populations.

ROS play an important role in neutrophil biology: ROS are principally used by neutrophils to destroy phagocytosed pathogens (Winterbourn et al., 2016). However, ROS have also been shown to affect intracellular signalling within neutrophils, and ROS released from neutrophils can have effects on local cells, activating or modifying signalling pathways (Winterbourn et al., 2016, Dupré-Crochet et al., 2013). Therefore, neutrophil ROS levels can indicate a range of potential functional activities. Additionally, in functional assays I have observed neutrophils suppressing T cells and boosting cancer cell growth, both of these functions can be mediated through ROS (Mensurado et al., 2018, Reczek and Chandel, 2017), and thus investigating ROS levels may provide mechanistic insight into how neutrophils interact with T cells and cancer cells in these assays.

I used flow cytometry to assay intracellular ROS levels in bone marrow, blood and spleen neutrophils from control and pre-metastatic tumour-bearing mice. I first found that neutrophils in control bone marrow have significantly higher ROS levels than neutrophils in tumour-bearing bone marrow (Figure 5.13a, b). In the blood and spleen, ROS levels were identical across both tissues and between control and tumour-bearing neutrophils, with ROS levels in these tissues being significantly lower compared to the bone marrow.

I next determined ROS levels in $CXCR2^+$ $CD62L^+$ and $CXCR2^+$ $CD62L^-$ neutrophils, from both control and tumour-bearing mice. I found no difference between $CD62L^{+/-}$

neutrophil populations, in any tissue, regardless of control or tumour-bearing background (Figure 5.13c,d). As observed with the total neutrophil population, control $CXCR2^+$ $CD62L^{+/-}$ neutrophils in the bone marrow had higher ROS levels than the same population in tumour-bearing bone marrow.

Having observed that bone marrow neutrophils have higher ROS levels in control mice compared to tumour-bearing mice, I wanted to look at specific populations of neutrophils within the bone marrow, to see whether this difference in ROS levels occurred at a specific stage of neutrophil development. I therefore compared ROS levels in immature CXCR2- neutrophils and mature $CXCR2^+$ neutrophils from control and tumour-bearing mice, and also compared the $CD62L^+$ and $CD62L^-$ fractions within the $CXCR2^+$ population. I found that ROS levels are decreased significantly in all neutrophil populations in tumour-bearing mice compared to control mice (Figure 5.14a, b). The immature neutrophils also have lower ROS levels than the mature neutrophils, in both control and tumour-bearing contexts.

These results suggest that the presence of a tumour perturbs the bone marrow microenvironment, resulting in decreased ROS levels in immature and mature neutrophils. The precise consequences of this are unclear; however, ROS can play a role in numerous intracellular signalling pathways (Zhang et al., 2016), and can also affect cell metabolic pathways, thus it is possible that the differences in ROS levels may result in altered cell signalling or metabolism between control and tumour-bearing bone marrow neutrophils. Moreover, the shift in ROS levels between immature and mature bone marrow neutrophils indicates possible alterations in cell signalling or metabolism between these developmental states, which fits with published literature on neutrophil development (Coffelt et al., 2016).

Conclusions

- **Bone marrow neutrophils from tumour-bearing mice have lower ROS levels**
- **This is found at all stages of $Ly6g^+$ neutrophil development, with immature $CXCR2^-$ neutrophils having lower ROS levels than mature $CXCR2^+$ neutrophils**

- **Blood and spleen neutrophils have lower ROS levels than bone marrow neutrophils**
- **There is no difference in ROS levels between $CXCR2^+$ $CD62L^-$ and $CXCR2^+$ $CD62L^+$ neutrophils, regardless of tissue or mouse tumour presence**

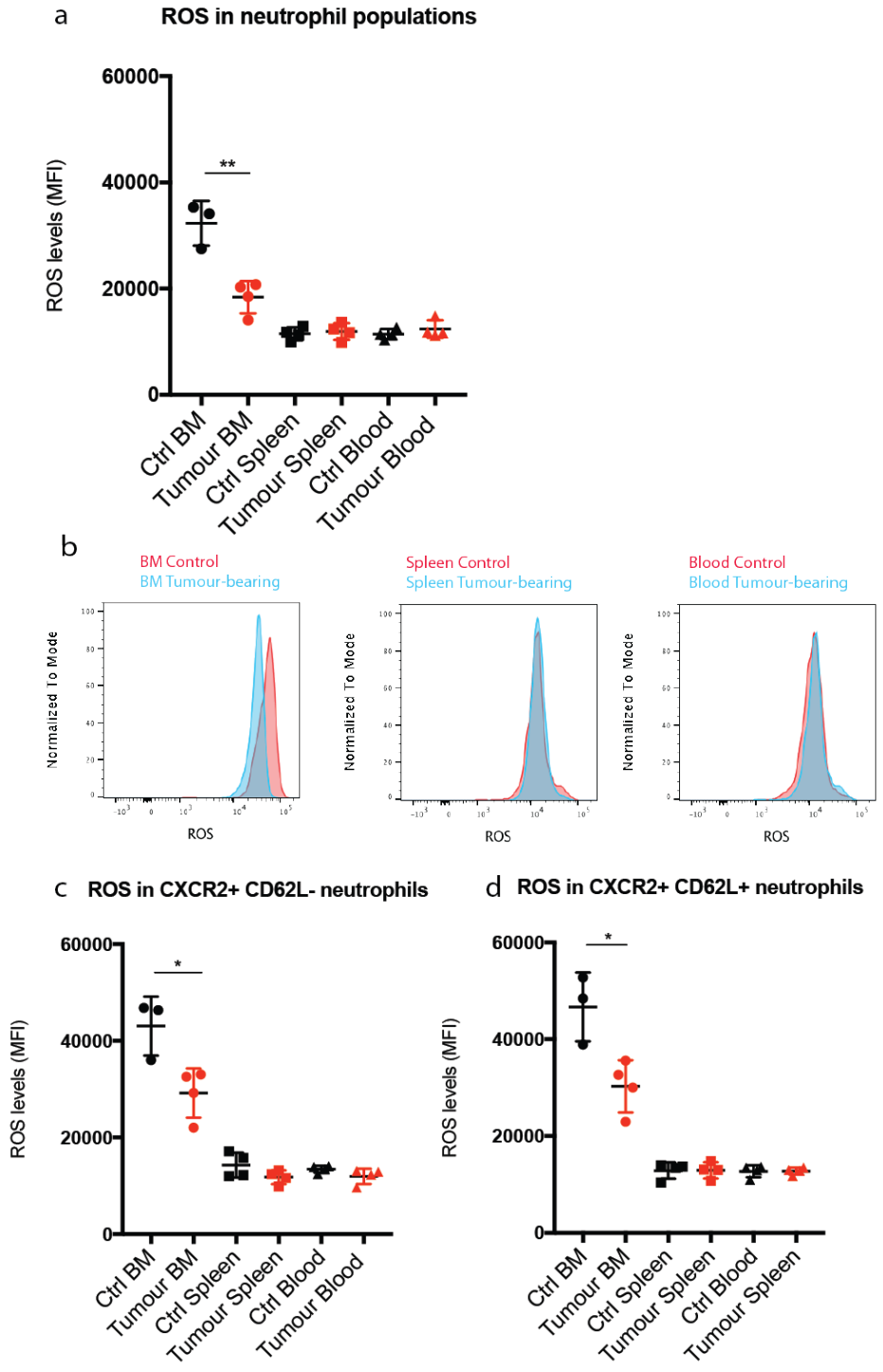

Figure 5.13 Higher ROS levels in neutrophils in the bone marrow of control mice

(**a**) Flow cytometric quantification of ROS levels (in mean fluorescence intensity, MFI) in Ly6g+ CD11b+ neutrophils across tissues from control and tumour-bearing mice. n=4 mice for all conditions except Ctrl BM for which n=3 mice. (**b**) Representative histograms displaying ROS levels in neutrophils across tissues. Red = neutrophils from control mice, blue = neutrophils from tumour-bearing mice. (**c**) ROS levels in CXCR2+ CD62L- neutrophils. (**d**) ROS levels in CXCR2+ CD62L+ neutrophils. For (**c, d)** .n=4 mice for all conditions except Ctrl BM for which n=3 mice. Data displayed as mean ± SD. Statistical analysis by two-sided t test. *P < 0.05, ** P < 0.01.

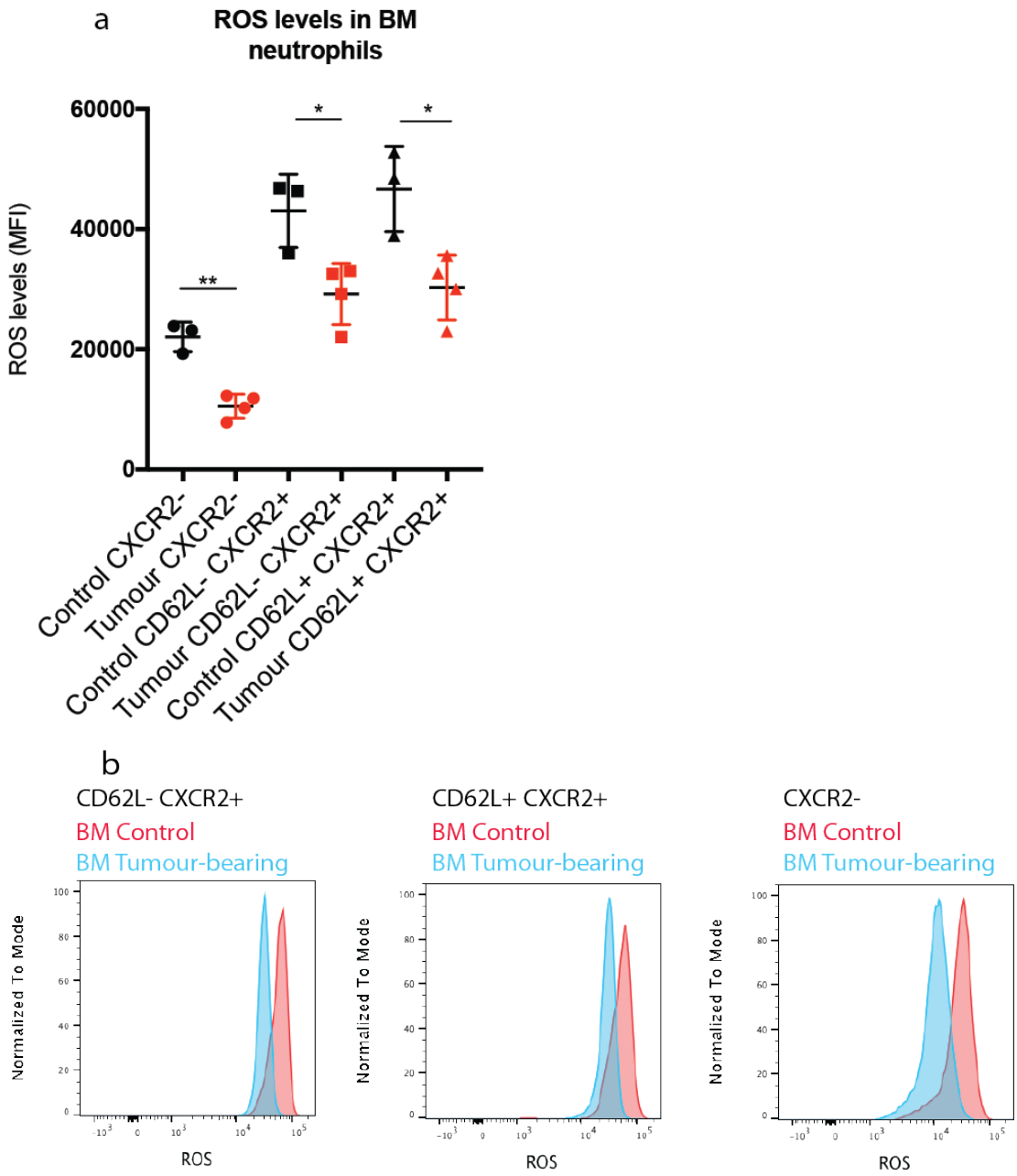

Figure 5.14 Higher ROS levels in mature and immature neutrophils in control bone marrow

(**a**) Flow cytometric quantification of ROS levels (in MFI) in neutrophil bone marrow populations from control and tumour-bearing mice. n=3 mice for control samples, n=4 mice for tumour-bearing samples. Data are displayed as mean ± SD. Statistical analysis by two-sided t test. *P < 0.05, ** P < 0.01. (**b**) Representative histograms displaying ROS levels in bone marrow neutrophil populations. Red = neutrophils from control mice, blue = neutrophils from tumour-bearing mice.

5.8 Differences in kinase activity between neutrophil populations in control and tumour-bearing mice

In the previous sections I have found differences in functionality and ROS levels between neutrophils from control mice and tumour-bearing mice. I next wanted to further explore differences between these neutrophil populations using an approach less focused on one specific function (such as immune suppression), and instead examine shifts in overall cell activity between neutrophil populations. To do this I took advantage of a technique that can assay the kinase activity of numerous proteins in cells. The assay is based on a chip that contains target phosphorylation sites for a multitude of kinases. Cell lysates are incubated with ATP on the chip, providing substrate for kinases in the lysate to phosphorylate their target sequences. This phosphorylation is then detected with fluorescent antibodies (Figure 5.15). The chip can contain sequences for tyrosine kinases (196 peptide kinase sites) or serine/threonine kinases (144 peptide kinase sites). The chip thus allows determination of the activity of numerous kinases within a sample. This technique therefore offers an advantage over more commonly used approaches such as RNA-sequencing and proteomics because it provides information on the actual activity of kinases, rather than levels of mRNA or protein, which do not necessarily correlate with the functional activity of a protein or pathway. Thus, the kinase assay provides a more functionally relevant readout than other approaches, though it is not an unbiased approach like transcriptomics and proteomics are.

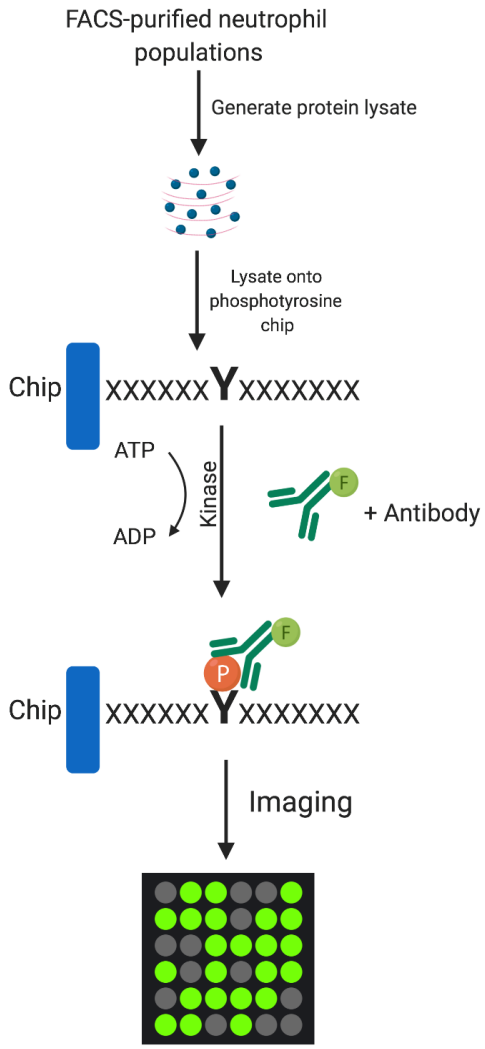

Figure 5.15 Schematic of Pamgene tyrosine kinase chip assays

Neutrophils were purified using FACS and then lysed. Lysate is combined with ATP and fluorophore-conjugated antibodies against phosphorylated tyrosine kinase target sequences. This mixture is then incubated on the chip. Active kinases can use ATP to phosphorylate tyrosines on their target sequences, which can then be bound by fluorescent-labelled antibodies, which are detected by imaging. Created with Biorender.com

I ran this assay with tyrosine kinase chip (PTK) using samples from control mice and mice with spontaneous PyMT tumours. In previous sections I showed that spontaneous PyMT tumours had the strongest effect on neutrophil expansion and the expansion of the $CXCR2^{+}$ $CD62L^{-}$ neutrophil population (Chapter 4 Section 4.6, Figure 4.8), and therefore I predicted that these tumours would have the strongest effect on neutrophil kinase activity, thereby facilitating the identification of difference in kinase activity that a tumour may induce in neutrophils. I analysed kinase activity in $CXCR2^{+}$ mature neutrophils and $CXCR2^{-}$ immature neutrophils from the bone marrow, and $CXCR2^{+}$ mature neutrophils from the blood. These populations were selected because in the previous section I found that ROS levels are significantly decreased in bone marrow neutrophils (mature and immature) in tumour-bearing mice, indicating possible differences in intracellular signalling and hence kinase activity. I also found a difference in ROS levels between immature and mature neutrophils, and this may also suggest differences in kinase activity. Mature blood neutrophils were selected because these cells form the main circulating component of mature neutrophils. It is important to note that this is a single experiment performed with three mice per condition, thus these findings are preliminary and will need further repetition and replication to be confirmed.

Kinase assay data were analysed using ClustVis (Metsalu and Vilo, 2015). A full table of all kinase target sequences used in the analysis can be found in Appendix 7.1.

In both the bone marrow immature and mature populations, and in the blood mature populations I find shifts in the activity of numerous kinases between control and tumour-bearing mice. I find that immature neutrophils from control mice having increased kinase activity compared to those from tumour-bearing mice (Figure 5.16). In the mature neutrophils in the bone marrow, the kinase activity of a number of kinases is raised in tumour-bearing mice (Figure 5.17). The shift is less strong than in the mature blood neutrophils, but a number of kinases increase in activity in samples Tumour 2 and Tumour 3. As with the immature bone marrow population, there is the suggestion of a link between tumour burden and differences in kinase activity: mature bone marrow neutrophils from sample Tumour 1 show much more modest increases in kinase activity than those from Tumour 2 and Tumour 3.

In the blood mature neutrophils, there is an increase in kinase activity in almost all kinases in the tumour-bearing samples compared to the control samples (Figure 5.18). This indicates a broad shift in kinase activity in mature blood neutrophils of tumour-bearing mice, with the increases in kinase activity much stronger than in the bone marrow mature population.

It is also possible to compare kinase activity between the neutrophil populations within a given mouse. For samples Tumour 2 and Tumour 3 this reveals large shifts in kinase activity between the neutrophil populations (Figure 5.19). The immature bone marrow neutrophils have reduced activity compared the mature bone marrow and blood neutrophils, with the mature bone marrow neutrophils having the highest kinase activity. These results suggest neutrophils undergo changes in kinase activity during development, and during egress from the bone marrow into the circulation.

Conclusions

- **Kinase activity in different neutrophil populations can be extensively altered by the presence of a tumour**
- **The activity of different kinases varies between stages of neutrophil development, and between blood and bone marrow neutrophils**

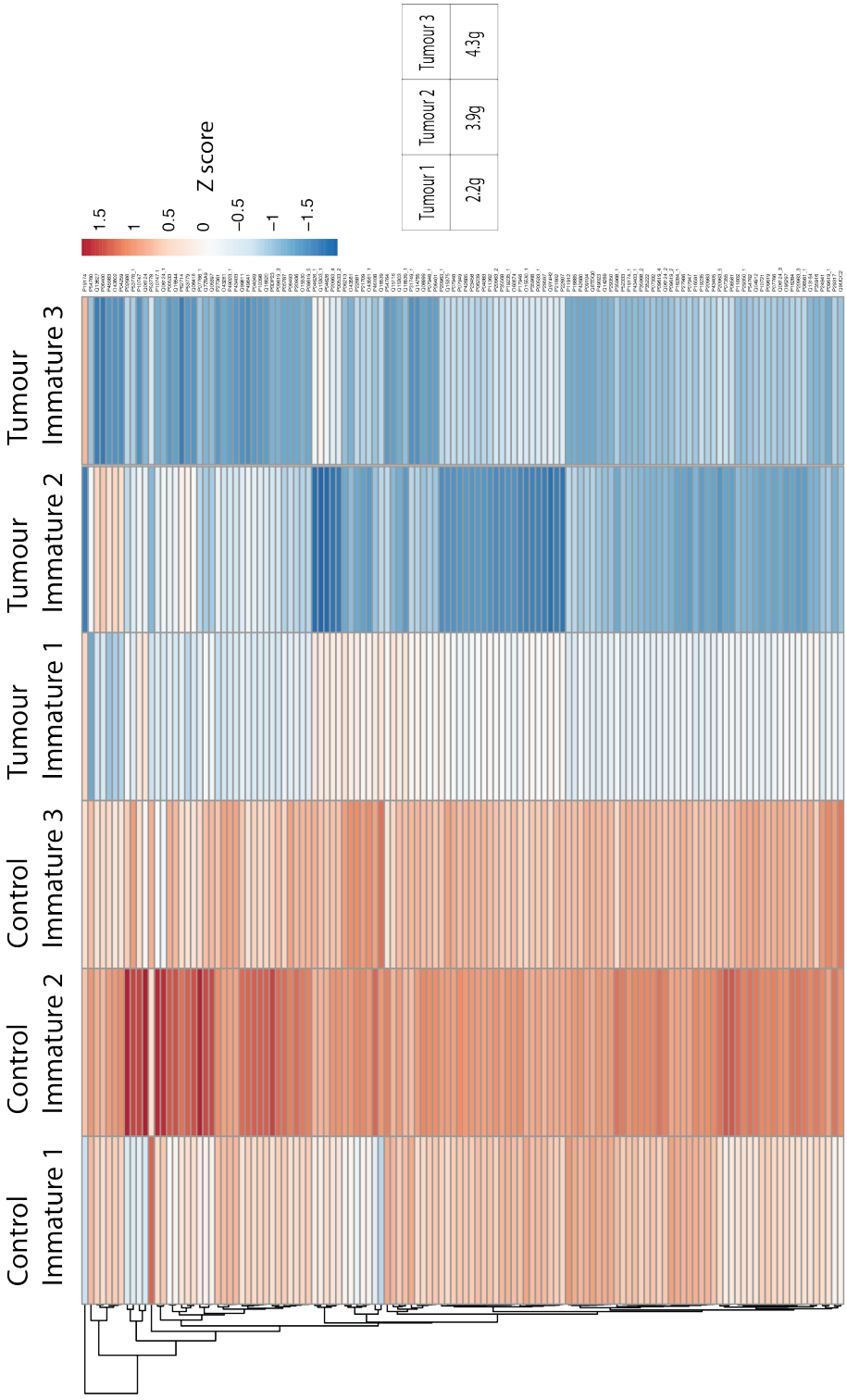

Figure 5.16 Differences in PTK activity between immature bone marrow neutrophils from control and tumour-bearing mice

Z score heatmaps of PTK kinase activity in immature neutrophils. Table displays tumour weights for tumour-bearing mice. Z score colour intensity indicates difference in relative kinase activity between kinases and samples. Kinase sequences are denoted by UniProt Protein database IDs (https://www.uniprot.org). Further information kinase sequences denoted by UniProt IDS can be found in Appendix 7.1

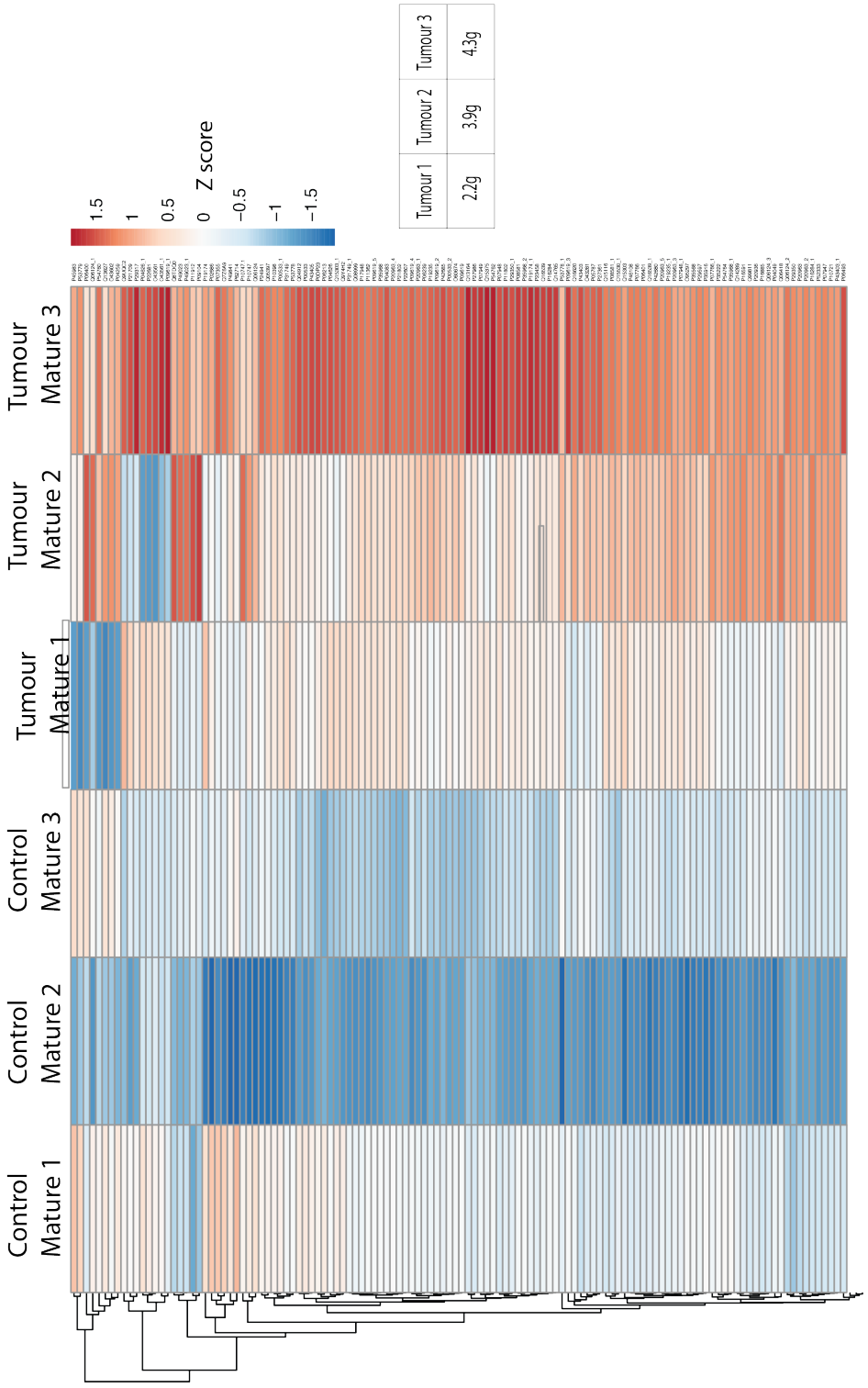

Figure 5.17 Differences in PTK activity between mature bone marrow neutrophils from control and tumour-bearing mice

Z score heatmaps of PTK kinase activity in mature neutrophils. Table displays tumour weights for tumour-bearing mice. Z score colour intensity indicates difference in relative kinase activity between kinases and samples. Kinase sequences are denoted by UniProt Protein database IDs (https://www.uniprot.org). Further information kinase sequences denoted by UniProt IDS can be found in Appendix 7.1

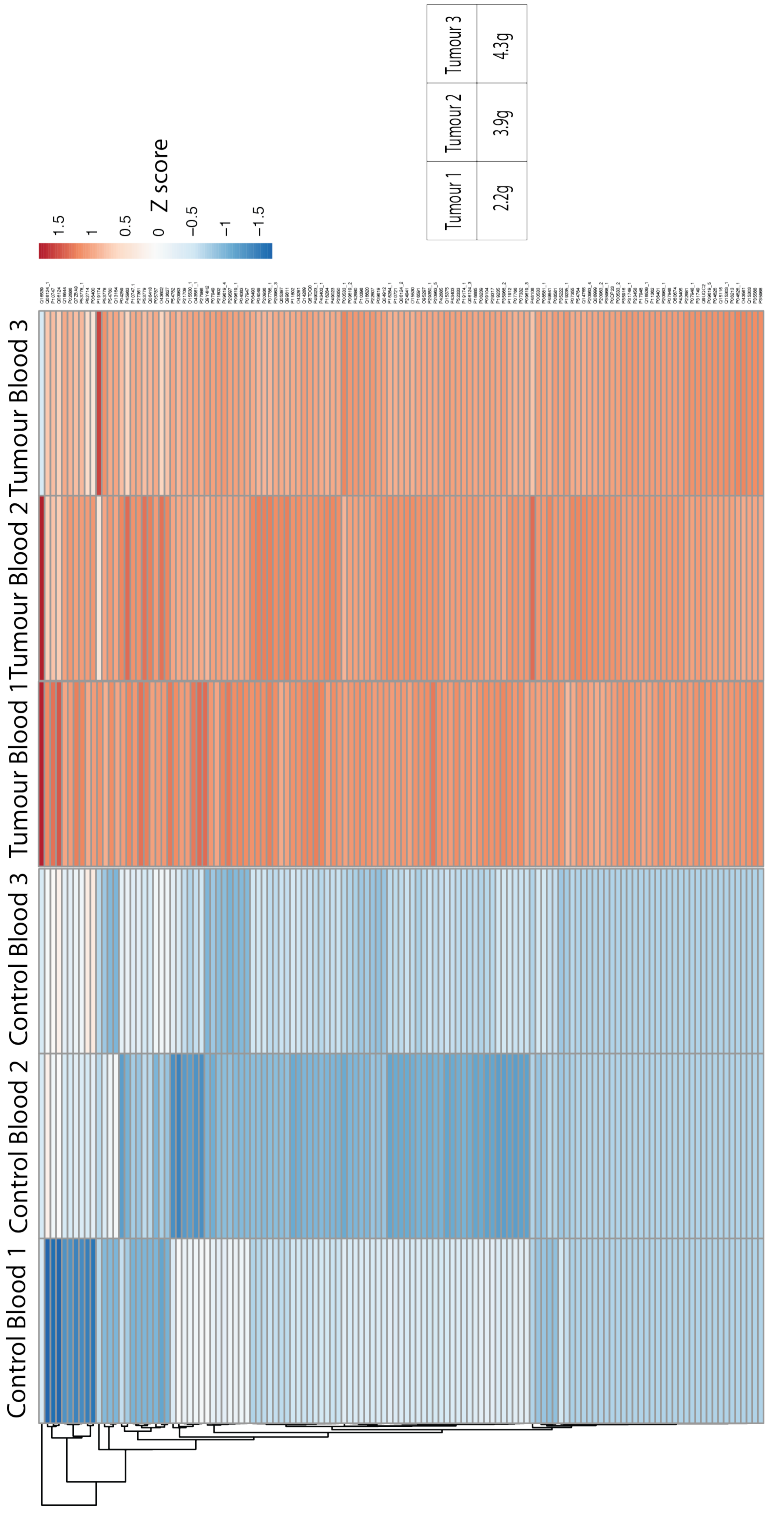

Figure 5.18 Differences in PTK activity between mature blood neutrophils from control and tumour-bearing mice

Z score heatmaps of PTK kinase activity in mature blood neutrophils. Table displays tumour weights for tumour-bearing mice. Z score colour intensity indicates difference in relative kinase activity between kinases and samples. Kinase sequences are denoted by UniProt Protein database IDs (https://www.uniprot.org). Further information kinase sequences denoted by UniProt IDS can be found in Appendix 7.1.

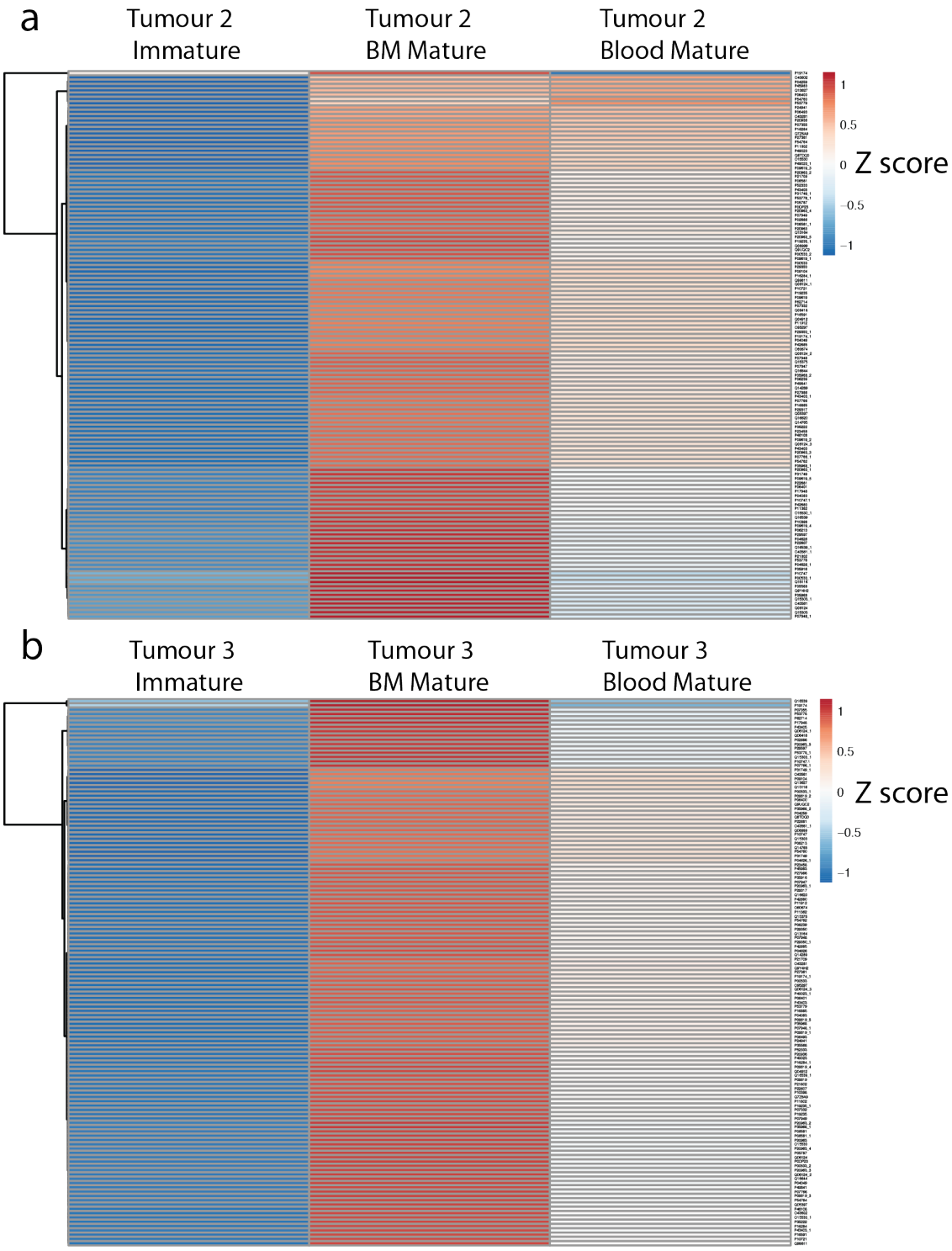

Figure 5.19 Differences in PTK activity between neutrophil populations from the same mouse

(**a, b**) Z score heatmaps of PTK kinase activity in neutrophil populations from (**a**) mouse Tumour 2, and (**b**) mouse Tumour 3. Z score colour intensity indicates difference in relative kinase activity between kinases and samples. Kinase sequences are denoted by UniProt Protein database IDs (https://www.uniprot.org). Further information kinase sequences denoted by UniProt IDS can be found in Appendix 7.1.

5.9 Chapter Conclusions

- **In tumour-bearing mice, $CXCR2^+$ $CD62L^-$ neutrophils have a more hypersegmented nuclear morphology than $CXCR2^+$ $CD62L^+$ neutrophils**
- **A range of assays do not find any differences in functionality between $CXCR2^+$ $CD62L^-$ and $CXCR2^+$ $CD62L^+$ neutrophils**
- **However, functional assays do show that neutrophils from tumour-bearing mice have enhanced immune suppression and greater capacity to boost cancer cell growth *in vitro***
- **In the bone marrow, neutrophils from control mice have higher ROS levels than neutrophils from tumour-bearing mice, at both immature and mature stages of neutrophil development**
- **Analysis of kinase activity in neutrophil populations finds shifts between bone marrow immature and mature and blood mature neutrophil populations**
- **These neutrophil populations in tumour-bearing mice have altered kinase activity compared to those in control mice**

Chapter 6. Discussion

6.1 Thesis aims

Evidence from both basic science and the clinic has implicated neutrophils in cancer. Whilst the bulk of evidence indicates a pro-tumour effect for neutrophils, a number of studies have also found neutrophils with anti-tumour phenotypes (Shaul and Fridlender, 2019). Neutrophil heterogeneity is an emerging concept that intersects with the roles of neutrophils in cancer, but the precise nature of neutrophil heterogeneity and its consequences for tumours remain to be established (Ng et al., 2019).

My aims in this thesis were to:

- Investigate neutrophil heterogeneity across tissues
- Determine how the presence of a tumour perturbs this heterogeneity
- Investigate the functional consequences of neutrophil heterogeneity for tumour cells

6.2 Neutrophil heterogeneity at the surface marker level

My first aim in this project was to investigate neutrophil heterogeneity across tissues. A number of different studies have identified different neutrophil populations by differential expression of surface molecules (Section 1.7) and this method is commonly used in immunology and other disciplines to define cell populations. My initial experiments used high-dimensional mass cytometry coupled with bioinformatics analysis to discern neutrophil heterogeneity in the bone marrow, lungs and spleen, identifying a range of populations defined by surface marker expression. I subsequently used flow cytometry to validate a number of the populations identified by mass cytometry, extending some of these findings to the blood and liver. In this way, I was able to achieve the first aim of the project, identifying inter- and intra-tissue heterogeneity of neutrophils. Before discussing my findings on how the

presence of a tumour can alter this heterogeneity, I will review my observations on neutrophil heterogeneity within control mice.

6.2.1 Bone marrow heterogeneity in control mice

Neutrophil heterogeneity is strongest in the bone marrow, this is to be expected given that the bone marrow is the site of neutrophil development, and will therefore contain neutrophils in various states of maturation (Borregaard, 2010). F4/80 and MHC-II respectively defined two populations of neutrophils in the bone marrow. I first investigated these populations in order to validate the mass cytometry findings, and was able to detect these populations with flow cytometry. Although MHC-II expression has been reported on neutrophils previously, this expression was on mature neutrophils within tissues and tumours (Singhal et al., 2016, Lin and Loré, 2017), not on neutrophils developing in the bone marrow. F4/80 expression has previously been reported on neutrophils in the bone marrow (Becher et al., 2014), however this study found that approximately 95% of neutrophils in the bone marrow were F4/80$^+$, in contrast to my findings that approximately 10% of bone marrow neutrophils are F4/80$^+$ (Figure 3.6). This may be due to mouse strain differences (the study in question used mice of C57/BL6 background whereas I used FvB background mice) or differences in animal housing, which in particular can affect the microbiome, which can significantly affect neutrophil phenotype (Zhang et al., 2015).

The functional significance of both MHC-II and F4/80 expression on neutrophils in the bone marrow is unclear. The role of F4/80 in macrophages remains unknown (Lin et al., 2010), and it is therefore difficult to even speculate about the importance of this marker on neutrophils. MHC-II is used to present antigens to T cells, but it is uncertain what purpose this could serve for neutrophils developing in the bone marrow.

I also observed heterogeneity in CXCR2 expression on bone marrow neutrophils. Neutrophils upregulate CXCR2 as they mature (McKinstry et al., 1997), so this finding is to be expected.

Finally, I was able to observe variable expression of CD62L on bone marrow neutrophils with positive, intermediate and negative populations. Variability in CD62L expression is observed in tandem with variability in CXCR2 expression: both immature and mature neutrophils display variability in CD62L expression, and this marker does not therefore appear to link to maturation state in the bone marrow.

6.2.2 Heterogeneity outside the bone marrow

Whilst I can observe quite extensive heterogeneity within the bone marrow, in the circulation and periphery the heterogeneity I find is more restricted. The principal axis of heterogeneity is the expression of CD62L. I can observe neutrophils with positive, negative and intermediate expression of this marker in the bone marrow, blood, spleen and liver. Variable expression of CD62L has been documented previously in both mice and humans (Pillay et al., 2012, Casanova-Acebes et al., 2013), thus this finding is not novel. However, it was important as it allowed detection of populations that shifted in response to the presence of a tumour.

6.2.3 Ly6g^{+} CD11b^{-} cells in the spleen

In the spleen, I detected a population of Ly6g^{+} CD11b^{-} cells. This combination of expression is highly unconventional: neutrophils upregulate both of these molecules during development (Coffelt et al., 2016), thus it was unclear how cells could be positive for Ly6g whilst lacking CD11b expression. This prompted my further investigation of this population, ultimately demonstrating that these cells are in fact not neutrophils but mature B cells (which do not express CD11b), which were detected as Ly6g^{+} by cytometry due to binding of their B cell receptor to the Ly6g antibody.

This phenomenon illustrates the potential pitfalls of defining cells by cytometry-based surface marker expression. In particular it demonstrates the limits of defining cell types by a specific marker, and positing that this marker uniquely identifies a given

population. This finding has implications for future mouse studies using the Ly6g antibody to delineate neutrophils from other immune cell populations. Ideally a combination of Ly6g and CD11b should be used, in order to exclude the $Ly6g^+$ B cell population from any experiments. In addition, analysis of nuclear morphology can ensure that cells positive for Ly6g can be confirmed as neutrophils.

6.2.4 Lung neutrophil heterogeneity

In the lungs, I was initially unable to detect any neutrophils expressing CD62L. Consequently, there appeared to be relatively limited heterogeneity within the lungs. However, I found that a gentler method of cell extraction allowed detection of some neutrophils expressing CD62L, but above 70% of neutrophils in the lungs remained $CD62L^-$ in control mice. This is in contrast to tissues such as bone marrow, blood, spleen and liver, where the $CD62L^-$ fraction was typically less than 15% of the neutrophil population. It appears that regardless of the method of tissue extraction at least 70% of lung neutrophils do not express CD62L on their surface.

It therefore seems that it is not solely lung tissue processing methods that are responsible for low CD62L expression in the lungs, but that the lung tissue microenvironment affects neutrophil expression of CD62L. The capillaries of the lungs are extremely narrow, therefore neutrophil movement through them may be slowed. Indeed, it has been observed that neutrophil trafficking times are much longer through the lungs than through other tissues, suggesting they are rolling and tethering to the endothelium constantly as they “crawl” through the lung capillary system, and extravasated neutrophils are found in the lungs in the steady state (Kreisel et al., 2010, Kolaczkowska and Kubes, 2013). Constant engagement of CD62L during tethering and rolling causes shedding of CD62L (Ivetic, 2018), this may explain why, regardless of the preparation method used, over 70% of lung neutrophils lack CD62L expression. However, this hypothesis has not been confirmed experimentally and further work is required to better understand the nature of lung neutrophils and the reason for their low CD62L expression.

Overall, the lack of CD62L expression means I can only find very limited neutrophil heterogeneity in the lungs. The lack of CD62L expression also prevents detection, in the lungs, of the shift in CD62L expression on neutrophils observed between control and tumour-bearing mice.

There is some evidence in the literature that the tight lung vasculature can induce downregulation of CD62L expression by lung neutrophils (Kolaczkowska and Kubes, 2013, Kreisel et al., 2010) and this may explain why even gentle dissociation does not restore lung neutrophil CD62L expression to that of neutrophils in other tissues

6.3 Effects of tumours on neutrophil heterogeneity

6.3.1 $CXCR2^+$ $CD62L^-$ neutrophils expand in tumour-bearing mice

My second aim in this thesis was to investigate how the presence of a tumour affects neutrophil heterogeneity. I find that tumours can have significant impacts on neutrophil numbers and heterogeneity, consistent with many previous reports in the literature (Ng et al., 2019, Coffelt et al., 2016). I observe increases in neutrophil numbers in the bone marrow, circulation and periphery, recapitulating previous findings (Wculek and Malanchi, 2015, Coffelt et al., 2015). I detect shifts in the relative proportions of a number of neutrophil populations across these tissues, and find these changes in a range of mouse tumour models. Importantly, when comparing control and tumour-bearing mice, I did not find novel neutrophil populations appearing in tumour-bearing mice, but instead observed shifts in the proportions of existing populations. This is consistent with a model of neutrophil heterogeneity in which neutrophils are plastic cells in different states of activation, polarization or maturation (Ng et al., 2019). The presence of a tumour thus appears to induce shifts in neutrophils towards different states.

The principal shift I observe is an expansion of $CXCR2^+$ $CD62L^-$ neutrophils in the bone marrow, blood, spleen and liver. This population is present at very low levels in

control mice, but expands significantly in mice bearing tumours, with this shift correlating with tumour size and stage. I am able to observe this change in a number of different tumour models in three strains of mice. This phenotype is thus not confined to a specific type of tumour or mouse strain.

$CD62L^-$ neutrophils have been observed in mice (Becher et al., 2014) and an expansion of these cells has been documented previously: neutrophils that have "aged" in the circulation are $CD62L^-$ and undergo expansion and reduction in a circadian manner (Casanova-Acebes et al., 2013). This phenomenon can be affected by the microbiome, demonstrating that CD62L expression can be affected by stimuli (Zhang et al., 2015). A recent study demonstrated the loss of CD62L in a tumour setting: cancer-associated fibroblast-conditioned media altered neutrophil phenotype *in vitro*, inducing loss of CD62L expression (Cheng et al., 2018). However, this study did not demonstrate *in vivo* changes in neutrophil CD62L expression in tumour-bearing mice. To my knowledge, my findings are the first to demonstrate a systemic expansion of $CXCR2^+$ CD62L- neutrophils in tumour-bearing mice. Future work should investigate a greater range of tumour models and mouse strains, to determine how many different cancer contexts this phenotype can be found in.

In humans, LPS injection results in the appearance of a hypersegmented $CD62L^-$ neutrophil population (Pillay et al., 2012). This population can suppress T cells more effectively than segmented $CD62L^+$ neutrophils, and has a different proteome profile (Tak et al., 2017). A subsequent study found that the $CD62L^-$ population could be detected in the blood of cancer patients and patients undergoing surgery for non-cancerous growths, but was not present in the circulation of healthy control donors (Hao et al., 2013). This study was limited by a small sample size of 31 patients spread over 9 types of cancer, but it is a tantalizing indication that the increase in $CXCR2^+$ $CD62L^-$ neutrophils I observe in tumour-bearing mice may occur in human cancer patients. A more recent study found increased $CD62L^-$ neutrophils in the blood of patients with head and neck squamous cell carcinoma, in whom they correlated with in improved survival (Millrud et al., 2017). These neutrophils were also found in tumour biopsies, and had enhanced NET-forming ability. Another study found an expansion of $CD62L^-$ neutrophils with enhanced immunosuppressive abilities in the circulation of patients with chronic lymphocytic leukaemia (Podaza et al., 2019). Thus,

there are a number of studies that link human cancers with increased levels of CD62L$^-$ neutrophils in the circulation, although it is important to note that there has been limited analysis of the functional phenotypes of these neutrophils. One of these studies found that CD62L$^-$ neutrophils correlated with improved prognosis, potentially through increased NET-formation (Millrud et al., 2017), whereas the other found CD62L$^-$ neutrophils had a more immunosuppressive phenotype, which suggests they may have a pro-tumour phenotype (Podaza et al., 2019).

A priority for future work is to perform more comprehensive analyses of blood and tumour samples from cancer patients, to determine whether these findings can be replicated. The results from the above studies suggest that my finding of an expansion of CD62L$^-$ neutrophils in tumour bearing mice may have some relevance to changes that occur in human disease; however, it will be important to carefully dissect the functional phenotypes of CD62L$^-$ neutrophils in different human cancers and different mouse cancer models. At this stage, it cannot be known if the CD62L$^-$ neutrophils I identify are functionally the same population as those observed in cancer patients. Furthermore, the finding of CD62L$^-$ neutrophils with pro-tumorigenic immunosuppressive capacity in one patient study, and CD62L$^-$ neutrophils with a more anti-tumour phenotype in another patient study suggest that CD62L$^-$ neutrophils can have differing phenotypes depending on the context. Therefore, careful elucidation will be necessary to discern the functional phenotypes and significance of CD62L$^-$ neutrophils in different cancer contexts.

6.3.2 Significance of CD62L expression

In neutrophils, the principal established function of CD62L is to bind to carbohydrate moieties on endothelial cells (Ivetic, 2018). This allows neutrophils to arrest in the circulation, tether to the endothelium, and then roll along the endothelium, ultimately migrating across the endothelium into tissues and sites of inflammation. Importantly, CD62L can be shed after neutrophil tethering, and also after neutrophil activation. This suggests that, compared to the CD62L$^+$ population, the CD62L$^-$ population may

have reduced ability to tether to endothelium and transmigrate into tissues, and also that this population may be in a more activated state. Moreover, CD62L has a cytoplasmic domain that can activate intracellular signalling pathways, linking CD62L engagement on the surface to alterations in activity within the cell (Ivetic et al., 2019). This can then affect neutrophil activation and function, for example it was recently shown that shedding of CD62L drove alterations in intracellular signalling that enhanced neutrophil effector functions in a mouse model of bacterial pneumonia (Cappenberg et al., 2019). Therefore, the $CD62L^-$ population may have differential activation of intracellular signalling pathways, altering its functional phenotype. I also found that the $CD62L^-$ population had low intracellular levels of CD62L, indicating that they have not just transiently lost surface expression of CD62L due to shedding but appear to have also downregulated internal expression of CD62L.

To investigate the above possibilities, I performed a number of assays to functionally characterize the $CD62L^-$ and $CD62L^+$ populations, but was unable to detect a difference in functionality between these populations in these assays (see Section 6.4 for further discussion). From my results, I cannot conclude that there is a functional significance for lack of CD62L expression on $CD62L^-$ neutrophils. However, given the above discussion, I cannot rule out the possibility that there may be functional differences between $CD62L^+$ and $CD62L^-$ neutrophils.

6.3.3 Expansion of mature neutrophils in tumour-bearing mice

A number of studies have observed immature neutrophils in the circulation of tumour-bearing mice and cancer patients (Sagiv et al., 2015, Wu et al., 2014, Mackey et al., 2019). This is generally believed to arise from extreme pressure on bone marrow granulopoiesis, resulting in the early egress of neutrophils from the bone marrow before they have fully differentiated (Coffelt et al., 2016). I am unable to observe this phenomenon in the mouse tumour models I investigated: I find that over 95% of neutrophils in the circulation and periphery of both control and tumour-bearing mice express CXCR2, indicating that they are mature, and thus there is no expansion of

immature neutrophils in tumour-bearing mice. Morphological analysis of the nuclei of $CXCR2^{+}$ $CD62L^{+/-}$ neutrophils from the blood and spleen of tumour-bearing mice found that less than 15% of these cells had banded nuclei (Figures 5.1 and 5.2), demonstrating that the majority of these cells are indeed mature. Moreover, I found that there is a small increase in hypersegmented neutrophils within the $CXCR2^{+}$ neutrophil population in the blood of tumour-bearing mice (Figure 5.2c), rather than an increase in neutrophils with more immature nuclear morphology. However, several studies have found an expansion of mature neutrophils in the circulation of mice and patients, thus my findings are not necessarily inconsistent with the literature (Granot et al., 2011, Fridlender et al., 2009, Singel et al., 2019). It is unclear why immature neutrophils appear to increase in some tumour contexts but not others. It is possible that different combinations of signals are responsible; G-CSF, GM-CSF, KIT and IL-6 can all induce granulopoiesis, but will not have identical effects, as they all impact upon other haematopoietic processes (Coffelt et al., 2016). Thus, in different tumour contexts there may be differing levels of these signals, leading to differential effects on granulopoiesis and release of immature neutrophils (Coffelt et al., 2016, Mackey et al., 2019).

An intriguing recent study demonstrated that loss of p53 can drive neutrophil expansion in breast cancer by causing cancer cells to upregulate WNT secretion, which stimulates macrophages to secrete IL-1ß, ultimately leading to the enhancement of G-CSF production, which boosts granulopoiesis and increases the numbers of immature neutrophils in the circulation (Wellenstein et al., 2019). The results of this study suggest that the genetic composition of a tumour may play a role in determining how a tumour affects neutrophil numbers and heterogeneity. It would be interesting to investigate this hypothesis using the mouse models I examined. I found that a range of mouse carcinoma models could affect neutrophils, but a melanoma model had no apparent effect on neutrophil numbers or phenotype, it is possible this difference may be due to genetic differences between the cancer cells. Extending my findings to a greater range of tumour models would allow the potential to explore how genetic mutations within cancer cells might impact upon neutrophil phenotype.

6.3.4 Changes in neutrophils in the bone marrow of tumour-bearing mice

The presence of a tumour has the strongest effect on neutrophils in the bone marrow: in tumour-bearing mice I observe an expansion of total neutrophils and within this population, mature neutrophils and $CD62L^-$ neutrophils. I also find a reduction in $MHC\text{-}II^+$ and $F4/80^+$ neutrophils in mice bearing PyMT tumours. As discussed above (Section 6.2.1) the significance of MHC-II and F4/80 expression on bone marrow neutrophils is uncertain. It is consequently difficult to establish the importance of the decrease of these populations in tumour-bearing mice.

In the literature, the presence of a tumour has been associated with expansion of granulocyte progenitor populations in the bone marrow in a range of contexts(Evrard et al., 2018, Coffelt et al., 2015, Zhu et al., 2018). I therefore attempted to determine the changes in granulopoiesis driving the expansion of neutrophils in the mouse models I used, by investigating populations of neutrophil precursors. I found only minor changes in GMP and CMP populations, and no increase in Pre-neutrophils or immature neutrophils, with significant variability between experiments. Therefore, from my results it is difficult to ascertain the precise mechanisms by which neutrophil expansion is driven. It is likely that there are a number of factors influencing granulopoiesis in a tumour-bearing context, and my experiments do not provide sufficient evidence to reach a conclusion on how a tumour can affect granulopoiesis.

Overall, it is clear that the presence of a tumour can significantly perturb the bone marrow and granulopoiesis. I can find a major expansion of neutrophil production and mature neutrophils in the bone marrow of tumour-bearing mice, but in the mouse models I have investigated I cannot determine how a tumour alters the earlier stages of granulopoiesis to effect these changes.

6.4 No differences in activity between CD62L$^+$ and CD62L$^-$ neutrophils from tumour-bearing mice

The third aim of my thesis was to investigate the functional consequences of neutrophil heterogeneity for tumour cells. To achieve this, I performed functional assays with the primary aim of discerning differences between the CXCR2$^+$ CD62L$^+$ and CD62L$^-$ neutrophils from tumour-bearing mice, with the hypothesis that differential expression of CD62L indicated differences in functional phenotypes between these cells (Section 6.3.2). I first analysed the nuclear morphology of the two neutrophil populations from the blood and spleen, finding that an increased percentage of the CD62L$^-$ population have hypersegmented nuclei. In the literature, it has been shown that neutrophils with hypersegmented nuclei can have different functional characteristics to those with segmented or banded nuclei (Pillay et al., 2012, Tak et al., 2017, Zhang et al., 2015). My results therefore indicated the possibility that there were functional differences between the neutrophil populations, particularly given the potential functional roles of CD62L, which may be lost in CD62L$^-$ cells (Ivetic, 2018, Ivetic et al., 2019). However, I only found a shift in segmentation between these populations, not a total transformation between them; approximately 50% of CXCR2$^+$ CD62L$^-$ neutrophils still have a segmented or banded morphology (Figure 5.1). Furthermore, morphological analysis of neutrophil nuclei is fundamentally subjective, and indeed its relationship to underlying differences in functionality and maturation has been questioned (Ng et al., 2019).

Therefore, whilst the finding of increased hyper-segmentation in CXCR2$^+$ CD62L$^-$ neutrophils is intriguing and suggestive of functional differences it is not enough in itself to draw this conclusion. I therefore next turned to functional assays, including analysing ROS levels, NET formation, immune suppression and cancer cell growth. However, I was unable to discover any differences between CD62L$^+$ and CD62L$^-$ neutrophils from tumour-bearing mice in these assays.

This raises the possibility that there are no functional differences between these two populations of neutrophils; that despite their differential expression of CD62L, and differing nuclear morphology, they are functionally identical. This cannot be

concluded solely from my results, as I did not perform an exhaustive range of functional assays. Furthermore, I would argue that this possibility is unlikely for several reasons: firstly, the evidence in the literature for differential functional characteristics of $CD62L^-$ cells (Casanova-Acebes et al., 2013, Zhang et al., 2015, Pillay et al., 2012, Tak et al., 2017). Secondly the potential functional effects of CD62L (Ivetic, 2018, Ivetic et al., 2019) . Finally, my observation of increased hyper-segmentation in $CXCR2^+$ CD62L- neutrophils, which is suggestive of functional differences (Zhang et al., 2015).

Confirmation of my argument would require further functional characterization that demonstrated differences in activity between the populations. For example, analysis of cytokine secretion, or assays that further probe neutrophil-cancer cell interactions, such as sphere formation assays. Moving to an *in vivo* setting for these functional experiments may also provide further insights. For example, experiments could be performed using subcutaneous co-injection of cancer cells with different neutrophil populations, to test how the neutrophil populations affect cancer cell growth. Alternatively, intravenous injection of cancer cells and neutrophils to probe how neutrophils may affect metastasis. Findings from these experiments would also be more readily applicable to *in vivo* models and therefore may have greater translational relevance.

It is also possible that a focus on highly specific functional assays is the wrong approach to discover differences between these neutrophil populations, as it may require performing numerous different assays before finding the assay that actually reveals differences in functionality. Alternatively, unbiased methods such as transcriptomics, epigenomics and proteomics could provide broader information on whether these populations of neutrophils have differing functional phenotypes (Ng et al., 2019). These experiments could then inform further functional assays or *in* vivo experiments. The kinase activity technique that I performed with the $CXCR2^+$ neutrophils from control and tumour-bearing mice may provide particularly useful insights, as this method assays kinase activity rather than mRNA or protein levels, neither of which correlate perfectly with actual protein or pathway activity. However, the kinase assay is limited because it is not an unbiased approach as it can only

assay the activity of kinases with target sequences on the chip which cannot contain target sequences for all kinases.

Perhaps the most state-of-the-art approach would be to perform single-cell RNA sequencing of neutrophil populations. This may be technically challenging due to low RNA levels in neutrophils compared to, for example, other myeloid cell populations (Ng et al., 2019), but it could potentially offer the greatest insight into differences between neutrophil populations. It could also serve as a complimentary approach to the cytometry-based methods for defining neutrophil populations (i.e. defining neutrophils by surface marker expression): populations identified by single-cell RNA sequencing could then be linked to populations determined by surface marker expression, facilitating downstream experiments by allowing cytometric delineation and analysis of neutrophil populations.

6.5 Functional assays reveal differences between neutrophils from control and tumour-bearing mice

Despite being unable to find differences between $CXCR2^+$ $CD62L^+$ and $CXCR2^+$ $CD62L^-$ neutrophils from tumour-bearing mice, I was able to determine differences in functional assays between $CXCR2^+$ neutrophils from control and tumour-bearing mice. I found that mature $CXCR2^+$ neutrophils from tumour-bearing mice performed stronger immune suppression and had greater growth-boosting ability *in vitro*. Additionally, bone marrow neutrophils in tumour-bearing mice had lower intracellular ROS levels than their counterparts in control mice. Finally, I found extensive differences in kinase activity in mature blood and bone marrow neutrophils from control and tumour-bearing mice.

In the assays that I performed I found a pro-tumour effect of neutrophils: even neutrophils from control mice could suppress T cell proliferation and boost cancer cell growth *in vitro*, with this activity enhanced in neutrophils from tumour-bearing mice. It is well established that neutrophils can suppress T cells (Kumar et al., 2016, Veglia et al., 2018), and my finding of this behaviour is therefore not surprising. It is

interesting that neutrophils from tumour-bearing mice have greater suppressive capacity; this suggests that the presence of a tumour can alter neutrophil phenotype.

It is important to stress that the immunosuppression and 3D co-culture assays were performed *in vitro*, and consequently it is unclear if these behaviours translate to a pro-tumour phenotype *in vivo*. Given that the suppression of T cells is an established neutrophil function, I would focus future investigations on the 3D co-culture assay. Although it has been shown previously that neutrophils can boost cancer cell growth (Wculek and Malanchi, 2015), the co-culture assay utilizes a 3D scaffold system that recapitulates the 3D microenvironment found within tissues. Therefore, the behaviour of cells in this system may more faithfully recapitulate *in vivo* cell behaviours than traditional *in vitro* based methods that used 2D plastic systems, meaning this assay has the potential to provide more insight into *in vivo* cell activity and interactions. The 3D scaffold system can be easily manipulated; inhibitors could be added to probe the mechanisms by which neutrophils boost cancer cell growth. Alternatively, other cell types, such as fibroblasts, could be introduced to investigate how neutrophils may interact with cancer cells and cells within the tumour microenvironment.

The differences in intracellular ROS levels between bone marrow neutrophils from control and tumour-bearing mice are of particular interest. To my knowledge, this difference has not yet been demonstrated in the literature. ROS can be generated by a number of enzymes in neutrophils, typically during the respiratory burst that neutrophils use to destroy phagocytosed bacteria, and are also produced by metabolic processes in mitochondria (Forrester et al., 2018). Therefore, the differences in ROS levels may indicate differences in enzyme activity or metabolism between these neutrophils, suggesting potential functional differences between bone marrow neutrophils from control and tumour-bearing mice. In addition, ROS can participate in a range of processes, most prominently metabolism and cell signalling (Zhang et al., 2016). Consequently, the differences in ROS between these neutrophils further imply that there may be metabolic or signalling pathway differences between bone marrow neutrophils in control and tumour-bearing mice.

It is also important that these differences are observed only in bone marrow neutrophils, in both immature $CXCR2^-$ and mature $CXCR2^+$ populations. This suggests these effects are present at multiple stages of neutrophil development within the bone marrow. Moreover, neutrophils undergo extensive changes during their development, including major production of granules and functional proteins. Therefore ROS-mediated alterations in cell signalling or metabolism may affect these developmental processes, altering neutrophil development and ultimately producing differences in mature neutrophils between control and tumour-bearing mice. This may contribute to the differences I observe between control and tumour-bearing neutrophils in functional assays (immunosuppression and 3D co-culture).

Finally, the kinase activity assay I performed revealed extensive differences in kinase activity in neutrophils from control and tumour-bearing mice. I found these differences across immature and mature bone marrow neutrophils and mature blood neutrophils. This experiment was performed with three mice control and three tumour-bearing mice, thus it important to stress that the results are preliminary and require repetition and replication before robust conclusions can be drawn. Therefore, a critical priority for future work will be to expand the numbers of mice in these experiments. It would also be interesting to perform the assay with neutrophils from the spleen, as these neutrophils had strong immunosuppressive capacity, and the greatest ability to boost cancer cell growth *in vitro*. In addition, I investigated the activity of tyrosine kinases, it is also possible to investigate serine/threonine kinase activity with this assay, and this would provide further useful information on changes in neutrophil behaviour.

The kinase activity results mimic my findings of differing levels of ROS in bone marrow neutrophils between control and tumour-bearing mice. This suggests that the presence of a tumour perturbs the bone marrow environment, affecting neutrophil development, leading to shifts in ROS and kinase activity. Given the roles of kinases in numerous processes within cells, it is likely that the differential kinase activity results in changes in neutrophil development in the bone marrow. The differing kinase activity in blood neutrophils between control and tumour-bearing mice also implies a different phenotype between these populations. Given the limited numbers of mice used in this experiment it is difficult to draw robust conclusions from this

analysis, but the differences in kinase activity are reflected in the differences in functional assays I find between neutrophils from control and tumour-bearing mice. The kinase assay results therefore complement my findings from the other functional assays and point to major shifts in neutrophil phenotype induced by the presence of a tumour.

6.6 Signals involved in generating the expansion of $CXCR2^+$ $CD62L^-$ neutrophils in tumour-bearing mice

An interesting area for further investigation would be to determine the signals that cause the expansion of the $CXCR2^+$ $CD62L^-$ population in tumour-bearing mice. Of course, it would be necessary to first establish the functional significance of the $CXCR2^+$ $CD62L^-$ neutrophils (Section 6.4) before investigating how this population arises. But if this population does indeed have functional significance, then an understanding of the signals that cause its expansion in tumour-bearing mice could be useful for further experiments and translational investigations. For example, blockade of this signal(s) could decrease the expansion of $CXCR2^+$ $CD62L^-$ neutrophils in tumour-bearing mice, which may be of interest if this population were found to have a pro-tumour effect.

I found the expansion of neutrophils and of $CXCR2^+$ $CD62L^-$ neutrophils in a range of mouse carcinoma models. Given that these models were in several different strains of mice, and were all different tumour types this suggests common factor(s) across strains and tumour types involved in this process. In a melanoma model, I found the presence of a tumour had no effect on neutrophil numbers or the $CXCR2^+$ $CD62L^-$ population, showing that this phenomenon is not found in all tumour types. Further investigation of a greater range of mouse models would illuminate how common the expansion of neutrophils and $CXCR2^+$ $CD62L^-$ neutrophils is, and may provide insight into the factors that induce this phenotype, as the models where it occurs could be compared with those where it does not. Possible candidates for investigation include G-CSF, GM-CSF, IL-6 and KIT, which can all affect bone marrow granulopoiesis and also have effects on mature neutrophils (Coffelt et al., 2016).

In the literature, much work has been focused on signals involving immune cells, in particular T cells, and how these impinge upon neutrophils in cancer. It is therefore significant that I find the expansion of total neutrophils and the $CXCR2^{+}$ $CD62L^{-}$ neutrophil population in tumour-bearing $Rag^{-/-}$ mice, which lack mature T and B cells. This suggests that this phenomenon is not dependent T cells, in contrast to many findings in the literature (Pelletier et al., 2010a, Coffelt et al., 2015, Wu et al., 2014). However, this result is not necessarily unexpected: cancer cells, stromal cells, and other immune cells can all release immunomodulatory factors (Coffelt et al., 2016), but it does demonstrate that T cells are not necessary for neutrophil expansion and polarization in cancer. It may be informative to explore the effects of tumours in other immunodeficient mouse strains, to probe how other immune cell types may be involved in neutrophil expansion and polarization.

In humans, injection of LPS causes a hypersegmented $CD62L^{-}$ population to appear in the circulation (Pillay et al., 2012), this population was also found to have a different proteome from segmented $CD62L^{+}$ neutrophils (Tak et al., 2017). This suggests that the appearance of $CD62L^{-}$ neutrophils is not limited to a cancer context, it would therefore be of interest to explore other inflammatory contexts, such as infection or sterile injury, to see if these conditions recapitulate the expansion of the $CXCR2^{+}$ $CD62L^{-}$ population. These experiments may provide other settings to investigate the functional phenotypes of $CD62L^{-}$ neutrophils and the signals generating this population.

6.7 Final conclusions and future priorities

6.7.1 Final conclusions

My aims in this thesis were to:

- Investigate neutrophil heterogeneity across tissues
- Determine how the presence of a tumour perturbs this heterogeneity
- Investigate the functional consequences of neutrophil heterogeneity for tumour cells

I was able to achieve the first two aims of my project: I discovered neutrophil heterogeneity across tissues and demonstrated that the presence of a tumour alters this heterogeneity. The principal shift I identified is an expansion of $CXCR2^{+}$ $CD62L^{-}$ neutrophils across the bone marrow, blood, spleen and liver of tumour-bearing mice. I was less successful at achieving the third aim of my project: I was unable to determine a functional difference between the $CXCR2^{+}$ $CD62L^{-}$ and $CXCR2^{+}$ $CD62L^{+}$ neutrophil populations. Therefore, my results do not find functional consequences for the neutrophil heterogeneity that I observe. This is a limitation of my results: whilst I am able to define heterogeneity of neutrophils by the differential expression of CD62L, for this difference to be truly meaningful it must signify a deeper phenotypic difference, which, at least in my experiments, I am unable to discover.

However, I was able to find numerous differences in functional activity between the total neutrophil populations from control and tumour-bearing mice, most significantly in the bone marrow. This shows that tumours can alter neutrophil phenotype in various ways. My findings of differences in ROS levels and kinase activity are the most important, as they suggest more fundamental phenotypic differences between neutrophils from control and tumour-bearing mice, and indicate the mechanisms by which these differences might occur.

6.7.2 Future priorities

1. **Unbiased, high-throughput analysis comparing CD62L$^-$ and CD62L$^+$ neutrophils**.
    - For example, transcriptomics or proteomics, with the aim of determining functional differences between these neutrophil populations

2. **Analysis of neutrophil populations in other mouse tumour models and cancer patients**
    - Specifically focusing on determining whether CD62L$^-$ neutrophil populations expand in other settings, with the ultimate aim of discerning functional phenotypes of these populations with further experiments. The latter will be informed by the findings from (1).

3. **Further kinase activity assay experiments to confirm the initial findings and extend the observations to other neutrophil populations and cancer settings, including cancer patients**

4. **Investigation of the effects of ROS levels on bone marrow neutrophil development**
    - Focusing on metabolic changes that may be driving or driven by ROS and also signalling pathways that ROS may affect

5. **Investigate the signals generating the expansion of CD62L$^-$ neutrophils, in both a cancer context and also other inflammatory settings**

Appendix

Appendix 1. Key marker expression defining neutrophil clusters identified by Phenograph analysis of mass cytometry data

Cluster	Marker expression defining cluster
1	$CXCR2^{Intermediate}$
2	$CD62L^{-}$
3	$CD11c^{+}$
4	$CD115^{+}$
5	$CXCR2^{HI}$
6	$CD62L^{HI}$
7	$CD62L^{Intermediate}$
8	$F4/80^{+}$
9	$MHC\text{-}II^{+}$
10	$CD11b^{Intermediate}$
11	$CD11b^{-}$
12	$CD11b^{-}$, $Ly6G^{Low}$

Appendix 2. Phosphotyrosine kinase assay table

Peptide Sequence	Tyrosine position in primary sequence	Uniprot ID	Peptide label
YISKAEEYFLLKS	[383, 390]	Q07001	ACHD_383_395
KATGRYYAMKILK	[175, 176]	P31749	AKT1_170_182
FSGTPEYLAPEVL	[315]	P31749	AKT1_309_321_C310S
VLEDNDYGRAVDW	[326]	P31749	AKT1_320_332
EREGSKRYCIQTK	[12]	Q07075	AMPE_5_17
IENEEQEYVQTVK	[21]	P04083	ANXA1_14_26
HSTPPSAYGSVKA	[24]	P07355	ANXA2_17_29
RDSGYYWEVPP	[301, 302]	P10398	ARAF_297_307
TEATATDYHTTSH	[46]	P02730	B3AT_39_51
KPGIVYASLNH	[257]	Q7Z6A9	BTLA_252_262
TEASGYISSLEYP	[204, 210]	P00736	C1R_199_211
FDKDGNGYISAAE	[100]	P0DP23	CALM_93_105
KDGNGYISAAELR	[100]	P0DP23	CALM_95_107
EGEEDTEYMTPSS	[700]	P22681	CBL_693_705
RLLHSDYMNMTPR	[191]	P10747	CD28_185_197
RKHYQPYAPPRDF	[206, 209]	P10747	CD28_203_215
PVPNPDYEPIRKG	[188]	P07766	CD3E_182_194
KGQRDLYSGLNQR	[199]	P07766	CD3E_193_205
NPQEGLYNELQKD	[111]	P20963	CD3Z_105_117
KDKMAEAYSEIGM	[123]	P20963	CD3Z_116_128
DKMAEAYSEIGMK	[123]	P20963	CD3Z_117_129
KGHDGLYQGLSTA	[142]	P20963	CD3Z_135_147
STATKDTYDALHM	[153]	P20963	CD3Z_146_158
TATKDTYDALHMQ	[153]	P20963	CD3Z_146_158
LGRREEYDVLDKR	[83]	P20963	CD3Z_77_89
SVRRRPYGSVLRA	[15]	P32970	CD70_9_21_C17S
EYEDENLYEGLNL	[182, 188]	P11912	CD79A_181_193
KIGEGTYGVVYKG	[15, 19]	P06493	CDK1_9_21
EKIGEGTYGVVYK	[15, 19]	P24941	CDK2_8_20
EIGVGAYGTVYKA	[17, 21]	P11802	CDK4_11_23
GLAKSFGSPNRAY	[169]	P50613	CDK7_157_169
GPPEPGPYAQPSV	[221]	P46108	CRK_214_226
VADIDGQYAMTRA	[86]	P35222	CTNB1_79_91
GIVYAVSSDRFRS	[70]	O43602	DCX_67_79
LLLSNPAYRLLLA	[513]	Q08345	DDR1_506_518
KHDTEMKYYIVHL	[219, 220]	Q13627	DYR1A_212_224

CQLGQRIYQYIQS	[319, 321]	Q13627	DYR1A_312_324
GGTDEGIYDVPLL	[253]	O43281	EFS_246_258
GGTDEGIFDVPLL	[]	O43281	EFS_246_258_Y253F
EDSFLQRYSSDPT	[1069]	P00533	EGFR_1062_1074
GSVQNPVYHNQPL	[1110]	P00533	EGFR_1103_1115
APSRDPHYQDPHS	[1125]	P00533	EGFR_1118_1130
ISLDNPDYQQDFF	[1172]	P00533	EGFR_1165_1177
STAENAEYLRVAP	[1197]	P00533	EGFR_1190_1202
LGAEEKEYHAEGG	[869]	P00533	EGFR_862_874
MTFGSKPYDGIPA	[915]	P00533	EGFR_908_920
SGASTGIYEALEL	[44]	P09104	ENOG_37_49
LDDFDGTYETQGG	[781]	P21709	EPHA1_774_786
QLKPLKTYVDPHT	[588]	P29317	EPHA2_581_593
EDDPEATYTTSGG	[772]	P29317	EPHA2_765_777
LNQGVRTYVDPFT	[596]	P54764	EPHA4_589_601
QAIKMDRYKDNFT	[928]	P54764	EPHA4_921_933
TYIDPETYEDPNR	[608, 614]	Q15375	EPHA7_607_619
DDTSDPTYTSSLG	[778]	P54762	EPHB1_771_783
SAIKMVQYRDSFL	[928]	P54762	EPHB1_921_933
IGHGTKVYIDPFT	[590]	P54760	EPHB4_583_595
SEHAQDTYLVLDK	[368]	P19235	EPOR_361_373
ASAASFEYTILDP	[426]	P19235	EPOR_419_431
PTAENPEYLGLDV	[1248]	P04626	ERBB2_1241_1253
LDIDETEYHADGG	[877]	P04626	ERBB2_870_882
PASEQGYEEMRAF	[1289]	P21860	ERBB3_1283_1295
QALDNPEYHNASN	[1188]	Q15303	ERBB4_1181_1193
IVAENPEYLSEFS	[1284]	Q15303	ERBB4_1277_1289
DSKNFDDYMKSLG	[20]	P05413	FABPH_13_25
RYMEDSTYYKASK	[570, 576, 577]	Q05397	FAK1_569_581
RYIEDEDYYKASV	[573, 579, 580]	Q14289	FAK2_572_584
RQEDGGVYSSSGL	[714]	P16591	FER_707_719
REEADGVYAASGG	[713]	P07332	FES_706_718
TSNQEYLDLSMPL	[766]	P11362	FGFR1_761_773
TLTTNEEYLDLSQ	[769]	P21802	FGFR2_762_774
DVHNLDYYKKTTN	[647, 648]	P22607	FGFR3_641_653
TVTSTDEYLDLSA	[760]	P22607	FGFR3_753_765
KVDNEDIYESRHE	[387]	P42685	FRK_380_392
TATEPQYQPGENL	[531]	P06241	FYN_525_537
DKQVEYLDLDL	[627]	Q13480	GAB1_622_632

DEKVDYVQVDK	[643]	Q9UQC2	GAB2_638_648
GEPNVSYISSRYY	[216, 221, 222]	P49841	GSK3B_210_222_C218S
GIRSEENIYTI	[265]	Q8TDQ0	HAVR2_257_267
SLGFKRSYEEHIP	[1355]	P06213	INSR_1348_1360
YASSNPEYLSASD	[992, 999]	P06213	INSR_992_1004
PKSPGEYVNIEFG	[896]	P35568	IRS1_890_902
HPYPEDYGDIEIG	[628, 632]	Q9Y4H2	IRS2_626_638
AIETDKEYYTVKD	[1034,1035]	P23458	JAK1_ 1027_1039
DISYKRYIPETLN	[217, 220]	P23458	JAK1_214_226
LPQDKEYYKVKEP	[1007, 1008]	O60674	JAK2_1001_1013
VRREVGDYGQLHETE	[570]	O60674	JAK2_563_577
LPLDKDYYVVREP	[980, 981]	P52333	JAK3_974_986
GAGFGSRSLYGLG	[62]	P04259	K2C6B_53_65
SAYGGLTSPGLSY	[427, 437]	P05787	K2C8_425_437
ESTNHIYSNLANS	[936]	P10721	KIT_930_942_C942S
ALRADENYYKAQT	[525, 526]	P43405	KSYK_518_530
MESIDDYVNVPES	[200]	O43561	LAT_194_206
EEGAPDYENLQEL	[255]	O43561	LAT_249_261
RLIEDNEYTAREG	[394]	P06239	LCK_387_399
VIEDNEYTAREGA	[397]	P07948	LYN_391_403
YTATEGQYQQQP	[501, 508]	P07948	LYN_501_512
ALQTPSYTPYYVA	[204, 207, 208]	Q16644	MAPK3_198_210_C203S
ARTAHYGSLPQKS	[203]	P02686	MBP_198_210
FGYGGRASDYKSA	[261, 268]	P02686	MBP_259_271
GRASDYKSAHKGF	[268]	P02686	MBP_263_275
RDMYDKEYYSVHN	[1230, 1234, 1235]	P08581	MET_1227_1239
DMYDKEYYSVHNK	[1230, 1234, 1235]	P08581	MET_1228_1240
KSVAPYPSLLS	[1365]	P08581	MET_1360_1370_C1361S
HTGFLTEYVATRW	[187]	P28482	MK01_180_192
IMLNSKGYTKSID	[205]	P28482	MK01_198_210
LNSKGYTKSI	[205]	P28482	MK01_200_209
GFLTEYVATR	[204]	P27361	MK03_199_208
AEHQYFMTEYVAT	[216,221]	Q13164	MK07_ 212_224
MMTPYVVTRYY	[185, 190, 191]	P45983	MK08_181_191

TSFMMTPYVVTRY	[223, 228]	P53779	MK10_216_228
ADSEMTGYVVTRW	[185]	P53778	MK12_178_190
SEBTGYVVTR	[185]	P53778	MK12_180_189_M182B
RHTDDEMTGYVAT	[182]	Q16539	MK14_173_185
DEMTGYVATRW	[182]	Q16539	MK14_177_187
QGPVIYAQLDH	[241]	O95297	MPZL1_236_246
LHPNPMYQRMPLL	[554]	O15146	MUSK_548_560
QRSRKRLSQDAYR	[324]	P14598	NCF1_313_325
AKALGKRTAKYRW	[511]	Q06495	NPT2A_501_513
HIIENPQYFSDAC	[496]	P04629	NTRK1_489_501
PVIENPQYFGITN	[516]	Q16620	NTRK2_509_521
GMSRDVYSTDYYR	[702, 706, 707]	Q16620	NTRK2_696_708
KDSSAYRSVDEVN	[345]	P12694	ODBA_340_352_D340K
SMSDPGVSYRTRE	[299]	P29803	ODPAT_291_303
NENTEDQYSLVED	[607]	P27986	P85A_600_612
VGEEEHVYSFPNK	[118]	P49023	PAXI_111_123
FLSEETPYSYPTG	[31, 33]	P49023	PAXI_24_36
KKVDYGELDFQ	[223]	Q15116	PDCD1_221_229_FS219_220KK
ARTTSQLYDAVPI	[9]	O15530	PDPK1_2_14
DEDCYGNYDNLLS	[373, 376]	O15530	PDPK1_369_381
KKDTETVYSEVRK	[713]	P16284	PECA1_706_718
DTETVYSEVRK	[713]	P16284	PECA1_708_718
QRSELDKSSAHSY	[470]	P41219	PERI_458_470
LDTSSVLYTAVQP	[1009]	P09619	PGFRB_1002_1014
PNEGDNDYIIPLPDP	[1021]	P09619	PGFRB_1014_1028
VSSDGHEYIYVDP	[579, 581]	P09619	PGFRB_572_584
RPPSAELYSNALP	[716]	P09619	PGFRB_709_721
SSNYMAPYDNYVP	[771, 775, 778]	P09619	PGFRB_768_780
YMAPYDNYVPSAP	[771, 775, 778]	P09619	PGFRB_771_783
EGSFESRYQQPFE	[1253]	P19174	PLCG1_1246_1258
IGTAEPDYGALYE	[771, 775]	P19174	PLCG1_764_776
GRNPGFYVEANPM	[783]	P19174	PLCG1_777_789
ESEEELYSSSRQL	[1197]	P16885	PLCG2_1191_1203_C1200S
NNQLFLYDTHQNL	[1217]	P16885	PLCG2_1211_1223
EPHVTRRTPDYFL	[307]	P62714	PP2AB_297_309
LRPDSEASQSPQY	[557]	P06401	PRGR_545_557
EQRMKESSFYSLC	[795]	P06401	PRGR_786_798

WTASSPYSTVPPY	[208, 214]	Q99811	PRRX2_202_214
SKRKGHEYTNIKY	[546, 551]	Q06124	PTN11_539_551
RKGHEYTNIKY	[546, 551]	Q06124	PTN11_541_551
QNTGDYYDLYG	[62, 63, 66]	Q06124	PTN11_57_67
SARVYENVGLM	[584]	Q06124	PTN11_580_590
GQESEYGNITY	[536, 541]	P29350	PTN6_531_541
KHKEDVYENLHTK	[564]	P29350	PTN6_558_570
PRGQRDSSYYWEI	[340, 341]	P04049	RAF1_332_344
TVDGKEIYNTIRR	[460]	P20936	RASA1_453_465
IYISPLKSPYKIS	[805, 813]	P06400	RB_804_816
VPTVSKGTVEGNY	[111]	Q08999	RBL2_99_111
TPSDSLIYDDGLS	[1029]	P07949	RET_1022_1034
AQAFPVSYSSSGA	[687]	P07949	RET_680_692
SALLGDHYVQLPA	[1353]	Q04912	RON_1346_1358
ELRFKQYLRNPPK	[315]	P29353	SHC1_309_321
TSTEPQYQPGENL	[530]	P12931	SRC_524_536
LAKAVDGYVKPQI	[694]	P42229	STA5A_687_699
DGPKGTGYIKTEL	[701]	P42224	STAT1_694_706
LQERRKYLKHRLI	[690]	P52630	STAT2_684_696
DPGSAAPYLKTKF	[705]	P40763	STAT3_698_710
TERGDKGYVPSVF	[693]	Q14765	STAT4_686_698
PSDLLPMSPSVYA	[725]	Q14765	STAT4_714_726
MGKDGRGYVPATI	[641]	P42226	STAT6_634_646
RYFLDDQYTSSSG	[513, 519]	P42680	TEC_512_524
SRGQEVYVKKTMG	[992]	Q02763	TIE2_986_998
SDTEEQEYEEEQP	[9]	P13805	TNNT1_2_14
VPEGHEYYRVRED	[1054, 1055]	P29597	TYK2_1048_1060
KIYSGDYYRQGCA	[681, 685, 686]	Q06418	TYRO3_679_691
DFGLARDIYKNPD	[1048]	P17948	VGFR1_1040_1052
DIFKNPDYVRKGD	[1053]	P17948	VGFR1_1046_1058_Y1048F
KNPDYVRKGDTRL	[1053]	P17948	VGFR1_1049_1061
VQQDGKDYIPINA	[1169]	P17948	VGFR1_1162_1174
GSSDDVRYVNAFK	[1213]	P17948	VGFR1_1206_1218
ATSMFDDYQGDSS	[1242]	P17948	VGFR1_1235_1247
KKSPPPDYNSVVL	[1327]	P17948	VGFR1_1320_1332_C1320K/C1321K
DFGLARDIYKDPD	[1054]	P35968	VGFR2_1046_1058
AQQDGKDYIVLPI	[1175]	P35968	VGFR2_1168_1180
VSDPKFHYDNTAG	[1214]	P35968	VGFR2_1207_1219_C1208S

RFRQGKDYVGAIP	[951]	P35968	VGFR2_944_956
EEAPEDLYKDFLT	[996]	P35968	VGFR2_989_1001
DIYKDPDYVRKGS	[1063, 1068]	P35916	VGFR3_1061_1073
KSFLDSGYRILGA	[822]	P18206	VINC_815_827
RHPLSYVAQRQ	[265]	Q9H7M9	VISTA_260_270
LIEDNEYTARQGA	[426]	P07947	YES_420_432
SVYESPYSDPEEL	[315, 319]	P43403	ZAP70_313_325
ALGADDSYYTARS	[492, 493]	P43403	ZAP70_485_497
LRTHNGASPYQCT	[630]	Q05516	ZBT16_621_633

Table 4 Phosphotyrosine kinase assay peptide sequences

Appendix 3. One-way ANOVA statistical analysis of differences in neutrophils and neutrophil populations in mice with different stage tumours

Bonferroni's multiple comparisons test	Mean Diff.	95.00% CI of diff.	Significant?	Summary	Adjusted P Value
Bone marrow neutrophils					
Control vs. Small Induced	-5.425	-17.83 to 6.982	No	ns	>0.9999
Control vs. Medium Induced	-14.88	-27.28 to -2.468	Yes	*	0.0118
Control vs. Large induced	-24.33	-36.73 to -11.92	Yes	****	<0.0001
Control vs. Small Spontaneous	-15.67	-29.07 to -2.265	Yes	*	0.0146
Control vs. Large Spontaneous	-32.3	-45.7 to -18.9	Yes	****	<0.0001
Small Induced vs. Medium Induced	-9.45	-21.86 to 2.957	No	ns	0.2767
Small Induced vs. Large induced	-18.9	-31.31 to -6.493	Yes	**	0.0012
Small Induced vs. Small Spontaneous	-10.24	-23.64 to 3.16	No	ns	0.2717
Small Induced vs. Large Spontaneous	-26.88	-40.28 to -13.47	Yes	****	<0.0001
Medium Induced vs. Large induced	-9.45	-21.86 to 2.957	No	ns	0.2767
Medium Induced vs. Small Spontaneous	-0.7917	-14.19 to 12.61	No	ns	>0.9999
Medium Induced vs. Large Spontaneous	-17.43	-30.83 to -4.023	Yes	**	0.0057
Large induced vs. Small Spontaneous	8.658	-4.743 to 22.06	No	ns	0.6119
Large induced vs. Large Spontaneous	-7.975	-21.38 to 5.427	No	ns	0.8574
Small Spontaneous vs. Large Spontaneous	-16.63	-30.96 to -2.306	Yes	*	0.0155
Blood neutrophils					
Control vs. Small Induced	-4.363	-23.87 to 15.14	No	ns	>0.9999
Control vs. Medium Induced	-21.72	-41.23 to -2.22	Yes	*	0.0219
Control vs. Large induced	-34.22	-53.73 to -14.72	Yes	***	0.0003
Control vs. Small Spontaneous	-10.29	-31.35 to 10.78	No	ns	>0.9999
Control vs. Large Spontaneous	-52.62	-73.69 to -31.56	Yes	****	<0.0001
Small Induced vs. Medium Induced	-17.36	-36.86 to 2.143	No	ns	0.1108
Small Induced vs. Large induced	-29.86	-49.36 to -10.36	Yes	**	0.0011
Small Induced vs. Small Spontaneous	-5.927	-26.99 to 15.14	No	ns	>0.9999
Small Induced vs. Large Spontaneous	-48.26	-69.33 to -27.19	Yes	****	<0.0001
Medium Induced vs. Large induced	-12.5	-32 to 7.003	No	ns	0.6333
Medium Induced vs. Small Spontaneous	11.43	-9.632 to 32.5	No	ns	>0.9999
Medium Induced vs. Large Spontaneous	-30.9	-51.97 to -9.835	Yes	**	0.0018
Large induced vs. Small Spontaneous	23.93	2.868 to 45	Yes	*	0.0186
Large induced vs. Large Spontaneous	-18.4	-39.47 to 2.665	No	ns	0.125
Small Spontaneous vs. Large Spontaneous	-42.33	-64.85 to -19.81	Yes	***	0.0001
Spleen neutrophils					
Control vs. Small Induced	-1.08	-3.724 to 1.564	No	ns	>0.9999
Control vs. Medium Induced	-2.428	-5.071 to 0.2163	No	ns	0.0905
Control vs. Large induced	-6.92	-9.564 to -4.276	Yes	****	<0.0001
Control vs. Small Spontaneous	-6.3	-9.156 to -3.444	Yes	****	<0.0001
Control vs. Large Spontaneous	-11.47	-14.33 to -8.614	Yes	****	<0.0001
Small Induced vs. Medium Induced	-1.348	-3.991 to 1.296	No	ns	>0.9999
Small Induced vs. Large induced	-5.84	-8.484 to -3.196	Yes	****	<0.0001
Small Induced vs. Small Spontaneous	-5.22	-8.076 to -2.364	Yes	***	0.0002
Small Induced vs. Large Spontaneous	-10.39	-13.25 to -7.534	Yes	****	<0.0001
Medium Induced vs. Large induced	-4.493	-7.136 to -1.849	Yes	***	0.0004
Medium Induced vs. Small Spontaneous	-3.873	-6.728 to -1.017	Yes	**	0.0038
Medium Induced vs. Large Spontaneous	-9.043	-11.9 to -6.187	Yes	****	<0.0001
Large induced vs. Small Spontaneous	0.62	-2.236 to 3.476	No	ns	>0.9999
Large induced vs. Large Spontaneous	-4.55	-7.406 to -1.694	Yes	***	0.0007
Small Spontaneous vs. Large Spontaneous	-5.17	-8.223 to -2.117	Yes	***	0.0004

Table 5 One-way ANOVA of bone marrow, blood and spleen neutrophil neutrophil data from control and tumour-bearing mice (Figure 4.8)

Bonferroni's multiple comparisons test	Mean Diff.	95.00% CI of diff.	Significant?	Summary	Adjusted P Value
Bone marrow CXCR2+ CD62L- neutrophils of Ly6G+					
Control vs. Small Induced	-4.09	-8.103 to -0.07679	Yes	*	0.0435
Control vs. Medium Induced	-9.653	-13.67 to -5.639	Yes	****	<0.0001
Control vs. Large induced	-10.33	-14.34 to -6.314	Yes	****	<0.0001
Control vs. Small Spontaneous	-6.514	-10.85 to -2.179	Yes	**	0.0014
Control vs. Large Spontaneous	-11.36	-15.7 to -7.026	Yes	****	<0.0001
Small Induced vs. Medium Induced	-5.563	-9.576 to -1.549	Yes	**	0.0031
Small Induced vs. Large induced	-6.238	-10.25 to -2.224	Yes	***	0.001
Small Induced vs. Small Spontaneous	-2.424	-6.759 to 1.911	No	ns	>0.9999
Small Induced vs. Large Spontaneous	-7.271	-11.61 to -2.936	Yes	***	0.0004
Medium Induced vs. Large induced	-0.675	-4.688 to 3.338	No	ns	>0.9999
Medium Induced vs. Small Spontaneous	3.138	-1.196 to 7.473	No	ns	0.3597
Medium Induced vs. Large Spontaneous	-1.708	-6.043 to 2.626	No	ns	>0.9999
Large induced vs. Small Spontaneous	3.813	-0.5214 to 8.148	No	ns	0.1195
Large induced vs. Large Spontaneous	-1.033	-5.368 to 3.301	No	ns	>0.9999
Small Spontaneous vs. Large Spontaneous	-4.847	-9.481 to -0.2126	Yes	*	0.0358
Bone marrow CXCR2+ CD62L- neutrophils of alive					
Control vs. Small Induced	-1.885	-5.201 to 1.431	No	ns	>0.9999
Control vs. Medium Induced	-5.418	-8.733 to -2.102	Yes	***	0.0006
Control vs. Large induced	-6.608	-9.923 to -3.292	Yes	****	<0.0001
Control vs. Small Spontaneous	-5.19	-8.771 to -1.609	Yes	**	0.002
Control vs. Large Spontaneous	-8.083	-11.66 to -4.502	Yes	****	<0.0001
Small Induced vs. Medium Induced	-3.533	-6.848 to -0.2168	Yes	*	0.0311
Small Induced vs. Large induced	-4.723	-8.038 to -1.407	Yes	**	0.0024
Small Induced vs. Small Spontaneous	-3.305	-6.886 to 0.2763	No	ns	0.0875
Small Induced vs. Large Spontaneous	-6.198	-9.78 to -2.617	Yes	***	0.0003
Medium Induced vs. Large induced	-1.19	-4.506 to 2.126	No	ns	>0.9999
Medium Induced vs. Small Spontaneous	0.2275	-3.354 to 3.809	No	ns	>0.9999
Medium Induced vs. Large Spontaneous	-2.666	-6.247 to 0.9155	No	ns	0.3122
Large induced vs. Small Spontaneous	1.418	-2.164 to 4.999	No	ns	>0.9999
Large induced vs. Large Spontaneous	-1.476	-5.057 to 2.106	No	ns	>0.9999
Small Spontaneous vs. Large Spontaneous	-2.893	-6.722 to 0.9353	No	ns	0.2884

Table 6 One-way ANOVA of bone marrow CXCR2+ CD62L- neutrophil data from control and tumour-bearing mice (Figure 4.9)

Bonferroni's multiple comparisons test	Mean Diff.	95.00% CI of diff.	Significant?	Summary	Adjusted P Value
Blood CXCR2+ CD62L- neutrophils of Ly6G+					
Control vs. Small Induced	-5.495	-22.26 to 11.27	No	ns	>0.9999
Control vs. Medium Induced	-21.03	-37.8 to -4.262	Yes	**	0.0079
Control vs. Large induced	-67.63	-84.4 to -50.86	Yes	****	<0.0001
Control vs. Small Spontaneous	-16.91	-35.02 to 1.198	No	ns	0.0808
Control vs. Large Spontaneous	-76.88	-94.99 to -58.77	Yes	****	<0.0001
Small Induced vs. Medium Induced	-15.54	-32.3 to 1.233	No	ns	0.0853
Small Induced vs. Large induced	-62.14	-78.9 to -45.37	Yes	****	<0.0001
Small Induced vs. Small Spontaneous	-11.42	-29.53 to 6.693	No	ns	0.6792
Small Induced vs. Large Spontaneous	-71.39	-89.5 to -53.27	Yes	****	<0.0001
Medium Induced vs. Large induced	-46.6	-63.37 to -29.83	Yes	****	<0.0001
Medium Induced vs. Small Spontaneous	4.117	-13.99 to 22.23	No	ns	>0.9999
Medium Induced vs. Large Spontaneous	-55.85	-73.96 to -37.74	Yes	****	<0.0001
Large induced vs. Small Spontaneous	50.72	32.61 to 68.83	Yes	****	<0.0001
Large induced vs. Large Spontaneous	-9.25	-27.36 to 8.861	No	ns	>0.9999
Small Spontaneous vs. Large Spontaneous	-59.97	-79.33 to -40.6	Yes	****	<0.0001
Blood CXCR2+ CD62L- neutrophils of alive					
Control vs. Small Induced	-5.173	-13.42 to 3.072	No	ns	0.6931
Control vs. Medium Induced	-10.43	-18.67 to -2.183	Yes	**	0.0073
Control vs. Large induced	-17.23	-25.48 to -8.988	Yes	****	<0.0001
Control vs. Small Spontaneous	-6.276	-15.18 to 2.629	No	ns	0.4107
Control vs. Large Spontaneous	-40.56	-49.46 to -31.65	Yes	****	<0.0001
Small Induced vs. Medium Induced	-5.255	-13.5 to 2.989	No	ns	0.6484
Small Induced vs. Large induced	-12.06	-20.3 to -3.816	Yes	**	0.0018
Small Induced vs. Small Spontaneous	-1.103	-10.01 to 7.802	No	ns	>0.9999
Small Induced vs. Large Spontaneous	-35.38	-44.29 to -26.48	Yes	****	<0.0001
Medium Induced vs. Large induced	-6.805	-15.05 to 1.439	No	ns	0.1763
Medium Induced vs. Small Spontaneous	4.152	-4.753 to 13.06	No	ns	>0.9999
Medium Induced vs. Large Spontaneous	-30.13	-39.03 to -21.22	Yes	****	<0.0001
Large induced vs. Small Spontaneous	10.96	2.052 to 19.86	Yes	**	0.0094
Large induced vs. Large Spontaneous	-23.32	-32.23 to -14.42	Yes	****	<0.0001
Small Spontaneous vs. Large Spontaneous	-34.28	-43.8 to -24.76	Yes	****	<0.0001

Table 7 One-way ANOVA of blood CXCR2+ CD62L- neutrophil data from control and tumour-bearing mice (Figure 4.9)

Bonferroni's multiple comparisons test	Mean Diff.	95.00% CI of diff.	Significant?	Summary	Adjusted P Value
Spleen CXCR2+ CD62L- neutrophils of Ly6G+					
Control vs. Small Induced	-5.225	-19.14 to 8.69	No	ns	>0.9999
Control vs. Medium Induced	-26.13	-40.04 to -12.21	Yes	***	0.0001
Control vs. Large induced	-40.9	-54.81 to -26.99	Yes	****	<0.0001
Control vs. Small Spontaneous	-28.38	-43.4 to -13.35	Yes	***	0.0001
Control vs. Large Spontaneous	-64.24	-79.27 to -49.21	Yes	****	<0.0001
Small Induced vs. Medium Induced	-20.9	-34.81 to -6.985	Yes	**	0.0014
Small Induced vs. Large induced	-35.68	-49.59 to -21.76	Yes	****	<0.0001
Small Induced vs. Small Spontaneous	-23.15	-38.18 to -8.12	Yes	**	0.0011
Small Induced vs. Large Spontaneous	-59.02	-74.05 to -43.99	Yes	****	<0.0001
Medium Induced vs. Large induced	-14.78	-28.69 to -0.8604	Yes	*	0.0319
Medium Induced vs. Small Spontaneous	-2.25	-17.28 to 12.78	No	ns	>0.9999
Medium Induced vs. Large Spontaneous	-38.12	-53.15 to -23.09	Yes	****	<0.0001
Large induced vs. Small Spontaneous	12.53	-2.505 to 27.55	No	ns	0.1665
Large induced vs. Large Spontaneous	-23.34	-38.37 to -8.312	Yes	***	0.001
Small Spontaneous vs. Large Spontaneous	-35.87	-51.93 to -19.8	Yes	****	<0.0001
Spleen CXCR2+ CD62L- neutrophils of alive					
Control vs. Small Induced	-0.8838	-2.919 to 1.152	No	ns	>0.9999
Control vs. Medium Induced	-1.836	-3.872 to 0.1992	No	ns	0.1017
Control vs. Large induced	-4.394	-6.429 to -2.358	Yes	****	<0.0001
Control vs. Small Spontaneous	-3.895	-6.094 to -1.697	Yes	***	0.0002
Control vs. Large Spontaneous	-7.855	-10.05 to -5.657	Yes	****	<0.0001
Small Induced vs. Medium Induced	-0.9525	-2.988 to 1.083	No	ns	>0.9999
Small Induced vs. Large induced	-3.51	-5.545 to -1.475	Yes	***	0.0003
Small Induced vs. Small Spontaneous	-3.012	-5.21 to -0.8131	Yes	**	0.0035
Small Induced vs. Large Spontaneous	-6.972	-9.17 to -4.773	Yes	****	<0.0001
Medium Induced vs. Large induced	-2.558	-4.593 to -0.522	Yes	**	0.0078
Medium Induced vs. Small Spontaneous	-2.059	-4.258 to 0.1394	No	ns	0.0792
Medium Induced vs. Large Spontaneous	-6.019	-8.218 to -3.821	Yes	****	<0.0001
Large induced vs. Small Spontaneous	0.4983	-1.7 to 2.697	No	ns	>0.9999
Large induced vs. Large Spontaneous	-3.462	-5.66 to -1.263	Yes	***	0.0008
Small Spontaneous vs. Large Spontaneous	-3.96	-6.31 to -1.61	Yes	***	0.0004

Table 8 One-way ANOVA of spleen CXCR2+ CD62L- neutrophil data from control and tumour-bearing mice (Figure 4.10)

Reference List

AL-HAIDARI, A. A., ALGETHAMI, N., LEPSENYI, M., RAHMAN, M., SYK, I. & THORLACIUS, H. 2019. Neutrophil extracellular traps promote peritoneal metastasis of colon cancer cells. *Oncotarget,* 10**,** 1238-1249.

ALLMAN, D. & PILLAI, S. 2008. Peripheral B cell subsets. *Current opinion in immunology,* 20**,** 149-157.

AUTENGRUBER, A., GEREKE, M., HANSEN, G., HENNIG, C. & BRUDER, D. 2012. Impact of enzymatic tissue disintegration on the level of surface molecule expression and immune cell function. *European journal of microbiology & immunology,* 2**,** 112-120.

BALD, T., QUAST, T., LANDSBERG, J., ROGAVA, M., GLODDE, N., LOPEZ-RAMOS, D., KOHLMEYER, J., RIESENBERG, S., VAN DEN BOORN-KONIJNENBERG, D., HÖMIG-HÖLZEL, C., REUTEN, R., SCHADOW, B., WEIGHARDT, H., WENZEL, D., HELFRICH, I., SCHADENDORF, D., BLOCH, W., BIANCHI, M. E., LUGASSY, C., BARNHILL, R. L., KOCH, M., FLEISCHMANN, B. K., FÖRSTER, I., KASTENMÜLLER, W., KOLANUS, W., HÖLZEL, M., GAFFAL, E. & TÜTING, T. 2014. Ultraviolet-radiation-induced inflammation promotes angiotropism and metastasis in melanoma. *Nature,* 507**,** 109.

BALKWILL, F. R., CAPASSO, M. & HAGEMANN, T. 2012. The tumor microenvironment at a glance. *Journal of Cell Science,* 125**,** 5591.

BANK, U. & ANSORGE, S. 2001. More than destructive: neutrophil-derived serine proteases in cytokine bioactivity control. *Journal of Leukocyte Biology,* 69**,** 197-206.

BECHER, B., SCHLITZER, A., CHEN, J., MAIR, F., SUMATOH, H. R., TENG, K. W. W., LOW, D., RUEDL, C., RICCARDI-CASTAGNOLI, P., POIDINGER, M., GRETER, M., GINHOUX, F. & NEWELL, E. W. 2014. High-dimensional analysis of the murine myeloid cell system. *Nat Immunol,* 15**,** 1181-1189.

BEKES, E. M., SCHWEIGHOFER, B., KUPRIYANOVA, T. A., ZAJAC, E., ARDI, V. C., QUIGLEY, J. P. & DERYUGINA, E. I. 2011. Tumor-recruited neutrophils and neutrophil TIMP-free MMP-9 regulate coordinately the levels of tumor angiogenesis and efficiency of malignant cell intravasation. *The American journal of pathology,* 179**,** 1455-1470.

BELGODERE, J. A., KING, C. T., BURSAVICH, J. B., BUROW, M. E., MARTIN, E. C. & JUNG, J. P. 2018. Engineering Breast Cancer Microenvironments and 3D Bioprinting. *Frontiers in Bioengineering and Biotechnology,* 6**,** 66.

BENDALL, L. J. & BRADSTOCK, K. F. 2014. G-CSF: From granulopoietic stimulant to bone marrow stem cell mobilizing agent. *Cytokine & Growth Factor Reviews,* 25**,** 355-367.

BLAISDELL, A., CREQUER, A., COLUMBUS, D., DAIKOKU, T., MITTAL, K., DEY, SUDHANSU K. & ERLEBACHER, A. 2015. Neutrophils Oppose Uterine Epithelial Carcinogenesis via Debridement of Hypoxic Tumor Cells. *Cancer Cell,* 28**,** 785-799.

BLANPAIN, C. 2013. Tracing the cellular origin of cancer. *Nat Cell Biol,* 15**,** 126-34.

BORREGAARD, N. 2010. Neutrophils, from Marrow to Microbes. *Immunity,* 33**,** 657-670.

BRAY, F., JEMAL, A., GREY, N., FERLAY, J. & FORMAN, D. 2012. Global cancer transitions according to the Human Development Index (2008–2030): a population-based study. *The Lancet Oncology,* 13**,** 790-801.

BRINKMANN, V., REICHARD, U., GOOSMANN, C., FAULER, B., UHLEMANN, Y., WEISS, D. S., WEINRAUCH, Y. & ZYCHLINSKY, A. 2004. Neutrophil Extracellular Traps Kill Bacteria. *Science,* 303**,** 1532.

BRONTE, V., BRANDAU, S., CHEN, S.-H., COLOMBO, M. P., FREY, A. B., GRETEN, T. F., MANDRUZZATO, S., MURRAY, P. J., OCHOA, A., OSTRAND-ROSENBERG, S., RODRIGUEZ, P. C., SICA, A., UMANSKY, V., VONDERHEIDE, R. H. & GABRILOVICH, D. I. 2016a. Recommendations for myeloid-derived suppressor cell nomenclature and characterization standards. *Nature communications,* 7**,** 12150-12150.

BRONTE, V., BRANDAU, S., CHEN, S.-H., COLOMBO, M. P., FREY, A. B., GRETEN, T. F., MANDRUZZATO, S., MURRAY, P. J., OCHOA, A., OSTRAND-ROSENBERG, S., RODRIGUEZ, P. C., SICA, A., UMANSKY, V., VONDERHEIDE, R. H. & GABRILOVICH, D. I. 2016b. Recommendations for myeloid-derived suppressor cell nomenclature and characterization standards. *Nature Communications,* 7**,** 12150.

BUI, T. M., MASCARENHAS, L. A. & SUMAGIN, R. 2018. Extracellular vesicles regulate immune responses and cellular function in intestinal inflammation and repair. *Tissue Barriers,* 6**,** e1431038.

CALIS, J. J. A. & ROSENBERG, B. R. 2014. Characterizing immune repertoires by high throughput sequencing: strategies and applications. *Trends in immunology,* 35**,** 581-590.

CAPPENBERG, A., MARGRAF, A., THOMAS, K., BARDEL, B., MCCREEDY, D. A., VAN MARCK, V., MELLMANN, A., LOWELL, C. A. & ZARBOCK, A. 2019. L-selectin shedding affects bacterial clearance in the lung - a new regulatory pathway for integrin-outside-in signaling. *Blood***,** blood.2019000685.

CARUS, A., LADEKARL, M., HAGER, H., PILEGAARD, H., NIELSEN, P. S. & DONSKOV, F. 2013. Tumor-associated neutrophils and macrophages in non-small cell lung cancer: No immediate impact on patient outcome. *Lung Cancer,* 81**,** 130-137.

CARUSO, R. A., BELLOCCO, R., PAGANO, M., BERTOLI, G., RIGOLI, L. & INFERRERA, C. 2002. Prognostic Value of Intratumoral Neutrophils in Advanced Gastric Carcinoma in a High-Risk Area in Northern Italy. *Mod Pathol,* 15**,** 831-837.

CASANOVA-ACEBES, M., PITAVAL, C., WEISS, L. A., NOMBELA-ARRIETA, C., CHEVRE, R., N, A. G., KUNISAKI, Y., ZHANG, D., VAN ROOIJEN, N., SILBERSTEIN, L. E., WEBER, C., NAGASAWA, T., FRENETTE, P. S., CASTRILLO, A. & HIDALGO, A. 2013. Rhythmic modulation of the hematopoietic niche through neutrophil clearance. *Cell,* 153**,** 1025-35.

CASEY, A. E., LASTER, W. R. & ROSS, G. L. 1951. Sustained Enhanced Growth of Carcinoma EO771 in C57 Black Mice. *Proceedings of the Society for Experimental Biology and Medicine,* 77**,** 358-362.

CATENA, R., BHATTACHARYA, N., EL RAYES, T., WANG, S., CHOI, H., GAO, D., RYU, S., JOSHI, N., BIELENBERG, D., LEE, S. B., HAUKAAS, S. A., GRAVDAL, K., HALVORSEN, O. J., AKSLEN, L. A., WATNICK, R. S. & MITTAL, V. 2013. Bone marrow-derived Gr1+ cells can generate a metastasis-resistant microenvironment via induced secretion of thrombospondin-1. *Cancer discovery,* 3**,** 578-589.

CHAFFER, C. L. & WEINBERG, R. A. 2015. How does multistep tumorigenesis really proceed? *Cancer discovery,* 5**,** 22-24.

CHANG, C. Y., TAI, J. A., LI, S., NISHIKAWA, T. & KANEDA, Y. 2016. Virus-stimulated neutrophils in the tumor microenvironment enhance T cell-mediated anti-tumor immunity. *Oncotarget,* 7**,** 42195-42207.

CHARLES, K. A., KULBE, H., SOPER, R., ESCORCIO-CORREIA, M., LAWRENCE, T., SCHULTHEIS, A., CHAKRAVARTY, P., THOMPSON, R. G., KOLLIAS, G., SMYTH, J. F., BALKWILL, F. R. & HAGEMANN, T. 2009. The tumor-promoting actions of TNF-alpha involve TNFR1 and IL-17 in ovarian cancer in mice and humans. *The Journal of clinical investigation,* 119**,** 3011-3023.

CHENG, Y., LI, H., DENG, Y., TAI, Y., ZENG, K., ZHANG, Y., LIU, W., ZHANG, Q. & YANG, Y. 2018. Cancer-associated fibroblasts induce PDL1+ neutrophils through the IL6-STAT3 pathway that foster immune suppression in hepatocellular carcinoma. *Cell Death & Disease,* 9**,** 422.

CHORNY, A., CASAS-RECASENS, S., SINTES, J., SHAN, M., POLENTARUTTI, N., GARCÍA-ESCUDERO, R., WALLAND, A. C., YEISER, J. R., CASSIS, L., CARRILLO, J., PUGA, I., CUNHA, C., BASTOS, H., RODRIGUES, F., LACERDA, J. F., MORAIS, A., DIEGUEZ-GONZALEZ, R., HEEGER, P. S., SALVATORI, G., CARVALHO, A., GARCIA-SASTRE, A., BLANDER, J. M., MANTOVANI, A., GARLANDA, C. & CERUTTI, A. 2016. The soluble pattern recognition receptor PTX3 links humoral innate and adaptive immune responses by helping marginal zone B cells. *The Journal of Experimental Medicine,* 213**,** 2167-2185.

CHRISTENSON, J. L., BUTTERFIELD, K. T., SPOELSTRA, N. S., NORRIS, J. D., JOSAN, J. S., POLLOCK, J. A., MCDONNELL, D. P., KATZENELLENBOGEN, B. S., KATZENELLENBOGEN, J. A. & RICHER, J. K. 2017. MMTV-PyMT and Derived Met-1 Mouse Mammary Tumor Cells as Models for Studying the Role of the Androgen Receptor in Triple-Negative Breast Cancer Progression. *Hormones & cancer,* 8**,** 69-77.

CHRISTOFFERSSON, G., LOMEI, J., O'CALLAGHAN, P., KREUGER, J., ENGBLOM, S. & PHILLIPSON, M. 2017. Vascular sprouts induce local attraction of proangiogenic neutrophils. *Journal of Leukocyte Biology,* 102**,** 741-751.

CHRISTOFFERSSON, G., VÅGESJÖ, E., VANDOOREN, J., LIDÉN, M., MASSENA, S., REINERT, R. B., BRISSOVA, M., POWERS, A. C., OPDENAKKER, G. & PHILLIPSON, M. 2012a. VEGF-A recruits a proangiogenic MMP-9–delivering neutrophil subset that induces angiogenesis in transplanted hypoxic tissue. *Blood,* 120**,** 4653-4662.

CHRISTOFFERSSON, G., VÅGESJÖ, E., VANDOOREN, J., LIDÉN, M., MASSENA, S., REINERT, R. B., BRISSOVA, M., POWERS, A. C., OPDENAKKER, G. & PHILLIPSON, M. 2012b. VEGF-A recruits a proangiogenic MMP-9–delivering neutrophil subset that induces angiogenesis in transplanted hypoxic tissue. *Blood,* 120**,** 4653.

COFFELT, S. B., KERSTEN, K., DOORNEBAL, C. W., WEIDEN, J., VRIJLAND, K., HAU, C. S., VERSTEGEN, N. J., CIAMPRICOTTI, M., HAWINKELS, L. J., JONKERS, J. & DE VISSER, K. E. 2015. IL-17-producing gammadelta T cells and neutrophils conspire to promote breast cancer metastasis. *Nature,* 522**,** 345-8.

COFFELT, S. B., WELLENSTEIN, M. D. & DE VISSER, K. E. 2016. Neutrophils in cancer: neutral no more. *Nat Rev Cancer,* 16**,** 431-446.

COLOM, B., BODKIN, J. V., BEYRAU, M., WOODFIN, A., ODY, C., ROURKE, C., CHAVAKIS, T., BROHI, K., IMHOF, B. A. & NOURSHARGH, S. 2015. Leukotriene B4-Neutrophil Elastase Axis Drives Neutrophil Reverse Transendothelial Cell Migration In Vivo. *Immunity,* 42**,** 1075-1086.

COLOTTA, F., RE, F., POLENTARUTTI, N., SOZZANI, S. & MANTOVANI, A. 1992. Modulation of granulocyte survival and programmed cell death by cytokines and bacterial products. *Blood,* 80**,** 2012.

CUI, T. X., KRYCZEK, I., ZHAO, L., ZHAO, E., KUICK, R., ROH, M. H., VATAN, L., SZELIGA, W., MAO, Y., THOMAS, D. G., KOTARSKI, J., TARKOWSKI, R., WICHA, M., CHO, K., GIORDANO, T., LIU, R. & ZOU, W. 2013. Myeloid-derived suppressor cells enhance stemness of cancer cells by inducing microRNA101 and suppressing the corepressor CtBP2. *Immunity,* 39**,** 611-621.

DALEY, J. M., THOMAY, A. A., CONNOLLY, M. D., REICHNER, J. S. & ALBINA, J. E. 2008. Use of Ly6G-specific monoclonal antibody to deplete neutrophils in mice. *J Leukoc Biol,* 83**,** 64-70.

DENNY, M. F., YALAVARTHI, S., ZHAO, W., THACKER, S. G., ANDERSON, M., SANDY, A. R., MCCUNE, W. J. & KAPLAN, M. J. 2010. A distinct subset of proinflammatory neutrophils isolated from patients with systemic lupus erythematosus induces vascular damage and synthesizes type I Interferons. *Journal of immunology (Baltimore, Md. : 1950),* 184**,** 3284-3297.

DEVALARAJA, R. M., NANNEY, L. B., QIAN, Q., DU, J., YU, Y., DEVALARAJA, M. N. & RICHMOND, A. 2000. Delayed Wound Healing in CXCR2 Knockout Mice. *Journal of Investigative Dermatology,* 115**,** 234-244.

DI MITRI, D., TOSO, A., CHEN, J. J., SARTI, M., PINTON, S., JOST, T. R., D'ANTUONO, R., MONTANI, E., GARCIA-ESCUDERO, R., GUCCINI, I., DA SILVA-ALVAREZ, S., COLLADO, M., EISENBERGER, M., ZHANG, Z., CATAPANO, C., GRASSI, F. & ALIMONTI, A. 2014. Tumour-infiltrating Gr-1+ myeloid cells antagonize senescence in cancer. *Nature,* 515**,** 134.

DOS ANJOS CASSADO, A. 2017. F4/80 as a Major Macrophage Marker: The Case of the Peritoneum and Spleen. *In:* KLOC, M. (ed.) *Macrophages: Origin, Functions and Biointervention.* Cham: Springer International Publishing.

DOUGAN, M., DRANOFF, G. & DOUGAN, S. K. 2019. Cancer Immunotherapy: Beyond Checkpoint Blockade. *Annual Review of Cancer Biology,* 3**,** 55-75.

DUPRÉ-CROCHET, S., ERARD, M. & NÜBE, O. 2013. ROS production in phagocytes: why, when, and where? *Journal of Leukocyte Biology,* 94**,** 657-670.

EASH, K. J., GREENBAUM, A. M., GOPALAN, P. K. & LINK, D. C. 2010. CXCR2 and CXCR4 antagonistically regulate neutrophil trafficking from murine bone marrow. *The Journal of clinical investigation,* 120**,** 2423-2431.

ENGBLOM, C., PFIRSCHKE, C., ZILIONIS, R., DA SILVA MARTINS, J., BOS, S. A., COURTIES, G., RICKELT, S., SEVERE, N., BARYAWNO, N., FAGET, J., SAVOVA, V., ZEMMOUR, D., KLINE, J., SIWICKI, M., GARRIS, C., PUCCI, F., LIAO, H.-W., LIN, Y.-J., NEWTON, A., YAGHI, O. K., IWAMOTO, Y., TRICOT, B., WOJTKIEWICZ, G. R., NAHRENDORF, M., CORTEZ-RETAMOZO, V., MEYLAN, E., HYNES, R. O., DEMAY, M., KLEIN, A., BREDELLA, M. A., SCADDEN, D. T., WEISSLEDER, R. & PITTET, M. J. 2017. Osteoblasts remotely supply lung tumors with cancer-promoting SiglecF(high) neutrophils. *Science (New York, N.Y.),* 358**,** eaal5081.

ERPENBECK, L. & SCHÖN, M. P. 2016. Neutrophil extracellular traps: protagonists of cancer progression? *Oncogene,* 36**,** 2483.

ERUSLANOV, E. B., BHOJNAGARWALA, P. S., QUATROMONI, J. G., STEPHEN, T. L., RANGANATHAN, A., DESHPANDE, C., AKIMOVA, T., VACHANI, A., LITZKY, L., HANCOCK, W. W., CONEJO-GARCIA, J. R., FELDMAN, M., ALBELDA, S. M. & SINGHAL, S. 2014. Tumor-associated neutrophils stimulate T cell responses in early-stage human lung cancer. *The Journal of clinical investigation,* 124**,** 5466-5480.

EVRARD, M., KWOK, I. W. H., CHONG, S. Z., TENG, K. W. W., BECHT, E., CHEN, J., SIEOW, J. L., PENNY, H. L., CHING, G. C., DEVI, S., ADROVER, J. M., LI, J.

L. Y., LIONG, K. H., TAN, L., POON, Z., FOO, S., CHUA, J. W., SU, I. H., BALABANIAN, K., BACHELERIE, F., BISWAS, S. K., LARBI, A., HWANG, W. Y. K., MADAN, V., KOEFFLER, H. P., WONG, S. C., NEWELL, E. W., HIDALGO, A., GINHOUX, F. & NG, L. G. 2018. Developmental Analysis of Bone Marrow Neutrophils Reveals Populations Specialized in Expansion, Trafficking, and Effector Functions. *Immunity,* 48**,** 364-379.e8.

FAGERHOLM, S. C., GUENTHER, C., LLORT ASENS, M., SAVINKO, T. & UOTILA, L. M. 2019. Beta2-Integrins and Interacting Proteins in Leukocyte Trafficking, Immune Suppression, and Immunodeficiency Disease. *Frontiers in Immunology,* 10**,** 254.

FERLAY, J., SOERJOMATARAM, I., DIKSHIT, R., ESER, S., MATHERS, C., REBELO, M., PARKIN, D. M., FORMAN, D. & BRAY, F. 2015. Cancer incidence and mortality worldwide: Sources, methods and major patterns in GLOBOCAN 2012. *International Journal of Cancer,* 136**,** E359-E386.

FINISGUERRA, V., DI CONZA, G., DI MATTEO, M., SERNEELS, J., COSTA, S., THOMPSON, A. A., WAUTERS, E., WALMSLEY, S., PRENEN, H., GRANOT, Z., CASAZZA, A. & MAZZONE, M. 2015. MET is required for the recruitment of anti-tumoural neutrophils. *Nature,* 522**,** 349-53.

FLEMING, V., HU, X., WEBER, R., NAGIBIN, V., GROTH, C., ALTEVOGT, P., UTIKAL, J. & UMANSKY, V. 2018. Targeting Myeloid-Derived Suppressor Cells to Bypass Tumor-Induced Immunosuppression. *Frontiers in immunology,* 9**,** 398-398.

FORRESTER, S. J., KIKUCHI, D. S., HERNANDES, M. S., XU, Q. & GRIENDLING, K. K. 2018. Reactive Oxygen Species in Metabolic and Inflammatory Signaling. *Circulation research,* 122**,** 877-902.

FRIDLENDER, Z. G., SUN, J., KIM, S., KAPOOR, V., CHENG, G., LING, L., WORTHEN, G. S. & ALBELDA, S. M. 2009. Polarization of Tumor-Associated Neutrophil (TAN) Phenotype by TGF-β: “N1” versus “N2” TAN. *Cancer cell,* 16**,** 183-194.

GALLI, S. J., BORREGAARD, N. & WYNN, T. A. 2011. Phenotypic and functional plasticity of cells of innate immunity: macrophages, mast cells and neutrophils. *Nature immunology,* 12**,** 1035-1044.

GARNER, H. & DE VISSER, K. E. 2017. Neutrophils take a round-trip. *Science,* 358**,** 42.

GEERING, B., STOECKLE, C., CONUS, S. & SIMON, H.-U. 2013. Living and dying for inflammation: neutrophils, eosinophils, basophils. *Trends in Immunology,* 34**,** 398-409.

GENTLES, A. J., NEWMAN, A. M., LIU, C. L., BRATMAN, S. V., FENG, W., KIM, D., NAIR, V. S., XU, Y., KHUONG, A., HOANG, C. D., DIEHN, M., WEST, R. B., PLEVRITIS, S. K. & ALIZADEH, A. A. 2015. The prognostic landscape of genes and infiltrating immune cells across human cancers. *Nature Medicine,* 21**,** 938.

GERSHKOVITZ, M., FAINSOD-LEVI, T., ZELTER, T., SIONOV, R. V. & GRANOT, Z. 2019. TRPM2 modulates neutrophil attraction to murine tumor cells by regulating CXCL2 expression. *Cancer Immunology, Immunotherapy,* 68**,** 33-43.

GIESE, M. A., HIND, L. E. & HUTTENLOCHER, A. 2019. Neutrophil plasticity in the tumor microenvironment. *Blood,* 133**,** 2159-2167.

GONG, L., CUMPIAN, A. M., CAETANO, M. S., OCHOA, C. E., DE LA GARZA, M. M., LAPID, D. J., MIRABOLFATHINEJAD, S. G., DICKEY, B. F., ZHOU, Q. & MOGHADDAM, S. J. 2013. Promoting effect of neutrophils on lung tumorigenesis is mediated by CXCR2 and neutrophil elastase. *Molecular Cancer,* 12**,** 154-154.

GOODEN, M. J. M., DE BOCK, G. H., LEFFERS, N., DAEMEN, T. & NIJMAN, H. W. 2011. The prognostic influence of tumour-infiltrating lymphocytes in cancer: a systematic review with meta-analysis. *British Journal Of Cancer,* 105**,** 93.

GOODNOW, C. C., CROSBIE, J., ADELSTEIN, S., LAVOIE, T. B., SMITH-GILL, S. J., BRINK, R. A., PRITCHARD-BRISCOE, H., WOTHERSPOON, J. S., LOBLAY, R. H., RAPHAEL, K., TRENT, R. J. & BASTEN, A. 1988. Altered immunoglobulin expression and functional silencing of self-reactive B lymphocytes in transgenic mice. *Nature,* 334**,** 676-682.

GOVERNA, V., TRELLA, E., MELE, V., TORNILLO, L., AMICARELLA, F., CREMONESI, E., MURARO, M. G., XU, H., DROESER, R., DÄSTER, S. R., BOLLI, M., ROSSO, R., OERTLI, D., EPPENBERGER-CASTORI, S., TERRACCIANO, L. M., IEZZI, G. & SPAGNOLI, G. C. 2017. The Interplay Between Neutrophils and CD8⁺ T Cells Improves Survival in Human Colorectal Cancer. *Clinical Cancer Research,* 23**,** 3847.

GRANOT, Z., HENKE, E., COMEN, E., KING, T., NORTON, L. & BENEZRA, R. 2011. Tumor entrained neutrophils inhibit seeding in the premetastatic lung. *Cancer cell,* 20**,** 300-314.

GRIVENNIKOV, S. I., GRETEN, F. R. & KARIN, M. 2010. Immunity, Inflammation, and Cancer. *Cell,* 140**,** 883-899.

GUY, C. T., CARDIFF, R. D. & MULLER, W. J. 1992. Induction of mammary tumors by expression of polyomavirus middle T oncogene: a transgenic mouse model for metastatic disease. *Molecular and Cellular Biology,* 12**,** 954-961.

HÄGER, M., COWLAND, J. B. & BORREGAARD, N. 2010. Neutrophil granules in health and disease. *Journal of Internal Medicine,* 268**,** 25-34.

HANAHAN, D. & WEINBERG, R. A. 2000. The Hallmarks of Cancer. *Cell,* 100**,** 57-70.

HANAHAN, D. & WEINBERG, ROBERT A. 2011. Hallmarks of Cancer: The Next Generation. *Cell,* 144**,** 646-674.

HAO, S., ANDERSEN, M. & YU, H. 2013. Detection of immune suppressive neutrophils in peripheral blood samples of cancer patients. *American Journal of Blood Research,* 3**,** 239-245.

HE, G., ZHANG, H., ZHOU, J., WANG, B., CHEN, Y., KONG, Y., XIE, X., WANG, X., FEI, R., WEI, L., CHEN, H. & ZENG, H. 2015. Peritumoural neutrophils negatively regulate adaptive immunity via the PD-L1/PD-1 signalling pathway in hepatocellular carcinoma. *Journal of experimental & clinical cancer research : CR,* 34**,** 141-141.

HE, M., PENG, A., HUANG, X.-Z., SHI, D.-C., WANG, J.-C., ZHAO, Q., LIN, H., KUANG, D.-M., KE, P.-F. & LAO, X.-M. 2016. Peritumoral stromal neutrophils are essential for c-Met-elicited metastasis in human hepatocellular carcinoma. *Oncoimmunology,* 5**,** e1219828-e1219828.

HIDA, K., MAISHI, N., ANNAN, D. A. & HIDA, Y. 2018. Contribution of Tumor Endothelial Cells in Cancer Progression. *International journal of molecular sciences,* 19**,** 1272.

HIDALGO, A., CHILVERS, E. R., SUMMERS, C. & KOENDERMAN, L. 2019. The Neutrophil Life Cycle. *Trends in Immunology,* 40**,** 584-597.

HOFFMANN, K., SPERLING, K., OLINS, A. L. & OLINS, D. E. 2007. The granulocyte nucleus and lamin B receptor: avoiding the ovoid. *Chromosoma,* 116**,** 227-235.

HOUGHTON, A. M., RZYMKIEWICZ, D. M., JI, H., GREGORY, A. D., EGEA, E. E., METZ, H. E., STOLZ, D. B., LAND, S. R., MARCONCINI, L. A., KLIMENT, C. R., JENKINS, K. M., BEAULIEU, K. A., MOUDED, M., FRANK, S. J., WONG, K. K. & SHAPIRO, S. D. 2010. Neutrophil elastase-mediated degradation of IRS-1 accelerates lung tumor growth. *Nature medicine,* 16**,** 219-223.

IVETIC, A. 2018. A head-to-tail view of L-selectin and its impact on neutrophil behaviour. *Cell and Tissue Research,* 371**,** 437-453.

IVETIC, A., HOSKINS GREEN, H. L. & HART, S. J. 2019. L-selectin: A Major Regulator of Leukocyte Adhesion, Migration and Signaling. *Frontiers in immunology,* 10**,** 1068-1068.

JAMIESON, T., CLARKE, M., STEELE, C. W., SAMUEL, M. S., NEUMANN, J., JUNG, A., HUELS, D., OLSON, M. F., DAS, S., NIBBS, R. J. B. & SANSOM, O. J. 2012. Inhibition of CXCR2 profoundly suppresses inflammation-driven and spontaneous tumorigenesis. *The Journal of Clinical Investigation,* 122**,** 3127-3144.

JAWHARA, S., PLUSKOTA, E., CAO, W., PLOW, E. F. & SOLOVIEV, D. A. 2016. Distinct Effects of Integrins αXβ2 and αMβ2 on Leukocyte Subpopulations during Inflammation and Antimicrobial Responses. *Infection and immunity,* 85**,** e00644-16.

JENSEN, H. K., DONSKOV, F., MARCUSSEN, N., NORDSMARK, M., LUNDBECK, F. & VON DER MAASE, H. 2009. Presence of Intratumoral Neutrophils Is an Independent Prognostic Factor in Localized Renal Cell Carcinoma. *Journal of Clinical Oncology,* 27**,** 4709-4717.

JENSEN, T. O., SCHMIDT, H., MØLLER, H. J., DONSKOV, F., HØYER, M., SJOEGREN, P., CHRISTENSEN, I. J. & STEINICHE, T. 2012. Intratumoral neutrophils and plasmacytoid dendritic cells indicate poor prognosis and are associated with pSTAT3 expression in AJCC stage I/II melanoma. *Cancer,* 118**,** 2476-2485.

JOHNSTONE, C. N., SMITH, Y. E., CAO, Y., BURROWS, A. D., CROSS, R. S. N., LING, X., REDVERS, R. P., DOHERTY, J. P., ECKHARDT, B. L., NATOLI, A. L., RESTALL, C. M., LUCAS, E., PEARSON, H. B., DEB, S., BRITT, K. L., RIZZITELLI, A., LI, J., HARMEY, J. H., POULIOT, N. & ANDERSON, R. L. 2015. Functional and molecular characterisation of EO771.LMB tumours, a new C57BL/6-mouse-derived model of spontaneously metastatic mammary cancer. *Disease models & mechanisms,* 8**,** 237-251.

KALLURI, R. 2016. The biology and function of fibroblasts in cancer. *Nature Reviews Cancer,* 16**,** 582.

KATOH, H., WANG, D., DAIKOKU, T., SUN, H., DEY, S. K. & DUBOIS, R. N. 2013. CXCR2-expressing myeloid-derived suppressor cells are essential to promote colitis-associated tumorigenesis. *Cancer cell,* 24**,** 631-644.

KERDILES, Y. M., ALMEIDA, F. F., THOMPSON, T., CHOPIN, M., VIENNE, M., BRUHNS, P., HUNTINGTON, N. D., RAULET, D. H., NUTT, S. L., BELZ, G. T. & VIVIER, E. 2017. Natural-Killer-like B Cells Display the Phenotypic and Functional Characteristics of Conventional B Cells. *Immunity,* 47**,** 199-200.

KIM, C. H. 2010. Homeostatic and pathogenic extramedullary hematopoiesis. *Journal of blood medicine,* 1**,** 13-19.

KIM, H. K., DE LA LUZ SIERRA, M., WILLIAMS, C. K., GULINO, A. V. & TOSATO, G. 2006. G-CSF down-regulation of CXCR4 expression identified as a mechanism for mobilization of myeloid cells. *Blood,* 108**,** 812-820.

KÖHLER, A., DE FILIPPO, K., HASENBERG, M., VAN DEN BRANDT, C., NYE, E., HOSKING, M. P., LANE, T. E., MÄNN, L., RANSOHOFF, R. M., HAUSER, A. E., WINTER, O., SCHRAVEN, B., GEIGER, H., HOGG, N. & GUNZER, M. 2011. G-CSF–mediated thrombopoietin release triggers neutrophil motility and mobilization from bone marrow via induction of Cxcr2 ligands. *Blood,* 117**,** 4349.

KOLACZKOWSKA, E. & KUBES, P. 2013. Neutrophil recruitment and function in health and inflammation. *Nat Rev Immunol,* 13**,** 159-75.

KOTECHA, N., KRUTZIK, P. O. & IRISH, J. M. 2010. Web-Based Analysis and Publication of Flow Cytometry Experiments. *Current protocols in cytometry /*

editorial board, J. Paul Robinson, managing editor ... [et al.], 0 10**,** Unit10.17-Unit10.17.

KREISEL, D., NAVA, R. G., LI, W., ZINSELMEYER, B. H., WANG, B., LAI, J., PLESS, R., GELMAN, A. E., KRUPNICK, A. S. & MILLER, M. J. 2010. In vivo two-photon imaging reveals monocyte-dependent neutrophil extravasation during pulmonary inflammation. *Proceedings of the National Academy of Sciences of the United States of America,* 107**,** 18073-18078.

KRUGER, P., SAFFARZADEH, M., WEBER, A. N., RIEBER, N., RADSAK, M., VON BERNUTH, H., BENARAFA, C., ROOS, D., SKOKOWA, J. & HARTL, D. 2015. Neutrophils: Between host defence, immune modulation, and tissue injury. *PLoS Pathog,* 11**,** e1004651.

KUMAR, V., PATEL, S., TCYGANOV, E. & GABRILOVICH, D. I. 2016. The Nature of Myeloid-Derived Suppressor Cells in the Tumor Microenvironment. *Trends in immunology,* 37**,** 208-220.

KUNDU, J. K. & SURH, Y.-J. 2008. Inflammation: Gearing the journey to cancer. *Mutation Research/Reviews in Mutation Research,* 659**,** 15-30.

LANG, S., BRUDEREK, K., KASPAR, C., HÖING, B., KANAAN, O., DOMINAS, N., HUSSAIN, T., DROEGE, F., EYTH, C., HADASCHIK, B. & BRANDAU, S. 2018. Clinical Relevance and Suppressive Capacity of Human Myeloid-Derived Suppressor Cell Subsets. *Clinical Cancer Research,* 24**,** 4834.

LEE, J. W., KOMAR, C. A., BENGSCH, F., GRAHAM, K. & BEATTY, G. L. 2016. Genetically Engineered Mouse Models of Pancreatic Cancer: The KPC Model (LSL-Kras(G12D/+) ;LSL-Trp53(R172H/+) ;Pdx-1-Cre), Its Variants, and Their Application in Immuno-oncology Drug Discovery. *Current protocols in pharmacology,* 73**,** 14.39.1-14.39.20.

LEE, P. Y., WANG, J.-X., PARISINI, E., DASCHER, C. C. & NIGROVIC, P. A. 2013. Ly6 family proteins in neutrophil biology. *Journal of Leukocyte Biology,* 94**,** 585-594.

LELIEFELD, P. H. C., KOENDERMAN, L. & PILLAY, J. 2015. How Neutrophils Shape Adaptive Immune Responses. *Frontiers in Immunology,* 6**,** 471.

LERMAN, I., GARCIA-HERNANDEZ, M. D. L. L., RANGEL-MORENO, J., CHIRIBOGA, L., PAN, C., NASTIUK, K. L., KROLEWSKI, J. J., SEN, A. & HAMMES, S. R. 2017. Infiltrating Myeloid Cells Exert Protumorigenic Actions via Neutrophil Elastase. *Molecular Cancer Research,* 15**,** 1138.

LEVINE, JACOB H., SIMONDS, ERIN F., BENDALL, SEAN C., DAVIS, KARA L., AMIR, E.-AD D., TADMOR, MICHELLE D., LITVIN, O., FIENBERG, HARRIS G., JAGER, A., ZUNDER, ELI R., FINCK, R., GEDMAN, AMANDA L., RADTKE, I., DOWNING, JAMES R., PE'ER, D. & NOLAN, GARRY P. Data-Driven Phenotypic Dissection of AML Reveals Progenitor-like Cells that Correlate with Prognosis. *Cell,* 162**,** 184-197.

LEWIS, S. M., TREACHER, D. F., EDGEWORTH, J., MAHALINGAM, G., BROWN, C. S., MARE, T. A., STACEY, M., BEALE, R. & BROWN, K. A. 2015. Expression of CD11c and EMR2 on neutrophils: potential diagnostic biomarkers for sepsis and systemic inflammation. *Clinical and experimental immunology,* 182**,** 184-194.

LIN, A. & LORÉ, K. 2017. Granulocytes: New Members of the Antigen-Presenting Cell Family. *Frontiers in Immunology,* 8**,** 1781.

LIN, E. Y., JONES, J. G., LI, P., ZHU, L., WHITNEY, K. D., MULLER, W. J. & POLLARD, J. W. 2003. Progression to malignancy in the polyoma middle T oncoprotein mouse breast cancer model provides a reliable model for human diseases. *The American journal of pathology,* 163**,** 2113-2126.

LIN, H.-H., STACEY, M., STEIN-STREILEIN, J. & GORDON, S. 2010. F4/80: The Macrophage-Specific Adhesion-GPCR and its Role in Immunoregulation. *In:*

YONA, S. & STACEY, M. (eds.) *Adhesion-GPCRs: Structure to Function.* Boston, MA: Springer US.
LIU, F., WU, H. Y., WESSELSCHMIDT, R., KORNAGA, T. & LINK, D. C. 1996. Impaired Production and Increased Apoptosis of Neutrophils in Granulocyte Colony-Stimulating Factor Receptor–Deficient Mice. *Immunity,* 5**,** 491-501.
LÓPEZ-LAGO, M. A., POSNER, S., THODIMA, V. J., MOLINA, A. M., MOTZER, R. J. & CHAGANTI, R. S. K. 2013. Neutrophil chemokines secreted by tumor cells mount a lung antimetastatic response during renal cell carcinoma progression. *Oncogene,* 32**,** 1752-1760.
LUND-JOHANSEN, F. & TERSTAPPEN, L. W. M. M. 1993. Differential surface expression of cell adhesion molecules during granulocyte maturation. *Journal of Leukocyte Biology,* 54**,** 47-55.
MAATEN, L. V. D. & HINTON, G. 2008. Visualizing data using t-SNE. *Journal of machine learning research,* 9**,** 2579-2605.
MACKEY, J. B. G., COFFELT, S. B. & CARLIN, L. M. 2019. Neutrophil Maturity in Cancer. *Frontiers in Immunology,* 10**,** 1912.
MANTOVANI, A., ALLAVENA, P., SICA, A. & BALKWILL, F. 2008. Cancer-related inflammation. *Nature,* 454**,** 436-444.
MANTOVANI, A., CASSATELLA, M. A., COSTANTINI, C. & JAILLON, S. 2011. Neutrophils in the activation and regulation of innate and adaptive immunity. *Nat Rev Immunol,* 11**,** 519-31.
MANZ, M. G. & BOETTCHER, S. 2014. Emergency granulopoiesis. *Nature Reviews Immunology,* 14**,** 302.
MARINI, O., COSTA, S., BEVILACQUA, D., CALZETTI, F., TAMASSIA, N., SPINA, C., DE SABATA, D., TINAZZI, E., LUNARDI, C., SCUPOLI, M. T., CAVALLINI, C., ZORATTI, E., TINAZZI, I., MARCHETTA, A., VASSANELLI, A., CANTINI, M., GANDINI, G., RUZZENENTE, A., GUGLIELMI, A., MISSALE, F., VERMI, W., TECCHIO, C., CASSATELLA, M. A. & SCAPINI, P. 2017. Mature CD10⁺ and immature CD10[−] neutrophils present in G-CSF–treated donors display opposite effects on T cells. *Blood,* 129**,** 1343.
MAYADAS, T. N., CULLERE, X. & LOWELL, C. A. 2014. The multifaceted functions of neutrophils. *Annu Rev Pathol,* 9**,** 181-218.
MAZZONI, A., BRONTE, V., VISINTIN, A., SPITZER, J. H., APOLLONI, E., SERAFINI, P., ZANOVELLO, P. & SEGAL, D. M. 2002. Myeloid Suppressor Lines Inhibit T Cell Responses by an NO-Dependent Mechanism. *The Journal of Immunology,* 168**,** 689.
MCARDEL, S. L., TERHORST, C. & SHARPE, A. H. 2016. Roles of CD48 in regulating immunity and tolerance. *Clinical immunology (Orlando, Fla.),* 164**,** 10-20.
MCKINSTRY, W. J., LI, C.-L., RASKO, J. E. J., NICOLA, N. A., JOHNSON, G. R. & METCALF, D. 1997. Cytokine Receptor Expression on Hematopoietic Stem and Progenitor Cells. *Blood,* 89**,** 65.
MENSURADO, S., REI, M., LANÇA, T., IOANNOU, M., GONÇALVES-SOUSA, N., KUBO, H., MALISSEN, M., PAPAYANNOPOULOS, V., SERRE, K. & SILVA-SANTOS, B. 2018. Tumor-associated neutrophils suppress pro-tumoral IL-17+ γδ T cells through induction of oxidative stress. *PLoS biology,* 16**,** e2004990-e2004990.
MESTAS, J. & HUGHES, C. C. W. 2004. Of Mice and Not Men: Differences between Mouse and Human Immunology. *The Journal of Immunology,* 172**,** 2731.
METSALU, T. & VILO, J. 2015. ClustVis: a web tool for visualizing clustering of multivariate data using Principal Component Analysis and heatmap. *Nucleic Acids Research,* 43**,** W566-W570.

MILLRUD, C. R., KÅGEDAL, Å., KUMLIEN GEORÉN, S., WINQVIST, O., UDDMAN, R., RAZAVI, R., MUNCK-WIKLAND, E. & CARDELL, L. O. 2017. NET-producing CD16high CD62Ldim neutrophils migrate to tumor sites and predict improved survival in patients with HNSCC. *International Journal of Cancer,* 140**,** 2557-2567.

MISHALIAN, I., GRANOT, Z. & FRIDLENDER, Z. G. 2016. The diversity of circulating neutrophils in cancer. *Immunobiology*.

MOMBAERTS, P., IACOMINI, J., JOHNSON, R. S., HERRUP, K., TONEGAWA, S. & PAPAIOANNOU, V. E. 1992. RAG-1-deficient mice have no mature B and T lymphocytes. *Cell,* 68**,** 869-877.

MORRIS, K. T., KHAN, H., AHMAD, A., WESTON, L. L., NOFCHISSEY, R. A., PINCHUK, I. V. & BESWICK, E. J. 2014. G-CSF and G-CSFR are highly expressed in human gastric and colon cancers and promote carcinoma cell proliferation and migration. *British Journal of Cancer,* 110**,** 1211-1220.

MURPHY, G. P. & HRUSHESKY, W. J. 1973. A Murine Renal Cell Carcinoma. *JNCI: Journal of the National Cancer Institute,* 50**,** 1013-1025.

NEUBERT, E., SENGER-SANDER, S. N., MANZKE, V. S., BUSSE, J., POLO, E., SCHEIDMANN, S. E. F., SCHÖN, M. P., KRUSS, S. & ERPENBECK, L. 2019. Serum and Serum Albumin Inhibit in vitro Formation of Neutrophil Extracellular Traps (NETs). *Frontiers in immunology,* 10**,** 12-12.

NG, L. G., OSTUNI, R. & HIDALGO, A. 2019. Heterogeneity of neutrophils. *Nature Reviews Immunology,* 19**,** 255-265.

NOURSHARGH, S., RENSHAW, S. A. & IMHOF, B. A. 2016. Reverse Migration of Neutrophils: Where, When, How, and Why? *Trends in Immunology,* 37**,** 273-286.

NOWOSAD, C. R., SPILLANE, K. M. & TOLAR, P. 2016. Germinal center B cells recognize antigen through a specialized immune synapse architecture. *Nature immunology,* 17**,** 870-877.

NOZAWA, H., CHIU, C. & HANAHAN, D. 2006. Infiltrating neutrophils mediate the initial angiogenic switch in a mouse model of multistage carcinogenesis. *Proceedings of the National Academy of Sciences of the United States of America,* 103**,** 12493-12498.

OVERWIJK, W. W. & RESTIFO, N. P. 2001. B16 as a mouse model for human melanoma. *Current protocols in immunology,* Chapter 20**,** Unit-20.1.

PAPAYANNOPOULOS, V. 2017. Neutrophil extracellular traps in immunity and disease. *Nature Reviews Immunology,* 18**,** 134.

PARK, J., WYSOCKI, R. W., AMOOZGAR, Z., MAIORINO, L., FEIN, M. R., JORNS, J., SCHOTT, A. F., KINUGASA-KATAYAMA, Y., LEE, Y., WON, N. H., NAKASONE, E. S., HEARN, S. A., KÜTTNER, V., QIU, J., ALMEIDA, A. S., PERURENA, N., KESSENBROCK, K., GOLDBERG, M. S. & EGEBLAD, M. 2016. Cancer cells induce metastasis-supporting neutrophil extracellular DNA traps. *Science translational medicine,* 8**,** 361ra138-361ra138.

PARLATO, M., SOUZA-FONSECA-GUIMARAES, F., PHILIPPART, F., MISSET, B., ADIB-CONQUY, M. & CAVAILLON, J. M. 2012. CD24-mediated neutrophil death in inflammation: ex vivo study suggesting a potential role in sepsis. *Critical Care,* 16**,** P81-P81.

PELLETIER, M., MAGGI, L., MICHELETTI, A., LAZZERI, E., TAMASSIA, N., COSTANTINI, C., COSMI, L., LUNARDI, C., ANNUNZIATO, F., ROMAGNANI, S. & CASSATELLA, M. A. 2010a. Evidence for a cross-talk between human neutrophils and Th17 cells. *Blood,* 115**,** 335-43.

PELLETIER, M., MAGGI, L., MICHELETTI, A., LAZZERI, E., TAMASSIA, N., COSTANTINI, C., COSMI, L., LUNARDI, C., ANNUNZIATO, F., ROMAGNANI,

S. & CASSATELLA, M. A. 2010b. Evidence for a cross-talk between human neutrophils and Th17 cells. *Blood,* 115**,** 335.

PEYSSONNAUX, C., DATTA, V., CRAMER, T., DOEDENS, A., THEODORAKIS, E. A., GALLO, R. L., HURTADO-ZIOLA, N., NIZET, V. & JOHNSON, R. S. 2005. HIF-1alpha expression regulates the bactericidal capacity of phagocytes. *The Journal of clinical investigation,* 115**,** 1806-1815.

PHILLIPSON, M. & KUBES, P. 2019. The Healing Power of Neutrophils. *Trends in Immunology,* 40**,** 635-647.

PILLAY, J., DEN BRABER, I., VRISEKOOP, N., KWAST, L. M., DE BOER, R. J., BORGHANS, J. A. M., TESSELAAR, K. & KOENDERMAN, L. 2010. In vivo labeling with 2H2O reveals a human neutrophil lifespan of 5.4 days. *Blood,* 116**,** 625.

PILLAY, J., KAMP, V. M., VAN HOFFEN, E., VISSER, T., TAK, T., LAMMERS, J.-W., ULFMAN, L. H., LEENEN, L. P., PICKKERS, P. & KOENDERMAN, L. 2012. A subset of neutrophils in human systemic inflammation inhibits T cell responses through Mac-1. *The Journal of Clinical Investigation,* 122**,** 327-336.

PILLAY, J., TAK, T., KAMP, V. M. & KOENDERMAN, L. 2013. Immune suppression by neutrophils and granulocytic myeloid-derived suppressor cells: similarities and differences. *Cellular and Molecular Life Sciences,* 70**,** 3813-3827.

PODAZA, E., RISNIK, D., COLADO, A., ELÍAS, E., ALMEJÚN, M. B., FERNANDEZ GRECCO, H., BEZARES, R. F., BORGE, M., GAMBERALE, R. & GIORDANO, M. 2019. Chronic lymphocytic leukemia cells increase neutrophils survival and promote their differentiation into CD16highCD62Ldim immunosuppressive subset. *International Journal of Cancer,* 144**,** 1128-1134.

POWELL, D. R. & HUTTENLOCHER, A. 2016. Neutrophils in the Tumor Microenvironment. *Trends in Immunology,* 37**,** 41-52.

PULASKI, B. A. & OSTRAND-ROSENBERG, S. 2000. Mouse 4T1 Breast Tumor Model. *Current Protocols in Immunology,* 39**,** 20.2.1-20.2.16.

QUAIL, D. F. & JOYCE, J. A. 2013. Microenvironmental regulation of tumor progression and metastasis. *Nat Med,* 19**,** 1423-37.

QUARESMA, M., COLEMAN, M. P. & RACHET, B. 2015. 40-year trends in an index of survival for all cancers combined and survival adjusted for age and sex for each cancer in England and Wales, 1971–2011: a population-based study. *The Lancet,* 385**,** 1206-1218.

RECZEK, C. R. & CHANDEL, N. S. 2017. The Two Faces of Reactive Oxygen Species in Cancer. *Annual Review of Cancer Biology,* 1**,** 79-98.

REICHEL, C. A., KHANDOGA, A., ANDERS, H.-J., SCHLÖNDORFF, D., LUCKOW, B. & KROMBACH, F. 2006. Chemokine receptors Ccr1, Ccr2, and Ccr5 mediate neutrophil migration to postischemic tissue. *Journal of Leukocyte Biology,* 79**,** 114-122.

SACK, U. 2017. CD64 expression by neutrophil granulocytes. *Cytometry Part B: Clinical Cytometry,* 92**,** 189-191.

SAGIV, J. Y., MICHAELI, J., ASSI, S., MISHALIAN, I., KISOS, H., LEVY, L., DAMTI, P., LUMBROSO, D., POLYANSKY, L., SIONOV, R. V., ARIEL, A., HOVAV, A. H., HENKE, E., FRIDLENDER, Z. G. & GRANOT, Z. 2015. Phenotypic diversity and plasticity in circulating neutrophil subpopulations in cancer. *Cell Rep,* 10**,** 562-73.

SCENEAY, J., SMYTH, M. J. & MÖLLER, A. 2013. The pre-metastatic niche: finding common ground. *Cancer and Metastasis Reviews,* 32**,** 449-464.

SCHMIDT, H., BASTHOLT, L., GEERTSEN, P., CHRISTENSEN, I. J., LARSEN, S., GEHL, J. & VON DER MAASE, H. 2005. Elevated neutrophil and monocyte counts in peripheral blood are associated with poor survival in patients with

metastatic melanoma: a prognostic model. *British journal of cancer,* 93**,** 273-278.

SEITA, J. & WEISSMAN, I. L. 2010. Hematopoietic stem cell: self-renewal versus differentiation. *Wiley interdisciplinary reviews. Systems biology and medicine,* 2**,** 640-653.

SHAUL, M. E. & FRIDLENDER, Z. G. 2019. Tumour-associated neutrophils in patients with cancer. *Nature Reviews Clinical Oncology*.

SHEN, M., HU, P., DONSKOV, F., WANG, G., LIU, Q. & DU, J. 2014. Tumor-associated neutrophils as a new prognostic factor in cancer: a systematic review and meta-analysis. *PloS one,* 9**,** e98259-e98259.

SIEGEL, R. L., MILLER, K. D. & JEMAL, A. 2019. Cancer statistics, 2019. *CA: A Cancer Journal for Clinicians,* 69**,** 7-34.

SILVESTRE-ROIG, C., HIDALGO, A. & SOEHNLEIN, O. 2016. Neutrophil heterogeneity: implications for homeostasis and pathogenesis. *Blood,* 127**,** 2173-2181.

SINGEL, K. L., EMMONS, T. R., KHAN, A. N. H., MAYOR, P. C., SHEN, S., WONG, J. T., MORRELL, K., ENG, K. H., MARK, J., BANKERT, R. B., MATSUZAKI, J., KOYA, R. C., BLOM, A. M., MCLEISH, K. R., QU, J., RAM, S., MOYSICH, K. B., ABRAMS, S. I., ODUNSI, K., ZSIROS, E. & SEGAL, B. H. 2019. Mature neutrophils suppress T cell immunity in ovarian cancer microenvironment. *JCI insight,* 4**,** e122311.

SINGHAL, S., BHOJNAGARWALA, P. S., O'BRIEN, S., MOON, E. K., GARFALL, A. L., RAO, A., QUATROMONI, J. G., STEPHEN, T. L., LITZKY, L., DESHPANDE, C., FELDMAN, M., HANCOCK, W. W., CONEJO-GARCIA, J. R., ALBELDA, S. M. & ERUSLANOV, E. B. 2016. Origin and Role of a Subset of Tumor-Associated Neutrophils with Antigen Presenting Cell Features (Hybrid TANs) in Early-Stage Human Lung Cancer. *Cancer cell,* 30**,** 120-135.

SKINNER, B. M. & JOHNSON, E. E. P. 2017. Nuclear morphologies: their diversity and functional relevance. *Chromosoma,* 126**,** 195-212.

SMITH, I., SILVEIRINHA, V., STEIN, J. L., DE LA TORRE-UBIETA, L., FARRIMOND, J. A., WILLIAMSON, E. M. & WHALLEY, B. J. 2017. Human neural stem cell-derived cultures in three-dimensional substrates form spontaneously functional neuronal networks. *Journal of Tissue Engineering and Regenerative Medicine,* 11**,** 1022-1033.

SONODA, E., PEWZNER-JUNG, Y., SCHWERS, S., TAKI, S., JUNG, S., EILAT, D. & RAJEWSKY, K. 1997. B Cell Development under the Condition of Allelic Inclusion. *Immunity,* 6**,** 225-233.

SPITZER, M. H. & NOLAN, G. P. 2016. Mass Cytometry: Single Cells, Many Features. *Cell,* 165**,** 780-91.

SZCZERBA, B. M., CASTRO-GINER, F., VETTER, M., KROL, I., GKOUNTELA, S., LANDIN, J., SCHEIDMANN, M. C., DONATO, C., SCHERRER, R., SINGER, J., BEISEL, C., KURZEDER, C., HEINZELMANN-SCHWARZ, V., ROCHLITZ, C., WEBER, W. P., BEERENWINKEL, N. & ACETO, N. 2019. Neutrophils escort circulating tumour cells to enable cell cycle progression. *Nature,* 566**,** 553-557.

TAK, T., WIJTEN, P., HEERES, M., PICKKERS, P., SCHOLTEN, A., HECK, A. J. R., VRISEKOOP, N., LEENEN, L. P., BORGHANS, J., AMP, AMP, EACUTE, A. M., TESSELAAR, K. & KOENDERMAN, L. 2017. Human CD62L- Neutrophils Identified as a Separate Subset by Proteome Profiling and In Vivo Pulse-Chase Labelling. *Blood*.

TALMADGE, J. E. & GABRILOVICH, D. I. 2013. History of myeloid-derived suppressor cells. *Nat Rev Cancer,* 13**,** 739-52.

TAZZYMAN, S., BARRY, S. T., ASHTON, S., WOOD, P., BLAKEY, D., LEWIS, C. E. & MURDOCH, C. 2011. Inhibition of neutrophil infiltration into A549 lung tumors in

vitro and in vivo using a CXCR2-specific antagonist is associated with reduced tumor growth. *International Journal of Cancer,* 129**,** 847-858.
TEMPLETON, A. J., MCNAMARA, M. G., ŠERUGA, B., VERA-BADILLO, F. E., ANEJA, P., OCAÑA, A., LEIBOWITZ-AMIT, R., SONPAVDE, G., KNOX, J. J., TRAN, B., TANNOCK, I. F. & AMIR, E. 2014. Prognostic Role of Neutrophil-to-Lymphocyte Ratio in Solid Tumors: A Systematic Review and Meta-Analysis. *JNCI: Journal of the National Cancer Institute,* 106**,** dju124-dju124.
THUN, M. J. & JEMAL, A. 2006. How much of the decrease in cancer death rates in the United States is attributable to reductions in tobacco smoking? *Tobacco control,* 15**,** 345-347.
TOFTS, P. S., CHEVASSUT, T., CUTAJAR, M., DOWELL, N. G. & PETERS, A. M. 2011. Doubts concerning the recently reported human neutrophil lifespan of 5.4 days. *Blood,* 117**,** 6050.
UEDA, Y., KONDO, M. & KELSOE, G. 2005. Inflammation and the reciprocal production of granulocytes and lymphocytes in bone marrow. *The Journal of experimental medicine,* 201**,** 1771-1780.
URIBE-QUEROL, E. & ROSALES, C. 2015. Neutrophils in Cancer: Two Sides of the Same Coin. *J Immunol Res,* 2015**,** 983698.
VALASTYAN, S. & WEINBERG, R. A. 2011. Tumor metastasis: molecular insights and evolving paradigms. *Cell,* 147**,** 275-92.
VAN GRINSVEN, E., TEXTOR, J., HUSTIN, L. S. P., WOLF, K., KOENDERMAN, L. & VRISEKOOP, N. 2018. Immature Neutrophils Released in Acute Inflammation Exhibit Efficient Migration despite Incomplete Segmentation of the Nucleus. *The Journal of Immunology***,** ji1801255.
VAN LOCHEM, E. G., VAN DER VELDEN, V. H. J., WIND, H. K., TE MARVELDE, J. G., WESTERDAAL, N. A. C. & VAN DONGEN, J. J. M. 2004. Immunophenotypic differentiation patterns of normal hematopoiesis in human bone marrow: Reference patterns for age-related changes and disease-induced shifts. *Cytometry Part B: Clinical Cytometry,* 60B**,** 1-13.
VEENSTRA, M. & RANSOHOFF, R. M. 2012. Chemokine receptor CXCR2: physiology regulator and neuroinflammation controller? *Journal of neuroimmunology,* 246**,** 1-9.
VEGLIA, F., PEREGO, M. & GABRILOVICH, D. 2018. Myeloid-derived suppressor cells coming of age. *Nature immunology,* 19**,** 108-119.
VEGLIA, F., TYURIN, V. A., BLASI, M., DE LEO, A., KOSSENKOV, A. V., DONTHIREDDY, L., TO, T. K. J., SCHUG, Z., BASU, S., WANG, F., RICCIOTTI, E., DIRUSSO, C., MURPHY, M. E., VONDERHEIDE, R. H., LIEBERMAN, P. M., MULLIGAN, C., NAM, B., HOCKSTEIN, N., MASTERS, G., GUARINO, M., LIN, C., NEFEDOVA, Y., BLACK, P., KAGAN, V. E. & GABRILOVICH, D. I. 2019. Fatty acid transport protein 2 reprograms neutrophils in cancer. *Nature,* 569**,** 73-78.
VILLANUEVA, E., YALAVARTHI, S., BERTHIER, C. C., HODGIN, J. B., KHANDPUR, R., LIN, A. M., RUBIN, C. J., ZHAO, W., OLSEN, S. H., KLINKER, M., SHEALY, D., DENNY, M. F., PLUMAS, J., CHAPEROT, L., KRETZLER, M., BRUCE, A. T. & KAPLAN, M. J. 2011. Netting neutrophils induce endothelial damage, infiltrate tissues and expose immunostimulatory molecules in systemic lupus erythematosus. *Journal of immunology (Baltimore, Md. : 1950),* 187**,** 538-552.
VIRCHOW, R. L. K. 1863. *Die krankhaften Geschwülste,* Berlin, August Hirschwald.
VISVADER, J. E. 2011. Cells of origin in cancer. *Nature,* 469**,** 314-322.
WANG, J., HOSSAIN, M., THANABALASURIAR, A., GUNZER, M., MEININGER, C. & KUBES, P. 2017. Visualizing the function and fate of neutrophils in sterile injury and repair. *Science,* 358**,** 111.

WANG, J.-X., BAIR, A. M., KING, S. L., SHNAYDER, R., HUANG, Y.-F., SHIEH, C.-C., SOBERMAN, R. J., FUHLBRIGGE, R. C. & NIGROVIC, P. A. 2012a. Ly6G ligation blocks recruitment of neutrophils via a β2-integrin–dependent mechanism. *Blood,* 120**,** 1489-1498.

WANG, K., WEI, G. & LIU, D. 2012b. CD19: a biomarker for B cell development, lymphoma diagnosis and therapy. *Experimental hematology & oncology,* 1**,** 36-36.

WANG, S., XIA, P., CHEN, Y., HUANG, G., XIONG, Z., LIU, J., LI, C., YE, B., DU, Y. & FAN, Z. 2016. Natural Killer-like B Cells Prime Innate Lymphocytes against Microbial Infection. *Immunity,* 45**,** 131-144.

WCULEK, S. K. & MALANCHI, I. 2015. Neutrophils support lung colonization of metastasis-initiating breast cancer cells. *Nature,* 528**,** 413-7.

WELLENSTEIN, M. D., COFFELT, S. B., DUITS, D. E. M., VAN MILTENBURG, M. H., SLAGTER, M., DE RINK, I., HENNEMAN, L., KAS, S. M., PREKOVIC, S., HAU, C.-S., VRIJLAND, K., DRENTH, A. P., DE KORTE-GRIMMERINK, R., SCHUT, E., VAN DER HEIJDEN, I., ZWART, W., WESSELS, L. F. A., SCHUMACHER, T. N., JONKERS, J. & DE VISSER, K. E. 2019. Loss of p53 triggers WNT-dependent systemic inflammation to drive breast cancer metastasis. *Nature,* 572**,** 538-542.

WHITMORE, L. C., WEEMS, M. N. & ALLEN, L.-A. H. 2017. Cutting Edge: Helicobacter pylori Induces Nuclear Hypersegmentation and Subtype Differentiation of Human Neutrophils In Vitro. *Journal of immunology (Baltimore, Md. : 1950),* 198**,** 1793-1797.

WILCOX, R. A. 2010. Cancer-associated myeloproliferation: old association, new therapeutic target. *Mayo Clinic proceedings,* 85**,** 656-663.

WINTERBOURN, C. C., KETTLE, A. J. & HAMPTON, M. B. 2016. Reactive Oxygen Species and Neutrophil Function. *Annual Review of Biochemistry,* 85**,** 765-792.

WIRTHS, S., BUGL, S. & KOPP, H.-G. 2014. Neutrophil homeostasis and its regulation by danger signaling. *Blood,* 123**,** 3563.

WU, P., WU, D., NI, C., YE, J., CHEN, W., HU, G., WANG, Z., WANG, C., ZHANG, Z., XIA, W., CHEN, Z., WANG, K., ZHANG, T., XU, J., HAN, Y., ZHANG, T., WU, X., WANG, J., GONG, W., ZHENG, S., QIU, F., YAN, J. & HUANG, J. 2014. γδT17 cells promote the accumulation and expansion of myeloid-derived suppressor cells in human colorectal cancer. *Immunity,* 40**,** 785-800.

YANG, L., DEBUSK, L. M., FUKUDA, K., FINGLETON, B., GREEN-JARVIS, B., SHYR, Y., MATRISIAN, L. M., CARBONE, D. P. & LIN, P. C. 2004. Expansion of myeloid immune suppressor Gr+CD11b+ cells in tumor-bearing host directly promotes tumor angiogenesis. *Cancer Cell,* 6**,** 409-421.

YANG, M., MCKAY, D., POLLARD, J. W. & LEWIS, C. E. 2018. Diverse Functions of Macrophages in Different Tumor Microenvironments. *Cancer Research,* 78**,** 5492.

YAO, Y., MATSUSHIMA, H., OHTOLA, J. A., GENG, S., LU, R. & TAKASHIMA, A. 2015. Neutrophil priming occurs in a sequential manner and can be visualized in living animals by monitoring IL-1β promoter activation. *Journal of immunology (Baltimore, Md. : 1950),* 194**,** 1211-1224.

ZHANG, D., CHEN, G., MANWANI, D., MORTHA, A., XU, C., FAITH, J. J., BURK, R. D., KUNISAKI, Y., JANG, J.-E., SCHEIERMANN, C., MERAD, M. & FRENETTE, P. S. 2015. Neutrophil ageing is regulated by the microbiome. *Nature,* 525**,** 528-532.

ZHANG, J., WANG, X., VIKASH, V., YE, Q., WU, D., LIU, Y. & DONG, W. 2016. ROS and ROS-Mediated Cellular Signaling. *Oxidative medicine and cellular longevity,* 2016**,** 4350965-4350965.

ZHOU, S.-L., ZHOU, Z.-J., HU, Z.-Q., HUANG, X.-W., WANG, Z., CHEN, E.-B., FAN, J., CAO, Y., DAI, Z. & ZHOU, J. 2016. Tumor-Associated Neutrophils Recruit Macrophages and T-Regulatory Cells to Promote Progression of Hepatocellular Carcinoma and Resistance to Sorafenib. *Gastroenterology,* 150**,** 1646-1658.e17.

ZHU, Y. P., PADGETT, L., DINH, H. Q., MARCOVECCHIO, P., BLATCHLEY, A., WU, R., EHINGER, E., KIM, C., MIKULSKI, Z., SEUMOIS, G., MADRIGAL, A., VIJAYANAND, P. & HEDRICK, C. C. 2018. Identification of an Early Unipotent Neutrophil Progenitor with Pro-tumoral Activity in Mouse and Human Bone Marrow. *Cell reports,* 24**,** 2329-2341.e8.

ZOU, Y. R., TAKEDA, S. & RAJEWSKY, K. 1993. Gene targeting in the Ig kappa locus: efficient generation of lambda chain-expressing B cells, independent of gene rearrangements in Ig kappa. *The EMBO journal,* 12**,** 811-820.